FINAL REPORT

La Conchita Slope Stabilization Project

Geological Study

La Conchita, Ventura County

Contract No. 3108855 (CRN 17600307169846)
Project No. 122259A

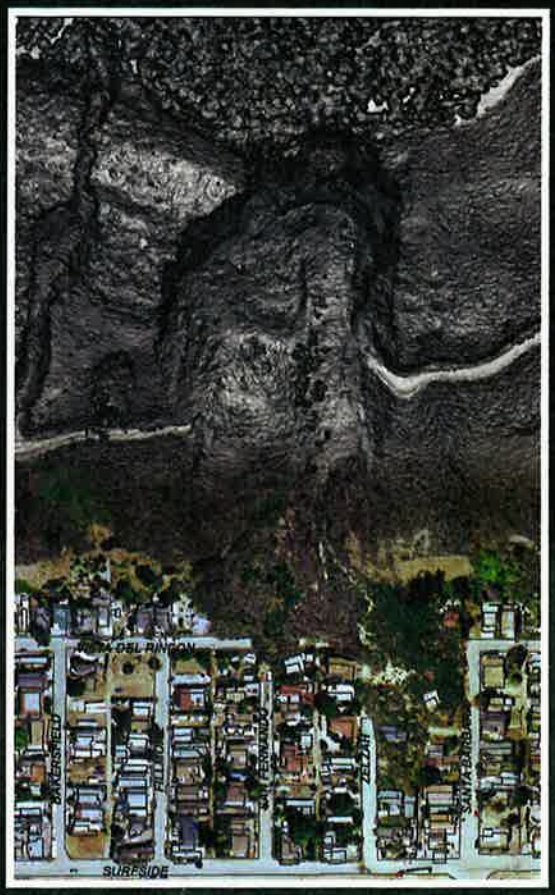

SUBMITTED TO
Department of General Services
Real Estate Services Division
BOPP Contract Management Section
707 Third Street, Suite 4-062
West Sacramento, CA 95605

SUBMITTED BY
WILLIAM LETTIS & ASSOCIATES, INC.
1777 Botelho Drive, Suite 262
Walnut Creek, CA 94596

August 28, 2009

WLA - William Lettis & Associates, Inc.

WLA

FINAL REPORT

La Conchita Slope Stabilization Project

Geological Study

La Conchita, Ventura County

Prepared by:

William Lettis & Associates, Inc.
1777 Botelho Drive, Suite 262
Walnut Creek, CA 94596

Submitted to:

Alan Kropp and Associates, Inc
GEOTECHNICAL ENGINEERING CONSULTANTS
2140 Shattuck Avenue, Suite 910
Berkeley, CA 94704

August 2009

SIGNATURE PAGE

La Conchita Slope Stabilization Project Geological Study, La Conchita, Ventura County
William Lettis & Associates, Inc. Project No. 1885

This investigation and report was prepared by the following qualified William Lettis & Associates personnel:

August 28, 2009

Christopher S. Hitchcock, CEG 2017 — Date
Principal Geologist

This investigation and report were reviewed by the following qualified senior WLA personnel and demonstrate WLA's best effort towards achieving the project objectives:

August 28, 2009

Scott C. Lindvall, CEG 1711 — Date
Senior Principal Geologist

TABLE OF CONTENTS

LIST OF TABLES

LIST OF FIGURES

LIST OF FIGURES - CONTINUED

LIST OF APPENDICES

1.0 INTRODUCTION

This report presents results from the William Lettis & Associates, Inc. (WLA) geological study of the La Conchita Study Area (Figure 1.1). This study was conducted as part of the La Conchita Slope Stabilization Project. Information collected for this study and presented within this report, and the earlier Phase 1 report (AKA, 2007), is intended to provide the necessary framework for characterization of the overall risk posed to the community of La Conchita, within the context of all major geologic and seismic hazards to the town.

1.1 Site Location

La Conchita is located on the California coast about ten miles northwest of the City of Ventura, approximately three miles southeast of Carpinteria (Figure 1.1). At this general location, the coastline trends approximately northwest to southeast. To simplify results presented in this report, we have adopted the local convention that the Pacific Ocean borders the south side of the Study Area. We also have rotated the orientation in all map figures approximately 54 degrees counterclockwise, with the Pacific Ocean margin shown as horizontal and major canyons (West and East Barrancas) shown as vertical. The landward, vertical direction is depicted as "project north" on all maps and figures, as shown on Figure 1.2. Consistent with our Phase 1 report (AKA, 2007), we use the following terminology:

Landward – The landward direction is approximately northeast.

Seaward – The seaward direction is approximately southwest and towards the Pacific Ocean.

Upcoast – The upcoast direction is approximately northwest and towards Carpinteria.

Downcoast – The downcoast direction is approximately southeast and towards Ventura.

As shown on Figure 1.2, the Study Area includes the community of La Conchita and adjacent lands of La Conchita Ranch. Two major canyons form the upcoast and downcoast limits of the Study Area. We refer to these canyons by their local names. West Barranca is a northeast to southwest flowing drainage, typically dry, that bounds the western margin of the Study Area and enters the ocean on the upcoast margin of the community of La Conchita. East Barranca is a smaller, northeast to southwest flowing drainage, also typically dry, that enters the coastal plain near Punta Gorda point and bounds the downcoast limit of the Study Area.

We further describe the Study Area in terms of the other major topographic features present (AKA, 2007). These features include the coastal plain upon which the community of La Conchita is built; the cliff area landward of La Conchita that is the source of the 1995 and 2005 landslides; and, the broad plateau above the cliff that is covered with avocado and citrus orchards of La Conchita Ranch.

1.2 Purpose of Study

The primary purpose of this report is to characterize the geologic and geotechnical conditions, and associated geologic hazards, of the La Conchita Study Area, as defined above. Results from the hazard assessment will be used to develop design criteria for conceptual mitigation schemes for slope hazards to the community of La Conchita. This investigation focused on characterization of geologic, seismic, and groundwater conditions.

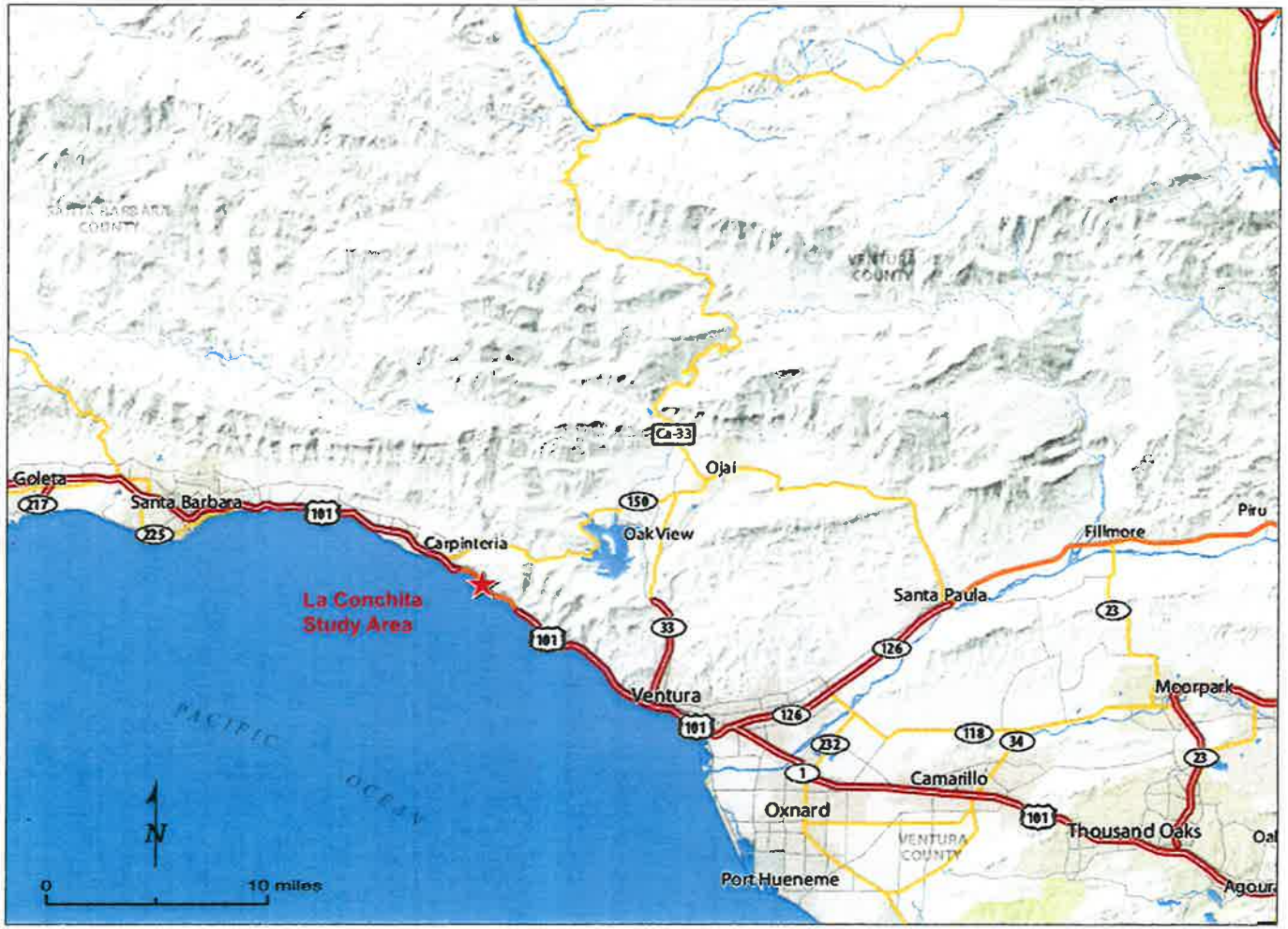

Regional Map of La Conchita Area

LA CONCHITA LANDSLIDE – PHASE 2
Figure 1.1

18 MARCH 08, 1885, REV 1, CSH

0 1000 ft

WLA

Map Showing Limits of La Conchita Study Area

LA CONCHITA LANDSLIDE – PHASE 2
Figure 1.2

18 MARCH 08, 1885, REV 1, CSH

1.3 Report Organization

Geologic and geotechnical information presented in this report is organized in eleven main sections. Basic data collected for this study, including boring logs, and interpretative products, including geologic maps and cross-sections, are presented in Appendices A through E at the end of this report.

Section 2.0 – *Scope of Work*. This section describes the scope of work performed, data collected, and activities completed for this investigation.

Section 3.0 – *Regional Tectonic Setting*. This section provides a review of the regional geologic, tectonic, and seismic setting of the La Conchita Study Area. Historical seismicity and nearby active faults are discussed. This section also includes brief description of the seismic sources incorporated in the hazard evaluation completed for this study, documented in detail within Appendix A.

Section 4.0 – *Site Geology*. This section describes site-specific geologic and geotechnical information for the La Conchita Study Area, based on data compiled from previous work and new geologic and geotechnical information collected during for investigation. The three-dimensional geologic model developed for this study is presented, based on the geologic map and cross-sections (provided in Appendix B), results of subsurface exploration, including small and large-diameter borings (provided in Appendix C), down-hole geophysical data (provided in Appendix D), and radiocarbon dating laboratory results (Appendix E). Also included in Section 4.0 is discussion of the late Quaternary geologic evolution of the main geologic features within the La Conchita Study Area. Included in this section is presentation and discussion of radiocarbon dates obtained from debris flow deposits in the community of La Conchita, with a full report on the laboratory testing provided in Appendix E. These dates, combined with down-hole observations of pre-historic debris flow deposits in large-diameter borings, provide constraints on the recurrence of debris flows in La Conchita.

Section 5.0 – *Red Mountain Fault.* This section discusses the Red Mountain fault, including results of new mapping conducted for this study. In addition to summary of existing published and unpublished information on the fault, this section presents interpretation of seismic parameters to evaluate surface fault rupture hazard to the community of La Conchita.

Section 6.0 – *Groundwater*. This section presents information on surface runoff and groundwater, based on interpretation of compiled data from previous studies and the geologic model developed for this study. A brief summary of ongoing groundwater level monitoring efforts also is presented.

Section 7.0 – *Landslides and Debris Flows*. This section presents information on historical slope failures, including major and minor landslides and debris flows, within the vicinity of the La Conchita Study Area. The section also presents and discusses our inventory of previously undocumented historical and pre-historic slope failures, and associated deposits. The slope failure inventory is based on interpretation of available aerial photography and new subsurface exploration conducted for this study.

Section 8.0 – *Evaluation of Slope Hazards*. This section presents and discusses landslide and debris flow hazards.

Section 9.0 – *Evaluation of Seismic Hazards*. This section presents and discusses individual seismic hazards.

Section 10.0 - *Conclusions and Recommendations.* This section provides a summary of key conclusions derived from our study.

Section 11.0 – *References.* References cited in this report, including previous unpublished geotechnical reports for the La Conchita Study Area, are provided in this section.

1.4 Project Team

This investigation was directed and managed by Mr. Christopher Hitchcock of WLA (CEG 2017), with assistance from Dr. Ross Hartleb, Mr. Kevin Clahan (CEG 2100), Mr. Michael Strane, and technical oversight from Mr. Scott Lindvall (CEG 1711). Mr. Jeffrey Hemphill compiled GIS layers of compiled and digitized datasets. Mr. Hemphill was assisted by Mr. Mark Zellman in the processing of detailed LiDAR elevation data. Dr. Dan O'Connell completed numerical modeling of debris flow run-out distances and depths. Hartleb and Strane conducted the geologic mapping with input and oversight by Hitchcock and Clahan. Hitchcock and Hartleb logged the geotechnical borings. This draft report has been prepared by Hitchcock, with graphical assistance from Mr. Rick Zeeb and Ms. Carolyn Mosher of WLA. Technical review of the report was performed by Hartleb and Lindvall.

1.5 Limitations

This report has been prepared specifically for Alan Kropp and Associates (AKA), under a master contract to the State of California Department of General Services (DGS) and the Governor's Office of Emergency Services (OES). It is to be used solely in support of AKA's development of conceptual hazard mitigation/management plans for the Study Area delineated in this report. No warranty, expressed or implied, is made as to the professional advice included in this report. This report has not been prepared for use by other parties, and may not contain sufficient information for more site-specific design. The conclusions and recommendations apply only to the existing study area and are based only on information made available to us by the date of submittal. Our findings are based on existing compiled geologic and geotechnical data from previous studies of varying quality, supplemented by reconnaissance-level mapping and limited field exploration. In the event that future development occurs for the Study Area, the conclusions and recommendations contained in this report shall not necessarily be considered applicable as new field data may modify the conclusions and recommendations of this report. The conclusions and recommendations contained in this report are professional opinions derived in accordance with current standards of professional practice.

2.0 SCOPE OF WORK

This study consists of geologic assessment for input into the development of conceptual hazard mitigation/management plans. The project scope of work for the entire study is divided into three primary phases, as follows:

Phase 1 – Initial Assessments
Phase 2 – Detailed Assessments
Phase 3 – Risk Management Options and Report

Primary objectives of Phases 1 and 2, including the focus of the geotechnical results provided in this report, include characterization the La Conchita Study Area from both a geologic and hazard perspective. Information contained within this report, and the earlier Phase 1 report (AKA, 2007), is intended to provide the necessary framework for characterization of the overall risk posed to the community of La Conchita, within the context of all major geologic and seismic hazards to the town. The data compiled as part of Phase 1, and new information collected in Phase 2 as presented in this report, are the product of a project data collection plan designed to provide reasonably detailed information necessary for development of a suite of possible conceptual designs towards possible mitigation of slope hazards to La Conchita. Towards this end, within the constraints of the project budget, the scope of work of our Phase 1 activities included:

- ***Review of previous work***, including existing reports, maps, aerial photographs and other information relevant to the evaluation of the geology and hazards for the La Conchita Study Area;
- ***Development of a high-resolution topographic base map***, derived from airplane-based imaging (LiDAR) of the La Conchita Study Area;
- ***Development of a preliminary geologic map***, based on compilation of existing published and unpublished (consultant's reports) geologic mapping;
- ***Development of preliminary hazard maps***, based on existing published studies that show areas most susceptible to slope-related failure and other major geologic and seismic hazards; including tsunami inundation, strong ground shaking, fault rupture, and liquefaction;
- ***Identification of gaps in the available existing data*** relevant to the evaluation of geologic conditions and/or hazards;
- ***Preparation of a field investigation plan,*** including a drilling plan for field collection of subsurface geotechnical data using various drilling and geophysical techniques; and
- ***Preparation of a Phase 1 report***, summarizing compiled data (submitted previously as AKA, 2007).

The scope of our Phase 2 activities, conducted to provide more detailed geologic information for conceptual design including new data collected for this study, included the following:

- ***Additional data compilation,*** including review of existing reports, maps, aerial photographs and other information relevant to our evaluation of site geology and hazards;
- ***Development of a comprehensive geologic map***, based on interpretation of aerial photography and field reconnaissance mapping, including detailed mapping of the Red Mountain fault zone;
- ***Development of a groundwater model***, based on interpretation of compiled depth to water records from existing geotechnical borings and water wells;
- ***Limited subsurface investigation,*** including targeted geotechnical drilling consisting of large (24-inch) and small (5-inch) diameter borings. In addition, acquisition of shear wave velocities and

compressional wave velocities via downhole geophysics provides information for the evaluation of local site response to strong ground shaking.

- ***Radiocarbon dating,*** of samples obtained from large-diameter borings provide ages of debris flow deposits and hillslope deposits that constrain the return period of debris flows and timing of larger landslides.
- ***Construction of an inventory of historical slope failures***, including compilation of historical accounts of debris flows and landslides combined with interpretation of time-series of available aerial photography;
- ***Numeric modeling of debris flow run-out and depths***, including calculation of likely debris flow paths and lateral extent downslope;
- ***Evaluation of slope hazards***, including delineation of active and potentially active landslides, debris flow sources, debris flow run-out area, and calculation of likely debris flow volumes and inundation depths for return periods of interest (50, 500, and 1000 years);
- ***Evaluation of seismic hazards***, including examination of the probably return periods and possible associated impacts of earthquake-triggered liquefaction, strong ground shaking, and tsunami inundation;
- ***Preparation of a Phase 2 report***, submitted herein, that presents data collected for this study and summarizes our interpretations and conclusions.

2.1 Tasks and Methods

Below we describe each of the Phase 2 tasks in more detail, including relevant methods and procedures applied in compiling, collecting, and interpreting geologic and geotechnical data for the La Conchita Study Area. The Phase 2 tasks include the activities listed above.

2.1.1 Data Compilation

As part of our Phase 1 investigation, geologic and geotechnical data from previous geotechnical and hydrologic studies of the La Conchita area were compiled within a comprehensive database (AKA, 2007). Datasets compiled included geotechnical borings, water monitoring wells, historical spring locations, and locations of geochemical analyses. Logs for approximately sixty-nine borings, including seven water wells and three dewatering wells, were obtained, located, and evaluated as part of Phase 1 (AKA, 2007). Geotechnical boring logs and water well logs provide lithologic and hydrologic data that are useful for assessing the geotechnical and seismic response properties of geologic map units. Additional geotechnical properties recorded on logs include dry unit weight, moisture content, and depth to groundwater. Limited laboratory data are available for samples collected from smaller diameter wells that provide additional, useful information on unit shear strength.

We also compiled all available surface and groundwater data including locations and records from groundwater monitoring wells, obtained primarily from previous geotechnical studies and from La Conchita Ranch. All completed monitoring wells with measured water levels were compiled in database format with locations entered into the project GIS. First water encountered in geotechnical borings and subsequent water level measurements are included in the project database. We met with Ted Powers and Steven Bachman, consultants to La Conchita Ranch, to obtain basic data including well completion records, water level measurements, and water chemistry results.

Records from Ventura County and other sources, including published newspaper accounts, were compiled and interpreted to reconstruct an inventory of historical slope failures within the La Conchita Study Area.

Originals or copies of forty-nine sets of aerial photographs taken between 1927 and 2007, and obtained from various sources, were interpreted for changes in hillslope morphology and identification of specific slope failures.

2.1.2 Geologic Mapping

Detailed geologic field mapping of the Project Area, conducted to document geologic and hydrologic features (including springs and seeps), provides the baseline data for assessment of landslide and debris flow hazards. Of particular relevance are historic landslide features and potential future slope failures, including areas of over-steepened slopes, unstable debris or slope deposits, and other unique geologic features. Landslides and debris flows were identified based on review of 48 sets of stereo-paired aerial photographs dating back to 1927, including detailed photographs taken before and after 1995 and 2005 landslides by IK Curtis, Pacific Western Aerial Surveys, and Geo-Tech Imagery.

The final digital geologic map produced for this study is built upon merged digital aerial photographic and LiDAR-based terrain maps developed for the La Conchita Study Area as part of Phase I (AKA, 2007). The base map includes one-foot contours derived from the April 2007 LiDAR survey. These contours were interpreted to refine smaller geologic and landslide features previously mapped at a coarser, regional scale. Digital terrain data from the 2007 LiDAR survey were analyzed, along with compiled aerial photography, in order to register and update geologic map units and contacts, as needed.

During Phase 1, as part of the review process, WLA geologists compared the accuracy of mapped lines against high-resolution, geo-referenced topography and digital aerial photography. Geologic boundaries on the geologic map were directly overlain and compared to topographic features on the updated 2007 LiDAR topographic base map. The map boundaries also were compared with cultural and vegetation features identified on the 2006 digital aerial photographic base obtained from Air Photo USA.

Geologic mapping was conducted largely through compilation of existing mapping, supplemented by interpretation of several generations of aerial photographs and highly detailed LiDAR-based topography generated for this project, and field reconnaissance. Based on initial field reconnaissance, terrain data were analyzed along with compiled aerial photography to confirm the presence of identified landforms. This mapping was integrated with the compiled map layers to produce the interpretative map of surficial deposits and slope failures on the LiDAR-derived base map. As part of the mapping, we also reviewed and interpreted historical topographic maps, including evaluation of repeated slope failure and ongoing erosion.

Surficial information was correlated with subsurface data from borings previously drilled for geotechnical investigations to characterize the lithologic and engineering properties. The borehole data provided lithologic and engineering properties for key map units. Lithologic properties provided within compiled boring logs typically included soil color, type and texture; most often from field observation and less often from laboratory mechanical and hydrometer particle size distribution analysis. Engineering properties typically included dry unit weight in pounds per cubic foot (pcf), shear strength data, and relative moisture content.

As part of Phase 2, WLA geologists conducted extensive surface reconnaissance of the La Conchita Study Area between April and December of 2007. Additional field mapping was completed in January and February of 2008. Field reconnaissance included: (1) verification of previous mapping of geologic deposits, bedrock geology, and landslides, (2) examination and documentation of road cuts and canyon

walls for exposures of key geologic and fault contacts, and (3) identification of preferred boring locations and drill rig access for the evaluation of geologic conditions.

2.1.3 Subsurface Investigation

Small and large diameter borings were drilled in order to characterize key geologic relationships and to collect samples for laboratory testing in order to characterize and engineering properties. Borings were drilled to depths sufficient to document subsurface properties and identify potential slide planes. The locations of the borings were approximately determined by hand-held GPS, typically within 9 to 14 feet, supplemented by location on georectified aerial photographs merged with a detailed topographic contour map derived from high-resolution (30-cm spacing) LiDAR. Ground surface elevations at each boring location were approximately determined by interpolation between 1-ft contours on the LiDAR base map. The locations and elevations of the borings should be considered accurate only to the degree implied by the methods used.

The field exploration program consisted of advancing two rotary wash borings, five large-diameter ('bucket' auger) borings, and downhole geophysical measurements. The borings and geophysics were completed between October 10 and October 26, 2007. Boring logs are presented in Appendix C and the geophysical data are presented in report form within Appendix D. The rotary wash drilling subcontractor was C&L Drilling of Los Angeles, California. C&L Drilling used a truck-mounted rotary wash drill rig to advance two borings (WLA-B1 and WLA-B2) to depths of 161 and 151 feet, respectively, between October 23 and October 26, 2007. The small diameter borings were logged by Dr. Ross Hartleb, WLA Senior Geologist. Drill holes were sampled using a two-inch diameter Standard Penetration Test (SPT) split spoon sampler, and a three-inch diameter Shelby tube sampler. Split-spoon samplers were driven using a non-standard 300-pound hammer by means of an 18-inch drop. Groundwater levels could not be obtained from the rotary wash drill holes due to the rig's circulation of water during drilling.

Alluvial, colluvial, and bedrock conditions beneath the La Conchita Study Area also were explored by drilling and down-hole logging large diameter (24-inch diameter) 'bucket auger' borings. The borings were drilled by TriValley Drilling of Ventura, California, under the supervision of drillers James and Ron Hester. Five large diameter borings were completed to depths of 30 to 110 feet between October 9 and 11, 2007.

Each bucket auger boring was logged by Mr. Christopher Hitchcock, WLA Certified Engineering Geologist, after established methods for downhole logging of large-diameter borings (Scullin, 1994). Downhole measurements included use of hand-held shear torvane and pocket penetrometer instruments for assessment of the in-situ strength of materials. In addition, downhole photographs and samples were collected at key downhole localities. Charcoal samples were collected from in place deposits exposed within the borings, including two samples obtained in WLA-BA2 and one in WLA-BA4, and submitted for analyses. Results of these laboratory analyses provide ages of key deposits, provided in Appendix E.

Borehole geophysical measurements were collected in uncased, small-diameter borings WLA-B1 and WLA-B2 and are presented in Appendix D. Geophysical data acquisition was performed on October 23 and 26, 2007 by Mr. Rob Steller of GEOVision. Data analysis was performed by Mr. Steller, and reviewed by Mr. John Diehl of GEOVision. The purpose of these downhole measurements was to acquire shear wave velocities and compressional wave velocities as a function of depth. The testing consisted of lowering of instruments down each of the borings. The OYO Suspension PS Logging System (Suspension System) was used to obtain in-situ horizontal shear (Vs) and compressional (Vp) wave velocity measurements in the two borings at 1.6-foot intervals. Analysis of the acquired data

produced profiles of velocity versus depth for both compressional and horizontally polarized shear waves. Shear wave velocity is useful for the evaluation of local rock or soil conditions for ground motion calculations because it is dependant on basic physical properties of the material, including density, porosity, cementation of sediments and hardness and fracture spacing of rock (Fumal, 1978).

2.1.4 Geologic Characterization

A detailed geologic model was constructed of the Study Area that considers the totality of the relevant available data. Based on the geologic map prepared for this study, detailed geologic cross sections were developed depicting critical relationships warranting engineering analyses of slope stability. The geologic map and associated cross sections are provided in Appendix B. Geologic contacts, including landslide planes were described using available compiled data and downhole observations. Potential debris flow sources, volumes and run-out areas also were assessed.

2.1.5 Geologic and Seismic Hazard Characterization

The regional and local seismic source characteristics necessary for the calculation of site-specific seismic response spectra were developed for the La Conchita Project Area, including compilation of historic seismicity and nearby fault sources. In addition, detailed mapping of the Red Mountain fault completed for this study provides new information on the locations, style of deformation, and likely subsurface orientation of multiple active and inactive fault strands that cross the La Conchita Study Area. Estimates developed of recurrence interval and potential coseismic offsets on the Red Mountain fault provide direct input into seismic stability modeling of the large landslides within the cliff landward of La Conchita.

As part of this study, we prepared a comprehensive evaluation of potential geologic hazards (landslides and debris flows) including likely locations and probability of exceedence for major slope failures. Numerical modeling based on detailed terrain models allows prediction of realistic landslide run-out distances, depths, and travel times for the 2005 slide, and other potential debris flow sources located on the cliff adjacent to La Conchita.

The potential for liquefaction-related ground deformation was evaluated using available existing data. Our scope did not include performing supplemental subsurface investigations (e.g. borings or cone penetration tests) to evaluate liquefaction potential and/or effects. Tsunami recurrence and run-up were incorporated in the evaluation based on published studies.

2.1.6 Reporting

As part of Phase 1, a comprehensive data report was prepared. The Phase 1 report included compiled existing data and maps (AKA, 2007). This report presents final results of Phase 2, including supplemental data presented in Appendices A through E.

3.0 REGIONAL GEOLOGY AND TECTONIC SETTING

The La Conchita Study Area is located within an area of active tectonic uplift. The coastal terrace at La Conchita is bounded by a former sea cliff and plateau underlain by uplifted marine terrace deposits. Examination of marine terraces along approximately 900 miles (1,500 km) of the Pacific Coast documents that the highest rates of uplift and subsidence are associated with the intense fold-thrust tectonics of the western Transverse Ranges, in the Ventura-Santa Barbara County region (Figure 3.1; Orme, 1998).

In the Transverse Ranges, the "Big Bend" in the San Andreas fault system has caused north-south shortening of the crust and lithosphere that is expressed as a series of active thrust faults and folds, including the Red Mountain fault that extends through the La Conchita Study Area (Figure 3.2). Deformation within the Transverse Ranges and Santa Barbara Channel Region involves east-striking, left-lateral strike-slip and reverse oblique-slip faulting as well as west- northwest-striking thrust and reverse faulting. This ongoing tectonic uplift has not only shaped the La Conchita area but is a major factor in potential hazards.

3.1 Regional Faults

Investigators have identified a number of east-striking thrust and reverse faults in Santa Barbara Channel that are interpreted to be active and accommodate regional north-northeast to south-southwest shortening (e.g., Namson and Davis, 1992; Shaw and Suppe, 1994; Huftile and Yeats, 1995; Seeber and Sorlien, 2000; Sorlien and others, 2000, 2006). Major active faults near La Conchita that are incorporated in the 2003 U.S. Geological Survey/California Geological Survey (USGS/CGS) seismic source model include the Red Mountain fault, Channel Islands thrust, Oak Ridge fault, the Oak Ridge "Mid-Channel structure", and the Ventura-Pitas Point thrust fault (Figure 3.2; Cao and others, 2003). Other active faults within about 100 km of La Conchita incorporated in the USGS/CGS model include the Santa Cruz Island and Anacapa-Dume faults in the offshore region to the south, and the Ventura-Pitas Point, Red Mountain, Mission Ridge-Arroyo Parida-Santa Ana, Santa Ynez, and Oak Ridge faults to the north and east. Full fault parameters are provided in Appendix A, Table A.1.

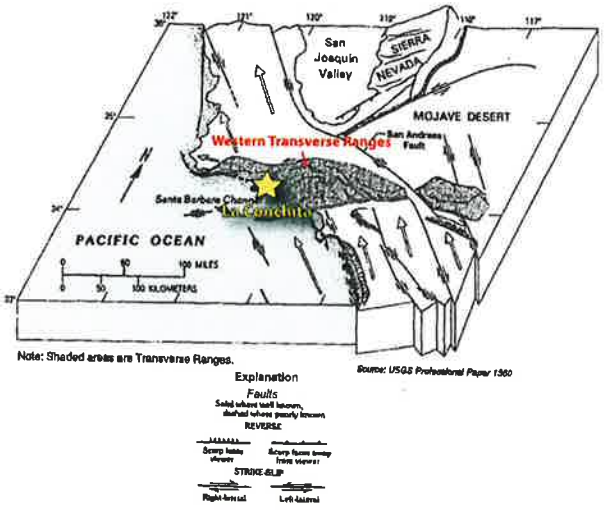

Figure 3.1. Regional tectonic diagram showing the western Transverse Ranges, including major faults and plate motions.

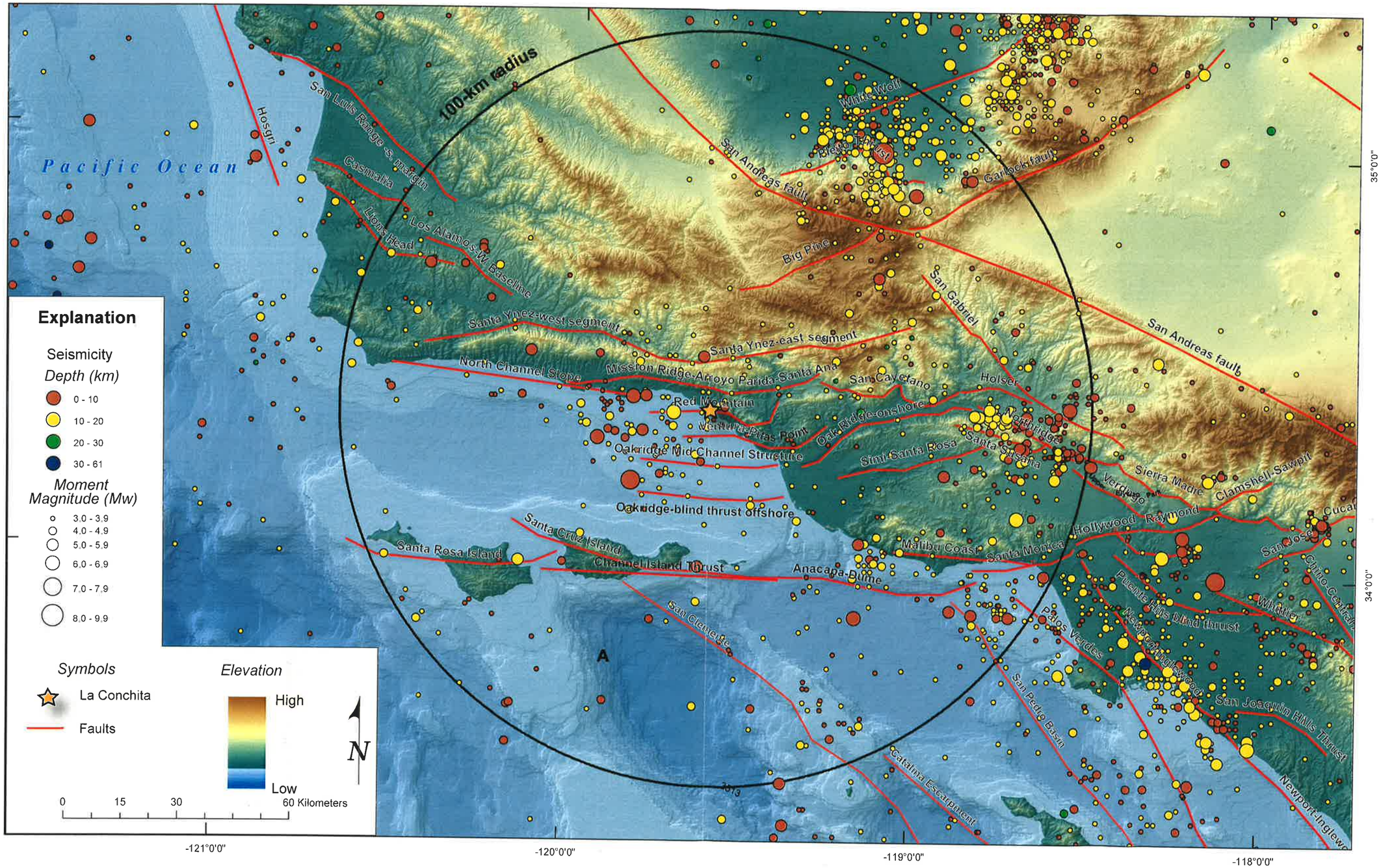

Historical seismicity within vicinity of La Conchita Study Area

Table 3.1 Known Active and Potentially Active Faults within 62 mile (100 km) Radius.

Fault	Activity	Slip-Rate (mm/yr)	Potential Rupture Length (km)	Probable Magnitudes (Mw)
Red Mountain Fault	Holocene	2	100	7.1
Oak Ridge Fault	Holocene	3	90	6.9
Ventura-Pitas Point Fault	Holocene	1	20	6.8
Santa Cruz Island Fault	Holocene	1	60	6.8
Simi Fault (Camarillo and Springville Faults	Holocene	1	40	6.7
Santa Susanna Fault	Late Quaternary	5	38	6.6
San Gabriel Fault	Late Quaternary	1	140	7.0
San Fernando Fault	Holocene	2	17	6.7
Sierra Madre Fault	Holocene	2	55	7
San Andreas Fault	Holocene	20-35	550	6.8-8.0
Verdugo Fault	Holocene	0.5	21	6.7
Santa Ynez Fault	Late Quaternary - Holocene	2	130	7
Holser Fault	Late Quaternary	0.4	20	6.5
San Cayetano Fault	Quaternary	6	45	6.8

Faults are summarized based on data from Wills and others, 2008, and Cao and others, 2003. See Appendix A for complete list.

Nearby faults include the Red Mountain and Padre Juan faults that bound the Rincon Anticline, and locally offset the uplifted Punta Gorda marine terrace. This older terrace (between 40,000 to 60,000 years old, herein referred to as 45,000 years old) is associated with the plateau that underlies La Conchita Ranch (Lajoie and others, 1982; Harden and others, 1986; Huftile and others, 1997). Locally, the uplifted terrace and folded bedrock has been eroded and dissected by deep canyons, including the West and East Barrancas that mark the boundaries of the La Conchita Study Area.

3.2 Historical Seismicity

The rugged and youthful topography of the Transverse Ranges is the physiographic expression of active crustal shortening. Both land-based and satellite geodesy document approximately 6 to 10 mm/yr of north-northeast to south-southwest shortening between Santa Cruz Island and the City of Santa Barbara (Larson and Webb, 1992; Larsen and others, 1993). This shortening rate is consistent with the moderate level of seismicity observed in the Santa Barbara Channel.

In 1812, an earthquake of about magnitude M7 occurred, probably in the Santa Barbara Channel (Ellsworth, 1990). The 1812 earthquake was widely felt in southern California and severely damaged Mission San Buenaventura in Ventura (Hamilton and others, 1969). The 1812 earthquake also is associated with a damaging tsunami along the coastline (Townley, 1939).

Other historical offshore earthquakes include ~M5 to M6 events in 1925 (M6.8), 1941 (M5.9), 1973 (M5.3), and 1978 (M6.0) (Table 3.2; Bailey, 1925; Townley, 1939). A large earthquake (M6.3) occurred offshore of Santa Barbara at 6:44 am on June 28, 1925 (Kirkbride, 1927). Significant structural damage

occurred within Santa Barbara. Following the earthquake, small landslides were removed along the railroad tracks between Santa Barbara and Ventura. Another moderate earthquake (M5.9), centered approximately eight miles from La Conchita, shook the Santa Barbara-Ventura coastal area at 11:53 pm on June 30, 1941 (Table 3.2). Occurring shortly before midnight, the quake appeared to be centered between Ventura and Santa Barbara, causing damage in both cities, and a landslide that blocked the coastal highway near the Ventura County line, north of La Conchita (The Oxnard Press-Courier, Vol. 34, no. 1, Jul. 1, 1941). In 1973, an earthquake offshore of Point Mugu (M5.3) caused widespread damage in the Oxnard area, including some structural damage to buildings (Lander, 1973).

On August 13, 1978, a M6.0 earthquake occurred in northeastern Santa Barbara Channel about 13 miles (20 kilometers) northwest of La Conchita (Corbett and Johnson, 1982). The earthquake focal mechanism suggests that rupture occurred on a west-northwest striking thrust or reverse fault, located sub-parallel to regional structural and topographic trends and normal to the geodetically determined direction of active crustal shortening. Based on the distribution of aftershocks, Corbett and Johnson (1982) interpreted that the earthquake likely occurred on a gently north-northeast-dipping thrust fault at a depth of about 8 miles (13 km). They noted that the up-dip projection of this shallow fault plane would intersect the earth's surface near Santa Cruz Island, implying that the entire eastern Santa Barbara Channel is underlain by a north-dipping thrust fault. However, Yeats and Olson (1984) argued that an alternative model, also feasible based on the focal mechanism, of a steeply south-dipping reverse fault was possible and more consistent with styles of faulting inferred from analysis of subsurface data from oil exploration and production.

On-shore faults in the vicinity of La Conchita and more distant faults within southern California also have produced several large historical earthquakes (Table 3.2; Weber and Kiessling, 1975; Toppozada and others, 2000). In 1857, the great Fort Tejon earthquake (about M8) ruptured about 200 miles of the San Andreas Fault, from Cholame to Wrightwood, and also severely damaged Mission San Buenaventura. The 1933 M6.4 Long Beach earthquake caused minor damage in the Ventura area. The 1994 M6.7 Northridge earthquake caused widespread minor damage in Ventura County (Barrows and others, 1995).

Table 3.2 Recorded Earthquakes >5.0 Magnitude within 62 miles (100 km) of La Conchita Study Area and Large (>6.0 Magnitude) Earthquakes within ~100 miles (161 km), 1800 to 2008. See Table A.2 in Appendix A for full record of historical earthquakes within 100 km.

Date	Estimated Magnitude (Mw)	Earthquake Name and/or Fault Name	Distance from La Conchita Study Area in miles (km)
12/08/1812	7.5	San Andreas Fault	86 (139)
12/21/1812	7.1	Santa Barbara Channel	18 (30)
01/09/1857	7.9	Ft. Tejon/San Andreas Fault	51 (82)
06/29/1925	6.8	Santa Barbara Channel	21 (33)
03/11/1933	6.4	Newport-Inglewood Fault	103 (166)
07/01/1941	5.9	Ventura-Pitas Point Fault	8 (12)
07/21/1952	7.3	Kern County Quake, White Wolf Fault	51 (82)
02/09/1971	6.6	Sylmar Quake, San Fernando Fault	58 (93)
02/21/1973	5.3	Anacapa/Dume Fault	31 (50)
08/13/1978	6.0	Santa Barbara	13 (20)
01/17/1994	6.7	Northridge Quake and Fault	52 (83)

Earthquake data are from Toppozada and others, 2000.

3.3 Seismic Source Model

Probabilistic Seismic Hazard Analysis (PSHA) has become standard practice in the evaluation and mitigation of seismic hazards to structures, infrastructure and lifelines. The PSHA methodology can condense the alternative interpretations of seismic source parameters, variability of seismic activity for various earthquake sources, and parameter uncertainties into a manageable data set. The seismotectonic setting of the southern coastal California region was evaluated in order to provide a seismic source model for input to the PSHA. As described above, the plate boundary is defined by: (a) the northwest-striking, right-lateral strike-slip faults of the San Andreas System; (b) the east-striking, left-lateral reverse-oblique faults that bound the northern and southern margins of the Western Transverse Ranges (WTR); and (c) the east-striking, north-dipping thrust faults within the WTR and Santa Barbara Channel. Additional tectonic features that may contribute to the seismic hazard include relatively minor faults within tectonic provinces that are bound by major active faults. Examples include the WTR, Inner Continental Borderland, Penninsular Ranges, and Southern Coast Ranges.

Appendix A includes major fault sources, including parameters for fault (line) sources and areal source zones. The fault parameters used in this study are derived from the seismic source model compiled by Cao and others (2003). Line sources represent specific active faults located in southern California for which data are sufficient to estimate maximum earthquake magnitude distribution and recurrence parameters. Areal source zones include regions of the shallow crust (i.e. <16 km depth) that are inferred

to have uniform style of faulting, earthquake magnitude, and recurrence characteristics, but for which sufficient data are not available to model specific faults.

4.0 SITE GEOLOGY

The community of La Conchita is located on a broad coastal plain bounded on the south by the Pacific Ocean and underlain by alluvial, debris flow, and landslide deposits that have accumulated along the base of a steep coastal cliff (Figure B-1, Appendix B). These young, predominately silty alluvial and debris fan deposits are up to 70 feet thick. The fan deposits cover a buried marine terrace, consisting of thin (four to ten feet thick) marine sand and beach cobbles deposited on an abrasion platform cut on siltstone of the underlying Pico Formation. This marine terrace is between 2,500 and 4,500 years old (Harden and others, 1986), and dips gradually toward the ocean.

The cliff adjacent to, and landward of, La Conchita is composed of relatively weak mudstone, siltstone, and sandstone of the Pico Formation, Sisquoc Shale, and Monterey Formations. The bedrock formations are separated by strands of the Red Mountain fault (CGS, 2003). Bedrock locally is obscured by slope wash and thick landslide deposits. These landslides include three relatively large, older block-type landslides that merge to form a landslide complex consisting of most of the cliff above La Conchita. Smaller active and potentially active slump-type landslides are mapped locally within the base of the cliff. Inset into the older landslide, these deposits typically are associated with localized vegetation and springs.

The cliff is bounded on the west (upcoast) and east (downcoast) by two major canyons, West and East Barrancas, that flow seaward and channel surface water from within a large coastal drainage area located landward of the Study Area. These canyons are v-shaped with steep walls mantled with shallow landslides and slope wash deposits. The floors of both West and East Barranca contain young, loose deposits of varying thickness that commonly are mobilized seaward as debris and flood material during large flood events triggered during major storms.

The plateau at the top of the cliff is covered by avocado and citrus orchards of La Conchita Ranch and is underlain by a thick (30 to 60 feet) mantle of older marine terrace deposits and associated paralic (non-marine) debris fan deposits overlying subvertical bedding of the Monterey Formation. The plateau underlying La Conchita Ranch is associated with the formation of the Punta Gorda marine terrace, and overlain by related paralic deposits. Marine terrace deposits of the 45,000-year-old Punta Gorda terrace consist of poorly consolidated clayey sand and gravel (Lajoie and others, 1982; Harden and others, 1986; Huftile and others, 1997). However, the Punta Gorda terrace deposits do not outcrop within the cliff face directly inland of La Conchita. Punta Gorda terrace deposits are partially exposed beneath Pleistocene debris deposits within the Eastern Barranca adjacent to the ranch and within Little "V" canyon located adjacent to Ocean View Road, west of the Western Barranca.

The distribution of the Punta Gorda terrace is in large part controlled by the location of active and inactive strands of the Red Mountain fault that extends across the plateau beneath La Conchita Ranch and the cliff face landward of the community of La Conchita. The location of the fault, and deposits offset across it, is obscured by landsliding and slope debris.

4.1 Previous Geologic Mapping

First mapped in part by Darton (1915), the geology of the La Conchita Study Area has been more recently mapped at 1:24,000-scale by Dibblee (1988) and CGS (2003). Portions of the Study Area also were mapped in detail by Leighton Consultants (1993) and Stoney Miller Consultants (1996; 1998). A digital copy of the most recent geologic map of the Pitas Point quadrangle was obtained from CGS for this study (Carlos Gutierrez of CGS, pers. Comm., 2007). The Arc export files were converted into ArcGIS shape

files; merged into discrete GIS map layers containing mapped geologic units, geologic contacts, and fault traces; and reprojected for direct comparison with the detailed LiDAR-derived topographic base map.

4.2 Geologic History

Deposits of the Punta Gorda marine terrace and related terrestrial (paralic) deposits form the broad plateau under La Conchita Ranch. Marine terrace deposits correlated to the Punta Gorda terrace were dated at roughly 45,000 years old by Lajoie and others (1979, 1982), based on amino acid analysis of marine shells found at the base of the terrace. The approximate age of the Punta Gorda terrace was corroborated by Harden and others (1986) based on detailed study of soil profiles and by Trecker and others (1998) based on oxygen isotope tests on fossil marine shells within exposed terrace deposits.

The Punta Gorda marine terrace formed as the Pacific Ocean cut a platform on bedrock of the Monterey, Sisquoc, and Pico Formations with resistant bedrock preserved in the areas immediately inland of La Conchita (see Figure 4.1A). During and following terrace deposition between 40,000 to 4,500 years ago (see Figure 4.1B), broad fans built out onto the terrace resulted in deposition of land-based debris and alluvial deposits (paralic deposits). Locally, the marine deposits composed of sand and beach pebbles are overlain by coarse terrestrial (paralic) deposits consisting of angular gravels. The upper portion of the paralic deposits capping the marine terrace deposits of the Punta Gorda terrace is distinguished by a five to ten feet thick silt layer with abundant clay. This laterally extensive layer is encountered in borings and exposed in outcrops throughout the Plateau area. It is interpreted to be a Pleistocene soil horizon ('paleosol') and may represent a period of relative stability for the landscape created following deposition of the Punta Gorda terrace.

After formation of the Punta Gorda terrace, the active Red Mountain fault locally offset and uplifted portions of the terrace and underlying wave-cut bedrock platform. The terrace formed at about 38 m (125 feet) below present-day sea level, during lower global ocean levels (Huftile and others, 1997). Ongoing regional uplift of at least 4 mm/yr has raised the terrace, and underlying wave-cut platform (Figures 4.1B and 4.1C). The wave-cut platform that underlies the base of the terrace within the footwall of the Red Mountain fault currently is at 400 to 555 feet above sea level.

Localized uplift and accompanying erosion prevented deposition of, or locally removed, the terrace deposits above the current cliff landward of La Conchita. At this location the Red Mountain fault splits into two distinct stands, producing a pronounced scarp and low hill within the plateau landward of the top of the cliff (Figure 4.1C). Mapped as the Red Mountain fault by Dibblee (1988), we initially mapped this seaward-facing feature as a potential older landslide scarp (map unit Qlso1) as part of our Phase 1 report (AKA, 2007). However, more detailed mapping conducted as part of Phase 2 documented the linear nature of the scarp and coincidence with surficial and subsurface fault-related features, including offset stratigraphy across the inferred fault strand. Map unit Qlso1 is no longer shown on the geologic map, or discussed in the text, but we have retained the associated numbering of landslide features and deposits to maintain consistency with the Phase 1 report (AKA, 2007).

The thick silt layer of the 'paleosol' at the top of the Punta Gorda terrace and associated paralic deposits is overlain by a mixture of colluvial, talus, and landslide debris. These deposits are differentiated from the underlying terrace-related marine and paralic deposits by the presence of angular clasts of the Monterey Formation and the poorly consolidated nature of the debris deposits. This debris likely was deposited by large flows that extended outward from the ridge crests towards the ocean (Figure 4.1B). Based on relative thicknesses of the debris, the flows likely were diverted by ravines and low-lying hills,

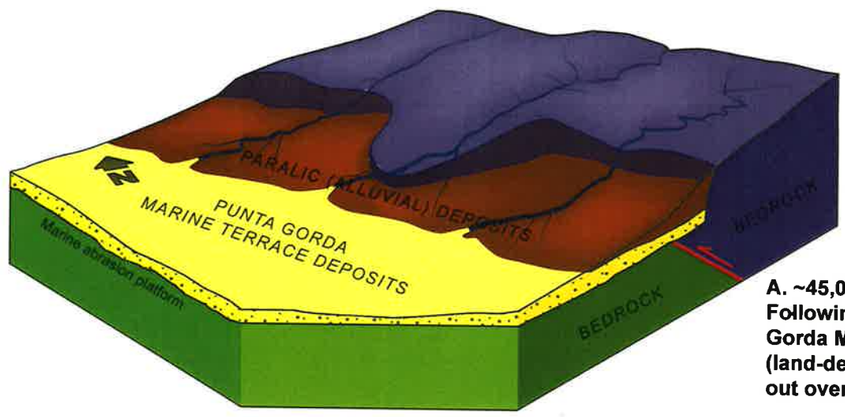

A. ~45,000 to ~40,000 YEARS AGO
Following deposition of the Punta Gorda Marine Terrace, Paralic (land-derived) deposits prograde out over marine deposits

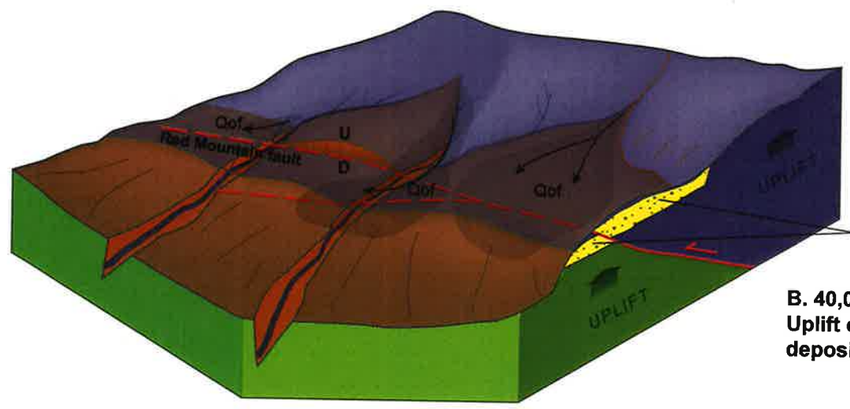

B. 40,000 to 4,500 YEARS AGO
Uplift of Punta Gorda Terrace and deposition of older debris Ffans (Qof)

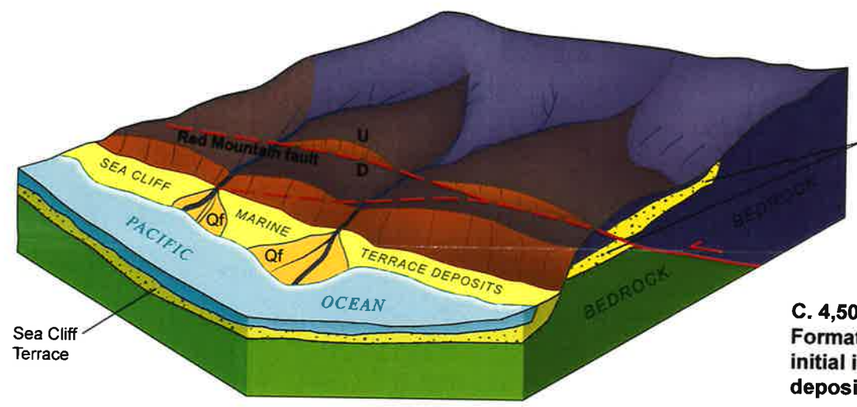

C. 4,500 to 2,500 YEARS AGO
Formation of the Sea Cliff Marine Terrace, initial incision of Barrancas and deposition of debris fans (Qf)

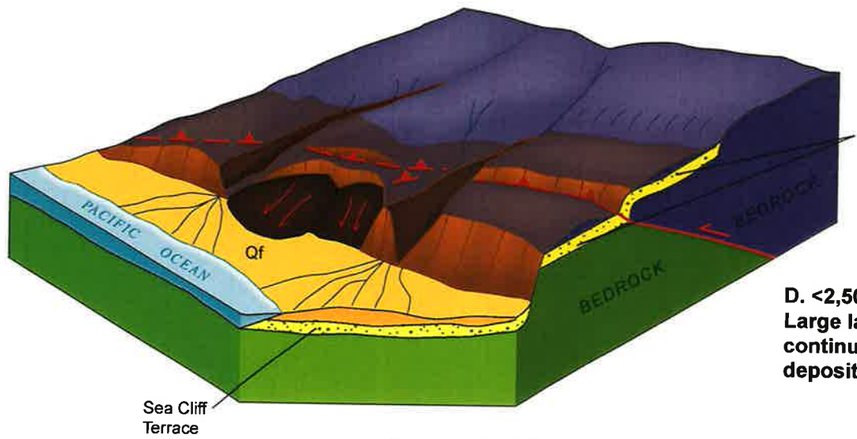

D. <2,500 to 100 YEARS AGO
Large landslides in cliff, continued incision of Barrancas and depositions of debris fans (Qf)

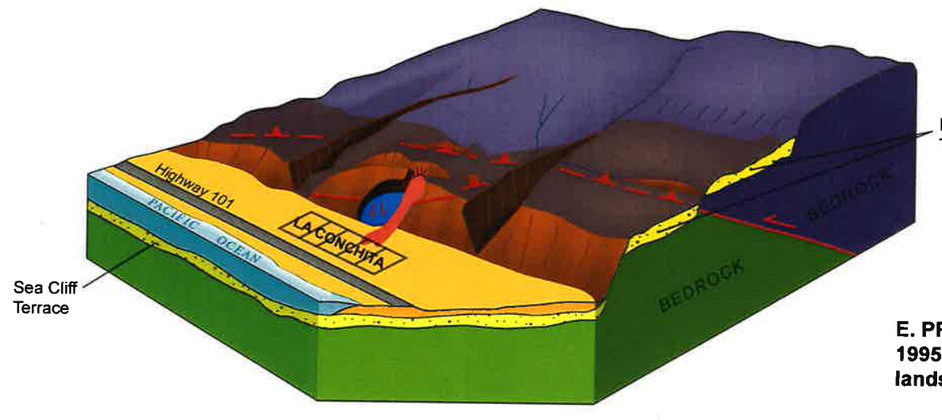

E. PRESENT DAY
1995 (blue) and 2005 (pink) landslides

including features associated with localized uplift along the Red Mountain fault, including the low-lying hill on the plateau above the sea cliff area. In particular, the debris was diverted to the downcoast side of the sea cliff above La Conchita, forming a thick package of material several hundred feet thick beneath the La Conchita Ranch office and extending to the area of the 1995/2005 slides.

Sea-level rise resulted in the development of a wave-cut platform, development of the Sea Cliff marine terrace about 4,500 to 2,500 years ago (Figure 4.1C; Harden and others, 1986), and a likely near-vertical sea cliff. Formation and incision of the barrancas likely occurred during this time as the stream levels equilibrated to the new base level elevation, resulting in accelerated downcutting of the East and West Barrancas.

Following creation of the Sea Cliff marine terrace, large landslides formed in the sea cliff area, likely as a result of undercutting of the slope and erosion of the sea cliff (Figure 4.1D). The landslide deposits are underlain by, and are younger than, the marine terrace deposits. The terrace deposits, and associated paralic deposits, have been covered by a sequence of up to 70 feet of alluvial and debris flow deposits, including deposits from debris flows into the community of La Conchita in the late 1930s. Debris flow fans from uphill sources have built broad, convex mounds out onto the coastal plain since formation of the underlying terrace. More recently, large slope failures in 1995 and 2005 contributed more sediment to these fans and damaged numerous houses within La Conchita (Figure 4.1E)

4.3 Geologic Map Units (This Study)

We prepared an updated geologic map, and accompanying geologic cross sections, of the Study Area that integrate: (1) previous published geologic mapping and subsurface data compiled as part of Phase 1 (AKA, 2007); (2) interpretation of LiDAR-based topography; (3) limited geotechnical borings completed for this study; and, (4) new detailed field mapping. The geologic map and cross sections are presented in Appendix B.

The 1:2,400-scale Geologic Map presented in Appendix B depicts bedrock units, faults, small landslides, debris flow deposits, and deep-seated landslide deposits of the Study Area. We identify fifteen Quaternary map units in the Study Area, in addition to bedrock of the Pliocene Pico Formation (map unit Tp), Pliocene-Miocene Sisquoc Shale (Tsq), and Miocene Monterey Formation (map unit Tm). Quaternary geologic mapping units identified during this investigation are generally younger than 60,000 years, although absolute dates are not available for mapped deposits within the La Conchita Study Area. Ages are estimated based on comparison with similar dated deposits elsewhere in Ventura County. Geologic unit descriptions, lithology, and estimated thicknesses are compiled from previous mapping augmented by limited field inspection of surface exposures and review of compiled subsurface borings and the engineering properties. Full descriptions for each unit are provided in Appendix B.

4.3.1 Principal Bedrock Units

Three principal in-place bedrock units exist within the La Conchita Study Area; all generally consisting of sedimentary rock that was deposited in a marine environment. The following rock descriptions and age estimates are based on mapping by CGS (2003). The oldest of the bedrock units, the Monterey Formation, was deposited about 23.2 to 5.2 million years ago during the Miocene age. The Sisquoc Shale was deposited in the Tertiary Period, and the Pico Formation, was deposited in the late Tertiary and early Quaternary, about 2.5 to 1 million years ago. Brief descriptions of these units (from oldest to youngest) follow.

Monterey Formation (unit symbol Tm) - The Miocene Monterey Formation consists siliceous and diatomaceous shale with some sandstone and limestone and is considered generally susceptible to landsliding. The Monterey Formation is mapped beneath much of the plateau beneath La Conchita Ranch and is exposed within the walls of West and East Barrancas.

Sisquoc Formation (unit symbol Tsq) – The Piocene-Miocene Sisquoc Formation consists of interbedded silty shale and claystone, with layers of tuffaceous sandstone, and is considered generally susceptible to landsliding.

Pico Formation-undivided (unit symbol Tp) – The Plio-Pleistocene Pico Formation consists of massive gray mudstone that includes light gray sandstone and conglomerate with pebbles of hard sandstone and white siliceous shale. Rock of the Pico Formation is very weakly cemented and is considered generally susceptible to landsliding (Parise and Jibson, 2000; Jibson, 2005).

Within the Study Area, the principal bedrock units are covered or obscured by younger alluvial, colluvial, and landslide deposits (Figure B-1; Appendix B). Where exposed within the West and East Barrancas, the marine Monterey Formation consists of thin-bedded siltstone and sandstone with interbeds of soft, fissile clay shale to hard siliceous shale (Dibblee, 1988; CGS, 2003). Late Miocene marine Sisquoc Shale (Tsq) is exposed upcoast (north) of La Conchita, seaward of the Red Mountain fault. Although overlying the Monterey Formation, locally the Sisquoc Shale is exposed as steeply south-dipping to overturned beds faulted against the Monterey Formation by the Red Mountain fault. The formation consists of light-gray, silty shale that is locally slightly siliceous and diatomaceous, with layers of tuffaceous sandstone (CGS, 2003). The Sisquoc Shale is not exposed in the cliff directly above (landward of) La Conchita but is exposed in the canyon walls of West Barranca. The Sisquoc Shale is inferred to be present within the upper cliff area as a tapering structural wedge bounded by strands of the Red Mountain fault. The Pico Formation (Tp) is marine, early Pleistocene to possibly late Pliocene age, and, where exposed in the Study Area, consists of massive gray mudstone that includes light gray sandstone and conglomerate with pebbles of hard sandstone and white siliceous shale (Dibblee, 1988).

4.3.2 Principal Alluvial and Colluvial Units

All of the alluvial and colluvial units within the La Conchita Study Area were deposited during the Quaternary Period (within the past 1.8 million years). Late Pleistocene-age deposits (symbol includes a lower case letter "p") are the oldest and were deposited between 11,000 and 300,000 years ago. Holocene-age deposits were deposited during the past 11,000 years (symbol may include a lower case letter "h"). Brief descriptions of these units (from youngest to oldest) follow.

Pleistocene Punta Gorda marine terrace (unit symbol Qppr-p) – The Punta Gorda marine terrace consists predominantly of clayey sand with lenses of rounded gravels and cobbles. These materials were deposited in a near-shore environment and are locally preserved on uplifted wave-cut bedrock platforms. Overlying paralic (terrestrial or land-derived) deposits, consisting primarily of semi-consolidated, poorly-sorted gravels, likely covered the marine terrace deposits shortly after formation and are believed to be roughly the same age (CGS, 2003).

Pleistocene Debris Deposits (unit symbol Qpmw)- Pleistocene debris flow deposits found locally include abundant angular fragments of Monterey Formation rocks within a poorly-sorted matrix of silt. These deposits have been transported downslope from higher inland areas and are also found on uplifted wave-cut platforms. The lower case "mw" within the unit symbol refers to "mass wasting", a general term that includes debris flows.

Holocene Marine Terrace Deposits (unit symbol Qhmt) - Holocene marine terrace deposits found locally consist predominantly of loose sand with rounded cobbles. These materials were overlie lower wave-cut platforms below the base of the modern cliffs, beneath the coastal plain and the community of La Conchita.

Holocene Alluvial Fan and Paralic Deposits (unit symbol Qf) - Holocene alluvial and debris fan deposits found locally generally consist of stratified layers of gravel, sand, silt and clay. This sediment primarily was deposited onto the coastal plain by streams and debris flows emanating from the barrancas and smaller drainages.

Holocene though Historic Debris Deposits (unit symbol Qdf) - Holocene debris fan deposits generally consist of sand, silt and clay deposited near base of modern cliffs. These deposits are differentiated from unit Qf based on relative geomorphic expression and review of archival aerial photographs and maps.

Holocene through Historic Stream Wash Deposits (unit symbol Qw) – Holocene through historic stream wash deposits identified within flat-floored active stream channels and arroyos, including the East and West Barrancas. Deposits generally are coarse grained, consisting of poorly-sorted sand, silty sands and clayey sands, often with gravel and in the upland drainages, boulders.

Holocene through Historic Beach Deposits (unit symbol Qb) – Holocene through historic beach sand deposits consisting of loose to dense, fine to coarse sand. This unit includes active beaches.

Artificial Fill (unit symbol af) - Man-made fills of historical age and variable composition constructed by humans include both engineered and non-engineered material (map unit af). Artificial fill is mapped based on comparison of historical topographic maps and photographs with modern conditions.

The ages of terrestrial deposits (paralic deposits), consisting primarily of debris and alluvial fan deposits (unit Qppr-p), associated with deposition of the Punta Gorda marine terrace are not well constrained. If sedimentation processes are similar on the Punta Gorda and Sea Cliff marine terraces, the terrestrial deposits probably postdate platform cutting by at least 3,000 years (Harden and others, 1986). If sedimentation was continuous since formation of the bedrock platform, or if sedimentation rates were relatively low in comparison with those on the Sea Cliff marine terrace, the paralic deposits and surface of the Punta Gorda terrace could be significantly younger than the underlying bedrock platform. Fluctuation of the clay content of the sediment with depth indicates cycles of clay and silt deposition and, possibly, pulses of sedimentation. Although soil developed on the Punta Gorda marine terrace has been estimated to have an age of 45,000 years, the actual terrace surface could be as young as 35,000 years old (Harden and others, 1986).

In addition, the upper portion of the Punta Gorda marine deposits and paralic deposits are associated with a thick, clay-rich layer. This dark-brown layer is laterally extensive and overlain by poorly sorted, sub-angular gravel containing fragments of Monterey Formation siltstone and sandstone. The clay-rich layer appears to be the upper surface, and possibly associated soil horizon, formed on paralic deposits of the Punta Gorda terrace. Locally, this horizon is developed directly on underlying bedrock with the marine terrace deposits missing. It may represent a relatively stable land surface that has been partially to fully covered by debris flow deposits (unit Qpmw) or a basal, laterally extensive debris flow deposit.

Undifferentiated Holocene alluvial fan and paralic (land-derived) deposits (unit Qf) are present on broad areas of the coastal plain. Borehole data from within the community of La Conchita suggests that the alluvial fan and other paralic deposits overlie a five- to ten-foot thick layer of Holocene marine terrace deposits that sit directly atop a wave-cut platform on bedrock of the Pico Formation. These deposits locally are overlain by younger deposits, including active and potentially active landslides (Qlsa, Qlsu, and Qlsu?) and debris flow deposits (Qdf) present along the base of the cliff. The recency of deposition is based on young geomorphic features interpreted from aerial photographs and historic accounts of flooding or other active processes. Historical deposits mapped within the La Conchita Study Area include active stream wash deposits (map unit Qw), beach sand (map unit Qb), and active landslides (map unit Qlsa). Active wash deposits are identified within channels of the East and West Barrancas, and other smaller canyons and gullies.

4.3.3 Principal Landslide and Debris Flow Units

Slope failure deposits include: (1) shallow debris or earth flows, which typically contain recent slope wash deposits; (2) shallow slumps and translational slides, which typically contain slope deposits and weathered bedrock; and, (3) underlying, deep rotational and translational landslides that typically involve underlying bedrock of the Monterey, Sisqouc, and Pico Formations. Brief descriptions of these units (from oldest to youngest) follow.

> ***Deep rotational and translational landslides*** – Large landslides (map units Qlso2 through Qlso4) are present within the cliff behind La Conchita. The scarp associated with map unit Qlso1, shown in our Phase 1 report, has been reinterpreted as a fault scarp of the Red Mountain fault. The older (possibly Holocene or Pleistocene) slides (map unit Qlso2, Qlso3, and Qlso4) are distinguished by internal hummocky terrain and well-defined headscarps, including down-dropped portions of the upper wave-cut plateau surface.
>
> ***Shallow slumps and landslides*** - Shallow translational and rotational slides and slumps typically are located in canyon (barranca) walls and near the base of slopes, including the toes of older landslides. Active landslides (map unit Qlsa) are slide masses that are associated with clearly defined landslide features, unique vegetation and springs associated with local groundwater flow, and/or have evidence of movement based on analysis of available historical aerial photographs and topographic maps.
>
> ***Shallow debris flows*** – Debris flow source deposits and debris flow fan deposits are mapped as a single map unit (unit Qdf). The accumulated debris flow deposits, intermingled with and built on larger alluvial fan and debris flow deposits from the East and West Barrancas, record late Holocene mass wasting of the cliff front due to ongoing erosion and slope failure.

We have delineated two main, large landslide complexes in the cliff directly above (landward of) La Conchita. We refer to the complexes and associated landslides by their location along the coast. The upcoast landslide (unit Qlso4) consists of a single large landslide located upslope of much of the community of La Conchita. This landslide is located upcoast of the intersection of Vista Del Rincon with San Fernando Avenue and is crossed by lower Ranch Road. The landslide predominately is composed of bedrock of the Pico and Sisquoc formations.

The downcoast landslide complex consists of two large nested landslides (units Qlso2 and Qlso3) that intersect, and apparently offset, the upcoast slide in the area of the 1995 and 2005 landslides. The larger

landslide (Qlso2) extends landward and downcoast of the intersection of Vista Del Rincon and Zelzah Avenue and is crossed by upper Ranch Road. Qlso3 is inset into Qlso2 and located downslope of Ranch Road.

Active landslides (unit Qlsa) are defined as slope failures with evidence for historical movement or recent movement, defined as occurring within the past 300 years. These typically small slides generally are well expressed within the terrain with developed headscarps and locally are associated with springs and vegetation consistent with shallow groundwater. Landslides with less prominent surface expression include older, yet potentially active landslides (unit Qlsu). Features potentially related to slope failure (Qlsu?) are mapped as possible landslides pending additional study. During or following heavy rainfall, active or potentially active slides may fail. Failure locally may result in movement of the base of the hillslope outward onto the La Conchita plain or within canyon floors.

Deposition of multiple debris flows at the foot of the cliff and the mouths of West and East Barrancas has resulted in the formation of fan-shaped mounds that underlie much of the coastal plain including La Conchita. Debris flows (unit Qdf) typically occur where slope wash deposits (colluvium) collect in topographic swales or hollows. During heavy rainfall, this stored material becomes saturated and may flow rapidly down incised channels. Poorly sorted debris within a debris flow may be deposited at the base of the hill, where the slope angle decreases, or at the mouth of the transport. The primary potential hazard posed by debris flows is the movement of the saturated soil, and associated burial and/or displacement of structures within the flow path of the debris.

Debris flows consist of an uphill source area, typically consisting of hollows filled with loose slope wash. The source area is connected to an area of deposition, typically at the coastal plain along the base of the hillside, by incised gullies that serve as paths for downhill movement of the collected debris. Deposition of multiple debris flows at the foot of the cliff, including at the mouth of gullies, has resulted in the formation of fan-shaped mounds that underlie much of the coastal plain including La Conchita (Geologic Map; Appendix B).

4.4 Geotechnical Properties of Map Units

As part of the overall evaluation of landslide hazards for this project, AKA is evaluating the stability of landslide deposits under earthquake conditions. Towards this goal, geologic map units have been initially ranked and grouped on the basis of their shear strength. This initial grouping is based on general, regional classification of geologic materials by CGS (2002) as part of seismic hazard zoning for the Pitas Point quadrangle. To evaluate the stability of geologic materials under earthquake conditions, CGS ranked and grouped geologic map units in the La Conchita vicinity on the basis of their shear strength (CGS, 2002). The primary source for shear-strength measurements was geotechnical reports prepared by consultants on file with local government permitting departments, obtained from the County of Ventura Public Works Agency. Thirty-one shear tests were conducted on seventeen borehole or trench samples within the Pitas Point 7.5-minute quadrangle, which includes the La Conchita Study Area. Shear test data from adjoining quadrangles, primarily the Ventura Quadrangle, were used to augment the data for several geologic formations for which little or no information was available. We have incorporated the regional CGS dataset with laboratory data from local geotechnical studies completed in the La Conchita Study Area. Laboratory testing of samples from the toe of the 1995 landslide indicates that the landslide debris has dry densities ranging from 76 to 100 pounds per cubic foot (pcf) with moisture contents between 20 and 24 percent, strength parameters of 250 pcf cohesion, with an internal friction angle of 34 degrees. Laboratory testing of samples from debris flow and fan deposits at the base of the cliff within La Conchita, in the vicinity of the 1995 landslide, indicates that the debris has dry densities ranging from 75

to 94 pcf with moisture contents between 18 and 35 percent, strength parameters of 250 pcf cohesion, with an internal friction angle of 27 to 34 degrees. The properties of the alluvial and debris derived from the landslide deposits appear similar to the source deposits.

Table 4.1 Preliminary classification of geotechnical strength parameters of major geologic map units.

Map Unit	Friction Angle (phi in degrees)	Dry Density (pcf)	Cohesion (pcf)
Monterey Formation (Tm)	35 (CGS)	-	-
Pico Fm (Tp)	22 (CGS)	-	-
Quaternary Deposits, Qa, af, Qdf	30 (CGS)	75 to 100	250
Landslide, Qlsa, Qlso	9 (CGS), 20 to 34 from geotechnical studies.	76 to 100	250

4.4.1 Shear Wave Velocities

Downhole measurement of shear wave velocity, conducted to depths of over 100 feet in borings WLA-B1 and WLA-B2 by GeoVision for this study, provided geophysical parameters for evaluation of the site response of the landslide masses during strong ground shaking. This information is provided in full in Appendix D. Shear wave velocity is useful for the evaluation of local rock or soil conditions for ground motion calculations because it is dependant on basic physical properties of the material, including density, porosity, cementation of sediments and hardness and fracture spacing of rock (Fumal, 1978). Strong ground motions are more nearly a function of shear wave velocity (Vs) than compressional wave velocity (Vp) because shear and surface waves cause most of the damage associated with strong ground shaking (Joyner, 2000). Vs values are particularly useful in the evaluation of site-specific potential for amplification of shear waves and for categorization of geologic units in ground shaking calculations. The average shear wave velocity to 30 meters depth (Vs30) typically is used to develop site categories for modifying calculated ground motion to account for site conditions (Borcherdt, 1994).

Shear wave velocities were measured within the lower portion of the upcoast landslide (boring WLA-B1; Figure 4.2) and upper portion of the downcoast landslide (boring WLA-B2; Figure 4.3) using downhole suspension logging techniques (Nigbor and Imai, 1994). WLA-B1 penetrated the toe of the upcoast landslide (unit Qlso4), the basal slide plane, and underlying bedrock of the Pico Formation (Figure 4.2). Displaced bedrock is emplaced over slope deposits (colluvium). WLA-B2 penetrated a repeated section of relatively loose older debris flow deposits that cover the buried paralic and marine deposits of the Punta Gorda terrace (Figure 4.3). Although WLA-B2 did not penetrate bedrock, it did extend below the inferred basal slide plane and likely sampled the Red Mountain fault zone, a zone of clayey material.

4.5 Geologic Structure

The distribution and composition of bedrock units, and to a lesser degree the extent and thicknesses of more recent deposits, across the Study Area is controlled by displacement across strands of the Red Mountain fault and local, large landslides. The main fault trace has been mapped by CGS (2003) across the cliff face. It is this trace that was zoned as part of the official State of California Alquist-Priolo fault zone (CGS, 1991). The fault is coincident with a topographic break in the hillslope and displaces deposits of the Punta Gorda marine terrace. As mapped, it extends across the headscarps of both the 1995 and 2005 slope failures above La Conchita. An exposure of the fault was documented within the headscarp area of the 1995 landslide (pers. comm., Pam Irvine and Kevin Clahan, 2007).

The Red Mountain fault juxtaposes, from north to south, the Monterey Formation against the Sisquoc Shale. The Sisquoc Shale forms a thin wedge that tapers downcoast and extends under the cliff. The Sisquoc Shale is intensely folded and thrust over the Pico Formation that underlies the coastal plain and community of La Conchita. At the intersection of the two diverging strands of the Red Mountain fault, near the top of the cliff where Ranch Road emerges on the plateau, bedrock of the Monterey Formation is thrust over down-dropped bedrock of the Pico Formation.

The northeast-dipping Red Mountain fault also appears to be geomorphically expressed across the upper Plateau, landward of the top of the cliff, above the headscarp of the large upcoast and downcoast landslides. Local expression consistent with faulting includes a linear seaward-facing scarp and low hill imaged by LiDAR beneath the canopy of the avocado orchard. This scarp was previously believed to be a landslide headscarp associated with an older landslide (map unit Qlso1; AKA, 2007). However, the linear nature of the scarp and absence of a deeper slide plane within borings suggests that the scarp is associated with a landward-dipping strand of the Red Mountain fault. This inferred fault strand likely is connected to the fault exposed in the canyon upcoast of West Barranca (locally known as Little V Canyon). In the Little V canyon exposure, the fault dips northeast and vertically offsets the Punta Gorda terrace abrasion platform by about 20 feet. This strand exhibits significantly less displacement than that measured across the main fault exposed in paleoseismic trenching near Los Sausas Creek downcoast of the Study Area, documented by Huftile and others (1997) and Lindvall and others (2002). This discrepancy in slip suggests that the main fault exposed in the trench by Huftile and others (1997) bifurcates (splits) upcoast into multiple strands before reaching Little V Canyon.

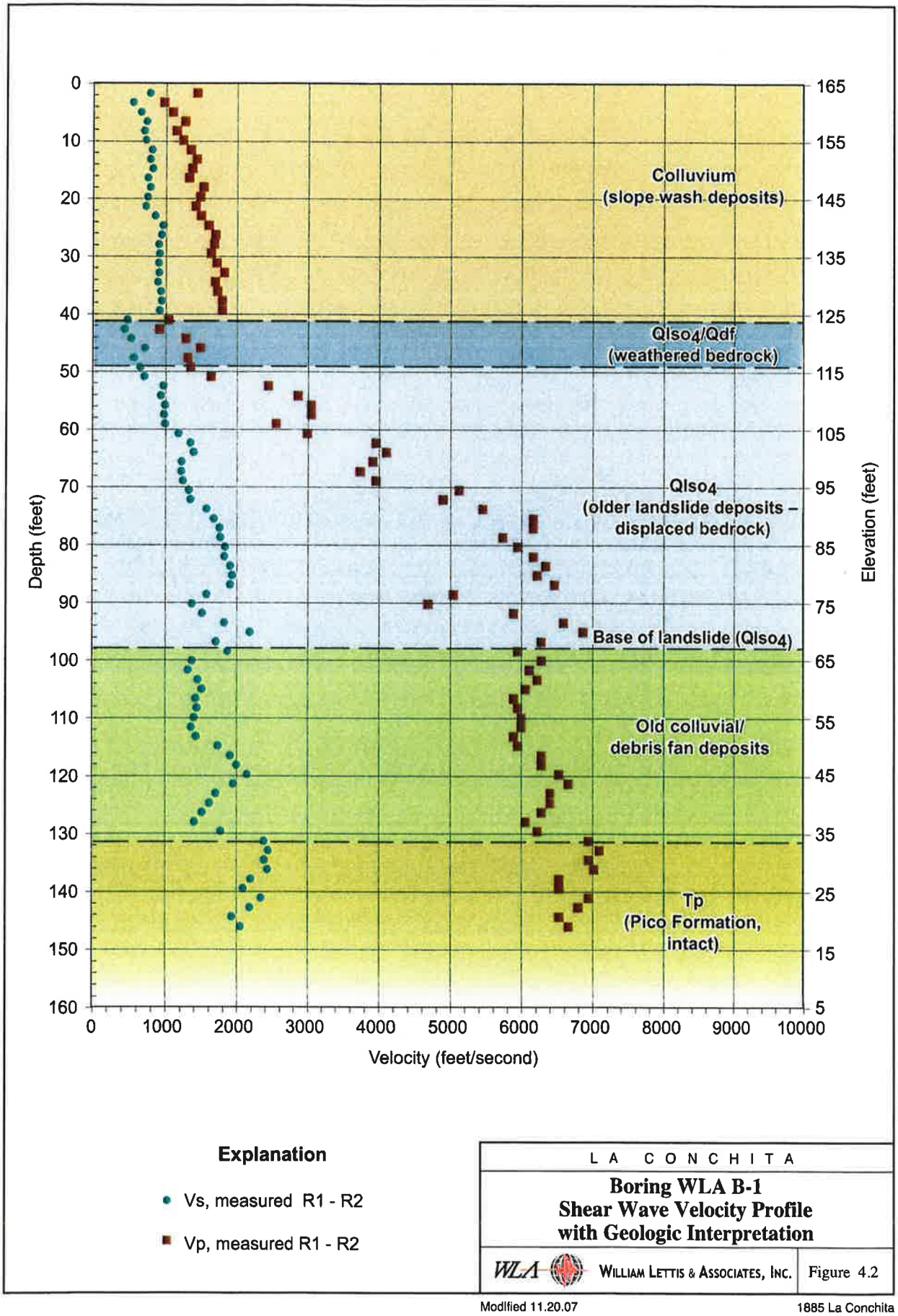

Explanation

- Vs, measured R1 - R2
- Vp, measured R1 - R2

L A C O N C H I T A

Boring WLA B-1
Shear Wave Velocity Profile
with Geologic Interpretation

WLA William Lettis & Associates, Inc. | Figure 4.2

Modified 11.20.07

1885 La Conchita

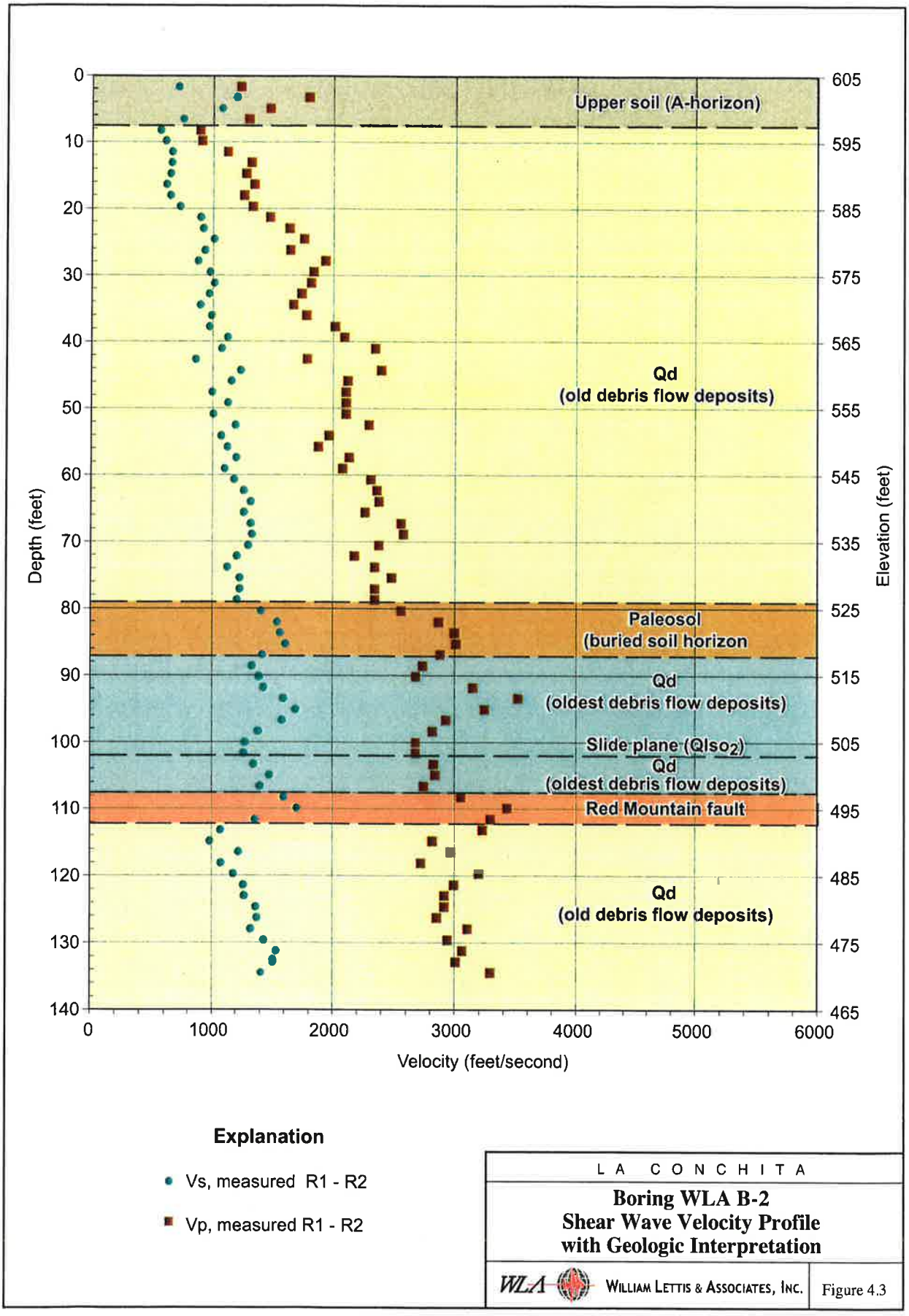

Explanation

- Vs, measured R1 - R2
- Vp, measured R1 - R2

LA CONCHITA

Boring WLA B-2
Shear Wave Velocity Profile
with Geologic Interpretation

WLA William Lettis & Associates, Inc. | Figure 4.3

Modified 11.20.07

5.0 RED MOUNTAIN FAULT

The Red Mountain fault is an east-striking, north-dipping reverse fault that, along much of its length, defines the transition from the uplifted Santa Ynez and Topatopa Mountains on the north to the Ventura basin on the south. South of the town of Carpinteria, the Red Mountain fault lies within the Ventura Basin, and structurally separates the Ventura Basin from the Carpinteria Basin.

The eastern end of the Red Mountain fault changes to a northeast strike and may terminate against the Mission Ridge-Arroyo Parida-Santa Ana fault, or may be connected by a blind thrust to the San Cayetano fault (Huftile and Yeats, 1995). Vertical separation of multiple distinct bedrock marker horizons across the Red Mountain fault decreases westward from 14,750 ft (4,500 m) north of the Rincon oil field to 1,150 ft (350 m) at Rincon Point (Jackson and Yeats, 1982). The western end of the Red Mountain fault projects offshore into the Santa Barbara Channel near Rincon Point and total measured offset decreases to less than 330 ft (100 m) south of Summerland. Slip along the Red Mountain fault may be transferred to the offshore North Channel Slope fault (Jackson and Yeats, 1982).

5.1 Associated Seismicity

No large historical earthquakes are associated with the Red Mountain fault, but microseismicity ($M < 3.0$) shows that it is presently active. These small earthquakes extend to a depth of 12 km and indicate an overall fault dip of about 60° to the north (Yeats and others 1987).

5.2 Previous Mapping of the Red Mountain Fault

Darton (1915) first mapped the Red Mountain fault as a near-vertical fault separating the Monterey Formation from the 'Fernando Formation', later subdivided into the Pico Formation and Sisquoc Shale (Figure 5.1). Dibblee (1998) mapped the Red Mountain fault in the La Conchita Study Area as a single, queried strand along the cliff landward of La Conchita. Upcoast (north) of West Barranca, Dibblee (1998) mapped a westward bifurcation in the Red Mountain fault, with two parallel strands extending offshore near Rincon Point.

In 1991, the fault was zoned as part of the official State of California map of earthquake fault zones (CGS, 1991). The Red Mountain fault extends across the La Conchita Study Area, with the official Alquist-Priolo fault zone extending northeast of the community of La Conchita, across the cliff face. The Alquist-Priolo zone map and fault traces are provided within our Phase 1 report (AKA, 2007). More recently, the CGS mapped strands of the Red Mountain fault during regional mapping activities (CGS, 2003). We incorporated the CGS (2003) digital mapping in our geologic mapping but remapped the location(s) of the fault based on interpretation of LiDAR-derived topography and field reconnaissance for this study (Figure 5.2).

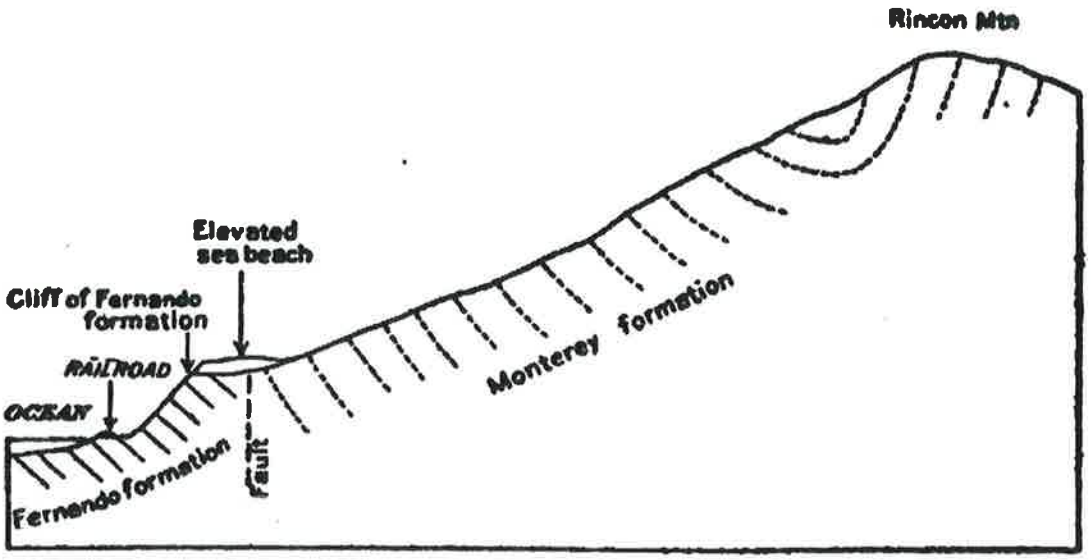

Figure 5.1 Generalized cross section from the Pacific Ocean to Rincon Mountain at Los Sauces Creek from Darton (1915). Cross section and accompanying map in report is the first documentation of the Punta Gorda marine terrace ('elevated sea beach') and faulting of the Monterey Formation against the 'Fernando Formation' (later renamed the Pico Formation and Sisquoc Shale) by the Red Mountain fault.

5.3 Location and Style of Deformation across the La Conchita Study Area

Trench exposures across the Red Mountain fault east of La Conchita indicate that a significant portion of the near-surface deformation is accommodated by folding (Lindvall and others, 2002). Based on oil well data and regional microseismicity, the Red Mountain fault dips about 60° to the north at depths of 3 km. Near the surface, the fault dips roughly ~30°. The main strand of the Red Mountain fault vertically separates the abrasion platform of the Punta Gorda marine terrace by over 110 feet (33 m) southeast of La Conchita near Los Sausas Creek, within the southeastern mapped limit of the terrace (Figure 5.2). A vertical slip rate of 1.5 millimeters (mm) per year has been estimated for this main fault strand based on vertical offset of the Punta Gorda wave-cut platform (Huftile and others, 1997; Lindvall and others, 2002).

5.3.1 Results of Field Mapping

The Red Mountain fault is geomorphically expressed across the upper Plateau (Figure 5.2). The main fault trace has been mapped by CGS (1991; 2003) across the cliff face, as well as across both the 1995 and 2005 slope failures above La Conchita. It is this trace that was zoned as part of the official State of California Alquist-Priolo fault zone (CGS, 1991). The inferred location of the exposed fault within the headscarp area of the 2005 slide is shown on Figure 5.3. The fault is coincident with a topographic break in the hillslope and appears to cut internal stratigraphy associated with the down-dropped Punta Gorda marine terrace (Figure 5.4).

Another strand of the fault is exposed in the canyon upcoast of West Barranca (locally known as Little V Canyon), as shown on Figure 5.5. In the Little V Canyon exposure, the fault dips northeast and vertically

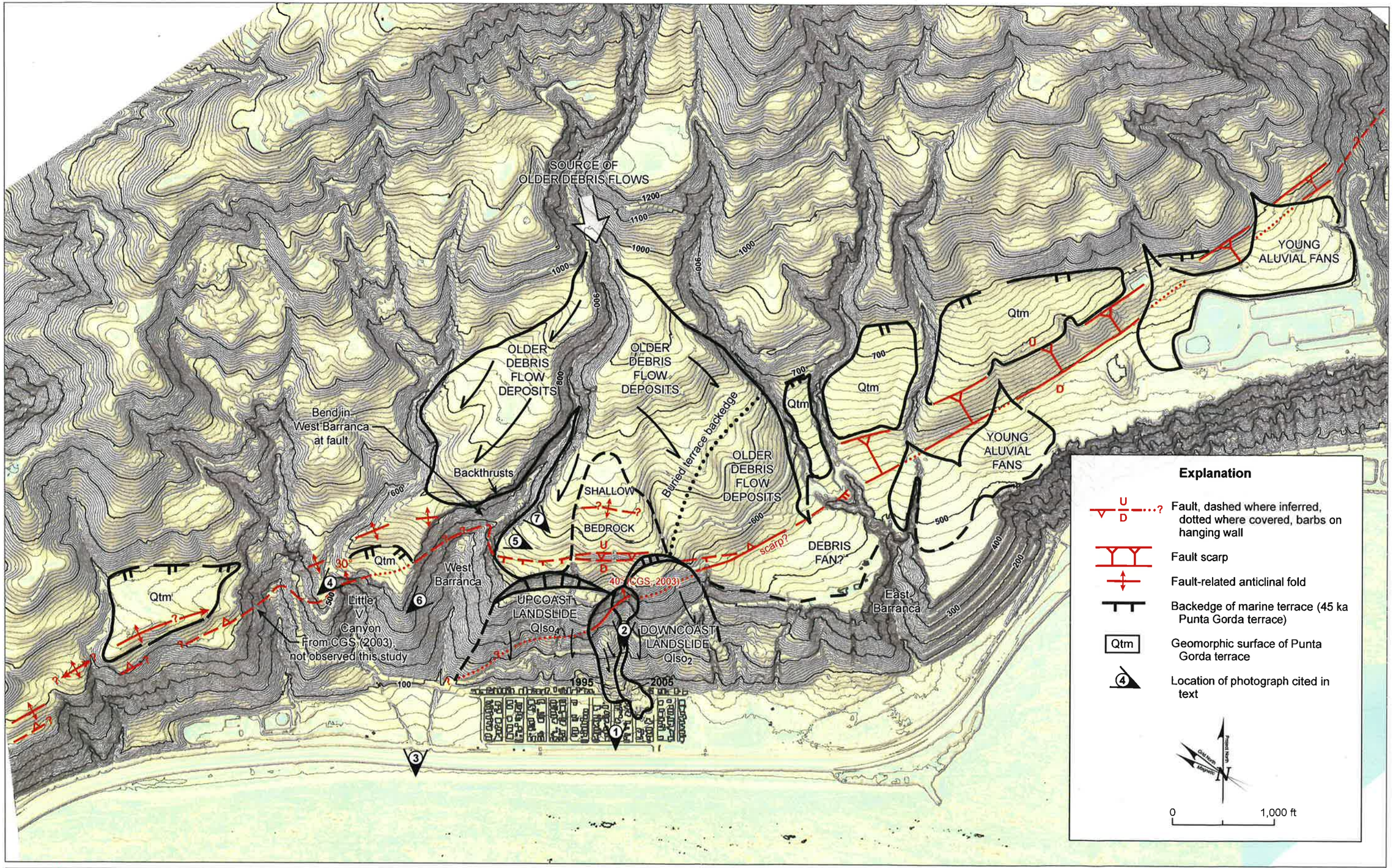

Map of Red Mountain Fault (this study) based on Geomorphic Features and Exposures (including observations from CGS, 2003)

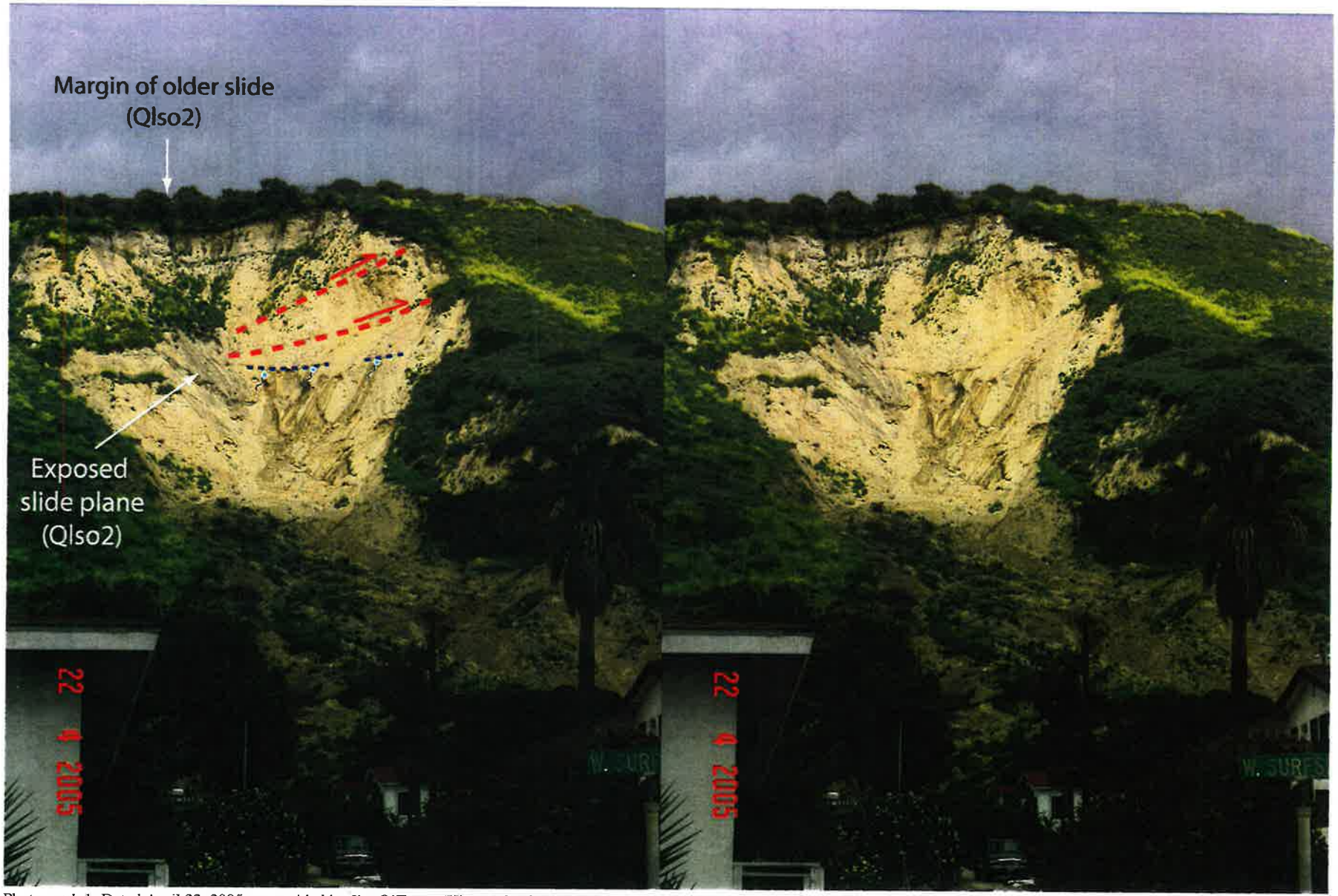

Photograph 1: Dated April 22, 2005 as provided by Jim O'Tousa (View to landward from La Conchita of 2005 slide, see Figure 5.2 for location)

WLA

View of 2005 headscarp area showing inferred location of Red Mountain fault strands (in red) and marine terrace abrasion platform (in blue)

LA CONCHITA LANDSLIDE – PHASE 2
Figure 5.3
02 JAN 08, 1885, CSH

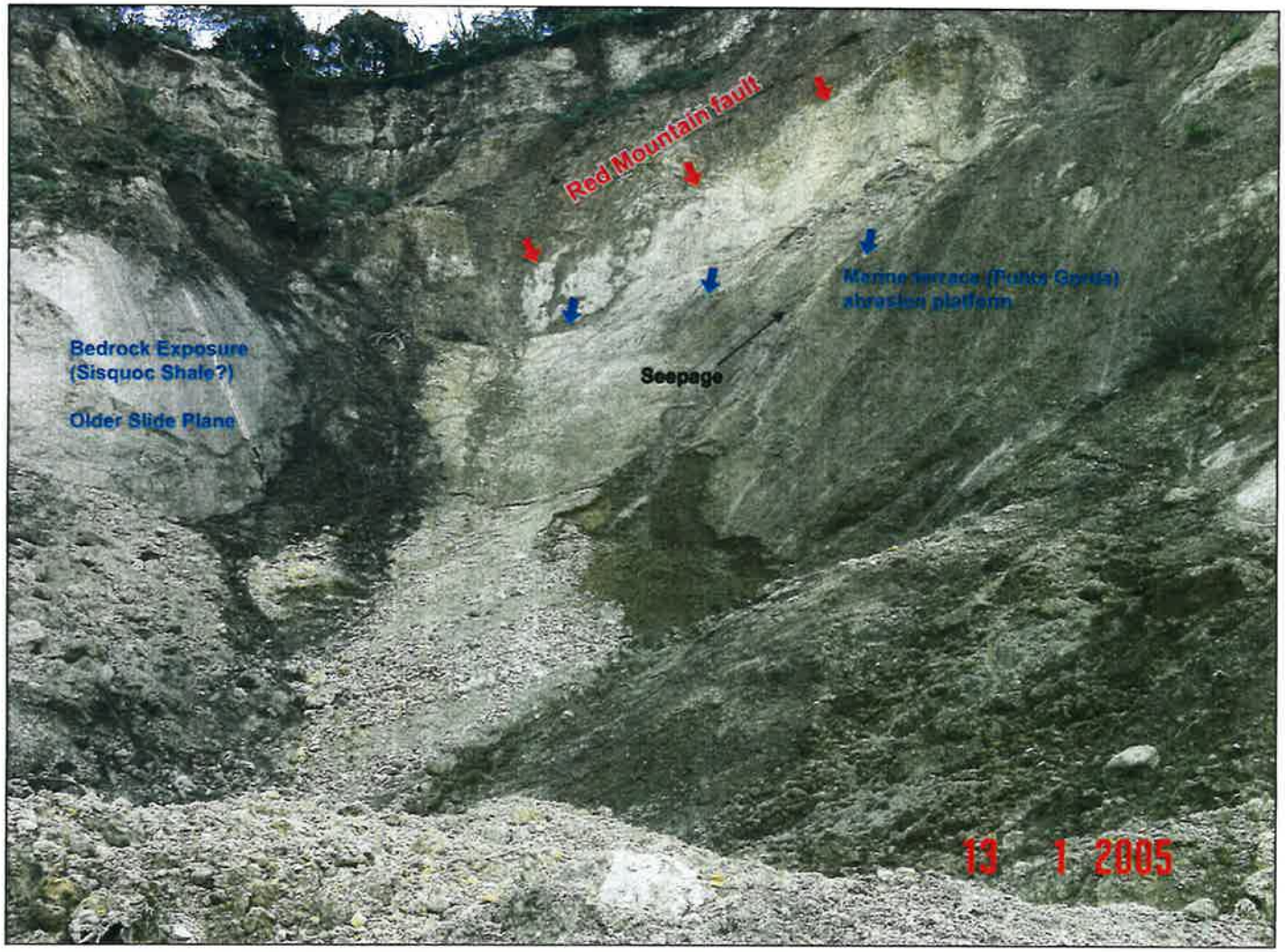

Photograph 2: Dated January 13, 2005 as provided by Jim O'Tousa (See Figure 5.2 for location)

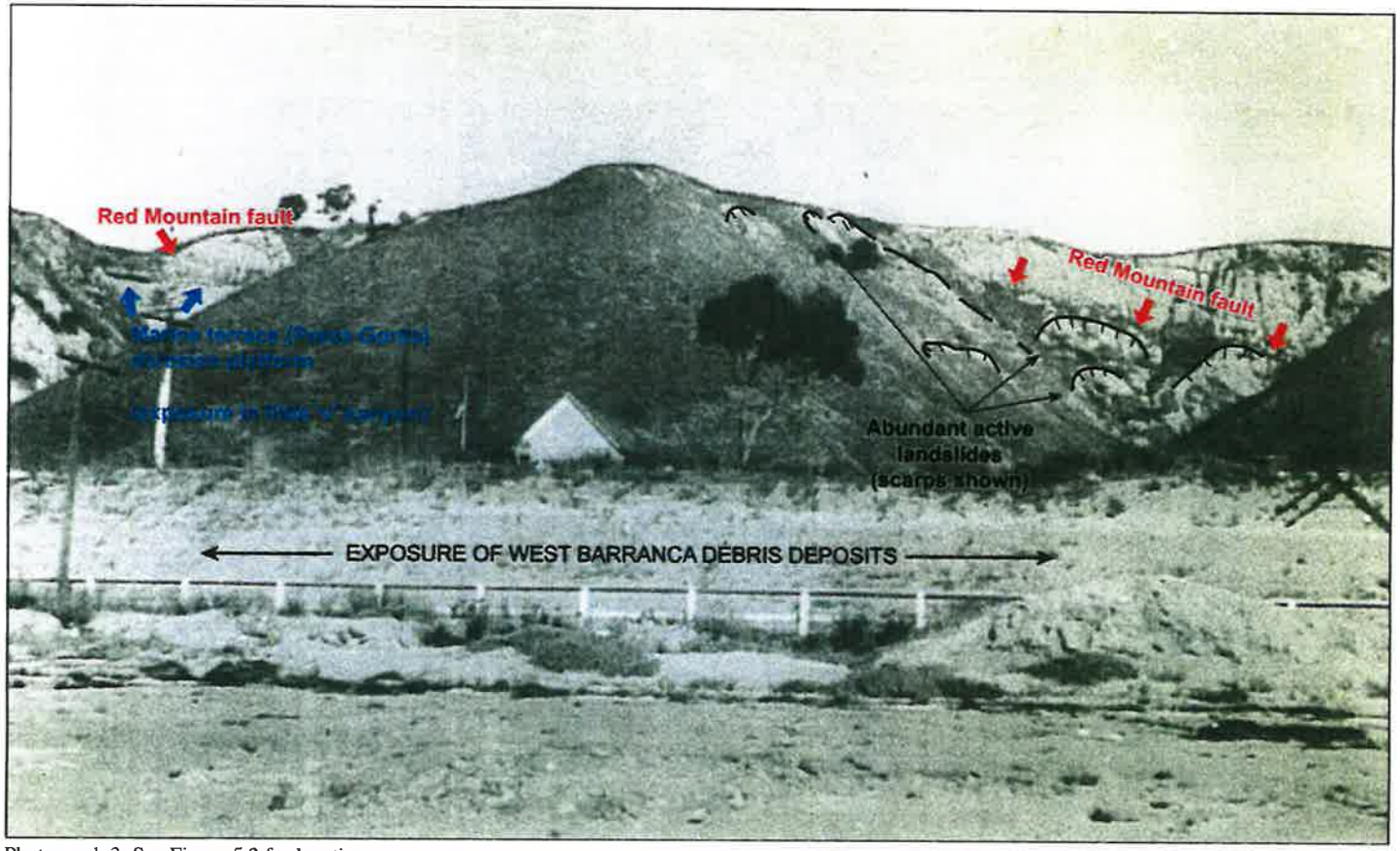

Photograph 3: See Figure 5.2 for location.

separates the Punta Gorda terrace abrasion platform by about 20 feet (Figure 5.6). This strand exhibits less displacement than the single, main strand of the Red Mountain fault exposed in the trench near Los Sausas Creek (Lindvall and others, 2002).

There is no obvious, direct connection between the CGS (1991; 2003) fault strand mapped in the cliff face above La Conchita and the strand located in the Little V Canyon upcoast of the West Barranca. Currently the Red Mountain fault within West Barranca, noted on the historical photograph reproduced in Figure 5.5, is obscured by recent landsliding. Figures 5.7 and 5.8 show possible exposures of the fault within the canyon walls of West Barranca photographed by Pam Irvine of CGS following the 1995 landslide. Figure 5.9 shows back-thrust faults exposed more recently, in December of 2007, within the west wall of West Barranca upstream of the inferred fault strand. The back-thrust faults offset the 'paleosol' layer and overlying older debris deposits. These seaward-dipping, secondary faults provide supporting evidence for the presence of a larger, landward-dipping active strand of the Red Mountain fault crossing the canyon downstream.

Based on examination of LiDAR-derived topography, we have identified potentially fault-related features upslope, landward, of the cliff area that are aligned with the inferred location of the fault across West Barranca (Figure 5.2). Specifically, a linear seaward-facing scarp and low hill imaged by LiDAR beneath the canopy of the avocado orchard are on strike with the mapped trace of the fault, as originally mapped by Dibblee (1998). The scarp was initially interpreted, prior to drilling performed for this study, as a possible headscarp of an older landslide (AKA, 2007). However, this inferred strand of the fault likely merges with the main active strand near the top of the cliff at Ranch Road.

Another north-dipping reverse fault is exposed in the East Barranca. This fault, which is located in the footwall of the main Red Mountain fault, does not displace the Punta Gorda marine terrace platform and therefore is no longer active.

5.4 Slip Rate

Slip rate estimates for the Red Mountain fault are poorly constrained and range from about 0.5 mm/yr to 5.9 mm/yr since the late Pleistocene (Petersen and Wesnousky, 1994; Huftile and Yeats, 1995). Huftile and Yeats (1995) modeled the Red Mountain fault as a north-dipping reverse fault that can be shown to extend down to seismogenic depths. The Ventura Avenue anticline was modeled as a north-vergent, lift-off fold uplifting Miocene and younger rocks above a decollement that is related to the south-dipping Oak Ridge fault. This model requires that the uplift rates of the footwall and hanging-wall blocks be combined to yield the slip rate on the Red Mountain fault at seismogenic depths. This would mean a total vertical uplift rate on the Red Mountain fault of 5.1 mm/yr, and a slip rate on a 60°-dipping fault of 5.9 mm/yr. The revised California probabilistic seismic hazard maps (Cao and others, 2003) assign a slip rate of 2.0 ± 1.0 mm/yr, based on data presented in Clark and others (1984).

A paleoseismic investigation of the Red Mountain fault downcoast (east) of the Study Area estimated the slip rate across the principal strand of the Red Mountain fault (Huftile and others, 1997; Lindvall and others, 2002). Based on trench exposures, bucket auger drilling, and local geologic mapping, Huftile and others (1997) concluded that the Red Mountain fault vertically separates the Punta Gorda marine terrace abrasion surface by about 112 feet (34 m). Lajoie and others (1979, 1982) and Trecker and others (1999) estimate a 45,000-year age for the Punta Gorda marine terrace based on amino acid racemization of marine shells found at the base of the terrace. Huftile and others (1997) combined these estimates of vertical separation and terrace age with an assumed 30° near-surface fault dip to estimate a minimum dip-slip rate on the Red Mountain fault of 1.5 mm/yr. This rate assumes no contribution from folding and

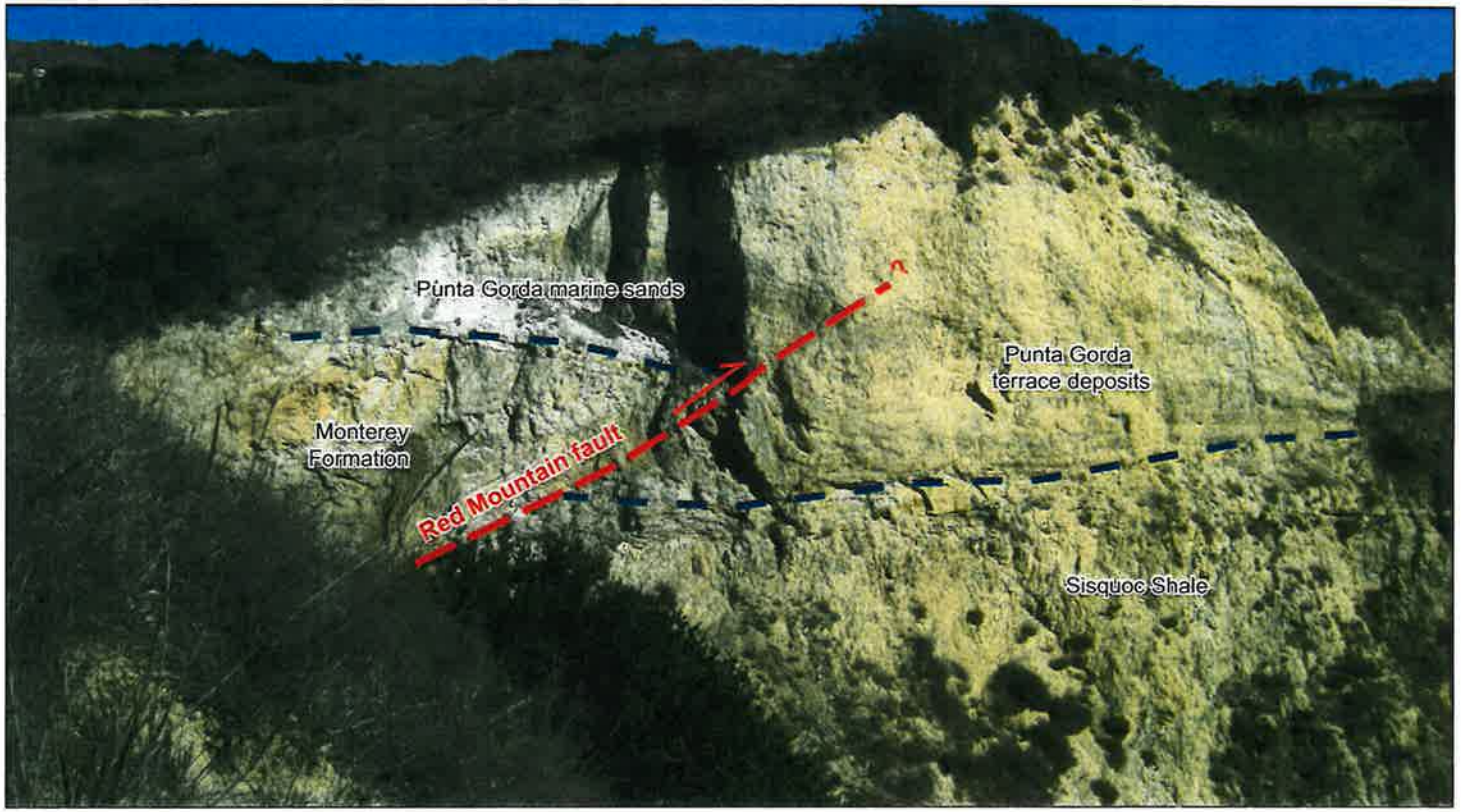

Photograph 4: Photograph by Christopher Hitchcock in December, 2007 (see Figure 5.2 for location)

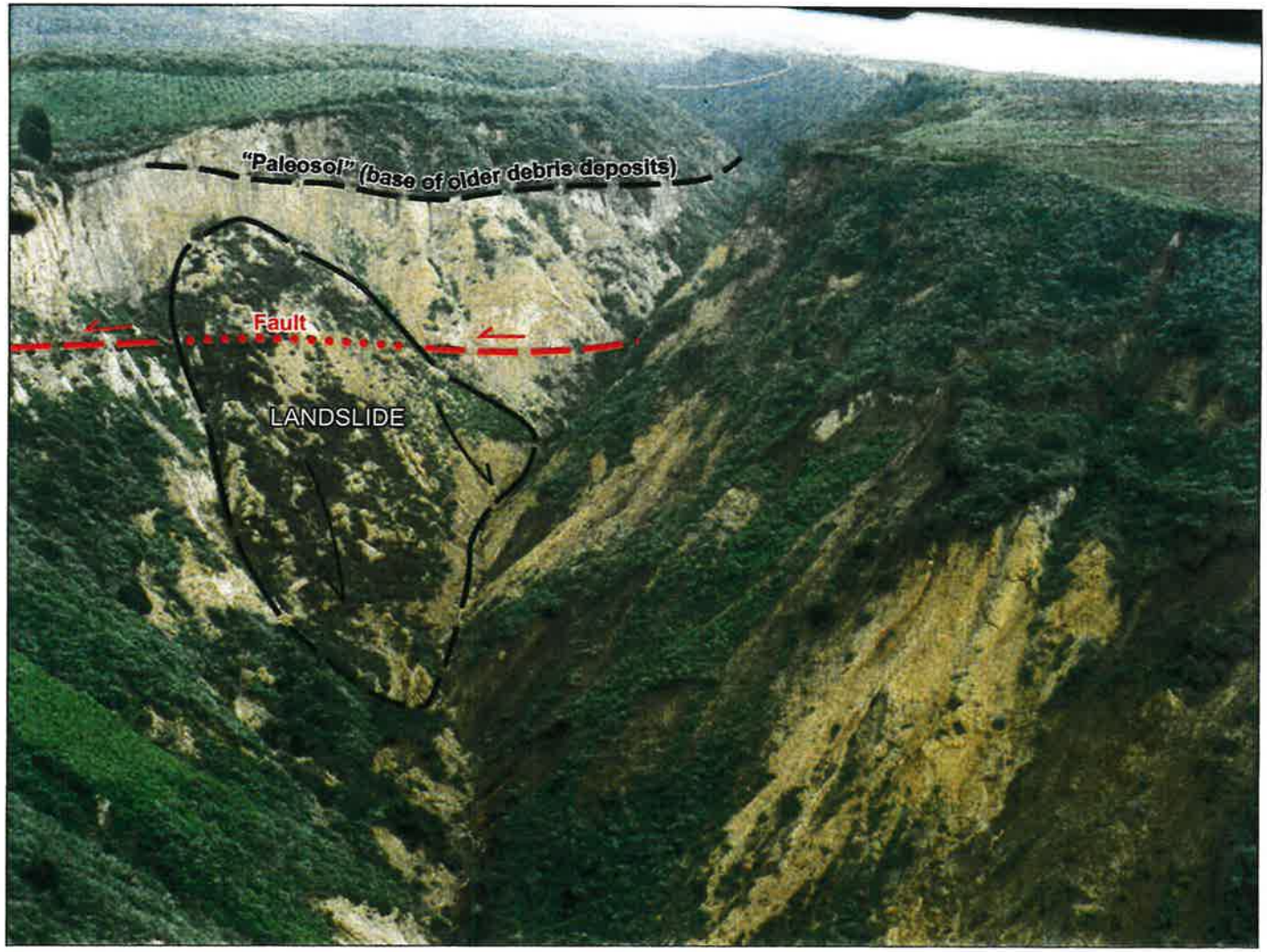

Photograph 6: Photograph of West Barranca taken in 1995 by Pam Irvine (see Figure 5.2 for location)

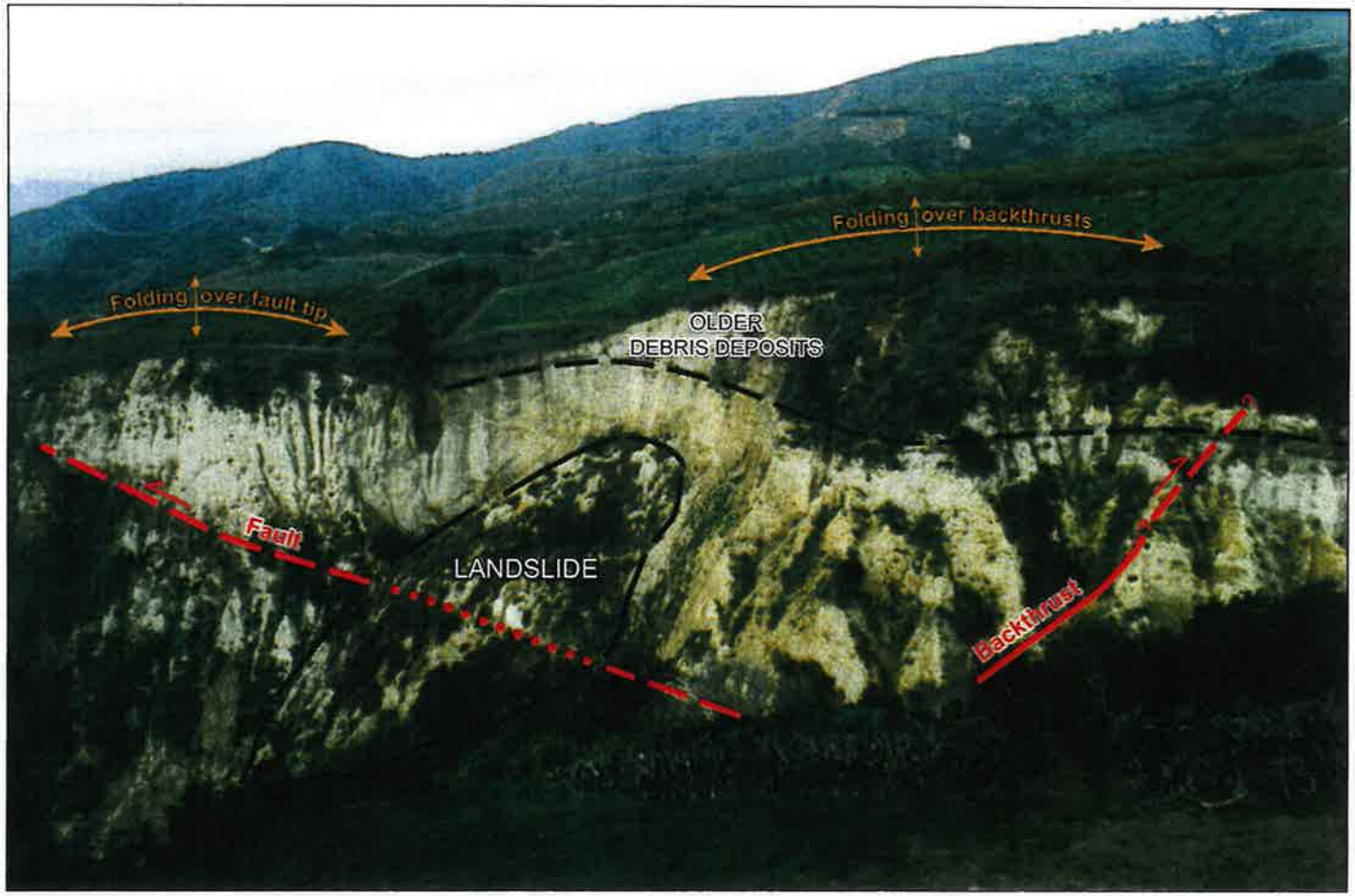

Photograph 5: Photograph by Pam Irvine taken in 1995 of west (upcoast) wall of West Barranca (see Figure 5.2 for location)

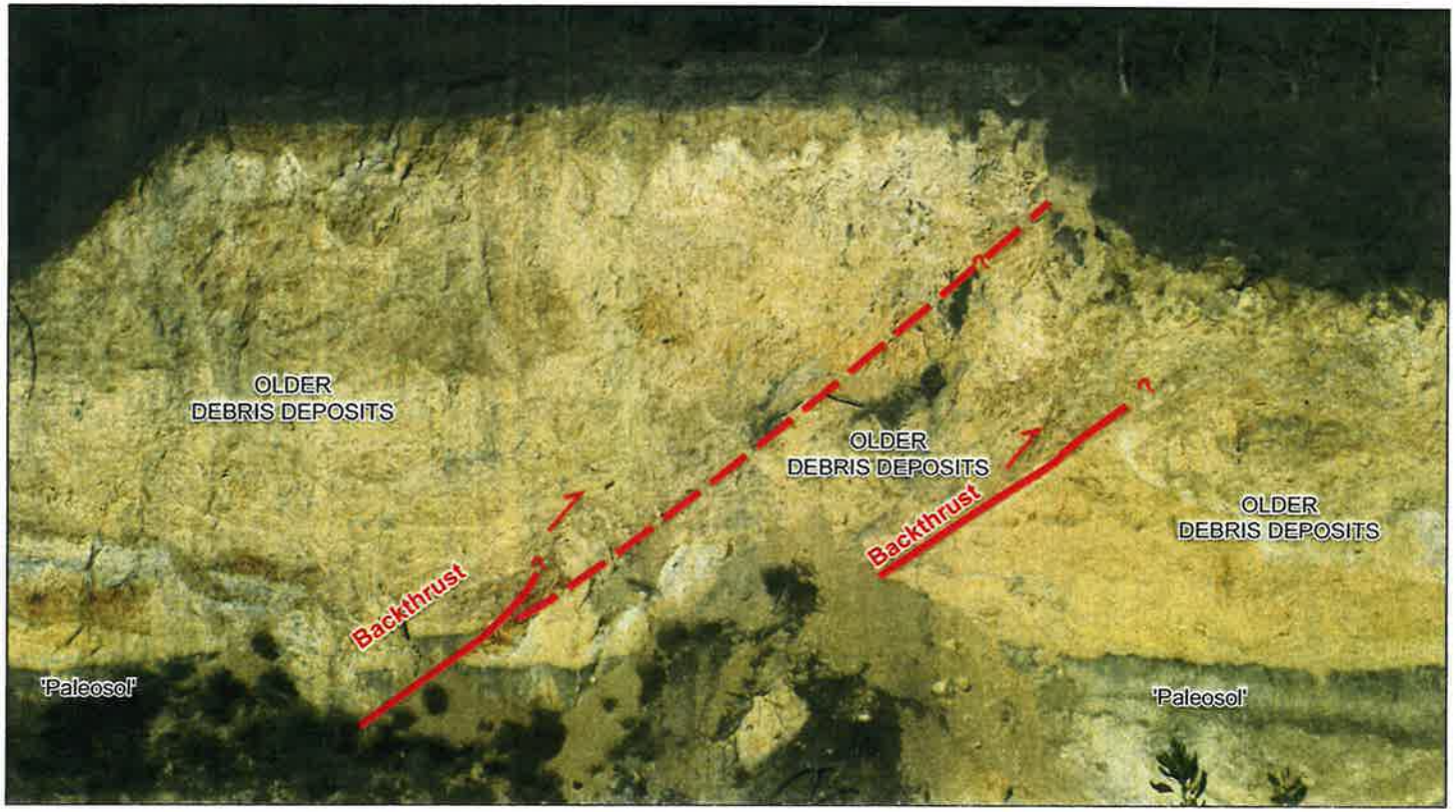

Photograph 7: Photograph by Chris Hitchcock of west (upcoast) wall of West Barranca in December, 2007 (see Figure 5.2 for location)

uplift associated with the Ventura-Rincon anticline in the fault footwall. The 1.5 mm/yr dip-slip rate is also a minimum slip-rate estimate because of the possibility that (1) other faults strands accommodate some of the motion along the fault zone, (2) the possibility that the fault may have some lateral component of slip, and/or (3) the possibility that the footwall block is being uplifted by regional folding (Lindvall and others, 2002). The 45,000-year-old Punta Gorda terrace was formed at about 38 meters (125 feet) below present-day sea level. However, near the trench, the terrace within the footwall block of the Red Mountain fault is at 169 meters (555 feet) elevation above sea level. Thus the footwall block of the fault is rising at over four mm/yr.

Yeats (1988) suggested that the slip rate on the Red Mountain fault is similar to that on the Oak Ridge and San Cayetano faults with slip rates well over 1.5 mm/yr. Based upon a balanced, retrodeformable cross section that includes the Saugus formation, Huftile and Yeats (1995) estimate 0.2 to 3.5 km (0.1 to 2.2 miles) of vertical displacement during the last 500,000 years, yielding a dip-slip rate of 0.4 to 7 mm/yr. However, recent geodetic measurements across the western Transverse Ranges preclude fault slip rates as high as 7 mm/yr.

5.5 Most Recent Surface Rupturing Event

There is evidence of past earthquakes in a colluvial wedge and a fissure fill in the hanging-wall block exposed in the trench (Lindvall and others, 2002). Attempts made to constrain the timing of the most recent event by using radiocarbon dating of detrital charcoal fragments found in the fissure fill proved inconclusive. Because the most recent event is not known, the probability of a large earthquake on the Red Mountain fault is not fully constrained.

6.0 GROUNDWATER

The hydrogeology of the La Conchita Study Area is poorly constrained with the sources, subsurface aquifers, and flow paths of groundwater largely undefined. The lack of detailed knowledge of subsurface groundwater flow paths and flow rates is the direct result of incomplete and contradictory borehole and water-well data. Available subsurface information, including water-well records, is of limited geographic extent within the La Conchita Study Area. Of the 84 borings and wells compiled for the Study Area, based on published and unpublished reports, less than 38 reported encountering groundwater and provided depth to water (Figure 6.1; AKA, 2007). In addition, seasonal variation in depth to groundwater in the Study Area is well documented, as are changes in groundwater elevation in response to periods of heavy rainfall or long-term drought (Bachman, 1998). The utility of the available groundwater information is limited by the broad range in dates over which borings and water wells were drilled, installed, and depths to water tables measured. On-going monitoring of piezometers within selected wells for this project may provide more information on changes in groundwater levels in response to rainfall.

The greatest uncertainty in characterizing groundwater in the Study Area is due to the subsurface variability of the surficial and bedrock geology, combined with structural complexity added by the presence of fracturing and faulting associated with strands of the Red Mountain fault. Based on the available subsurface data, combined with our revised mapping of the surficial geology, we have subdivided the Study Area in an attempt to provide a generalized model of groundwater flow. We identify five distinct hydrologic regions associated with groundwater recharge and flow, defined as follows:

Regional Catchment Basin upslope of La Conchita Study Area – The La Conchita Study Area is part of a much larger drainage basin that extends well inland to the ridge of the low-lying coastal range. Rainfall within this large basin likely reaches the ocean via surface flow within major canyons, including the East and West Barrancas. Subsurface flow is less well constrained but likely occurs within fractured bedrock and overlying older marine terrace and debris flow deposits that mantle the area.

East and West Barrancas – The East and West Barrancas are large canyons that bound the Study Area and extend landward, providing the primary conduit for surface drainage to the ocean and associated subsurface flow within young deposits that cover the canyon floors.

Plateau of La Conchita Ranch – The plateau area underlies orchards of La Conchita Ranch and extends between the East and West Barrancas. Locally the surface of plateau, and underlying wave-cut platform, is cut by the Red Mountain fault that serves to block or channel subsurface flow. Surface runoff is diverted into West Barranca via man-made, slope-parallel berms.

Cliff area, landward of La Conchita – The cliff behind (landward) of the community of La Conchita is exposed to rainfall during large storms. Surface runoff occurs within a series of gullies that drain into La Conchita. Locally springs within the cliff face are roughly coincident with the inferred projection of the Red Mountain fault. Springs along the base of the cliff coincide with the toe of small and large slope failures, and are localized within areas underlain by buried marine terrace sands.

Coastal plain underlying community of La Conchita – The coastal plain beneath La Conchita is bisected by West Barranca and similar through-going drainages. Locally groundwater is found in

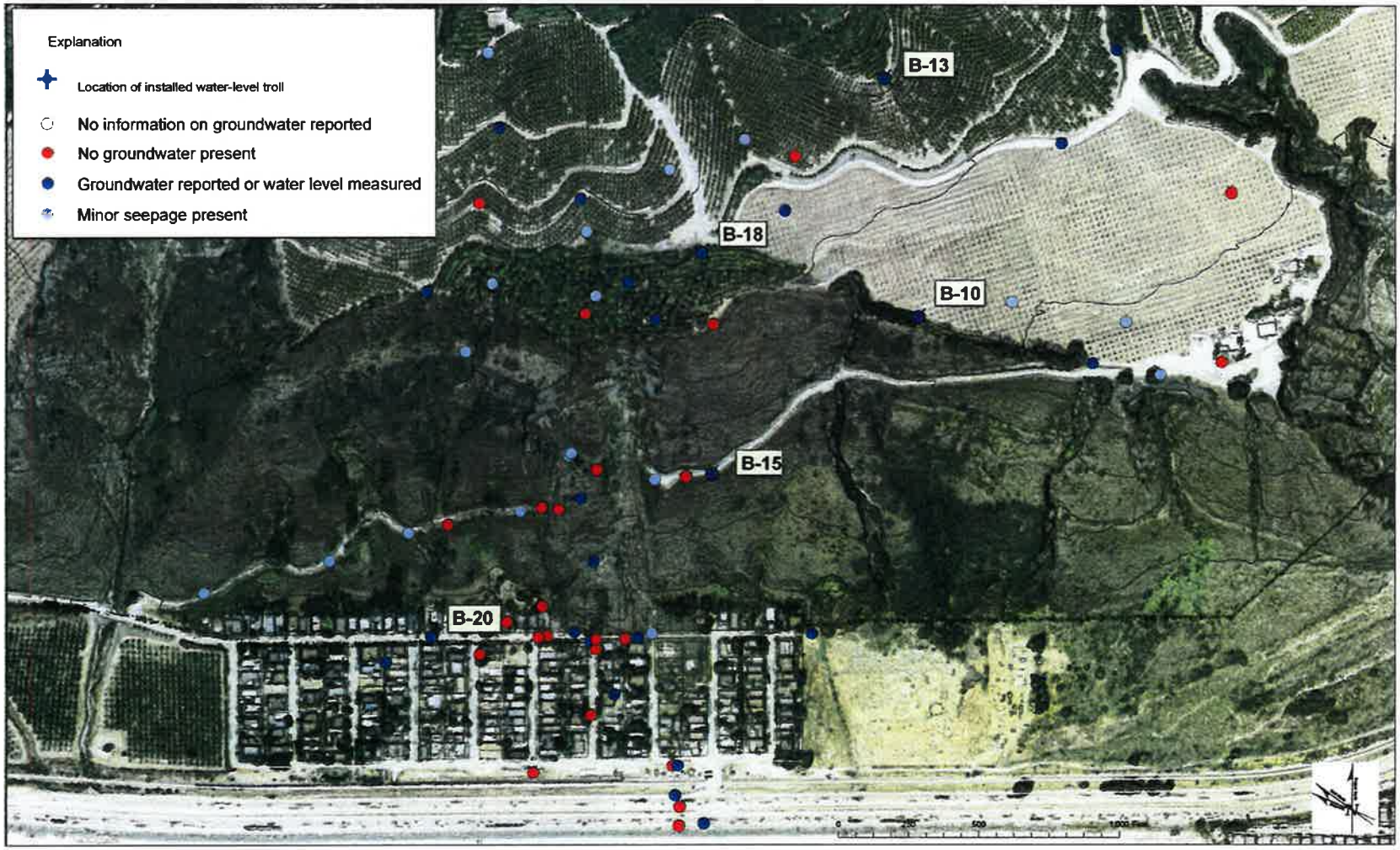

WLA

Map showing presence or absence of groundwater as recorded in compiled borings for Study Area

LA CONCHITA LANDSLIDE – PHASE 2
Figure 6.1
19 MARCH 08, 1885, CSH

buried marine terrace and beach deposits. These deposits also are saturated by saltwater infiltration near the coast.

Based on our review of available literature and observations from limited geotechnical drilling conducted for this study, we define the following major potential aquifers, or permeable units, that may host groundwater flow:

Older Debris Flow Deposits – The portion of the plateau within the Study Area landward of the cliff area upslope of La Conchita consists of younger, relatively thick mass wasting (debris) deposits (unit Qpmw) derived from higher elevation, inland areas. These poorly-sorted sediments predominately contain angular clasts of Monterey Formation sandstone and shale within a clayey matrix. Limited information is available on the permeability of these relatively loose deposits.

Permeable Deposits of the Punta Gorda marine terrace – Punta Gorda marine terrace deposits (unit Qppr-p) within the Study Area predominantly consist of clayey sand with lenses of rounded gravels. These deposits, where locally preserved, are laterally extensive and highly permeable. Because the terrace sediment is found at depth on relatively impermeable bedrock, available borings and water wells indicate that these deposits commonly are saturated. As these buried deposits extend within the headscarp area of the 1995 debris flow, and are the apparent source of springs within the cliff face in this area, the deposits may serve as a conduit across the Red Mountain fault in the plateau area. The Punta Gorda terrace deposits are only locally exposed within the headscarp area of the 1995 and 2005 slides and apparently do not extend within the cliff face upcoast of the slide area.

Bedrock Aquifers – The Pico Formation and Sisquoc Shale consist primarily of thinly-bedded shale with low permeability. These buried bedrock units locally are exposed within barranca walls and the cliff portions of the Study Area and, where exposed or encountered during drilling, generally are dry. The Monterey Formation predominately consists of shale with minor sandstone beds that may have limited permeability along bedding planes, allowing for localized groundwater storage and flow. Regional uplift and folding combined with local fracturing across the Red Mountain fault may also allow groundwater flow within, and across, these buried bedrock units.

Permeable Deposits of the Sea Cliff marine terrace beneath La Conchita– The Sea Cliff marine terrace consists predominantly of clean sand with lenses of rounded beach cobbles. These sediments locally are five to twenty feet thick and overlain by up to seventy feet of relatively impermeable, clayey debris flow and alluvial plain deposits.

We define the following major potential barriers to horizontal and vertical groundwater flow:

'Paleosol' developed on Punta Gorda deposits – A laterally extensive, buried silt deposit coincides with the upper portion of the Punta Gorda terrace and overlying paralic deposits. The clay-rich unit may retard downward infiltration and may locally be associated with perched groundwater and/or local horizontal groundwater flow.

Wave-cut Bedrock Platform beneath Plateau – The geomorphic plateau that forms much of the La Conchita Ranch orchard area is underlain by a wave-cut platform. This sub-horizontal surface formed on top of bedrock is a significant barrier to downward infiltration of groundwater and

commonly forms the base of perched groundwater within overlying, highly permeable marine sands of the Punta Gorda terrace.

Red Mountain fault – Multiple strands of the steeply-dipping Red Mountain fault offset water-bearing deposits and are associated with clay gouge material that form a barrier to lateral groundwater flow. The fault also may also serve to divert or dam subsurface flow and appears to be locally associated with springs within the cliff area, upslope and landward of La Conchita.

Wave-cut Bedrock Platform beneath Coastal Plain – The coastal plain that includes the community of La Conchita is underlain by a buried, wave-cut platform formed on relatively impermeable bedrock of the Pico Formation. This sub-horizontal bedrock surface is a significant barrier to downward infiltration of groundwater. Locally, the buried bedrock surface is covered with thin but highly permeable marine terrace and beach sands.

6.1 Previous Studies

Information on groundwater conditions within the community of La Conchita primarily consists of water levels reported on boring logs within geotechnical reports ('first water' encountered). Longer-term groundwater levels measured in installed water monitoring wells, including piezometers (installed down-hole tubes or instrumentation used to determine water-level elevation), primarily are available for the plateau area within La Conchita Ranch upslope of the cliff area (Bachman, 1998), and for isolated areas on the cliff face, principally within the 1995 landslide (Converse, 1994; Stoney-Miller, 1998). Additional groundwater monitoring data is available for saturated beach sands and marine terrace deposits located at depth at the entrance to the community of La Conchita near Highway 101 (Fugro West, 2007). The only active groundwater monitoring data is from limited piezometers installed within existing wells for this study.

Converse (1994) interpreted the presence of buried paleochannels beneath the plateau surface on La Conchita Ranch. These inferred paleochannels consist of channels incised into the Punta Gorda terrace filled with older debris flow deposits. Converse (1994) argued that the paleochannels formed subsurface conduits for groundwater flow across the plateau and cliff area. Evidence cited for the paleochannels included thick gravel deposits documented in deep dewatering wells.

Bachman (1998) provided a summary of groundwater levels recorded in multiple completion water wells drilled within La Conchita Ranch between 1992 and 1994, including the results of a well test in the hanging wall of the Red Mountain fault. Bachman (1998) concluded that water-bearing sediments beneath La Conchita Ranch are poorly connected and transmissivity is low. No transmission path for surface water through the groundwater system was identified. Rather, variations in depths of water levels recorded beneath the plateau were interpreted as evidence for isolated, hydraulically disconnected water-bearing sedimentary units (Bachman, 1998; Grismer and others, 2000).

Published data on infiltration rates of surface water within the plateau area provides constraints on infiltration and groundwater recharge from rainfall (Grismer and others, 1999; 2000). Measured recharge rates of about seven inches per year (180 mm/yr) were recorded during long-term soil moisture monitoring using neutron probes. The documented pattern of soil profile drying during summer irrigation followed by progressive wetting during the winter rainy season observed in both irrigated and non-irrigated areas of the Ranch suggests that groundwater recharge primarily consists of rainfall infiltration (Grismer and others, 2000).

Limited groundwater monitoring data is available for the cliff area landward of the community of La Conchita, downslope of the plateau underlying La Conchita Ranch. Reports documenting pre- and post-landslide water monitoring by Converse (1994) and Stoney-Miller (1998) discuss the area of the 1995 landslides. These reports include records of changes in water-table elevations prior to the landslide and incorporate post-landslide records for modeling of possible failure conditions.

Within the community of La Conchita, and for much of the coastal plain, groundwater data consists of water levels encountered in geotechnical borings and limited groundwater monitoring records. Groundwater data from monitoring wells at the La Conchita Mini Market at the intersection of Surfside Street and Santa Barbara Avenue (6905 Surfside Street), cited in Fugro West (2007), reported groundwater depths of approximately fifteen feet below ground surface from 2002 through 2004. CALTRANS (2002) reported groundwater levels at elevations above sea level of 11 to 13 feet in CPT explorations located about a quarter mile north of La Conchita near West Barranca. Fugro West (2007) provided groundwater depths within borings and a monitoring well near the entrance to La Conchita.

6.2 Surface Water

Rainfall within, and landward of, the Study Area is absorbed and stored within the soil, infiltrates to depth as part of deeper water levels, or becomes surface runoff. Grismer and others (2000) estimated that approximately 30 percent of yearly rainfall is stored within surface soils, 30 percent infiltrates into the ground and becomes groundwater recharge, and the remaining 40 percent flows downhill as runoff. Surface runoff primarily flows episodically within the West and East Barrancas, with occasional minor flow in incised gullies within canyon walls and the cliff behind La Conchita. The barrancas are sharply incised canyons that are generally V–shaped in cross-section with very narrow valley floors. Locally the barranca channels are filled in with soil and debris from adjacent upslope landslides, commonly resulting in temporary obstruction or diversion of downstream flow.

Stormwater also is channeled, and diverted, along established surface roads and associated berms and culverts. Ranch Road was constructed across the cliff, landward of the community of La Conchita, prior to 1914. Ocean View Road to the northeast of La Conchita was first graded under County contract in 1929. After the 1995 storms and slope failure, La Conchita Ranch installed two eight-foot diameter culverts beneath Ocean View Road at West Barranca. Ranch personnel also constructed a berm along the town side of the road. The town apparently was not inundated in the January 2005 mudflow from West Barranca that closed Highway 101. However, flooding resulting from blockage of either the drainage culverts or the canyon floor remains a significant concern.

Roads in the La Conchita subdivision were built in 1924 by the developers. In 1951, the roads were initially paved and street grades set by the County. In 1989, La Conchita Road at the entrance to La Conchita was widened in conjunction with efforts by CALTRANS to improve access off the freeway. The County, prior to the 1995 landslides, plowed or otherwise cleared the community streets of mud and other debris after heavy storms as part of their normal maintenance (undated memorandum obtained from County of Ventura, Road Maintenance Division). Records apparently were not kept on the frequency or amounts of debris removal within La Conchita, except that such maintenance was considered relatively common.

Above La Conchita, within La Conchita Ranch, changes were made to the natural drainage of the upland plateau in the early 1900s. Avocado and citrus trees at La Conchita Ranch, planted in the 1930s and 1940s, cover approximately 415 acres of the plateau. During the 1930s, slope-parallel diversion berms were installed on La Conchita Ranch (La Conchita Ranch, 1988). These dirt berms divert runoff along

unpaved ranch roads to West Barranca. Flow is discharged into West Barranca from large corrugated pipes. During our field reconnaissance, we noted erosion and slope failures downslope of these stormwater outfalls. However, the berms appear to capture and divert much of the available surface runoff with no apparent evidence of significant surface runoff over the cliff edge.

6.3 Groundwater Infiltration and Recharge

Much of the upper La Conchita Ranch plateau is covered by shaly, silty-clay loam soils of the Santa Lucia soil series (Edwards and others, 1970; Grismer and others, 2000). These soils have a low associated infiltration rate (about one-half to two inches per hour) and low overall water holding capacity (less than 0.14 to 0.16 inches per inch of soil; Edwards and others, 1970). Despite the low infiltration rates, the extensive surface area of the plateau and inland slopes of the larger drainage basin likely results in substantial cumulative subsurface flow through the underlying loose deposits of the older debris flow material. As noted above, bedrock platforms present beneath the portions of the plateau cut by wave action likely serve as barriers to deeper infiltration. These gently seaward-sloping buried surfaces, capped locally by marine terrace sands, may also serve to enhance seaward subsurface flow as part of the regional groundwater gradient. This gradient is from high (coast range) to low (beach) and is generally parallel to the regional surface drainages, including the East and West Barrancas.

Infiltration of surface water also occurs within the large barrancas and gullies that drain the Study Area and greater drainage basin. For the most part, within the Study Area, this infiltration likely occurs at elevations well below that of the plateau as East and West Barrancas are deeply incised with gully floors at elevations several hundred feet below that of the plateau. However, infiltration within the barrancas landward, upslope, of the Study Area likely does contribute significant groundwater recharge.

Infiltration at the base of the cliff behind (landward) of La Conchita is associated with surface water runoff within gullies that drain the cliff face. Groundwater beneath La Conchita appears to consist of a thin zone of locally saturated, highly permeable marine terrace deposits resting on impermeable bedrock and capped by relatively clay-rich, low permeability debris flow deposits. Recharge of this zone appears to occur at the cliff front at the mouths of several large gullies incised into the hillslope. At these locations, abundant vegetation and, in some cases, flowing or standing water is common. Where water has been encountered in subsurface borings, it has been at or near the mouths of these drainages (Figure 6.1).

6.4 Groundwater Aquifers, Water Levels, and Subsurface Flow

Although some limited water-well data are available for the lower portion of the older, large landslides that compose the cliff area adjacent to La Conchita, information is lacking below the top of the cliff within the upper portion of the landslides. There are no active monitoring wells within the community of La Conchita or at the base of the cliff within the toe of the 1995/2005 landslides or older, larger landslide masses, with the exception of piezometers installed for this study. There is no direct information on possible shallow groundwater flow within the headscarp area of the older and active landslides. Groundwater conditions likely vary seasonally due to changes in runoff, tidal and storm conditions, rainfall, and other factors.

6.4.1 Groundwater beneath La Conchita Ranch

Multiple completion wells within bedrock and longer-term water level records are available upslope of the mapped landslides in the orchard area of La Conchita Ranch. These wells, primarily installed to

detect deeper groundwater flow, typically are screened over intervals within bedrock of the Monterey Formation and do not record shallow, near-surface flow in overlying deposits.

Much of the available groundwater information for the Study Area is derived from three deep dewatering borings (WB-1A, WB-2, and WB-3) drilled by Converse (1994). These borings were later converted to monitoring wells. WB-1A was drilled to a depth of about 320 feet in the hanging-wall of the Red Mountain fault. First water was encountered at a depth of about 180 feet, with progressively more water encountered to a depth of 296 feet at the top of bedrock. The hole was cased to a depth of about 294.5 feet. WB-2 was drilled to a total depth of about 160 feet. No groundwater was found and the hole was abandoned. WB-3 was drilled in the headscarp of the large downcoast landslide to a total depth of about 380 feet with bedrock of the Pico formation encountered at a depth of about 335 feet. Groundwater was present from about 157 feet below the ground surface, with water also encountered at depths of about 250 and 300 feet.

Converse (1994) postulated that two deep wells (WB-1A and WB-3) that encountered thick sediment, with saturated zones, were located within the same connected subsurface channel. In part, this assumption was based on the presence of the marine terrace at a consistent elevation of about 400 feet above sea level elsewhere beneath the plateau and orchard area. However, the Punta Gorda terrace deposits are not found beneath the entire plateau, and the elevation of the associated wave-cut platform is not consistently at the same elevation. The platform is offset across the fault and locally warped or missing landward of the cliff.

Our interpretation is that the 'paleochannels' identified by Converse (1994) are in fact locations where strands of the Red Mountain fault have superimposed thick sections of deposits. Evidence of a 'paleochannel' cited by Converse (1994) included thick deposits exposed in WB-3. However, as noted above, WB-3 is located in a large landslide and penetrates the Red Mountain fault. The Red Mountain fault 'repeats section', that is, the fault thrusts the buried debris flow and underlying paralic deposits over younger deposits. Repetition of the depositional sequence across the fault was documented in our boring WLA-B2 and inferred from the down-hole shear wave profile (Figure 4.3).

WB-1A, with poor sample recovery due to the air rotary drilling technique, none the less appears to have encountered gravel zones at depth. The boring likely also penetrated a landward (east) dipping strand of the Red Mountain fault and extended into younger sediments at depth. WB-1A encountered a clay seam at 156 feet, roughly the depth of the inferred east-dipping fault strand mapped for this study. Within the well, the 'paleosol' silt layer was encountered at 56-foot depth (roughly 635 feet above sea level). No terrace deposits were encountered.

More detailed logs of HSA-2, drilled downslope by Stoney-Miller Consultants (1996) within the same drainage/'paleochannel' mapped by Converse (1994), encountered approximately 70 feet of older debris deposits before refusal within bedrock. No terrace deposits were encountered. The bedrock consists of hard, light gray diatomaceous shale, thinly bedded and dipping approximately 30 degrees from horizontal. During drilling the shale was interpreted to be bedrock of either the Sisquoc Shale or the Pico Formation. We have mapped the buried shale as bedrock of the Sisquoc Shale, preserved within a structural block located between the two identified strands of the Red Mountain fault.

Within WB-3, a pump test showed that groundwater levels dropped fastest when the water level reached 200 feet depth (Bachman, 1998), or roughly 470 feet above sea level. Bachman (1998) interpreted this rapid drawdown to represent intersection of the water level with a nearby impermeable boundary, likely the nearby Red Mountain fault. Our interpretation is that WB-3 penetrated the fault at approximately this

depth (Appendix B; Figure B.6) and, as shown on Cross Section BB-BB', the pump test likely drained an isolated aquifer of buried marine terrace sands within a narrow structural block bounded by two strands of the Red Mountain fault.

The pump test removed over 2,700 gallons of groundwater from the hanging wall of the fault but apparently did not influence spring flow (roughly 0.1 gallon per minute) in the headscarp area located approximately 300 feet away in the footwall of the fault (Bachman, 1998). This does not mean, however, that water does not leak across the fault barrier and recharge the water level within the exposed terrace deposits in the 1995/2005 headscarp area. The short duration of the pump test may have been insufficient to reduce the uphill water supply from the aquifer across the fault or allow the downhill spring to drain the local perched aquifer that feeds springs in the headscarp region. Given the steady flow from the springs in the headscarp area, the down-dropped terrace deposits feeding the springs may be fairly laterally extensive seaward of the fault.

6.4.2 Groundwater in the Cliff Area

Parts of the cliff face landward of the community of La Conchita are covered by dense brushy vegetation that locally obscures the ground surface. However, vegetation typically is absent in over-steepened areas, including sides of erosion gullies and the scarps of recent landslides. The presence of near surface water and, in some cases, flowing springs coincides with distinct young, green vegetation locally present within hollows upslope of Ranch Road. These springs include flowing water within the headscarp area of the 2005 landslide, at approximately 400 feet above sea level.

Upcoast of the 2005 failure, the springs and areas of lush vegetation are found progressively lower on the slope above Ranch Road, coincident with colluvial hollows filled with loose, clayey material. These hollows, source areas for historical and pre-historic debris flows, commonly are aligned with steep gullies that drain to the base of the cliff below. These hollows generally are located upslope of the inferred buried trace of the Red Mountain fault. The springs flow within saturated slope deposits developed on the Sisquoc Shale, upslope of, and separated from Pico Formation bedrock by the fault. The associated drainages are blocked by fill placed along Ranch Road. Locally water within the drainages is diverted within piping placed by Ranch personnel and along the road surface.

Groundwater measurements within the cliff area are generally lacking. However, depth to water within the 1995 slide mass, obtained from open-standpipe piezometers at borings SMC-B15 and SMC-B16, was monitored biweekly after installation of the wells in December of 1997. Groundwater measurements from late 1997 through 1998 showed minimum depths of approximately seventy feet (with a water level elevation of 184 to 210 feet above sea level). The recorded water levels were below that measured in borehole MB-3 in the same general location prior to failure in 1995. In MB-3, groundwater was detected within nineteen feet of the ground surface and the water level elevation reached at least 230 feet above sea level, or approximately 20 to 46 feet above the post-slide groundwater levels measured in 1997/1998 (Figure 6.2).

6.4.3 Groundwater beneath La Conchita

Groundwater beneath the community of La Conchita is localized within buried marine terrace and beach deposits. These highly permeable deposits are thin (five to twenty feet thick), dip gently seaward, and are underlain by a wave-cut platform on underlying impermeable bedrock of the Pico Formation. Where water is present, saturated terrace deposits form a discrete groundwater zone ('perched water table') capped by overlying dry, clay-rich debris deposits. Based on available borehole and monitoring well

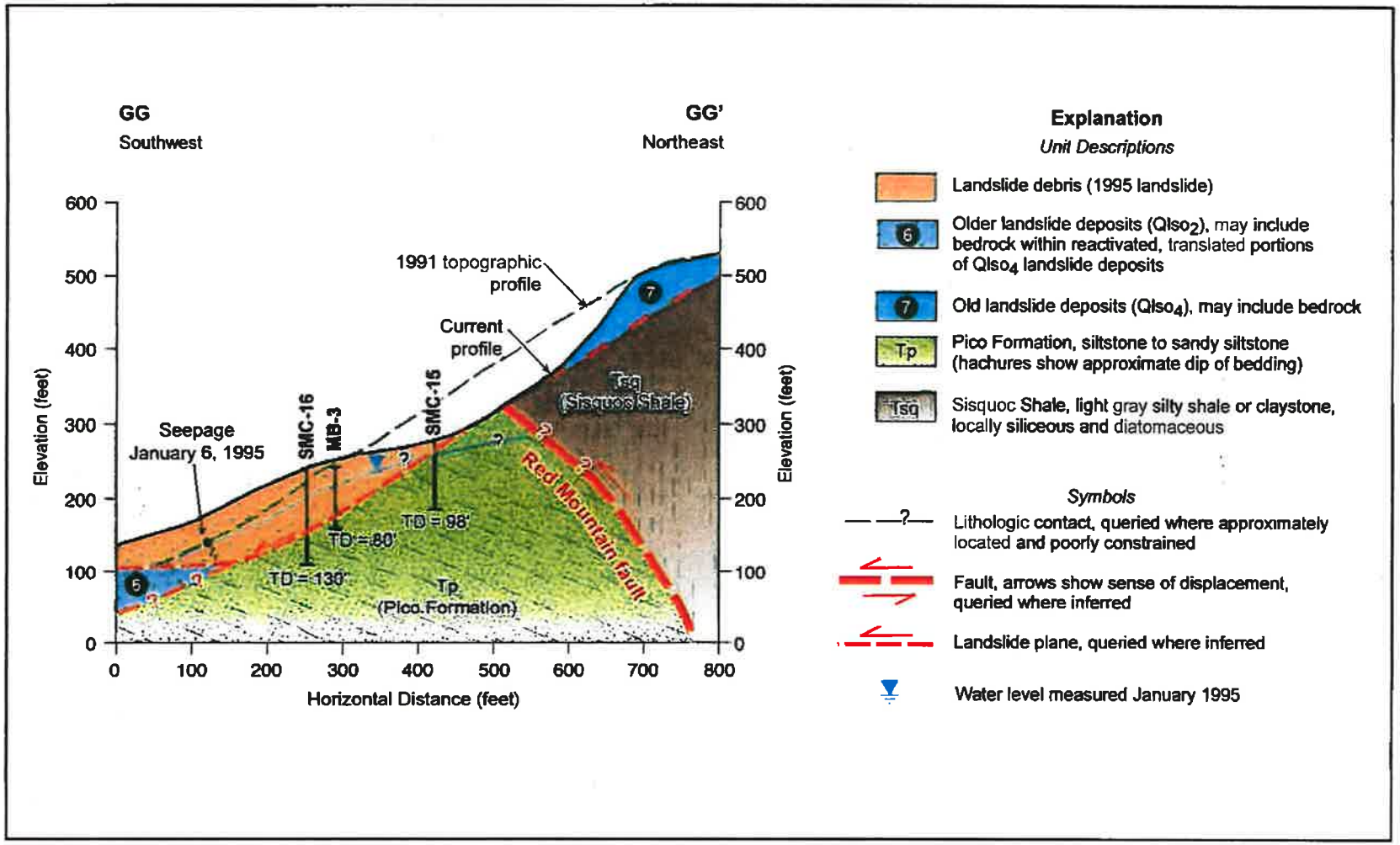

WLA

Geologic cross-section GG - GG' through 1995 landslide showing pre-failure water levels (see Figure B-1, Appendix B for location)

data, the saturated zone is discontinuous beneath La Conchita with much of the uphill (landward) portion of the community underlain by dry deposits. Within the buried deposits that do contain water, depth to the 'perched' groundwater likely is controlled by the thickness of overlying clay-rich debris and alluvial fan deposits and location relative to major gullies that provide recharge to the buried aquifer. This subsurface distribution of saturated sediment has important implications controlling the potential for liquefaction within the community.

Groundwater data from three monitoring wells at the La Conchita Mini Market at the intersection of Surfside Street and Santa Barbara Avenue (6905 Surfside Street), cited in Fugro West (2007), reported groundwater depths of approximately 15 feet below ground surface, at elevations above sea level of roughly 11 to 13 feet, from 2002 through 2004. Near the same location adjacent to Highway 101, Fugro West (2007) measured the elevation of the water table at an elevation of roughly 11 feet above sea level, based on multiple groundwater measurements. Caltrans (2002) reported groundwater levels at elevations of 11 to 13 feet above sea level in CPT explorations located on Highway 101 about a quarter mile north of La Conchita, near the outlet of West Barranca.

Groundwater elevations, within marine terrace and beach sand deposits preserved on the wave-cut top of underlying Pico Formation bedrock, therefore are relatively consistent along the portion of the coastal plain bounded by the beach and Highway 101. Locally, the groundwater gradient appears to be gradual and towards the beach (Fugro West, 2007). Beneath La Conchita, where encountered, groundwater is found at elevations of about ten to twenty feet above sea level. Where the buried deposits are saturated, within the perched groundwater zone, recharge likely occurs by percolation of surface and subsurface water at, or near, the base of the cliff. There is a relatively shallow groundwater mound beneath the central portion of Vista del Rincon, in the vicinity of Oxnard and Bakersfield Avenues. This zone of relatively shallow (forty to sixty foot deep) groundwater likely is related to the intersection of two gullies with extensive upslope vegetation. Based on available borings, the groundwater likely is localized within buried sands of the underlying marine terrace, and consists of a thin saturated zone on top of a relatively impermeable bedrock platform. However, groundwater recharge consisting of surface flow within the gullies and subsurface flow at, and within, the toe of the upcoast landslide likely is focused at this location.

An open, concrete-lined pit located on the uphill side of Vista del Rincon near the intersection with Oxnard Avenue contains undrained standing water (observed in February, 2008). This apparent water level is well above that measured within nearby well B-20 at an elevation of ten feet above sea level. Well B-20, converted from a large-diameter boring into a groundwater monitoring well, is located downcoast of the pit on Vista Del Rincon. The observed water level is also higher than the depth of water encountered at 46 feet (elevation of 25 feet above sea level) in nearby boring WLA-BA1. Following drilling, the water level in WLA-BA1 rapidly rose to a depth of 44 feet (elevation of 27 feet), suggesting that groundwater is confined at depth. Thus water within the pit likely does not represent the true depth of water beneath the ground surface but rather represents the piezometric surface of the confined water table. No drainage currently is available for near surface water from within the pit or for this area of apparent elevated water levels at the mouth of the cliff gully.

6.5 Influence of Red Mountain Fault on Groundwater Flow

Within the plateau at the top of the cliff, localized uplift and associated displacement of the buried permeable sands of the Punta Gorda terrace deposits appears to control seaward groundwater flow. Records of water levels encountered during drilling, borehole pump tests (within WB-3), and water-level

records from downhole monitoring devices provide information on groundwater elevations and possible flow in the vicinity of the fault.

In addition to separating permeable deposits, clay gouge along the fault strands is believed to serve as a local groundwater barrier. Geotechnical borings WB-3 and HSA-2 appear to have penetrated the Red Mountain fault. Within boring HSA-2, no consistent groundwater flows were documented but wet zones were encountered at depths of 19 and 59 feet (Leighton Associates, 1992). These wet zones are roughly coincident with the inferred subsurface intersection with the upper strand of the Red Mountain fault as mapped for this study.

Groundwater levels were not recorded in the immediate years prior to the 2005 failure. However, Stoney-Miller (1998) had noted that groundwater levels were generally constant in the vicinity of the 1995 failure for several years following 1995 with the exception of WB-3, the closest monitoring point to the 1995 landslides. Located on the plateau at the top of the cliff area, within the hanging wall of the Red Mountain fault, WB-3 is separated from the deposits exposed in the lower cliff by the fault. However, groundwater levels in WB-3 steadily rose after monitoring began in May of 1996. Stoney-Miller (1998) concluded that weathering-related obstruction of seepage in the scarp face exposed on the cliff face likely reduced flow paths. As noted above, Bachman (1998) concluded that the springs in the cliff are separated from the water level in well WB-3 by the Red Mountain fault and the two water levels likely are not directly connected. It is possible, based on our interpretation of two fault strands bounding the deep but relatively small aquifer penetrated by WB-3, that recharge of this aquifer may occur relatively quickly especially if groundwater flows preferentially along the fault strands at depth. More detailed groundwater monitoring, including additional piezometers across the faults at depth, would be required to test this model.

6.6 Inferred Groundwater Flow Paths

Converse (1994) concluded that buried channel provide pathways for flow beneath the plateau directly to, and within, the cliff area above La Conchita. Bachman (1998) provided a very different model that showed water-bearing sedimentary units beneath the plateau of La Conchita Ranch as hydraulically isolated (Bachman, 1998; Grismer and others, 2000). Our model incorporates the presence of the Red Mountain fault to explain the presence of thick gravel deposits that appear discontinuous at depth noted by both models. Groundwater likely consists of isolated water tables within thin but highly permeable units. These aquifers are segmented by fault displacement across the Red Mountain fault. However, it is possible that the water levels are somewhat interconnected as the fault is not a perfect impermeable barrier. Permeable terrace deposits are sufficiently thick that they may have some connectivity across the fault, even if locally offset. In addition, the basal slide plane of the downcoast landslide appears to cuts the fault, and the upcoast landslide plane, possibly forming a groundwater path from the terrace sands to the base of both landslides.

However, there appears to be no direct connectivity between the marine terrace deposits that underlie the plateau and those that underlie La Conchita. Rather a mixture of subsurface flow across the plateau with surface and near-surface flow within the cliff area allows for local groundwater recharge of the different hydrologic units. Minor fluctuations in groundwater elevation beneath La Conchita appear to coincide with daily tides. If tidal influence on groundwater beneath La Conchita can be documented, as suggested by anecdotal accounts of residents, connectivity of the terrace deposits beneath La Conchita may control flow paths towards the ocean.

7.0 HISTORICAL LANDSLIDES AND DEBRIS FLOWS

Reconstruction of the history of slope failures in the La Conchita Study Area provides valuable information on the past locations, types, and frequency of landslides and debris flows. As part of this study, historical accounts have been combined with interpretation of multiple sets of vintage aerial photographs, covering 1927 through 2007, to produce an inventory of past slope failures. This inventory of historical landslides and debris flows, although incomplete, provides the basis for evaluating both the likely locations and return periods of potential future failures.

In addition, because slope failure susceptibility is in large part dependent on precipitation, comparison of historical rainfall records with the dates of known slope failures provides useful information on likely triggering thresholds for slope failures from major storms. Because longer, more accurate historical records are available for rainfall amounts, the correlation of rainfall amounts, intensity, or duration to specific landslides or debris flows provides the basis for better predictive modeling of future rainfall-triggered slope failures. Such a detailed analysis is beyond the scope of this conceptual study but, to the degree possible, we have collected and presented available information on past slope failures and associated rainfall events.

7.1 Regional Landslide History

During the late 1800s and early 1900s, large storms battered the coast of Ventura but only limited accounts exist of associated coastal landslides. Pauline Gaynor, an early resident in the La Conchita area who grew up in a ranch house at the mouth of West Barranca just north of the current town, documented local events between 1901 and 1911 (Ventura County Historical Society (VCHS), Vol. 49, nos. 1 and 2). Although not a precise account, her memoirs note that *'once about every ten years the rains are very heavy and then the gullies coming from the canyons roar and boom with the water and boulders'*. She also remarked that *'the earth slid down the hills south of the school house several times'*, although locations of specific landslides or debris flows were not discussed (VCHS, 2005, p. 14). The school house was located on the fan of West Barranca, near the current railroad tracks.

Most of the published accounts of landslides are of damage to the coastal highway and railroad along the coast. The highway was built as a wagon trail circa 1865 (Hemphill, 2001). In one large landslide located south of La Conchita, approximately three miles northwest (upcoast) of Ventura, landslide debris moved four tenths of a mile seaward within a large canyon, covering the wave-cut platform at the base of a sea cliff (Figure 7.2; Putnam and Sharp, 1940). The debris formed a low hill blocking the canyon mouth. The slide likely occurred in 1875 and buried the original coast highway (Darton, 1915; Putnam and Sharp, 1940). A large cut was required to make room for the rebuilt coastal highway.

Figure 7.1 View to southeast from the former school house adjacent to the West Barranca of the coastal plain currently occupied by the community of La Conchita, vintage 1903-1911 (VCHS, 2005). Note the undulatory landscape composed of broad debris flow fans.

The coastal rail line was built through La Conchita in 1887 (Hemphill, 2001). Sections of the newly constructed railroad tracks were first buried by landslides between La Conchita and Rincon Point in 1889, based on accounts in the Ventura Free Press (Hemphill, 2001). In 1892, north- and south-bound trains were delayed by a landslide at Rincon, north (upcoast) of La Conchita, that blocked the tracks (Los Angeles Times, January 24, 1892). A decade later, in 1903, a major train derailment causing forty-five injuries occurred at Punta Gorda, near La Conchita (Los Angeles Times, May 30, 1903). The exact location of the wreck is approximate and the cause unknown, but the call for help required a three-mile hike north to the nearest telegraph station in Carpinteria and the relief train from Ventura that reached the wreck was stopped at Punta Gorda.

Another major accident caused by massive landsliding occurred north of Punta Gorda in 1909, taking the lives of four train company workers clearing the tracks of debris (Hemphill, 2001). Reported in extensive detail in the January 23rd edition of the Los Angeles Times, the landslide originated 'from a point hundreds of feet up on the mountainside' and took thirty seconds to inundate the tracks, reaching 'the ocean's brink' (Los Angeles Times, January 23, 1909). The source of the landslide was apparent, as the slide caused a 'tremendous hole in the high side of the mountain, looking as though the earth and rocks below had been scooped out by a mighty hand and cast on the tracks'.

Until the slide was repaired, passengers in south-bound trains disembarked in Benham, 'a mile north of the slide', and walked around the wreck of the buried work train, 'knee deep in the slimy mud, and in some places through the surf' (Los Angeles Times, January 25, 1909). The California Mining Bureau (1917), cited in Durham (2000), shows a small town called Benham located along the railroad about halfway between Carpinteria and the Santa Barbara-Ventura county line, in the vicinity of Rincon Point. Darton (1915) noted that the railroad crossed Rincon Creek at Benham.

One mile south of Rincon Creek, a set of prominent landslide scars, distinguished by small canyons, is present within the near-vertical sea cliffs along the coast. Located within a small canyon less than a mile north (upcoast) of La Conchita (likely geographic coordinates 34.373910°, -119.1458386°), CGS (2003) mapped these features as a large landslide within the Sisquoc Formation. The uphill headscarp of the landslide is bounded by the Red Mountain fault.

Later that same year, after several days of rain in March of 1909, a watchman died of a heart attack rushing to the scene of 'a slide of mud over the tracks of the Coast Line at Punta Gorda' (Los Angeles Times, March 26, 1909). The slide delayed trains for several hours until the debris could be cleared. The LA Times noted that Santa Barbara County had already broken the record in 1909 for a single season's rainfall, greater than the previous record rainfall of 34 inches recorded in Santa Barbara in 1884.

Repair of the 1909 landslide in 1910 required hydraulic mining equipment to sweep the debris into the ocean and over 1,300 railcars of imported boulders for a 2,400-foot-long fill embankment, that was over eighteen feet wide and ten feet high (Los Angeles Times, September 28, 1910). An even larger embankment and associated seawall completed in 1914 extended from Rincon Point to La Conchita. Sixty-foot piles were required in the La Conchita section of the seawall for embedment in the underlying bedrock (Los Angeles Times, December 24, 1914). A massive seawall over 6,400 feet long along the coastal highway, requiring nearly 16,000 cubic yards of concrete, was completed by CALTRANS in 1924. However, in 1926 high seas and localized slope failures washed away the earth behind the retaining wall of the second causeway of the 'Rincon grade' of the Coast Highway (Los Angeles Times, February 14, 1926). The La Conchita Dancehall also was swept away by high surf.

In the winter of 1937-1938, parts of southern California were flooded twice. During December 9-12, 1937, an intense storm moved rapidly from the northern Pacific across California and caused widespread flooding (Putnam and Sharp, 1940). In late January 1938, a pattern of almost continuous, and frequently intense, rainfall developed in southern California and culminated in a series of storms that affected an area much farther south than usual (Troxell and others, 1942). Rainfall in the Transverse Ranges from February 27 to March 4 averaged over twenty-two inches. In early March of 1938, a slow-moving warm storm resulted in near-record rainfall at Ventura, with over four inches falling in twenty-four hours on March 2 and 3 (Putnam and Sharp, 1940).

The pervasive impact of the storms on the coast was noted by Putnam and Sharp (1940) with the following: '*On some slopes in the Ventura region virtually every square foot of surface mantle has been moved by the earthflows originating in 1938*'. Putnam and Sharp (1940) noted several major coastal slides northwest of Ventura, southeast of (downcoast of) La Conchita (Figure 7.2). During this period, based on examination of aerial photography, substantial movement occurred within colluvial hollows upslope of the Ranch Road above La Conchita and a debris flow occurred with La Conchita.

More recently, in 1941, an M5.9 earthquake caused a large landslide near the Santa Barbara-Ventura County line, disrupting telephone communication and forcing auto traffic to one-way travel for more than two hours as the landslide covered part of the highway (Santa Barbara News Press, Vol. 78, no. 243, Jul. 1, 1941). Trains were also delayed because of repairs to the tracks. Telephone communications between Santa Barbara and Ventura also were disrupted, presumably because of the slide. Based on examination of available aerial photography, a large recent landslide with fresh scarp is present near the county line. No other historical accounts mention earthquake-triggered slope failures in the immediate vicinity of La Conchita, with the possible exception of accounts of small landslides observed along the railroad following the 1925 Santa Barbara earthquake (Kirkbride, 1927). From Santa Barbara to Ventura, the

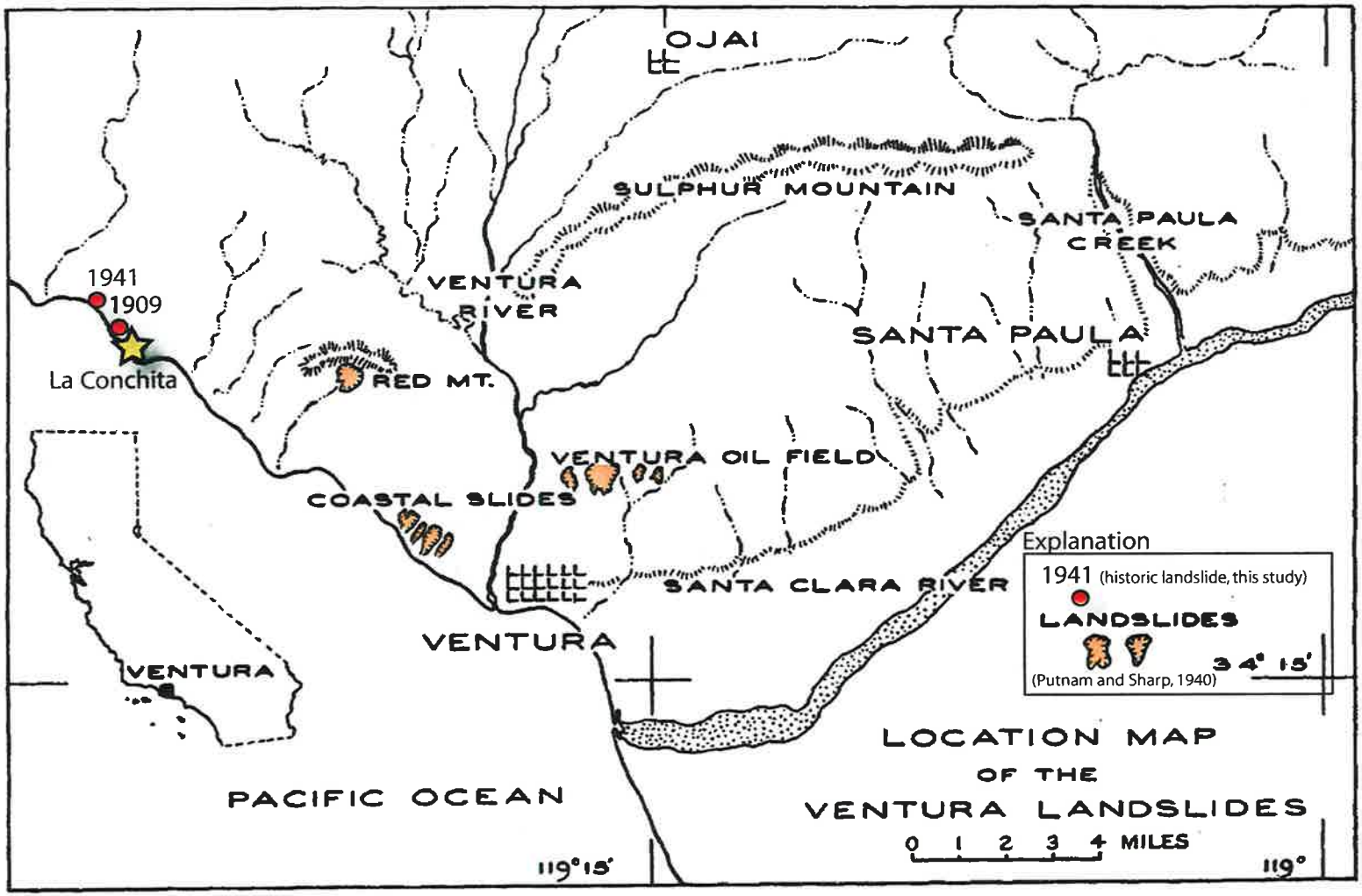

1937-1938 landslides mapped by Putnam and Sharp (1940), and additional slides located for this study based on historic accounts

LA CONCHITA LANDSLIDE – PHASE 2
Figure 7.2

02 JAN 08, 1885, RBZ

earthquake damage was 'largely confined to slides impinging on the track, which had to be cleaned away' (Kirkbride, 1927). However, locations of these smaller landslides were not documented in published accounts of the earthquake damage.

Historical accounts note similar earthquake-related slope failures in the greater Santa Barbara – Ventura region. During the 1925 Santa Barbara earthquake, landslide damage in the Hope Ranch area of Santa Barbara closed the railroad. The slide consisted of approximately 40,000 cubic yards of earth that moved a distance of thirteen feet toward the main rail tracks (Kirkbride, 1927). Strong ground shaking caused by the 1952 Kern County, California earthquake on the White Wolf fault at the south end of the San Joaquin Valley caused a large section of the cliff to collapse onto the beach at Hope Ranch Beach in Santa Barbara (Santa Barbara News Press, Jul. 21, 1952). Minor slides also were noted in San Marcos Pass but there were no reports of damage in the La Conchita area.

Harp and others (1978) noted that the M5.1 earthquake of August 13, 1978, caused settlement of a railroad fill embankment near Ellwood, west of Santa Barbara, resulting in a train derailment. However, aside from rockfalls that blocked San Marcos Pass, the only natural slope failures documented for this earthquake were small rockfalls in bedrock of the Sisquoc Shale and Monterey Formation in coastal cliffs near Santa Barbara and Goleta Point.

7.2 Landslide History of the La Conchita Study Area

The history of past landslides and debris flows in the La Conchita Study Area is based on interpretation of historical aerial photographs, accounts obtained from geotechnical reports, and available memorandum reviewed at the office of James O'Tousa, Ventura County Geologist. Within the La Conchita Study Area, individual landslides and debris flows in the walls of East and West Barranca are poorly documented. Most of the observed failures documented in County records, by residents, and by Ranch personnel occurred along Ranch Road on the cliff or at the base of the cliff behind residences. These locations, where known, are listed on Table 7.1 and shown on Figure 7.3. Ranch Road has been obstructed by smaller undocumented debris flows over the years. In part, berms built along the margin of Ranch Road have served to prevent debris within minor failures from flowing downslope. Where documented in Ranch and County correspondence, records of debris removal during maintenance of the road provides approximate constraints on the amount of material displaced from upslope during slide failures.

2005 photograph by Woodrow Higdon. See Table 7.1 for key to historic slope movement locations (shown as numbered locations).

Table 7.1 Documented Historical Slope Failures within La Conchita Study Area (See Figure 7.3 for locations).

Key	Date	Location	Source	Type of Failure
1	December, 1937	Vista del Rincon between Oxnard and Bakersfield Avenues	Ventura County Survey	Debris Flow
2	March 30, 1978	Ranch Road in area of 2005 slide	County of Ventura documents	Shallow landslide
3	March 30, 1978	Upslope of 6951 and 6955 Vista Del Rincon	County of Ventura documents	Debris Flow
4	March 30, 1978	Ranch Road in area of 2005 slide	County of Ventura	Debris Flow
5	December 22, 1987	Upper Ranch Road	LC Ranch letter	Shallow landslide
6	January 17, 1988	Upper Ranch Road	LC Ranch letter	Shallow landslide
7	September 17, 1989	Keller slide at base of slope, near Vista Del Rincon	LC Ranch correspondence	Shallow landslide
8	June 18, 1991	Upslope of 6835 and 6827 Vista Del Rincon	County of Ventura documents	Shallow landslide
9	February 14, 1992	Upslope of 6809 and 6823 Vista Del Rincon	County of Ventura	Shallow landslide
10	February 21, 1992	Upslope of 6873 Vista Del Rincon	County of Ventura	Shallow landslide
11	February 10, 1993	Lower Ranch Road above 6993 Vista Del Rincon	County of Ventura	Shallow landslide
12	March 4, 1995, 2:40 pm	Above Ranch Road to base of slope	Multiple eyewitness accounts, Stoney-Miller (1998)	Debris Flow
13	March 4, 1995	Above Ranch Road to Vista del Rincon	Multiple eyewitness accounts, O'Tousa (1995)	Deep landslide
14	July 3, 1995	In vicinity of 6809 and 6825 Vista Del Rincon	County of Ventura	Shallow landslide
15	February, 1998	Ocean View Road, north of La Conchita	Dames and Moore (1999)	Shallow landslide
16	January 10, 2005	Above Ranch Road into La Conchita	Multiple eyewitness accounts, Jibson (2005)	Shallow landslide
17	November 7, 2005	West Barranca	County of Ventura	Shallow landslide

7.2.1 1937 and 1938 Landslides (Debris Source Areas A, B, C, and D)

During the period between December 9th and 12th of 1937, an intense storm moved rapidly from the northern Pacific across California and caused widespread flooding. Within La Conchita, a large debris flow spilled into the community from the hillside above the intersection of Oxnard Avenue and Vista Del Rincon, from within debris flow source 'D' (Figure 7.3). A topographic map of the flow debris constructed by Ventura County is dated December 1937, drawn at a scale of one-inch to twenty feet, and retraced in February of 1938 (Ventura County Map #31600, provided by David Orr, La Conchita Ranch).

The map shows the western edge of the 'recent build up' along Oxnard Avenue, and the eastern edge along the range front with the 'line of principal flow' trending south along the range front before turning southwest, between Bakersfield Avenue and the ally to the east (Figure 7.4). Additional flow arrows suggest that flow also came in from the gully downcoast. At least seventeen parcels, and likely more,

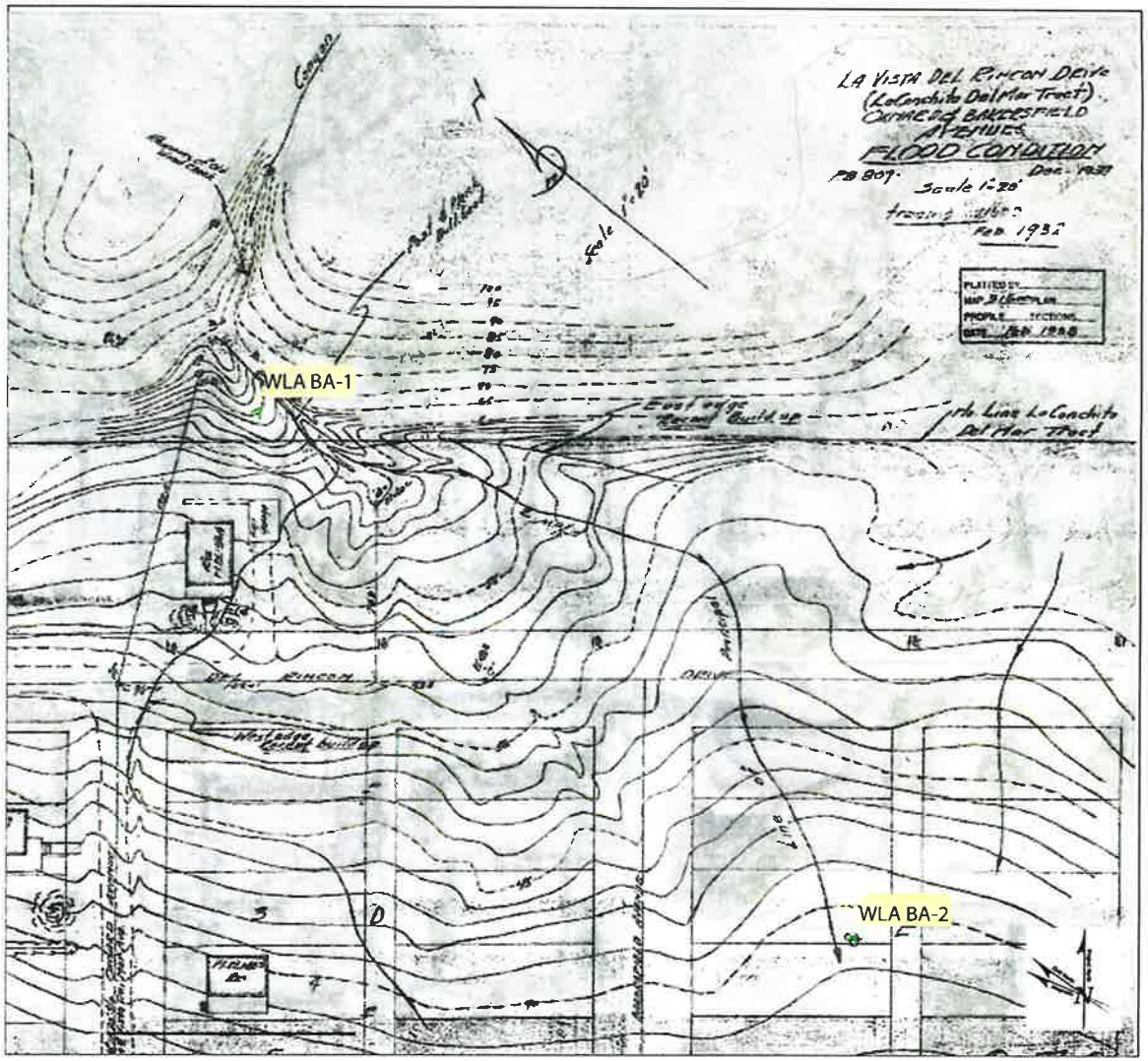

County of Ventura Map: Dated December 1937, drawn at a scale of one-inch to twenty feet, and retraced in February of 1938.

1937 Topographic Survey Map showing Depositional Area of Debris Fan

were covered by the debris flow. This debris flow can be seen on historical aerial photographs (Figure 7.5).

7.2.2 1969 Debris Flows (Debris Source Area A)

Interpretation of aerial photographs dated March 31, 1969 (Table 7.2), indicates that debris flows from source area A (Figure 7.3) may have crossed Ranch Road and extended several tens of feet downhill. The volumes and extent of the flows are unknown.

7.2.3 1978 Debris Flows (Debris Source Areas A and B)

Movement in debris source areas A and B (Figure 7.3), and associated debris that extended across Ranch Road, was documented by Blaise Cilweck (County of Ventura Senior Engineering Geologist) on March 30th, 1978 (unpublished files at Ventura County Public Works, 1978). The failure in area A consisted of a 120 by sixty feet wide slide that partially covered Ranch Road. The failure in area B consisted of a fifty- to seventy-foot-wide and 360-foot-long shallow slide that produced debris that extended across, and sixty feet downslope of, Ranch Road. Based on interpretation of color aerial photographs dated March 13, 1978, similar but less laterally extensive downslope displacement occurred in the other debris source areas (Table 7.2).

7.2.4 1987 and 1988 Debris Flows (Debris Source Areas A, B, C, and E)

A letter from David Orr to the County of Ventura dated January 27, 1988 noted that debris flow areas fed by springs on the hillside above Ranch Road had produced increased debris on the road in the previous several years. The Ranch stockpiled the slide debris along the roadside and then hauled the debris out to West Barranca (La Conchita Ranch, Letter to Joe Hanna, Ventura County Public Works, 1988). Based on examination of available aerial photographs (Table 7.2), movement within debris area E occurred between December 10, 1986 and June of 1987. The slope movement within source area E (Figure 7.3) occurred in a previously stable area with no established downslope gully.

On December 22, 1987, a large slide covered the entire road for a length of about eighty feet and was prevented from flowing downhill by a berm on the downhill side of Ranch Road. This slide required seven days to remove using a dump truck and front-end loader (La Conchita Ranch, 1988). A smaller slide occurred on January 17, 1988 blocking a drainage channel uphill of Ranch Road.

7.2.5 1989 Landslide (Keller Landslide)

A mudflow located near the toe of the slope in the vicinity of the intersection of Ojai and Vista Del Rincon was identified in early 1989 following heavy rains. This mudflow was associated with a ten-foot-high scarp in a strip cleared of vegetation on the lower cliff face. The slide was approximately five feet thick and had a total surface area of about 600 square feet (memo to David Orr, La Conchita Ranch, from Geotechnical Consultants (GTC) dated December 6, 1989). The slide mass was wet with associated flowing water from the toe when first identified in early September of 1989.

Continued movement of shallow slides behind 6835 and 6827 Vista Del Rincon was noted by Joe Hanna of Ventura County (Ventura County Water Resources and Development Department, 1991) and damage to hillside retaining walls was noted by Jim Fisher of Ventura County Development and Inspection Services behind 6873 Vista Del Rincon (Ventura County, memorandum dated December 12, 1991). In 1992, Fisher noted two additional homes threatened by landslides at 6809 and 6823 Vista del Rincon adjacent to each other and located between the existing failure at 6873 and the growing failure behind the

Table 7.2 Summary and evaluation of historic aerial photography for the La Conchita Study Area.

Year	Date	Source	Scale	Vertical/Oblique	Color/B&W	Flight Line: Frames	Photo Resolution	Project Relevance	Comments
1927	03/25/27	Fairchild, flown for Standard Oil°	1:15,000	Vertical	B&W	C-139: A1, A2, A3	Good	High	Whittier College Job 2702: 'old' debris fans visible beneath Oxnard and Zelzah Aves.
1929	01/01/29	Fairchild°	1:31,680	Vertical	B&W	A25, A26	Good	High	Older Oxnard Ave. debris fan clearly visible, house at fan apex.
1939	01/09/39	Soil Conservation Service (?)	1:24,000	Vertical	B&W	C4950: F156, 157, 158	Excellent	High	Approx. 15-20 houses, ranch road, gullies deeply incised.
1944	11/27/44	Military (?), Restricted°	1:7,200	Vertical	B&W	C9113: 72,73,74	Good	High	Hillside slide (above ranch road, above Santa Paula Ave), fan covers Oxnard Ave, house at apex missing.
1945	11/13/45	UC-Santa Barbara	1:14,400	Vertical	B&W	C9800: 14-1451, 14-1452	Excellent	High	Deposits on fan east (south) of La Conchita (from 1938/39?).
1947	08/20/47	Harry Tubis, Inc for USGS*	1:24,000	Vertical	B&W	GS-EM: 5-04, 5-05	Good	Moderate	Partial coverage of northern La Conchita, fault visible in West Barranca.
1948	07/30/48	Soil Conservation Service (?)°	1:12,000	Vertical	B&W	C12790: 9-32, 9-33	Excellent	High	Minor slump, headscarp area of 1995 slide, tank in downhill gully. 20+ houses.
1953	07/12/53	Soil Conservation Service°	1:22,000	Vertical	B&W	AXI-5K: 15,16	Poor	Moderate	Berms on ranch, first seen on 1948 photo, additional on 1953 photo. Oxnard Ave. regraded.
1954	05/04/54	Unknown (obtained from LCR)°	1:20,000	Vertical	B&W	BTM-10X: 185, 186	Poor	Moderate	Apparent movement of slump above ranch road, above Sunland Ave.
1957	03/07/57	Unknown (obtained from LCR)°	1:9,600	Vertical	B&W	HA-AX: 5	Good	High	No stereo coverage. Additional ranch berms.
1957	10/22/57	Unknown (obtained from LCR)°	1:9,600	Vertical	B&W	HA-AV: 21,22,24	Good	High	Minor incision in gullies, no other change, apparent expression of Red Mtn. fault. >55 houses.
1959	08/22/59	Soil Conservation Service	1:24,000	Vertical	B&W	AXI-12W: 114, 115	Poor	Moderate	Vegetation visible in slumps above ranch road, above Santa Paula and Sunland Aves.
1961	07/05/61	Soil Conservation Service (?)	1:18,000	Vertical	B&W	BRM-7BB: 111	Poor	Low	No stereo coverage. Vegetation still present in slumps.
1963	01/07/63	Mark Hund Aerial Surveys*	1:30,000	Vertical	B&W	HA-RR: 55, 56	Good	Moderate	Minor erosion in headscarp area of 1995/2005 slides.
1963	03/21/63	Unknown (obtained from LCR)°	1:6,000	Vertical	B&W	VII-Ven: 1-7 to 1-10	Good	High	Apparent movement (fresh scarps) of slumps above ranch road, Santa Paula and Sunland Aves.
1964	02/14/64	Mark Hund Aerial Surveys*	1:20,000	Vertical	B&W	HA-WE: 97 - 100	Good	Moderate	No coverage of La Conchita.
1964	02/17/64	Mark Hund Aerial Surveys°	1:24,000	Vertical	B&W	HA-WE: 348, 349, 272, 273	Poor	Low	No observable change.
1964	04/05/64	Unknown (obtained from LCR)°	1:9,600	Vertical	B&W	238V: 146, 147	Excellent	High	Minor erosion in hillside gullies, vegetation in slumps above ranch road less than previous years.
1966	04/13/66	Unknown (obtained from LCR)°	1:18,000	Vertical	B&W	266V: 95	Good	Low	No stereo coverage. Vegetation still present in slumps.
1967	05/14/67	Unknown (obtained from LCR)°	1:22,000	Vertical	B&W	BTM-1HH: 3, 4	Good	Moderate	Possible slump into ranch road below 2005 slide failure.
1967	11/27/67	Unknown (obtained from LCR)°	1:12,000	Vertical	B&W	TA-DS: 1,2,8	Good	Moderate	Vertical cut above ranch road below slide failures, slide removed (?).
1969	02/06/69	Unknown (obtained from LCR)°	1:6,000	Vertical	B&W	HB-NX: 142, 143	Good	High, significant rainfall	Small debris fans east (south) of La Conchita, Debris at base of 1995 slope, diversion structure below tank.
1969	02/13/69	Unknown (obtained from LCR)°	1:12,000	Vertical	B&W	HB-NX: 386, 387	Poor	High	Slump, indentation above ranch road below 2005 slide failure.
1970	12/10/70	Unknown (obtained from LCR)°	unknown	Oblique	B&W	HO-EQ-4	Poor	Moderate	Oblique view looking north above Pitas Point.
1974	01/14/74	Pacific Western Aerial Surveys	1:18,000	Vertical	B&W	PW-VEN: 147-152	Poor	Low	Coastline south of La Conchita.
1974	05/10/74	CALTRANS°	1:4,800	Vertical	B&W	7-VEN-101: 1-147, 148	Excellent	High	Partial coverage of southern La Conchita, minor debris on fans east (south) of La Conchita.
1975	02/06/75	Pacific Western Aerial Surveys°	1:20,000	Vertical	B&W	PW-4857: 1, 2	Good	Moderate	Vegetation visible in headscarp area of 1995 slide with minor erosion/incision.
1975	02/23/75	Unknown (obtained from LCR)°	1:9,600	Vertical	B&W	HB-XQ-131, 132	Poor	Moderate	Covers northern La Conchita.
1976	01/27/76	Pacific Western Aerial Surveys°	1:20,000	Vertical	Color	PW-5371: 25	Good	Low	No stereo coverage, no observed change.
1976	04/23/76	Pacific Western Aerial Surveys(?)°	1:12,000	Vertical	Color	NOS-23March76B	Good	Moderate	Minor vegetation in slumps, erosion unchanged.
1978	**03/13/78**	**Pacific Western Aerial Surveys**	1:12,000	Vertical	Color	PW7175:6,7	Good	High, significant rainfall	Erosion of 1995/2005 headscarp, deposition on fans to south, erosion/movement of slumps above ranch road.
1978	08/24/78	USDA	1:20,000	Vertical	Color	C615070: 678-1, 2	Poor	Moderate	Evidence of erosion from earlier storms, ranch is cleared terrain.
1981	06/15/81	Pacific Western Aerial Surveys	1:18,000	Vertical	Color	PW-VEN: 3-182, 183	Good	High	Growth of trees on headscarp area obscures topography, previous deposition on fans south is small, thin.
1984	06/09/84	Unknown (obtained from LCR)°	1:30,000	Vertical	Ifra-red	C341805:131-67, 68	Poor	Low	Renewed vegetation in slumps upslope of ranch road.
1986	04/20/86	Western Aerial Surveys	1:24,000	Vertical	B&W	WAC-85CA: 20-99, 20-100	Poor	Low	No observable change. Possible expression of Red Mt. fault across cliff face.
1986	12/10/86	Pacific Western Aerial Surveys°	1:22,000	Vertical	Color	PW-VEN: 5-20, 5-21	Good	Moderate	No stereo coverage.
1988	**05/27/88**	**Pacific Western Aerial Surveys°**	1:9,600	Vertical	Color	PW30630:1,2	Excellent	High	Slump above ranch road extends across road, uphill of Bakersfield Ave. Vegetation/seepage in other slumps.
1988	6/2/88	Pacific Western Aerial Surveys°	1:9,600	Vertical	Color	PW30630:3	Excellent	Moderate	No stereo coverage.
1989	05/23/89	Pacific Western Aerial Surveys°	1:18,000	Vertical	Color	PW-VEN: 7-170	Good	Low	No stereo coverage
1989	10/05/89	Pacific Western Aerial Surveys°	1:6,000	Vertical/Oblique	Color	PW35828: 2,3,4,5,6,8	Good	High	Vegetation within all slumps. 'Cliff' within 1995/2005 failure area above ranch road, apparent erosion.
1991	03/07/91	Pacific Western Aerial Surveys°	1:6,000	Vertical	B&W	PW: 1,2	Excellent	High, significant rainfall	Apparent slump, debris above ranch road in 1995/2005 failure area.
1992	11/01/92	Pacific Western Aerial Surveys°	1:20,000	Vertical	Color	PW-VEN: 9-169, 170, 209	Excellent	High	Vegetation visible in slumps above ranch road, above Santa Paula and Sunland Aves.
1994	11/29/94	Pacific Western Aerial Surveys	1:18,000	Vertical	Color	PW-VEN: 11-208, 209, 169	Excellent	Moderate	Increased vegetation in spring areas.
1995	**03/06/95**	**Pacific Western Aerial Surveys**	1:12,000	Vertical	Color	PW-999: 70-1, 3	Excellent	High	Post-1995 slide, significant erosion, movement of slumps above Santa Paula, Sunland, and Bakersfield Aves.
1995	08/30/95	Pacific Western Aerial Surveys	1:24,000	Vertical	Color	PW57016: 1	Excellent	Low	No stereo coverage. Minor vegetation growth.
1996	01/08/96	Pacific Western Aerial Surveys	1:20,000	Vertical	Color	PW-VEN: 12-170	Excellent	High	No stereo coverage. Minor vegetation growth.
1998	**02/26/98**	**Pacific Western Aerial Surveys**	1:9,600	Vertical	Color	PW64653: 1-1, 1-2	Excellent	High	Minor erosion in headscarp area of 1995/2005 slides. Minor debris on fans east (south) of La Conchita.
2005	**03/28/05**	**IK Curtis**	1:4,800	Vertical/Oblique	Color	-	Excellent	High	Post-2006 debris flow. Significant erosion and slope movement.
2006	**06/29/06**	**Air Photo USA**	1:2,400	Vertical	Color	-	Excellent	High	Used as base map.

° Obtained from La Conchita Ranch (LCR)
* Available from UC Santa Barbara Map and Imagery Library
in bold - purchased, this study

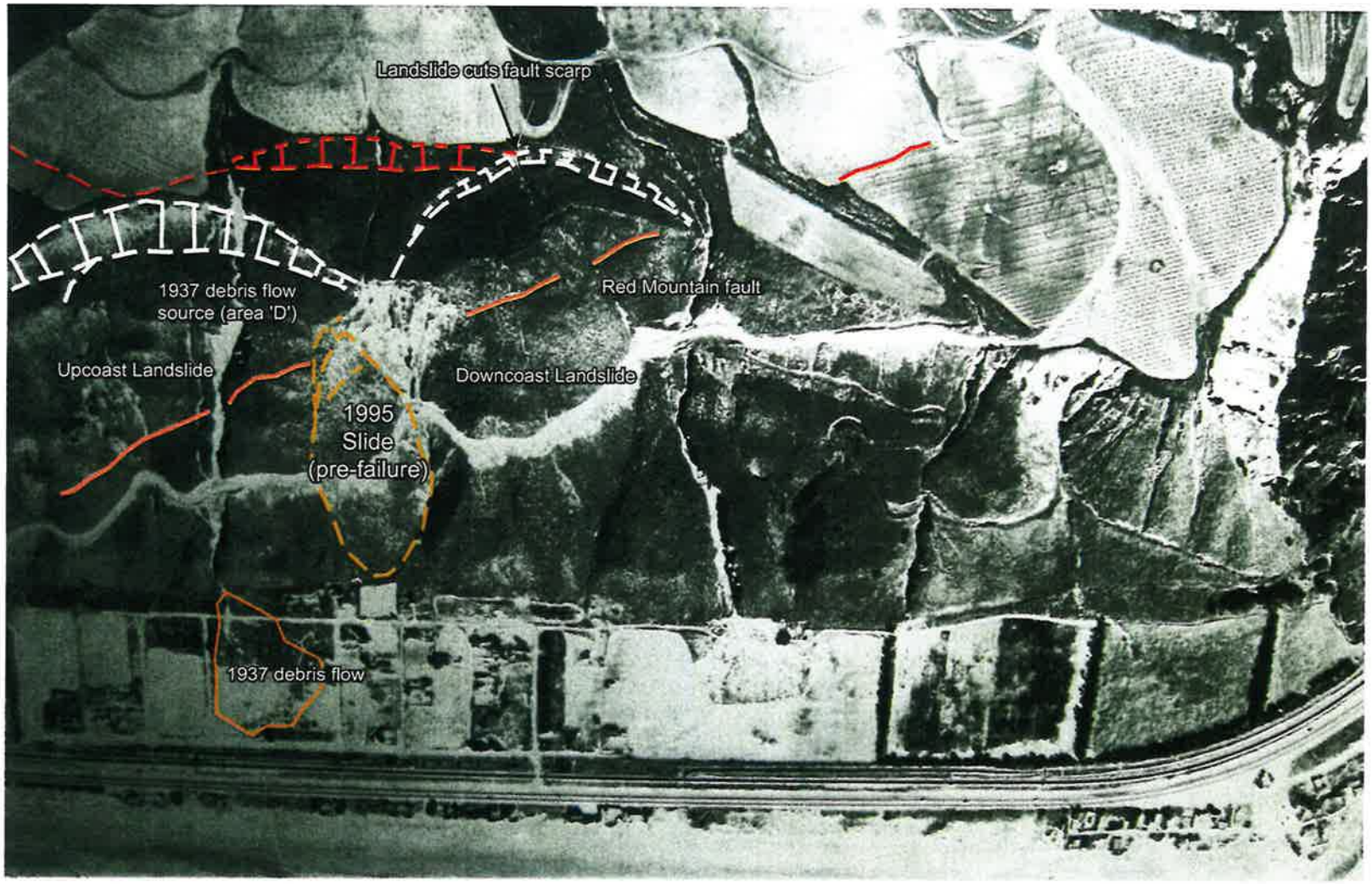

WLA

Annotated 1939 aerial photograph showing intersection of two older slides

LA CONCHITA LANDSLIDE – PHASE 2
Figure 7.5

02 JAN 08, 1885, RBZ

horse and mule corral. At this time the lateral margin was 100 feet from the structure at 6809 (Ventura County, memorandum dated February 14, 1992)

7.2.6 1993 Debris Flow (Debris Source Area A)

In early February of 1993, Dale Town of the Building and Safety Department of Ventura County and Jim Fisher, County Geologist, documented mudflow failure onto Ranch Road above Vista Del Rincon, near the intersection with Santa Paula Avenue (Ventura County, memorandum dated February 10, 1993). The origin of this mudflow was within the debris source area A (Figure 7.3). The mudflow was associated with a sixty-foot-wide scarp based on annotated field photographs examined at the County of Ventura offices. La Conchita Ranch personnel removed the debris covering portions of Ranch Road. A two-foot-high berm was constructed along the downhill side of the road to catch additional debris.

Despite the presence of the berm, Jim Fisher (Ventura County geologist) noted a potential for debris to cross the road and reach the town below if 'the entire failed mass 'let go' at once' (Ventura County, 1993). Fisher also noted topographic evidence of older debris flow deposits below the road, above the home located at 6993 Vista del Rincon. These pre-existing deposits likely are from the 1969 and 1978 debris flows noted above, or possibly the less-well documented debris flows of 1937 and 1938.

7.3 1995 Landslides and Debris Flows

The 1995 La Conchita landslide occurred on March 4, 1995. At about 2:40 pm, a section of the cliff near the top of the slope began sliding and a debris flow filled the gully, covering Ranch Road, and mantling the lower portions of the existing block landslide (Stoney-Miller, 1998). Apparently the debris did not reach Vista Del Rincon. According to eyewitness accounts, approximately twenty minutes after the debris flow, the main body of the landslide failed as a coherent block (Figure 7.6; GTC memorandum dated March 8, 1995; Stoney-Miller, 1998). The second slide buried Vista Del Rincon Drive in the vicinity of San Fernando Avenue. Instrumentation on a ten-inch diameter oil pipeline buried along Ranch Road, operated by Operators Offshore, appears to have recorded both slides.

Prior to failure, in June of 1994, initial movement of the block landslide was detected and identified as reactivation of an older landslide. The landslide impacted about 400 linear feet of Ranch Road, as recorded in the asphalt (Converse, 1994). New groundwater seeps at the toe of the slide mass were first reported in September of 1994 (Converse, 1994). The seeps were located adjacent to the existing gully at approximately 120 ft elevation and coincided with bulging of the slide toe into the gully.

Piezometers were installed in the incipient landslide mass in October of 1994 by Converse (1994). MB-1A was placed in the center of the slide mass and cased to a depth of 148 feet for emplacement of an inclinometer. Although no water was encountered during drilling, minor seepage of groundwater was noted into the well about one week after drilling (Converse, 1994). Groundwater was measured at a depth of about 110 feet (125 ft elevation) in MB-1 later. MB-2 drilled on Ranch Road about thirty feet within the east bounding lateral shear of the landslide was cased to a depth of 79.6 feet within displaced bedrock of the Pico Formation and remained dry throughout measurements. Although initially dry, well MB-3 located on Ranch Road about thirty feet within the eastern margin of the slide, and cased to a depth of 77 feet, filled with water. Initial measurements in October of 1994 showed that groundwater was about twenty feet below the top of the well (at an elevation of 230 feet) in boring MB-3, located on the downcoast portion of the landslide near the main gully. MB-4 was installed in the toe area of the slide and cased to 90 feet. Groundwater was encountered at a depth of 71 feet (24 ft elevation), roughly

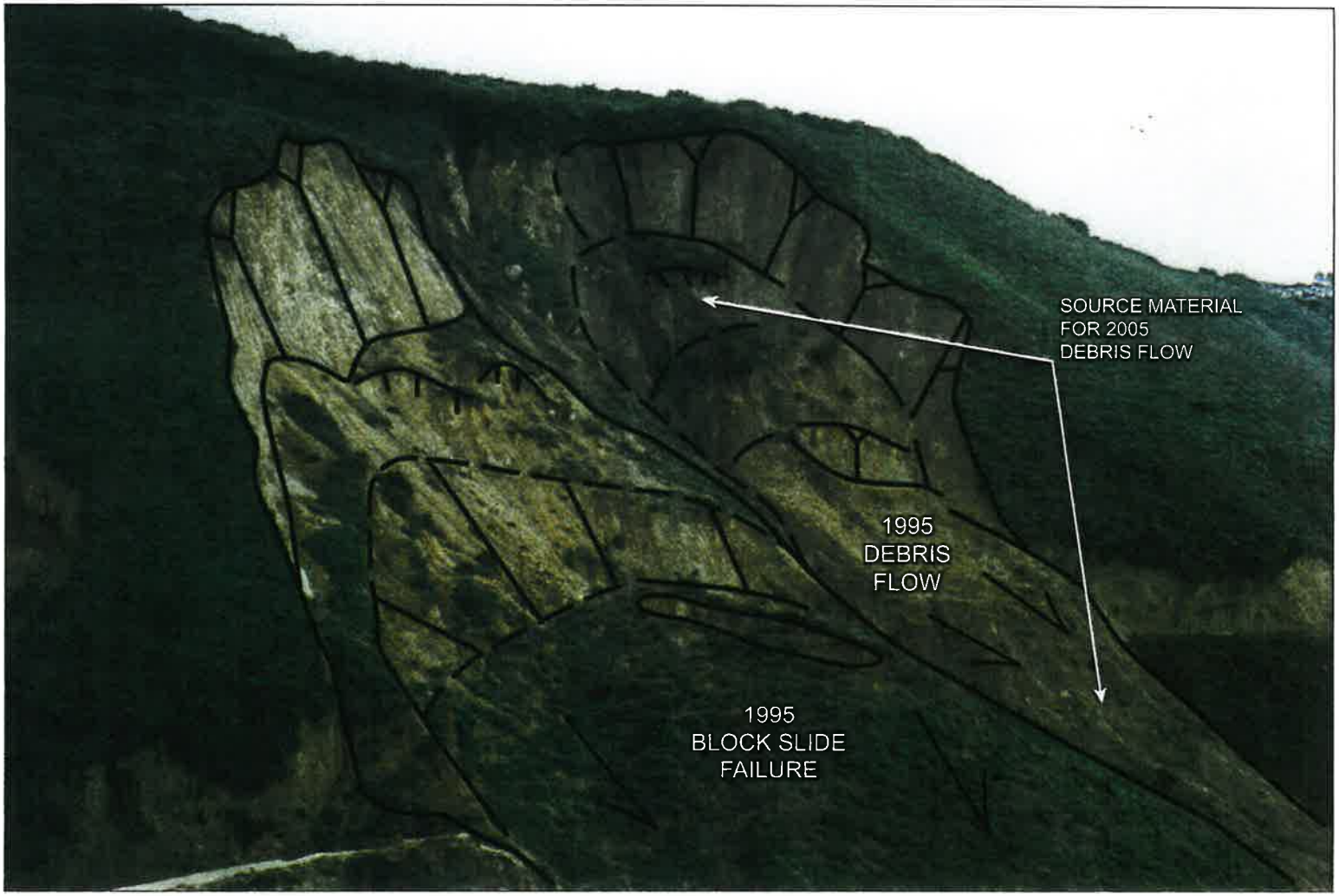

1995 photograph by Pam Irvine (CGS)

WLA

View to southeast of 1995 translational block slide failure and debris flow

LA CONCHITA LANDSLIDE – PHASE 2
Figure 7.6

02 JAN 08, 1885, RBZ

coincident with buried marine terrace sands. Groundwater rose to depth of about 67 feet (28 ft elevation) prior to failure. Stability analyses conducted by Stoney-Miller (1998) of the pre-failure mass of the 1995 block slide concluded that the incipient landslide mass was marginally stable (with a factor of safety of 1.1 or roughly ten percent more force resisting failure than causing failure). Based on the analyses, Stoney-Miller (1998) concluded that a groundwater rise of 30 feet from existing conditions was required to initiate failure. Stoney-Miller (1998) noted that the elevations of seeps observed prior to the slope failure suggest that groundwater levels exceeded those required for failure.

Following the March 4, 1995 landslide, in the evenings of March 9th and 10th, an intense series of storms triggered debris flows from the West Barranca, damaging three to five homes in the northwestern corner of La Conchita (Figure 7.7). Ventura County Geologist Jim O'Tousa noted mudflow debris had been cleared off of Carpinteria Avenue and pushed to the side, forming a crude berm up to three feet high (Ventura County, memorandum from Jim O'Tousa to Jim Fisher, dated March 21, 1995). At the intersection of Vista del Rincon and Ranch Road, O'Tousa noted that culverts beneath Ocean View Road had been clogged and evidence of two discrete mudflow events could be seen, an early flow that blocked the drainage and a subsequent flow that was diverted to the east, down the road and into the community.

Figure 7.7 Aerial oblique view of the destructive debris flow that emanated from West Barranca on the evening of March 10, 1995, damaging at least three homes. Photograph provided by Woodrow Higdon (copyrighted by Geo-Tech Imagery).

7.4 2005 Landslides and Debris Flows

The 2005 La Conchita slope failure occurred at about 12:30 pm on the 10th of January. The landslide was approximately 1,150 feet (350 meters) long and 260 to 300 feet (80 to 100 meters) wide (Jibson, 2006), The slide extended from about 450 feet above sea level to an elevation of about 60 feet (18 meters) within La Conchita, crossing Vista Del Rincon. Within La Conchita, debris within the fast moving toe of the flow destroyed thirteen houses and severely damaged twenty-three others, causing ten fatalities. The failure consisted of a remobilization of the southeastern portion of the 1995 landslide deposit, involving about 260,000 cubic yards of landslide material. Based on analysis of available video, Jibson (2006) concluded that the slope failure occurred as a thick debris flow mobilized on a saturated layer present within the 1995 deposit. Much of the overlying landslide mass was dry. In the West Barranca, landslides into the floor of the canyon with volumes of debris on the order of tens of thousands of cubic yards were noted and a major debris flow blocked Highway 101 and the railroad.

7.5 Comparison of the 1995 and 2005 Landslides

The massive 2005 debris flow appears to have evolved from conditions established prior to, and as a consequence of the 1995 slides, including small slope failures in 1978 and 1987 that produced a reservoir of loose sediment within the gully above Ranch Road. In addition, both the 1995 and 2005 slides occurred adjacent to a large gully at the intersection of two large, pre-existing landslides with the coastward strand of the Red Mountain fault (Figures 7.5 and 7.8). The gully is the source of a large fan on the coastal plain. At this complex structural intersection, groundwater flow along and across the fault within buried but permeable deposits of the Punta Gorda terrace feeds surface springs within the large gully. Sliding removed lateral support and weakened the hill. In addition, surface drainage of the gully was blocked by the 1995 slide, allowing saturation of slope material that had already been mobilized by earlier, smaller debris flows (Figure 7.9). These materials, primarily consisting of gravels derived from older debris deposits within the downcoast landslide, were remobilized during the 2005 slide.

The 1995 slide consisted of two distinct types of slides, a shallow debris flow within the gully followed closely by a block slide (Figures 7.6 and 7.8). The shallow debris flow did not completely extend into La Conchita and much of the associated debris was preserved on the hillslope, well upslope of Ranch Road (Figures 7.9). Figure 7.10 shows the change in relative elevation along the axis of the 2005 slide, using available topographic surveys (shown in Figure 7.9). In addition, the headscarp area and much of the 1995 debris covered active seeps within permeable sands of the Punta Gorda terrace at an elevation of approximately 400 feet. The toe of the 1995 bedrock slide completely blocked both surface and subsurface drainage. The 1995 debris flow and larger block failure therefore set up a combination of stored upslope debris and blocked subsurface drainage.

Results of our numeric modeling of the 2005 debris flow, described below, provide information on the underlying water conditions required to reproduce the debris run-out observed in 2005. Specifically, the zone of saturation at the base of the slide likely extended beneath the entire failure, well upslope of Ranch Road, to the headscarp area of the flow for the failure to achieve the run-out that occurred. This is consistent with observations and video evidence that the upper mass of the slide was relatively dry (Jibson, 2005; 2006). Since the 2005 slide, seepage has continue to occur along the contact between bedrock and overlying terrace and debris flow deposits in the headscarp area at approximately 400 feet above sea level. No other major springs were observed in this area during our field reconnaissance. It is likely that the source of saturation within the basal portions of the 1995 and 2005 debris flows is from subsurface flow within these deposits atop bedrock that daylights in the hillside.

Post-1995 Slide

Post-1995 Slide

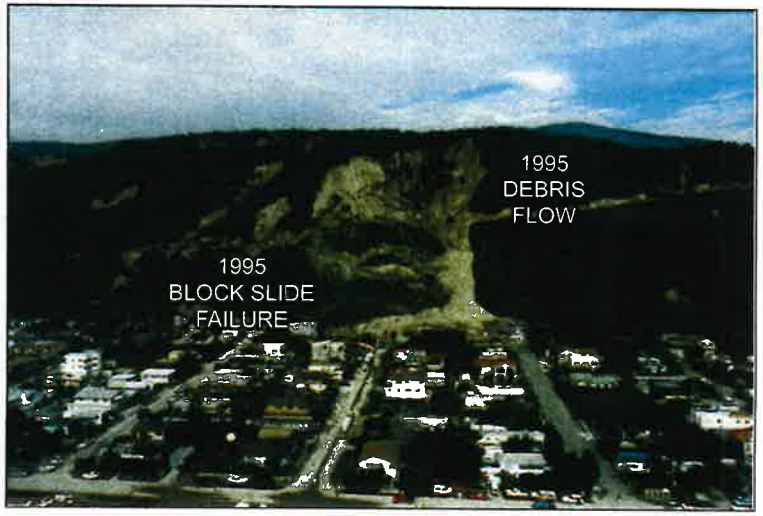

Post-2005 Slide

Post-2005 Slide

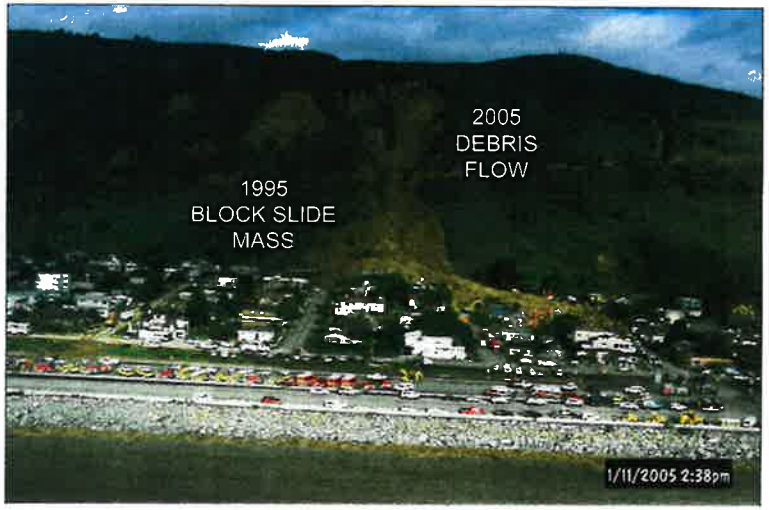

WLA

Photographs of 1995 slope failures compared to 2005 slope failures (photographs provided by Pam Irvine for 1995 and Jim O'Tousa for 2005)

Pre-1995 Slide

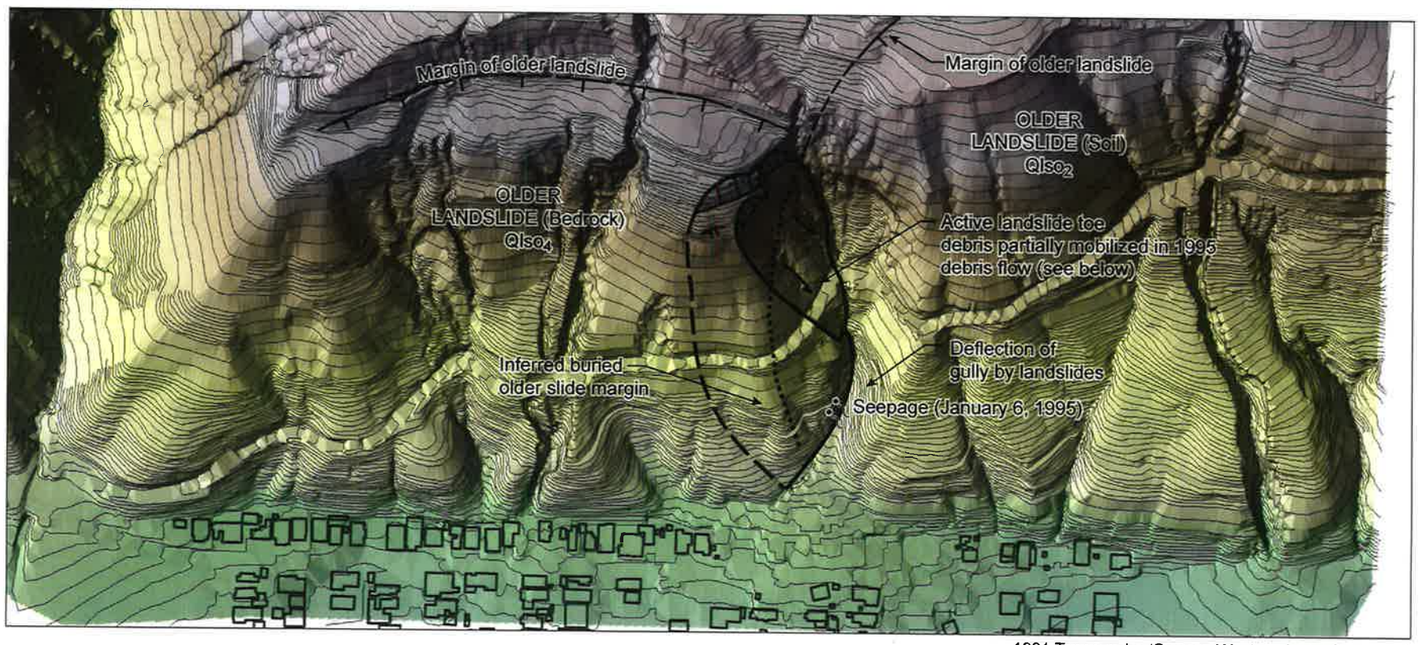

1991 Topography (Source: Western Aerial Surveyors)

Post-1995 Slide

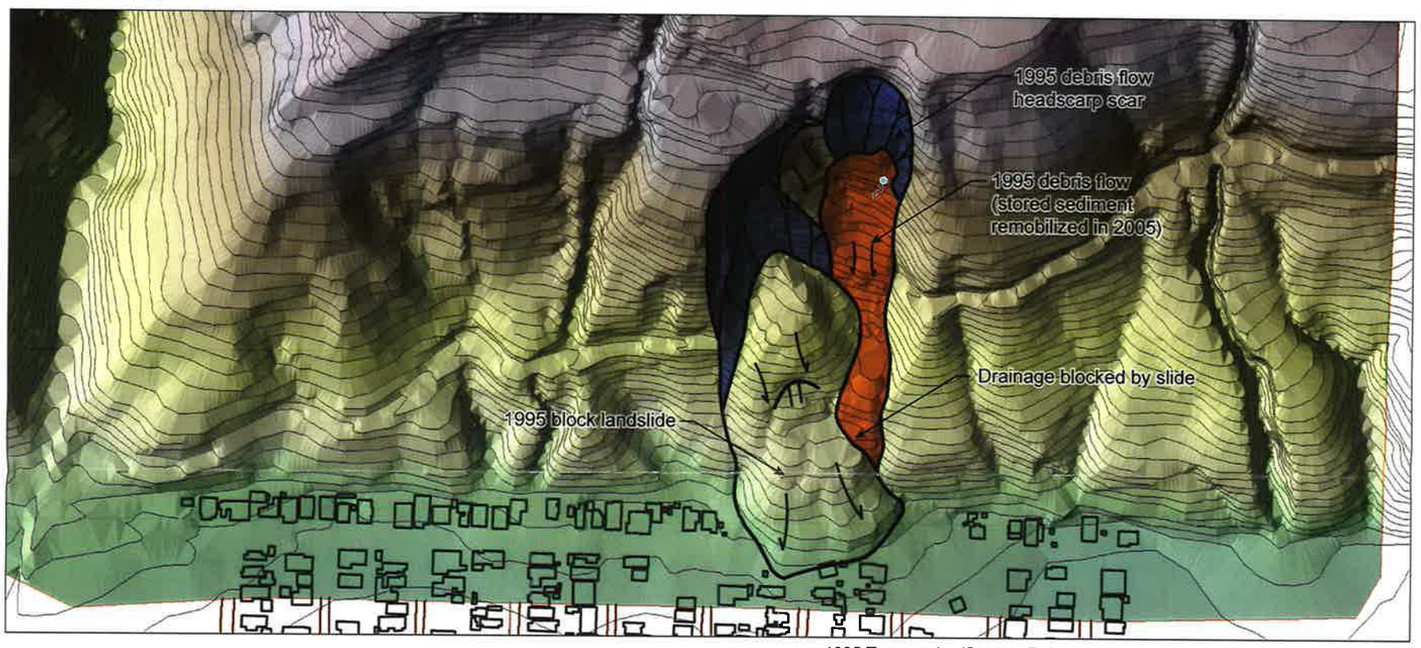

1995 Topography (Source: Robert J. Lung and Associates, Stoney Miller 1995)

Post-2005 Slide

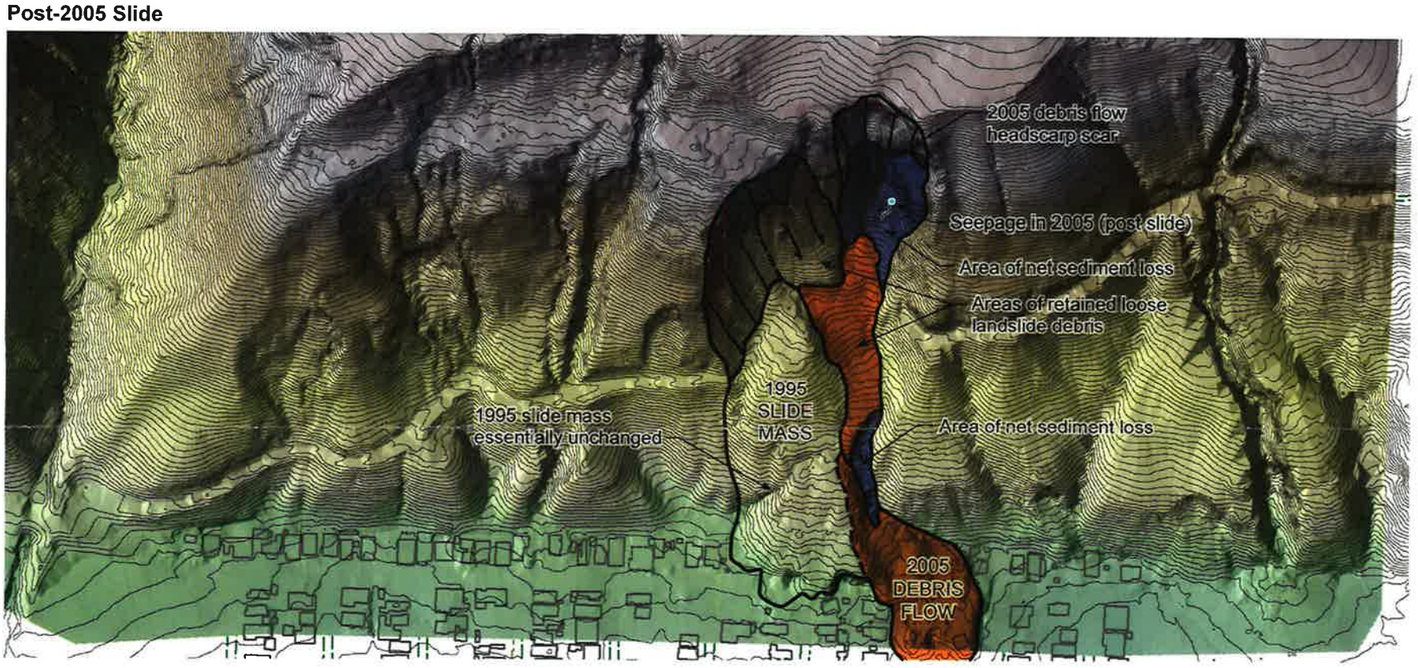

2006 Topography (Source: Robert J. Lung and Associates)

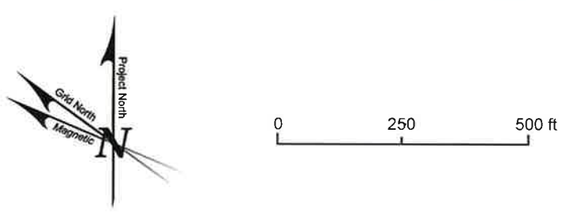

WLA

Evolution of 1995 and 2005 Slope Failures Shown on Digital Elevation Models Derived from of Civil Surveys (1991, 1995, and 2006)

LA CONCHITA LANDSLIDE – PHASE 2
Figure 7.9

03 JAN 08, 1885, RBZ

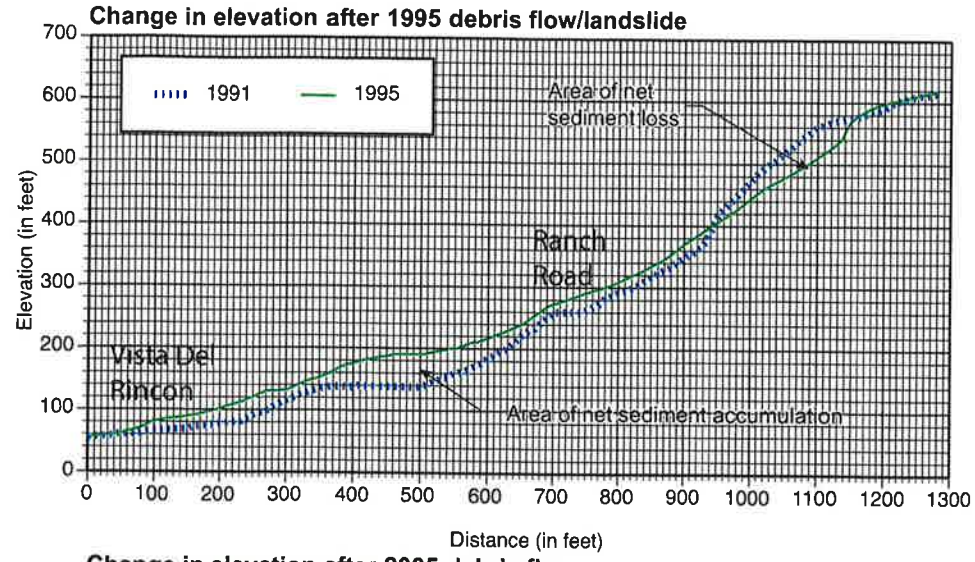

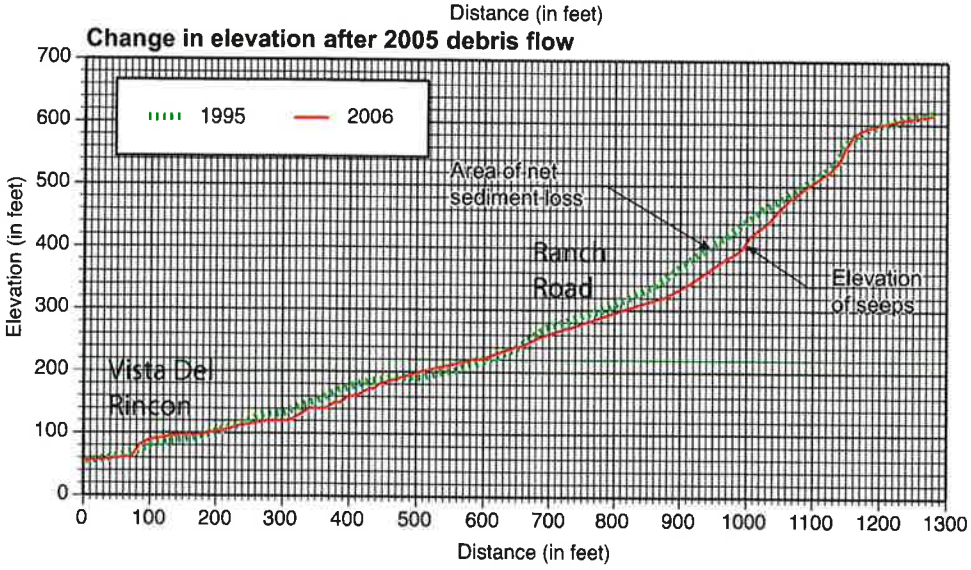

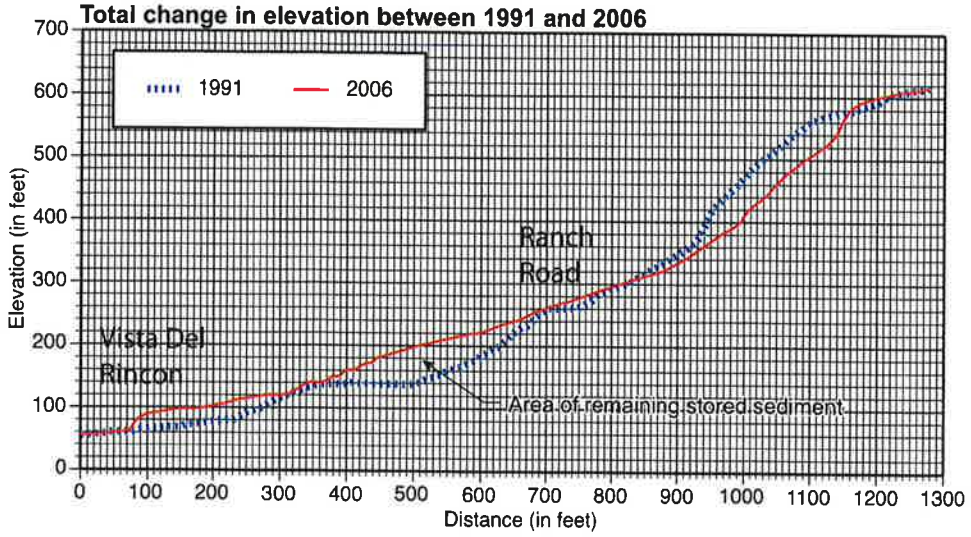

Comparison of topographic profiles along axis of 2005 debris flow between 1991 and 2006.

The system of interconnected subsurface and surface flow within the hillslope has two important implications for future slope hazard in the cliff area landward of the community of La Conchita. First, conditions that were favorable for large-scale failure in the 1995 and 2005 slides are less favorable at the present. Currently the water from the springs at the intersection of the two large, older landslides and the fault is unimpeded and flows within the gully. The springs currently are not covered by stored sediment and saturation of deposits occurs lower on the slope by infiltration from surface drainage within the small stream that flows within the gully. Although additional study would be required to confirm current water levels, subsurface flow likely is not significantly saturating the base of the 1995 or 2005 slides nor blocked enough to raise pore pressure.

The second implication of the likely confluence of localized groundwater flow at the intersection of the Red Mountain fault with buried deposits within the landslides is that subsurface flow may locally blocked in the future as slope deposits gradually cover the hillslope. In addition, similar blocked subsurface drainage of springs by overlying stored sediment is present elsewhere on the cliff. We discuss potential debris flow sources consisting of local confined flow beneath hillside deposits in the cliff area in the following section.

8.0 EVALUATION OF SLOPE HAZARDS

Slope failures in the La Conchita Study Area include: (1) deep rotational and translational landslides that typically involve underlying bedrock; (2) shallow slumps and translational landslides, which typically contain slope wash deposits and weathered bedrock; and, (3) shallow debris or earth flows, which typically contain recent slope wash deposits (Figure 8.1). Each of these types of slope failures is associated with distinct characteristics that can be used to identify and evaluate the associated hazard.

Deep landslides that involve underlying bedrock are relatively infrequent in the La Conchita area, compared to more common shallower slope failures. Most of the mapped bedrock landslides are older, pre-existing slides located along the coastal cliffs, based on mapping conducted for this study and previous published mapping by Dibblee (1988) and CGS (2003). These large landslides are topographically well expressed and the geographic extent of each individual landslide is relatively obvious, based on the presence of headscarps and hummocky terrain. The subsurface geometry of the landslides, including the depth and orientation of associated slide planes, is moderately constrained by information in the available geotechnical borings. Based on this information, the potential for failure (factor of safety) of the larger slides can be evaluated, along with the possible lateral extent of downslope movement, by construction of geologic cross-sections, estimates of groundwater depths, and modeling by geotechnical engineers.

Shallow translational and rotational slides and slumps typically are located in canyon walls and near the base of hillslopes. These slides generally are well expressed within the terrain with well-developed headscarps and locally are associated with springs and vegetation consistent with shallow groundwater. During or following heavy rainfall, these slides may fail, typically in semi-coherent fashion. Failure tends to be slow and may result in movement of the base of the hillslope outward onto the La Conchita plain or within canyon floors. Similar to the larger landslides, these hazards typically are associated with hillslope features that can be identified and mapped.

Debris flows typically occur where slope wash deposits (colluvium) collect in topographic swales or hollows. During heavy rainfall, this stored material becomes saturated and may flow rapidly down incised channels. Poorly sorted debris within a debris flow may be deposited at the base of the hill, where the slope angle decreases, or at the mouth of the transport. The primary potential hazard posed by debris flows is movement of the saturated soil, and associated burial and/or displacement of structures within the flow path of the debris.

8.1 Types of Landslide Hazards

During non-earthquake (static) conditions, shallow slope failures occur most frequently during the rainy season when high groundwater conditions persist. Debris flows typically are closely associated with high-intensity rainfall and can occur rapidly during and shortly after storms. The size and lateral extent of debris flows depends largely on the source and amount of material involved in the flow, while the duration of peak rainfall can determine whether failure occurs. Larger landslide failures typically occur following large storms and, in years with significant precipitation, may be associated with gradual changes in groundwater levels. These large block and translational slides may be associated with, and preceded by, hillslope cracking and scarp formation.

Landslides also can occur during earthquakes, triggered by the strain induced in soil and rock by the ground shaking vibrations. During non-saturated conditions, material within earthquake-induced

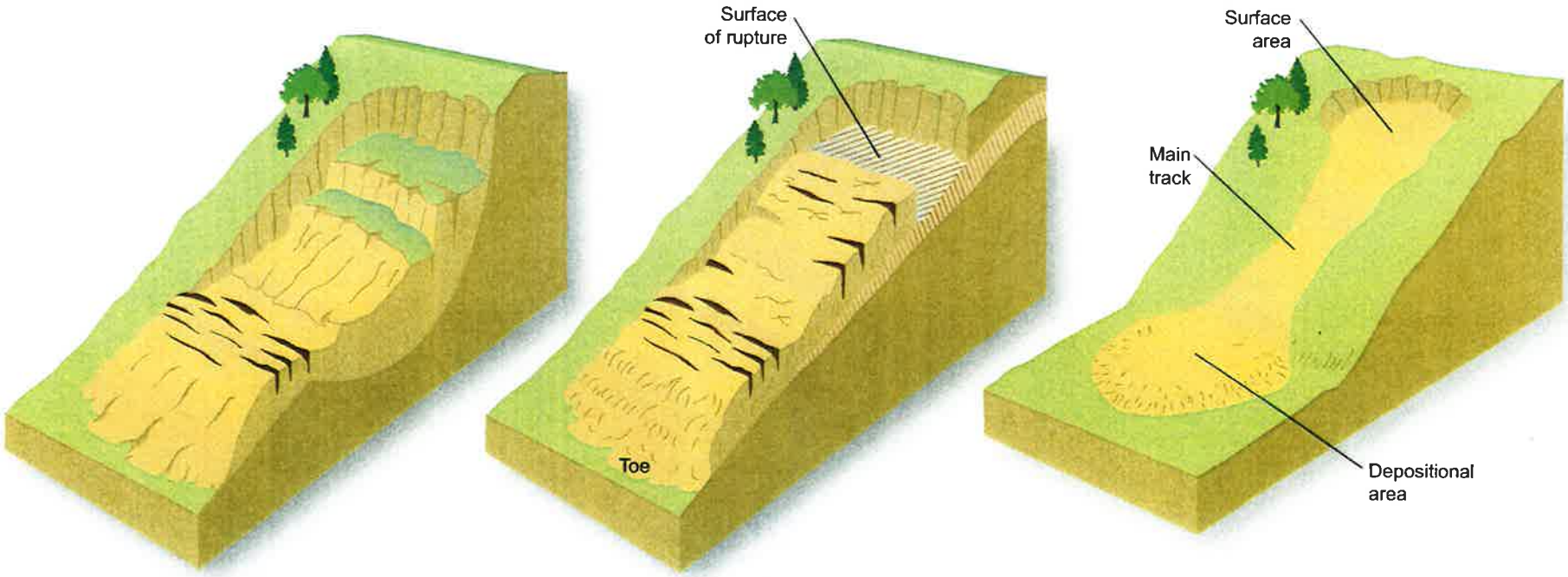

Rotational landslide

Translational landslide

Debris flow

landslides may fail as coherent blocks rather than debris flows or large-scale failures and translational movement downslope may be limited. Within historic time, La Conchita has been subjected to relatively strong ground motions from the 1925 Santa Barbara M6.8 earthquake and the nearby 1941 M5.9 earthquake. No slope movement was documented in the La Conchita Study Area during these earthquakes and no evidence of displacement was detected during examination of historical aerial photographs for this study.

8.2 Influence of Precipitation on Slope Failure

Coastal areas of Southern California are characterized by a high degree of variability in rainfall as a result of the extreme variability in seasonal precipitation (Engstrom, 1996). The cumulative departure of tree-ring indices and precipitation has been used to divide periods of the climatic record into wet and dry climatic periods (Hanson and others, 2003). Wet climatic periods are determined using the rising limb of the cumulative departure curve, and dry climatic periods are determined using the falling limb of the cumulative departure curve (Figure 8.2). The cumulative departure of tree-ring indices for southern California for 1458–1966 (National Atmospheric and Oceanic Administration, 1994) indicates an apparent shift in the frequency and amplitude of wet and dry periods after the early 1700s (Hanson and others, 2003). Prior to the early 1700s, wet and dry periods were relatively long (twenty to more than sixty years). After the early 1700s, wet and dry periods were shorter (five to twenty years). More detailed paleoclimatic records may provide better resolution for calculating the probability of 100-year and 500-year storm events, and associated landsliding, in the future.

The wet and dry periods determined from tree-ring indices for 1770 through 1965 generally are in agreement with available precipitation records for Port Hueneme and Santa Paula and are related to periods of major droughts and floods (e.g. Figure 8.2). The greatest storm in the written history of California struck the region in the winter of 1861–1862, and persisted for forty-five days as a series of storms impacted the California coast. The associated 1862 flood washed away much of the San Buenaventura township with a major portion of the community leveled. On February 1, 1862, the Los Angeles Star reported that flooding was sufficient to 'wash away the street to a depth of fifteen feet" and the town was abandoned. The other two largest historical storms floods occurred in December of 1867 and February of 1891 and were associated, respectively, with a moderate and a very strong El Nino (Sidler, 1968).

8.2.1 Return Periods of Rainfall Triggering Events

Because landslides and debris flows commonly are closely triggered by storm precipitation, review of the return period of large storms associated with past failures provides possible constraints on the likely recurrence of rainfall-triggered slope failures (Figure 8.3). Estimated recurrence frequencies include 100 to 200 years for the rainfall totals in January through February of 1969, 200 years for the 1983 rainfall totals, and 100 years for the thirty-day rainfall totals of January 1995. The historic flood peak discharges produced by the storms of January and February 1969 equaled or exceeded those of the March 1938 floods in southern California, that occurred approximately 30 years previously (Waananen, 1969). Less than thirty years later, major storms in 1995 contributed to the large landslide failure within La Conchita, followed by the damaging 2005 storms and landslides. All of these periods (1937-1938, 1969, 1983, 1995, and 2005) were associated with slope movement within the La Conchita Study Area.

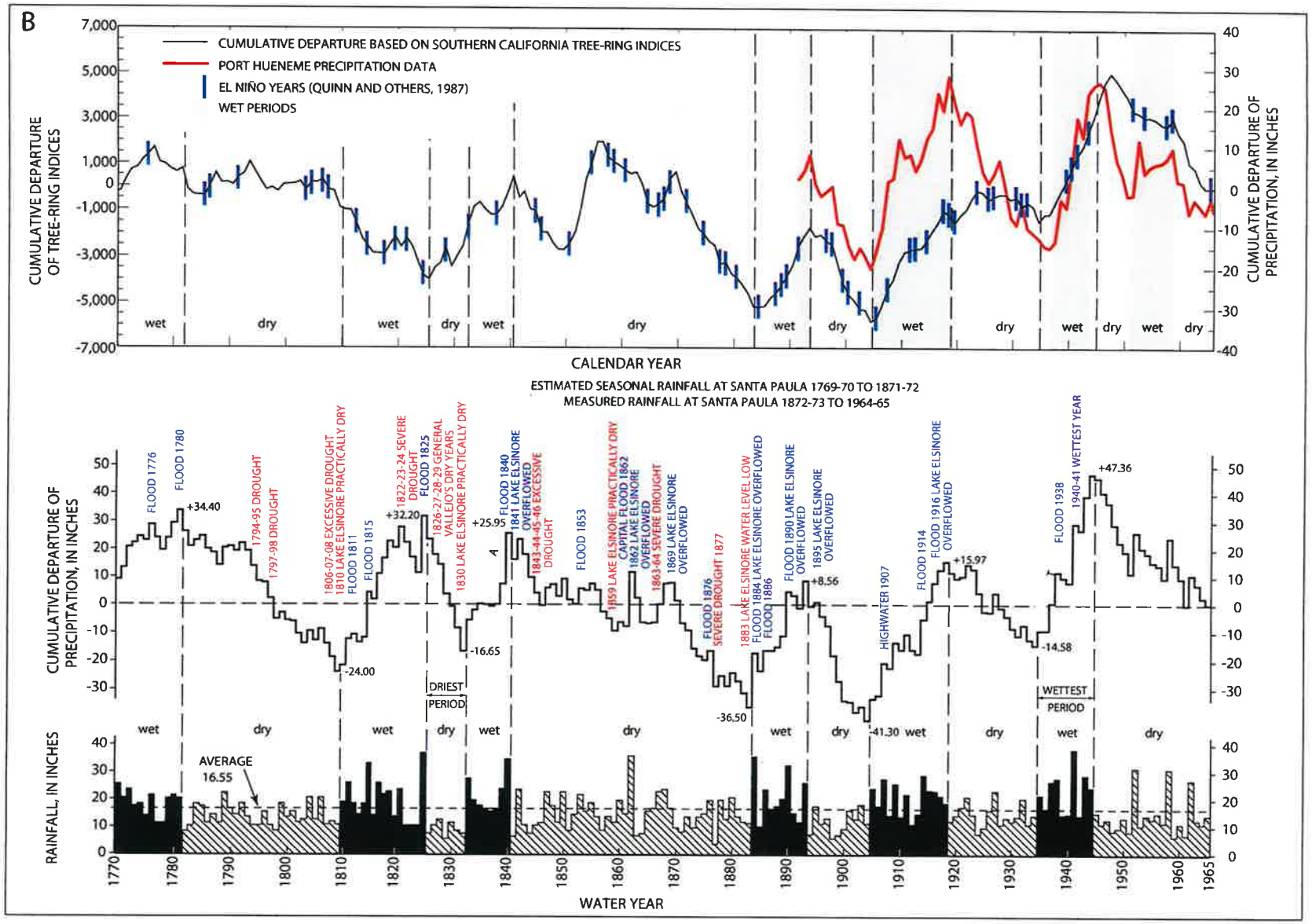

Figure from Hanson and others, 2003

Return Period for 24-hr Precipitation Totals
(NOAA Atlas 2, Vol. XI)

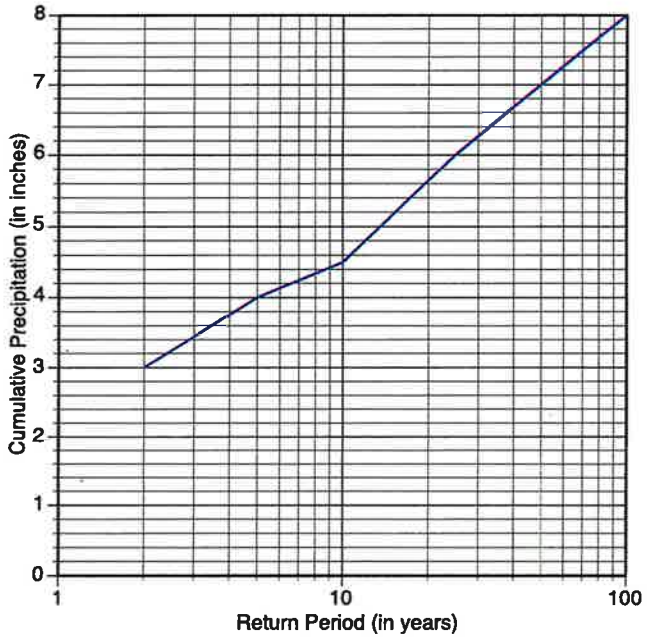

Return Period for 10-day Storm Precipitation Totals
(Technical Paper 49)

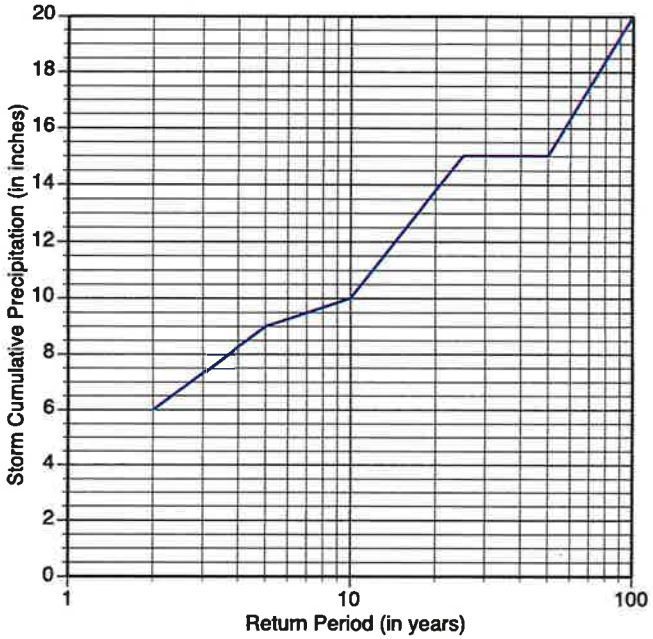

WLA

Return Period for 24-hour and 10-day Cumulative Rainfall Totals

LA CONCHITA LANDSLIDE – PHASE 2
Figure 8.3

02 JAN 08, 1885, CSH

The definition of a '100-year storm' is based on the average rainfall intensity for a given duration of time and/or the total volume of rain that falls over a given period of time (Robinson and others, 1982). The term '100-year storm' or '100-year frequency' does not refer to a rainfall event that occurs once every 100 years. Rather, in any given year, there is a one in one hundred (or one percent) chance of a 100-year storm event occurring. Over a 100-year period such a storm has a 63.5% chance of occurring. Over a thirty-year period, the storm has a twenty-six percent chance of occurring. Two 100-year storms could occur a year apart or even a month apart. Indeed, there is an eighteen percent chance that two 100-year storms will occur, and a nearly two percent chance that four 100-year storms might occur, within a given 100-year time period.

8.3 Major Landslides

The purpose of our evaluation of large landslides identified within the Study Area is to provide basic geologic, hydrologic, and seismic input parameters for the modeling of landslide displacement under static and dynamic conditions. Specifically, towards completion of the overall goals of the project, we have provided information on the likely locations, geometry, and composition of the slides along with inferred groundwater levels and flow paths. Although part of the overall hazard evaluation for the larger study, modeling of potential landslide displacement is not part of our scope of work. Results of the modeling conducted by Alan Kropp & Associates, Inc., for the purposes of developing a conceptual understanding of potential slope movement will be presented in their companion report.

Our geologic evaluation of the landslides mapped in the cliff area landward of La Conchita included detailed mapping of landslide morphology, large and small diameter geotechnical borings, collection of downhole geotechnical samples for analysis by AKA, downhole measurement of shear wave velocity within the landslide deposits, and construction of geologic cross sections showing the inferred geometry and subsurface extent of the landslide deposits. Combined with the mapped subsurface location, and orientation, of the Red Mountain fault across the cliff face and regional seismic information on likely ground shaking parameters provided in this report, this information provides the basis for more sophisticated modeling of possible landslide movement.

The discussions in this section refer to interpretative cross sections (AA-AA' through JJ-JJ') presented in Appendix B. Cross section locations are shown on the Geologic Map (Figure B-2), also provided in Appendix B.

8.3.1 Upcoast Landslide (Qlso4)

The upcoast landslide (Qlso4) is located landward of the community of La Conchita and is traversed by lower Ranch Road. The landslide is approximately 11,000 feet (3,352 meters) wide and extends from an elevation of approximately 600 feet to the base of the cliff at 60 to 80 feet (18 to 24 meters) above sea level (Figure B.3; Appendix B). The inferred lower landslide plane (main slide plane) was exposed at a depth of 66 feet in WLA-BA4 (Figure 8.4). The shear zone associated with the base of the landslide ranges from several inches to as thick as two feet.

The upper portion of the landslide consists primarily of the Siquoc Shale, overlain by approximately thirty feet of older debris flow material. The lower part of the landslide consists of siltstone of the Pico Formation. The landslide is traversed by the Red Mountain fault.

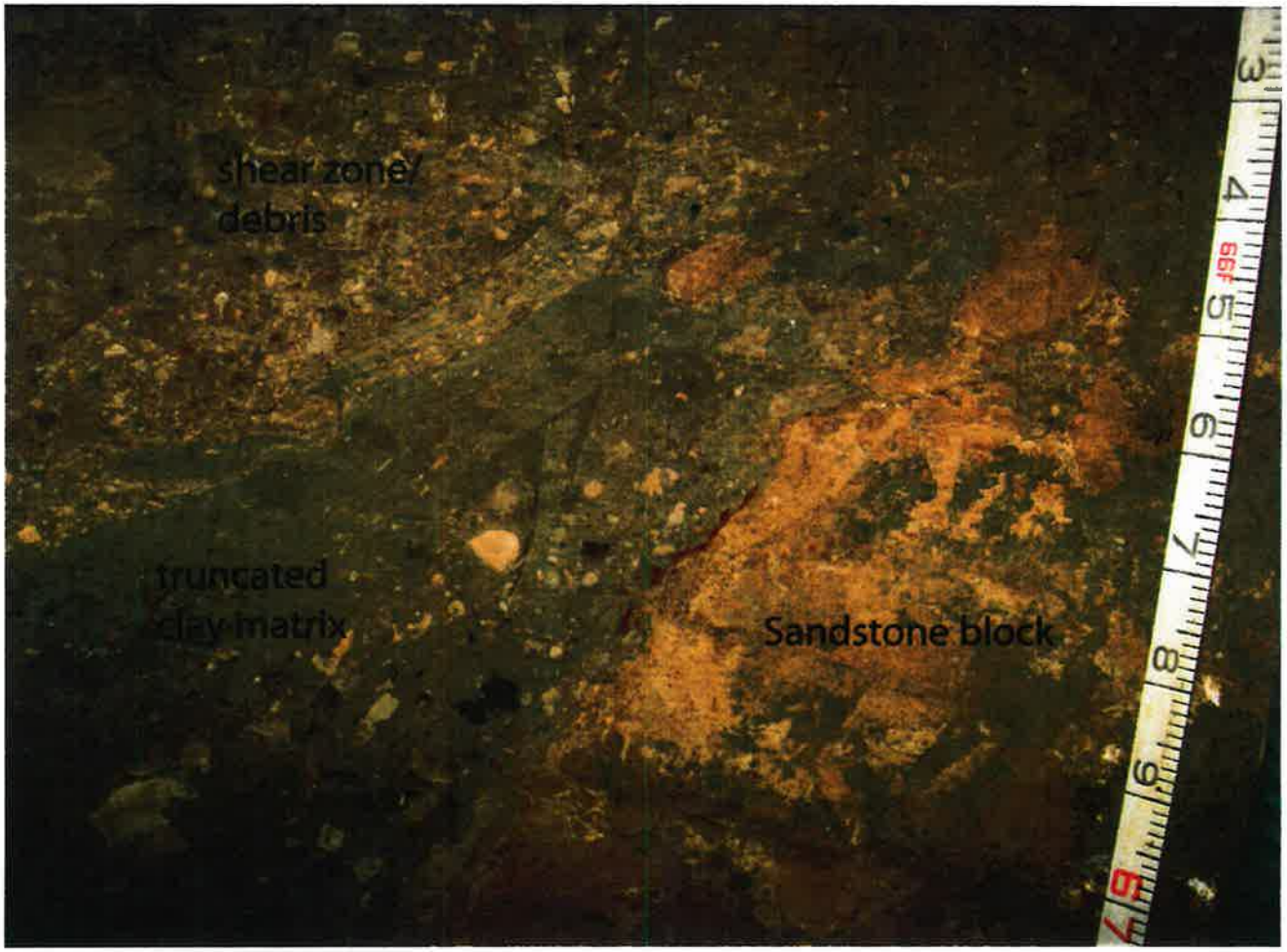

WLA

Photograph of upcoast landslide (Qlso4) slide plane exposed in boring WLA-BA4

LA CONCHITA LANDSLIDE – PHASE 2
Figure 8.4

02 JAN 08, 1885, RBZ

8.3.2 Downcoast Landslides (Qlso2 and Qlso3)

Downcoast landslides (Qlso2 and Qlso3) are located landward of Vista Del Rincon between San Fernando Avenue and the pasture downcoast of Ojai Avenue. The Qlso4 landslide is approximately 900 feet by approximately 1,300 feet long. The landslide is up to 100 feet thick (Figures B.6 and B.7; Appendix B). The base of the slide was encountered at a depth of forty-two to forty-four feet in WLA-BA5 (Figure 8.5). The inferred landslide shear zone is developed within blocky material of the older debris flow materials. This material is almost entirely clast supported and contains angular blocks of claystone and minor sandstone of the Monterey formation.

Lithology exerts a major influence on calculated shear wave ratios (Tatham and McCormack, 1991; Tatham, 1982). Compressional wave velocity (Vp) in particular is dependent upon the bulk modulus, the shear modulus and the density of the material (Christensen and Mooney, 1995). Comparison of p-wave with s-wave velocities, and the ratio between the two, measured in the two large landslides, shows an apparent increase in p-wave velocity in the upcoast slide versus the downcoast slide (Figure 8.6). This shift is consistent with the presence of displaced bedrock within the upcoast landslide ('bedrock' slide) versus relatively less dense, predominately loose older debris flow, paralic, and terrace deposits in the downcoast ('soil' slide).

8.3.3 Secondary Landslide Hazards

In addition to wholesale failure of the large landslides mapped within the cliff landward of the community of La Conchita, there is an associated hazard of failure of smaller portions of the existing landslide deposits, particularly within the headscarp areas of recent landslides. For deep-seated rotational and translational slides, reactivation of recent landslide debris and portions of pre-existing landslide scarps is a more frequent phenomenon, representing a higher hazard, than initiation of new landsliding within a landslide-prone area (Dewitte and others, 2005). Jibson (2006) noted that secondary landslides could be triggered from scarps or deposits within the uphill portions of the 1995 and 2005 landslides. Characterization of areas most susceptible to reactivation included construction of topographic sections and detailed mapping of existing landslide scarp features.

8.4 Ages of Landslide Deposits

The relative ages of the landslides that pre-date the historical record (older than about 120 years) have been inferred based on their relationship to other geologic units and limited radiocarbon dating of charcoal obtained in borings. The maximum age of the upcoast landslide (Qlso2) is less than 10,000 years based on an age date obtained from radiocarbon dating of charcoal collected within hillslope deposits beneath the slide plane, and landslide deposits (sample BA4-S1-65; Appendix E; Table 8.1). This sample was obtained from an apparent burn horizon within colluvial deposits at a depth of approximately 65 feet within large diameter boring WLA-BA4 (Appendix C).

There is evidence that the large upcoast and downcoast slides were active within the past 2,500 to 4,500 years. The age of the marine terrace at the base of the cliff is between 2,500 and 4,500 years. Consequently the sea cliff must have formed in the Holocene. In addition, deposits within the large slides locally cover, and thus likely are younger than, the marine terrace beneath La Conchita. Within large diameter boring WLA-BA1, displaced Pico Formation bedrock within the toe of the upcoast landslide is emplaced (thrust) over colluvial deposits and marine

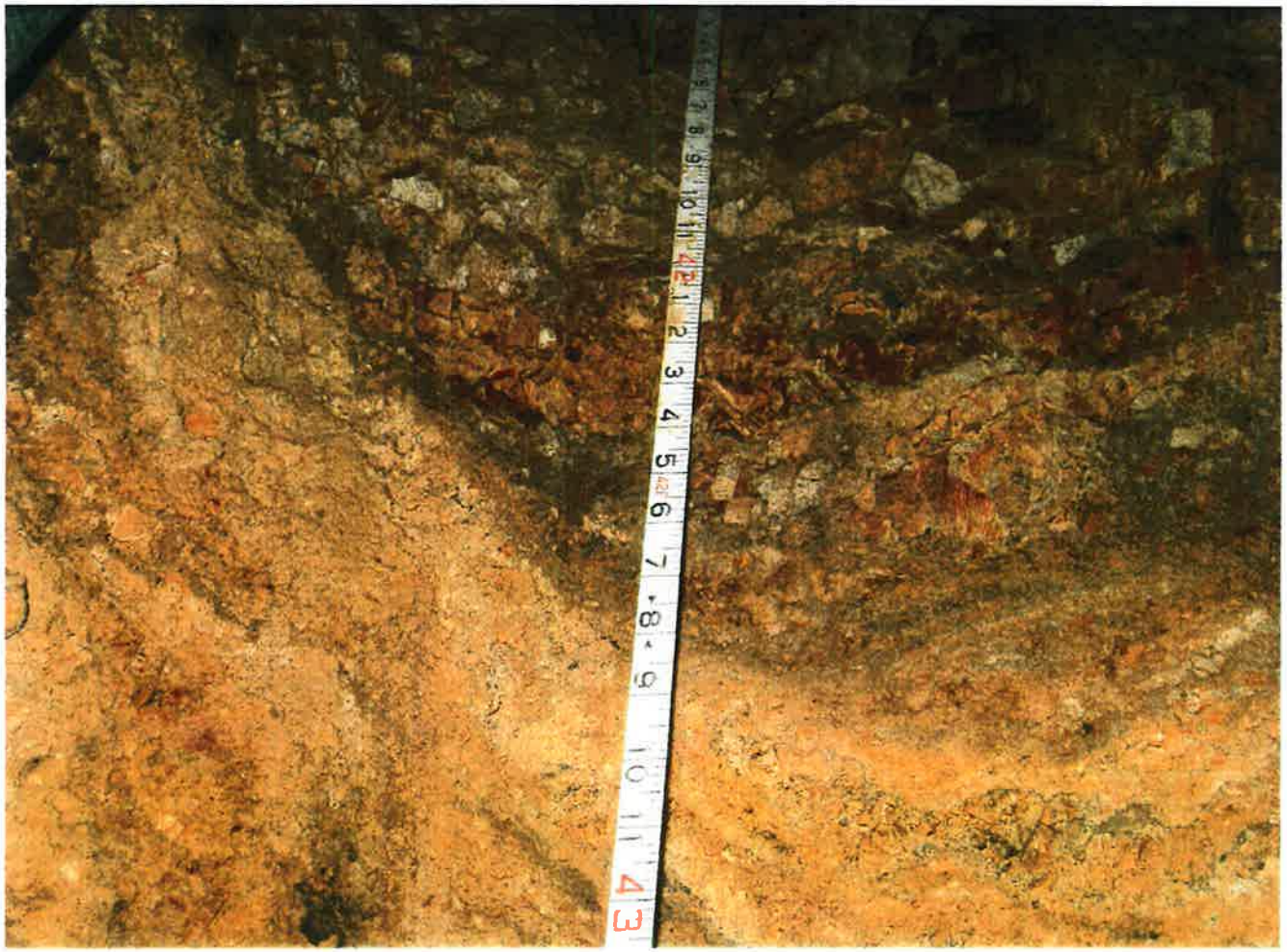

WLA

Photograph of downcoast landslide (Qlso2) slide plane exposed in boring WLA-BA5

LA CONCHITA LANDSLIDE – PHASE 2
Figure 8.5

02 JAN 08, 1885, RBZ

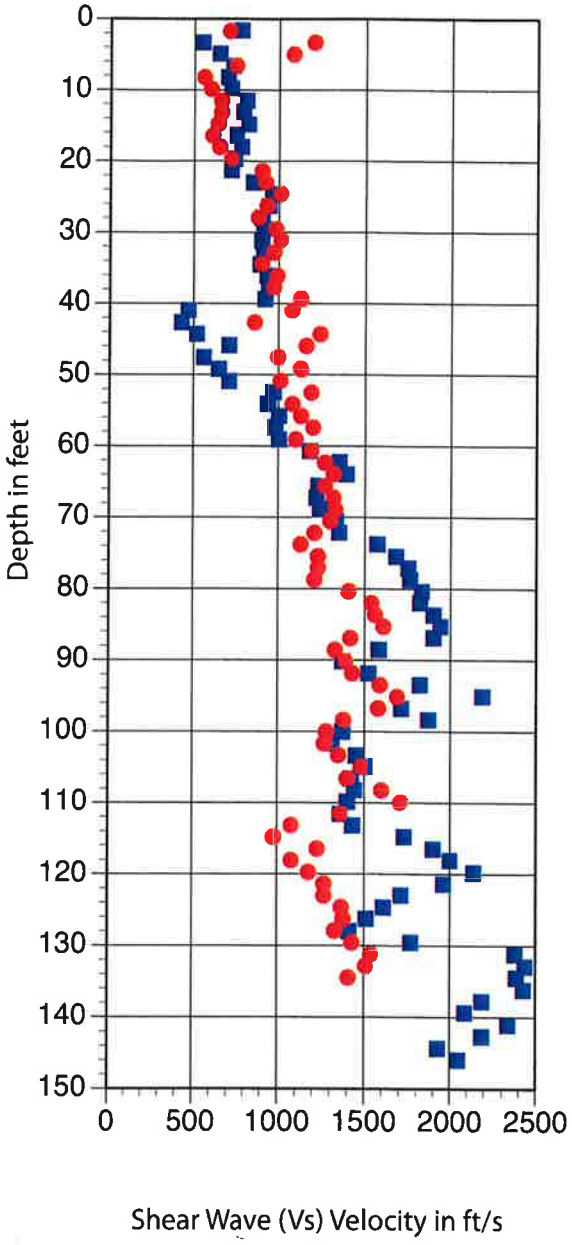

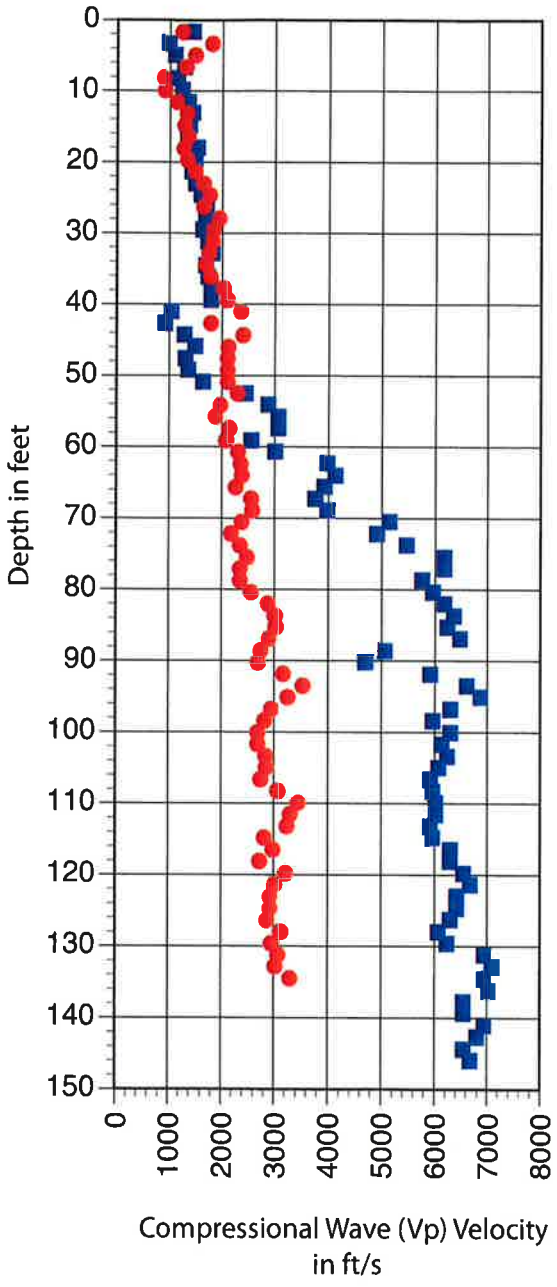

Explanation

■ B1 ● B2

LA CONCHITA

Comparison of Shear and Compressional Wave Velocity (Vp and Vs) of WLA B1 versus WLA B2

WLA William Lettis & Associates, Inc.

Figure 8.6

Modified 11.20.07

1885 La Conchita

terrace sands (Qlso2). There is no evidence, however, that the older slides (Qlso-2 through Qlso-4) have moved within historic time.

Radiocarbon dating of charcoal obtained within buried debris flow deposits within La Conchita provide constraints on the ages and return period of individual debris flows. Laboratory testing of charcoal samples collected at depths of fifteen and twenty feet in large-diameter boring WLA-BA2 (Appendix E). At a depth of fifteen feet, we obtained a date of 1,200 years before present (sample BA2-1; Table 8.1). This sample was collected from a debris flow buried beneath at least five other debris flows ranging in thickness from two to four feet. The overall debris accumulation, or sedimentation, rate is roughly 0.15 inch/year.

At the twenty-foot depth within large diameter boring WLA-BA2, a date of 1,570 years before present was obtained within the seventh identified buried debris flow (sample BA2-2; Table 8.1). This debris flow is approximately 370 years older that dated at fifteen feet, consistent with roughly 0.16 inches per year accumulation. If the deposition rate was consistent over time, that would make the base of the entire debris flow sequence (roughly 32 feet thick) about 2,500 years old. This correlates well to the inferred minimum age range of the underlying marine terrace (e.g., Harden and others, 1986).

Table 8.1 La Conchita Radiocarbon Results (See Appendix E for full laboratory results).

Sample ID	Measured Radiocarbon Age* (years before present)	13C/12C Ratio (‰)	Conventional Radiocarbon Age* (years before present)	2-Sigma Calibration* (calendric date)	2-Sigma Calibration, OxCal 4.0** (calendric date)	2-Sigma, OxCal Range*** (calendric date)
BA2-1	1,200 ± 40	-25.8	1,190 ± 40	710 - 750 760 - 900 920 - 960	695 - 699 [0.5] 708 - 748 [7.3] 766 - 902 [78.2] 916 - 967 [9.4]	700 - 970
BA2-2	1,570 ± 40	-23.8	1,590 ± 40	390 - 560	392 - 562 [95.4]	390 - 560
BA4-S1-65	9,910 ± 60	-22.5	9,950 ± 60	BC 9740 - 9730 BC 9680 - 9280	BC 9749 - 9723 [1.8] BC 9677 - 9285 [93.6]	BC 9750 - 9290

* reported by Beta Analytic (letter dated November 21, 2007).

** using "IntCal04" curve (atmospheric data of Reimer and others, 2004), weights shown in square brackets

*** rounded to nearest decade, as recommended in OxCal 3.10 manual

8.5 Evaluation of Debris Flow Inundation Hazard

Identification of debris flow hazard requires estimation of the debris flow inundation area, debris flow run-out distance and thickness, and debris flow recurrence. Debris flow run-out is a term that describes both the lateral distance that a debris flow travels and the type and thickness of material deposited (Hungr

and others, 1984). The run-out distance, and size of the inundation area, controls the associated hazard to a community. The volume of material deposited by individual debris flows and local thicknesses of debris flow run-out are critical factors that control how damaging individual debris flows may be to buildings. Also, because debris flows can occur with minimal warning and rapidly flow downhill, these types of slope failures have the greatest potential for causing loss of life.

We applied a multidisciplinary approach to develop a model of debris flow hazard at a local scale in La Conchita. First, we produced an inventory of past debris flows, based on historical accounts and comparison of observed changes on vintage aerial photographs, as discussed above (Figure 7.3). We then interpreted LiDAR-based topography and stereo-paired aerial photographs to delineate upslope debris flow source areas, map debris flow transport paths (gullies), and estimate the lateral extent and thicknesses of historical and pre-historic debris flow fans on the coastal plain. Debris flow source areas used in our model are shown on Figure 8.7.

Numeric modeling of debris flow run-out provided information on the probable lateral extent and depths of debris flow deposition. These data allowed us to estimate: (1) potential debris flow initiation zones, and (2) volumes of potential debris flow run-out for each mapped upslope debris flow source area.

Subsurface investigation, including detailed down-hole logging of debris flow deposits and buried soil horizons within La Conchita, provided information on the thicknesses and timing of individual debris flow events. Charcoal collected within large diameter borings provided ages of prehistoric debris flow deposits (Table 8.1; Appendix E). This information, combined with analysis of the number of historical debris flows and associated recurrence of major storms associated with past slope failures, provides the basis for establishing the likely return period of large debris flows.

8.5.1 Debris Flow Sources and Run-out Fan Morphology

The product of our mapping of deposits and possible source areas of historic and pre-historic debris flows includes a map showing debris fans, and transport gullies (Figure 8.7). We have identified past debris flows based on historic accounts, historic survey maps, and interpretation of aerial photography. Based on our examination of past movement, and the morphology of the hillslope, debris flows are localized within discrete areas distinguished by concave indentations (colluvial hollows) in the cliff area. These source areas are connected by gullies to convex fan areas formed by repeated deposition at the base of the cliff, on the coastal plain and within La Conchita.

For each area of historical and pre-historic debris flows, we delineated the uphill source area and estimated downslope run-out (inundation) area (Figure 8.7). Debris fan deposits (map unit Qdf) on the coastal plain and within the community of La Conchita were delineated on the basis of historical topographic maps, surveys of past debris flows, and interpretation of available soils and subsurface data. However, the mapped fans are geomorphic features built up by the repeated deposition of individual debris fans. To the extent possible we have delineated the likely lateral extent of past individual fans in order to predict future debris fan run-out. Geotechnical borings provide information on approximate thicknesses of historic and older debris flow deposits.

For example, a topographic map of a historic debris flow dated December 1937, shows the western edge of the 'recent build up' along Oxnard Avenue, and the eastern edge along the range front with the 'line of principal flow' trending south along the range front before turning southwest, between Bakersfield Avenue and the ally to the east (Figure 7.2; Ventura County Map #31600, provided by David Orr, La

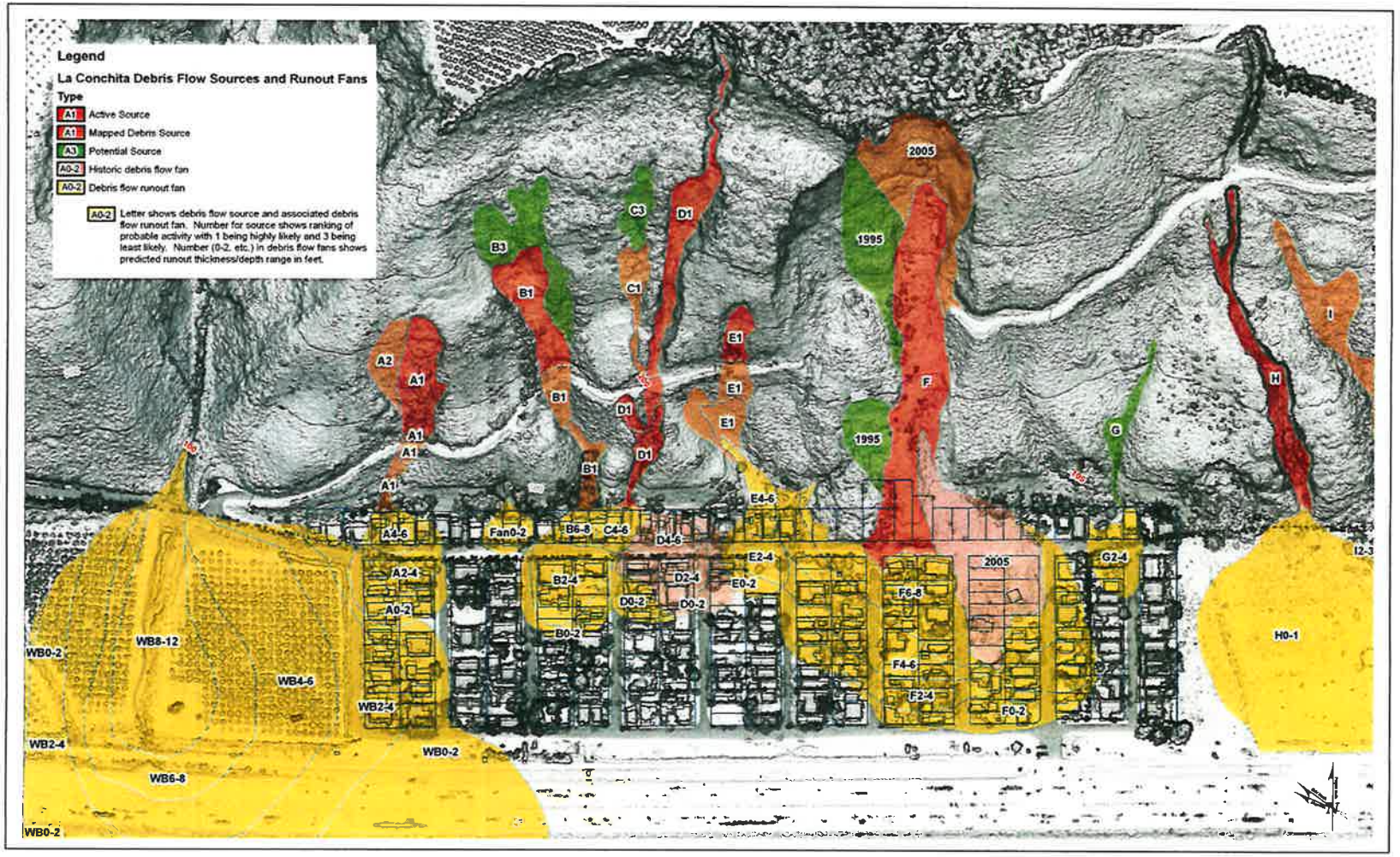

Map of Debris Flow Sources and Run-out Fans Showing Inferred Depth Ranges

LA CONCHITA LANDSLIDE – PHASE 2
Figure 8.7

02 JAN 08, 1885, CSH

Conchita Ranch). This debris flow likely was encountered in our large diameter borings WLA BA-1 and BA-2.

8.5.2 Results of Debris Flow Run-out Modeling

Numeric modeling performed for this study provides information on possible debris flow run-out and debris flow depths. Three-dimensional terrain can strongly influence the dynamics of debris flows. The modeling incorporates video of the 2005 landslide/debris, pre- and post-slide topography, and inferred physical properties of the slide material using the numerical physical model of Denlinger and Iverson (2001). This modeling is used to predict debris flow run-out distances, depths, and travel times for the 2005 slide and other potential landslides located on the slope adjacent to La Conchita.

Calculations were performed using a nonhydrostatic two-dimensional (2D) depth-averaged model that implements the Coulomb mixture theory for flow of variably fluidized granular masses across three-dimensional terrain from Iverson and Denlinger (2001) and Denlinger and Iverson (2001). The numerical approach combines computational schemes from Denlinger and Iverson (2001), Denlinger and Iverson (2004), and Denlinger and O'Connell (2007) to simulate depth-averaged shallow mixed granular solid-fluid flow, modified for a sloping bed and transient wetting and drying conditions.

Video of the 2005 landslide/debris shows that the slide developed and propagated as a fluidized granular flow that is adequately modeled using an approach similar to Denlinger and Iverson (2001), implemented in the nonhydrostatic depth-average flow model of Denlinger and O'Connell (submitted) that produces stable and accurate numerical solutions of the hyperbolic, nonlinear governing equations by using a Riemann technique.

For debris source D, source of the 1937 debris flow documented within La Conchita, several pore-pressure scenarios were investigated. The 2005 slide parameters and pore pressure rise time of five seconds produce maximum run-outs that barely extended beyond the base of the slope. Since slide D is located in a surface drainage channel that could effectively saturate the entire slide mass prior to movement, longer durations of saturation and high pore pressures were investigated than required to reproduce the 2005 slide run-out. The rise time to maximum pore pressure was increased from five seconds to fifteen seconds and the total duration over which elevated pore pressures were allowed to persist in the flow was increased from twenty to forty seconds.

The slide, as modeled, rapidly moves downslope during the first ten seconds of flow and develops sufficient downslope depth to breach the drainage divide and split a portion of the flow downcoast. After twenty-one seconds of flow, the lower portion of the slide decelerates, while the upper portion of the slide continues to move at high velocity, resulting complete breach of the drainage divide to produce substantial split flow toward the southeast. After about three minutes, the slide has extended over a large area south of the slope and developed a toe depth profile determined by the internal friction angle of fifteen degrees. The run-out extent is comparable to the mapped extent of the previous largest flows downstream of the 1995 and 2005 slide area.

In the absence of sustained high pore pressures and fluid saturation, the slide D scenario run-outs are comparable to the run-out observed from the 1995 slide. There is a very strong dependence of run-out distance and depths on the extent of initial fluid saturation of the slide mass. The composition of the slide mass is complex. The largest run-out distance scenario requires that the slide retain high pore pressures in the core of the flow for fifteen to forty seconds.

8.5.3 Numerical Simulation of the 2005 Slide

A numerical simulation can reproduce past events if realistic input parameters are incorporated. Information from 2005 slide includes pre- and post-slide topography, video of the slide that provides constraints on the duration of portions of the slide and the fluidization of the slide, and post-slide photographs that provide information about slide morphology. These data were combined with geotechnical estimates of the material properties of the slide material and highly detailed topographic information to perform numerical simulations of the 2005 slide. This modeling was conducted to evaluate the influences of specific parameters on slide run-out distances, depths, and overall behavior.

Pre- and post- 2005 slide topography were incorporated to model the 2005 slide. Digital elevation models (DEM) derived from two-foot elevation contours from 1995 and 2006 were used to reconstruct the initial slide mass of the 2005 slide. The 1995 and 2006 DEMs with eight-ft grid spacing were smoothed with a convolution filter to reduce artifacts associated with contours. The topographic differences between 2006 and 1995 in the slide source area were used to define the initial slide mass depths and slide base surface.

The 2005 slide provided several important constraints on debris flow parameters. First, a basal friction angle of about twenty degrees was required for the bulk of the slide to propagate to the base of the slope. Basal friction angles of twenty five or more resulted in the majority of the slide mass remaining between Ranch Road and the base of the slope, even when pore pressure ratios were allowed to remain > 0.7 for several tens of seconds. Second, internal friction angles less than ten degrees resulted in a slide toe that spread so much that the final slide toe depths were much less than observed in 2005. Third, internal friction angles were required to be between ten and fifteen degrees to allow the final slide toe to develop to the southeast of the initial slide path and attain the final slope along the top of the slide as it extended uphill from the toe.

In the absence of persistence of high-pore pressures for tens of seconds after the bulk of the slide mass encounters the base of the slope, the slide mass rapidly decelerates, and run-out distances and final depths of the thickness and densest portions of the flow are determined by the internal friction angle of the slide material. Only when large depth-averaged, high-pore pressures are maintained throughout the flow mass on both the hillside (slope) and on the "flat" area containing the community of La Conchita, does a 'runaway' fluidized debris flow propagate further than the 2005 slide. Such a debris flow generally produces shallow (one- to two-foot thick), highly liquid flow over a larger area than the 2005 slide, with a deep flow front confined to a width comparable to the width of the slide on the steep slope.

8.5.4 Estimated Debris Flow Run-out Volumes

For the conceptual design of catchment basins and other debris flow mitigation schemes, we developed estimates of possible debris flow volumes. These estimates represent amounts of material that could be mobilized as discrete flows from within existing debris flow source areas containing loose material (colluvial swales) on the hillslope to the base of the cliff (Table 8.2). Debris flow volumes are calculated for specific debris flow drainages identified based on our geomorphic mapping of potential sources. Volumes are estimated based on the surface extent of each source area, combined with limited information on thicknesses of stored slope deposits. Boring WLA-BA3 on Ranch Road exposed over thirty feet of colluvial deposits overlying landslide materials. The estimated uphill source volumes were matched to estimated downhill volumes within historic and pre-historic debris flows based on the surface extent of the debris fans and depths of associated debris flow deposits within La Conchita. These estimates were derived from the mapped areal extent of past flows and thicknesses of debris run-out estimated from limited subsurface exploration (borings WLA-BA1 and WLA-BA3) conducted for this

study. The estimates do not include future possible failure and mobilization of intermediate areas on the slope.

Hungr and others (1984) note that predictions of debris flow volume typically are based solely on storm runoff or peak surface discharge within drainages. However, they note that it is more logical to base predicted debris flow volume on the availability of upslope debris. This approach is particularly appropriate for conceptual design purposes within the La Conchita Study Area given that the apparent source of saturation of slope deposits and build up of pore pressure beneath these deposits is spring fed. Each of the debris flow sources shown on Figure 8.7 is associated with established gullies and drainages that have historic evidence for past, or the potential for future, transport of debris downslope. The volumetric estimates for each source provided in Table 8.2 are based on observed physical parameters including the mapped surface area and thicknesses of slope wash deposits for each source and associated debris fans.

Our volumetric estimates provide preliminary constraints on the total volume of stored debris flow material that may be mobilized in future events. Additional borings are required to more fully characterize thicknesses of uphill cliff slope deposits and better constrain likely volume per debris flow event.

Table 8.2 Estimated debris flow volumes for individual debris flow sources.

Debris Flow Source	Total Surficial Area (in feet2)	Average Thickness (in feet)	Maximum Thickness (thickness in feet)	Total Stored Volume (cubic yards)	Estimated Volume for 500-yr Debris Flow (cubic yards)
			SOURCE UPHILL OF RANCH ROAD		
A	49,207	16	30	29,000	6,114
B	81,866	12	30	19,300-33,000	9,692
C	25,232	12	25	5,270-9,800	2,241
D	48771	12	25	20,200	7,733
E	32,961	6	20	5,145	2,412

Debris Flow Source	Total Surficial Area (in feet2)	Average Thickness (in feet)	Maximum Thickness (thickness in feet)	Total Stored Volume (cubic yards)	Estimated Volume for 500-year Debris Flow (cubic yards mobilized in flow)
			SOURCE DOWNHILL OF RANCH ROAD		
A	2,825	10	20	520	112
B	8,599	10	30	1,600	875
C	0	0	0	-	-
D	8,275	8	15	1,200	475
E	14,384	10	20	2,500	2,250

Debris Flow Source	Total Stored Volume (in feet3)	Estimated Event‡ Debris Flow Volume (ft3)	Estimated Event‡ Debris Flow Volume (cubic yards)
		TOTAL UPHILL SOURCE	
A	797,000	168,106	6,226
B	535,180-905,970*	285,297	10,567
C	156,300-278,370*	60,520	2,241
D	577,820	221,626	8,208
E	206,415	125,876	4,662

However, the lateral extent of the 1937 debris flow fan and associated evacuation of the gully source strongly suggests that stored sediment within a source area may be completely mobilized downslope, and the source depleted, during an event. Combined with evidence for historic movement within all of the identified uphill debris sources, we believe that the volumetric estimates are reasonable input for the purpose of conceptual design.

8.5.5 Debris Flow Probability Map

An inventory of slope failures, including both landslides and debris flows, compiled from historical accounts and photogrammetry (the interpretation of available sets of historical aerial photographs) provides the basis for estimating the probability of future debris flows within the Study Area. The inventory represents a given historic time interval during which a minimum number of slope failures occurred. Sets of available aerial photographs (1927 through 2007) provide an eighty-year record, with historical accounts extending back a minimum of another twenty years, including accounts of major landslide impacts to the coastal highway and railroad. There is an eighty- to hundred-year historical record available within the Study Area with approximate estimates for the maximum debris flow deposition depths for most years (many years are zero).

Because large events (such as the 1937 and 2005 debris flows) are infrequent, they should be sampled over longer periods than smaller events (Hungr and others, 1984). To reduce the effects of data censoring (omission), we have examined the period of debris accumulation constrained by stratigraphic analysis, based on record of dated debris flow deposits that extends back to about 1,500 years before present. Radiocarbon ages from charcoal obtained at depths of fifteen and twenty feet (samples BA2-1 and BA2-2; Appendix E) in large-diameter boring WLA-BA2 provide constraints on number and return period of debris flows within La Conchita.

At a depth of fifteen feet, we obtained a date of 1,200 years before present (sample BA2-1; Table 8.1). This sample was collected from a debris flow buried beneath at least five other debris flows ranging in thickness from two to four feet. At the twenty-foot depth within large diameter boring WLA-BA2, a date of 1,570 years before present was obtained within the seventh identified buried debris flow (sample BA2-2; Table 8.1). This debris flow is approximately 370 years older that dated at 15 feet. Based on the dated deposits, an average return period of approximately 200 to 250 years is estimated between relatively large (greater than two-feet thick) individual debris flows extending within the community of La Conchita.

This approximate 1,500-year geologic record is used to generally constrain depth-frequency return periods of 500 to 1000 years. We calculated the likely lateral extent, depths, and frequency of debris flow inundation based on the following:

1. Estimates of periods of geologic/historical time where depth has not exceeded a particular value with some range of uncertainty for the nonexceedence depth and the duration of time that flows depths did not exceed the depth;
2. Evidence of individual event flow depths with some range of depth uncertainty and the approximate time that they occurred; and,
3. Individual events where the maximum depth is not known, but the depth was larger than some minimum depth and the approximate time the event occurred can be determined.

This information was integrated with our existing maps of debris fans, interpretation of available borings, and historical records to produce a map of the probable extent of two-feet run-out depths for return periods of 50, 475, and 1,000 years (Figure 8.8). This map is intended for conceptual design purposes

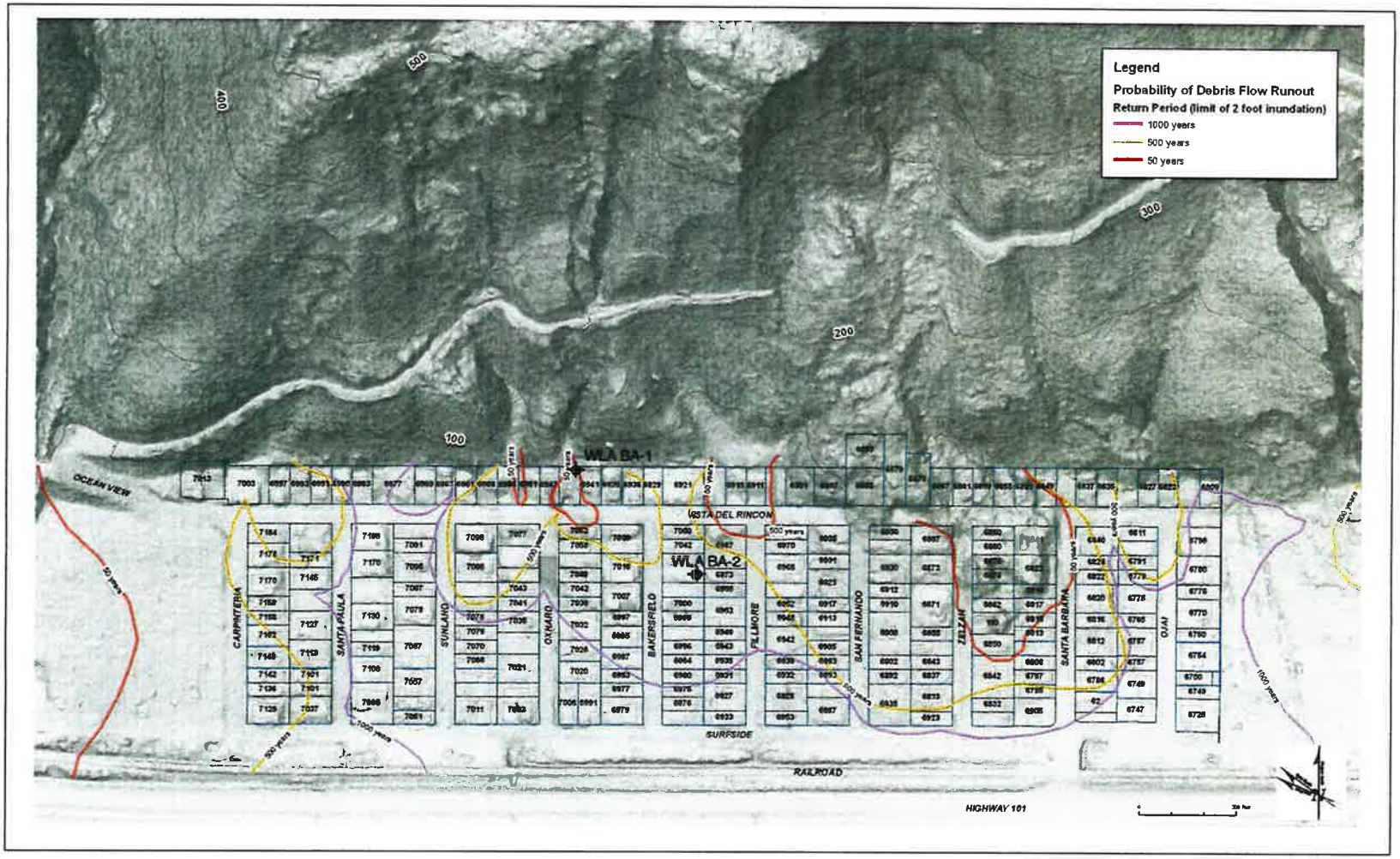

Map showing Probability of Debris Flow Run-out (limits of two-foot inundation)

LA CONCHITA LANDSLIDE – PHASE 2
Figure 8.8

02 JAN 08, 1885, CSH

only as more subsurface information is required to constrain past debris flow ages and run-out thicknesses within the Study Area. The 475-year return period is roughly approximate to a 500-year return period, used by AKA (2007), given the degree of uncertainty inherent within the available data.

8.6 Discussion of Landslide and Debris Flow Hazard

Jibson (2005; 2006) outlined several distinct landslide scenarios that pose potential future hazards to the community of La Conchita including the following:

(a) The remainder of the 1995 landslide could remobilize as a deep slump-earth flow similar to that in 1995;
(b) The 1995 (and possibly the 2005) deposit could mobilize into a rapid debris flow as occurred on 10 January 2005;
(c) Secondary landslides could be triggered from parts of the 1995 and 2005 deposits or scarps;
(d) Slumps and (or) earth flows on adjacent hillsides could mobilize; and,
(e) Intense rainfall could trigger rapid debris flows from various nearby slopes, particularly the ravines.

We have examined these potential slope hazards for this study. As part of our geologic evaluation, we also have collected new geophysical and geologic information, including radiocarbon and geotechnical samples, for evaluation of past and possible future large-scale landsliding of the larger landslides under static and seismic loading conditions. The possibility of earthquake-triggered landslide displacement is not discussed by Jibson (2005; 2006), but is addressed in additional modeling performed by AKA as part of this current study, and presented in their report.

Jibson (2006) concluded that remobilization of the 1995 landslide mass would likely be relatively slow, compared to the 2005 debris flow, but still could pose serious hazards to property and, perhaps, life. However, he questioned why the 1995 landslide did not fail in the same way that was observed in 2005.

> *'Why did the landslide material not mobilize into a rapid debris flow in 1995? What about the remaining 1995 deposit? Since only about 15% of the 1995 deposit remobilized in 2005, could the remainder also mobilize into a rapid debris flow, or is it more likely to remobilize as a deep slump-earth flow? Or will it remain metastable?' (Jibson, 2006)*

Our interpretation is that the 1995 slide debris consisted of two discrete sources; a bedrock-involved block landslide that was not reactivated in the 2005 slide and re-actived debris flow deposits. The upcoast bedrock landslide material blocked the drainage, allowing saturation of the downcoast debris. We infer that the upcoast material may be metastable but slope hazards are greatest where subsurface drainage is blocked and stored slope deposits are saturated. Debris flows appear to have the greatest hazard for future potential impacts to the community.

Finally, it is important to note that new landslides or debris flows could occur where none have been previously mapped. The hazard associated from previously unidentified features can not be directly evaluated. Debris flows may occur within the areas not shown that could impact the base of the cliff. However, as the cliff directly inland of the community of La Conchita is composed entirely of landslide debris, new failures could occur anywhere upslope of, east of, Vista del Rincon Drive. These failures may occur as portions of the cliff failing along buried landslide planes or as discrete debris flows. This is the apparent case with debris source area "E", which initially failed in 1986-1987 within a previously stable area and flowed onto Ranch Road.

9.0 EVALUATION OF SEISMIC HAZARDS

Because of the relative frequency of earthquakes in the Transverse Ranges, it is likely that during this century an earthquake will occur of sufficient size to cause damage to the community of La Conchita. We have evaluated associated seismic hazards to allow comparison of these earthquake-related hazards with the primary hazards from landslides and debris flows. This conceptual-level information is provided in support of decisions to be made relating to the safety and future of the community of La Conchita.

Based on the published and unpublished information available for the La Conchita Study Area, we have examined the likely return times, and overall probability, of seismic-related events and associated potential damage. The effects of strong ground shaking, associated ground deformation, fault rupture, and potential tsunami inundation are of primary concern. However, it is important to note that seismic hazards within the La Conchita Study Area are not unique within southern California and are comparable to those present for other developed portions of Ventura County.

9.1 Strong Ground Shaking

Ground shaking is the earthquake effect that results in the vast majority of structural damage and loss of life during large earthquakes. An earthquake produces seismic waves that emanate in all directions from the fault rupture surface. The seismic waves cause strong ground shaking, which typically is strongest near the fault and diminishes (attenuates) as the waves move through the earth away from the fault. The magnitude of an earthquake is a measure of the seismic waves or energy released by the earthquake.

Strong shaking from an earthquake can trigger landslides, ground lurching, and liquefaction. Structural damage from strong ground shaking may be accompanied by secondary damage from associated hazards including fire, releases of hazardous materials, or flood inundation as a result of broken water and sewer mains. The severity of ground shaking at a particular site is controlled by the interaction of several factors, including the distance from the earthquake source, earthquake magnitude, and the type, thickness, and condition of underlying geologic materials.

In 2002, the U.S. Geological Survey (USGS) completed an update of the national seismic hazard maps that depict the probabilistic ground-shaking hazard for the entire United States (Frankel and others, 2002). The hazard was calculated at a series of gridded locations (spaced 0.05 km apart) across the country using probabilistic seismic hazard analysis (PSHA) techniques. The USGS maps display contoured ground motion parameters (PGA and spectral accelerations) for a given probability of exceedence. The likely ground shaking level for the Study Area is approximately 0.6 to 0.7g within a 475-year return period (10% in 50 years). The 475-year return period is similar to the 500-year return period examined for this study by AKA.

More detailed information on probable ground shaking levels was developed by the California Geological Survey (CGS) for liquefaction zoning purposes, with ground motion parameters adjusted for the presence of alluvial deposits beneath the community of La Conchita (CGS, 2002). CGS (2002) calculated peak ground accelerations (PGAs) of 0.39 to 0.73g for the Pitas Point quadrangle resulting from a predominant earthquake of magnitude of Mw6.8. An average PGA of 0.65 for the 475-year return period was estimated for alluvial conditions within the community of La Conchita.

The severity of ground shaking at any particular point is referred to as "intensity" and is a subjective measure of the effects of ground shaking on people, structures, and earth materials. Ground shaking

intensity commonly is measured using the Mercalli Modified Scale, which provides a means of correlating felt effects of an earthquake to the size (magnitude) of an earthquake. Mercalli Intensity VIII is characterized by very strong to severe ground shaking, and commonly is associated with initiation of structural damage to buildings, including partial collapse (based on Wald and others, 1999). The associated ground motion value (PGA) at the lower end of Mercalli Intensity VII is 0.34g. This threshold PGA value clearly is exceeded within the 475-year return period commonly used for designing buildings under the State building code. For this study, we have incorporated the USGS analysis of potential ground shaking hazard based on the ten percent in 50-year hazard level (475-year return period) to derive the annual probability of exceedence of a PGA value of 0.34g required to produce damage (Figure 9.1).

9.2 Liquefaction-Induced Ground Failure

Liquefaction-related ground failure historically has caused extensive structural damage in urbanized areas around the world. Recent examples of these effects include damage produced during the 1989 Loma Prieta, 1994 Northridge, 1995 Kobe, and 1999 Turkey earthquakes. These and other historical earthquakes show that the distribution of liquefaction-related damage is not random, but generally is restricted to recently alluviated areas that contain low-density, saturated, granular sediments.

During the 1994 Northridge earthquake, liquefaction occurred at the mouth of the Santa Clara River in Oxnard/Ventura, in Simi Valley, and along the Santa Clara River between Fillmore and Newhall (Barrows and others, 1995). Settlement and lateral spreading caused by the earthquake resulted in rupture of an oil pipeline near the I-5 crossing of the river, directly east of Ventura County, and initiated an oil spill that contaminated large portions of the river downstream (Stewart and others, 1996). Distinctive and unusual patterns of ground shaking and localized damage in the alluvial areas of coastal Ventura County also have occurred during previous earthquakes, as interpreted from historical reports (Weber, Jr., and Kiessling, 1976). However, there are no historical accounts of liquefaction within the vicinity of La Conchita.

The potential for liquefaction depends on both the *susceptibility* of a deposit to liquefy and the *opportunity* for ground motions to exceed a specified threshold level. Liquefaction susceptibility is the relative resistance of a deposit to loss of strength when subjected to ground shaking. Loss of soil strength can result in ground failures at the earth's surface. These failures, including localized ground settlement and lateral spreading, can cause significant property damage. Physical properties of surficial deposits govern the degree of resistance to liquefaction during an earthquake. These properties include sediment grain-size distribution, density, cementation, saturation, and depth. Sediments that lack resistance (susceptible deposits) commonly include saturated young sediments that are sandy and loose. Sediments resistant to liquefaction include older surficial deposits that are dry or sufficiently dense.

Historical and geologic evidence of large earthquakes in Ventura County, and evidence of past liquefaction during these earthquakes (Barrows and others, 1995), demonstrates that the opportunity exists to produce liquefaction in susceptible sediments in Ventura County. Given the widespread occurrence of active faults in Ventura County, virtually all parts of Ventura County will be exposed to long duration peak ground acceleration in excess of 0.15g, the typical threshold for initiation of liquefaction. These ground motions are produced by earthquakes typically greater than Mw 6.5.

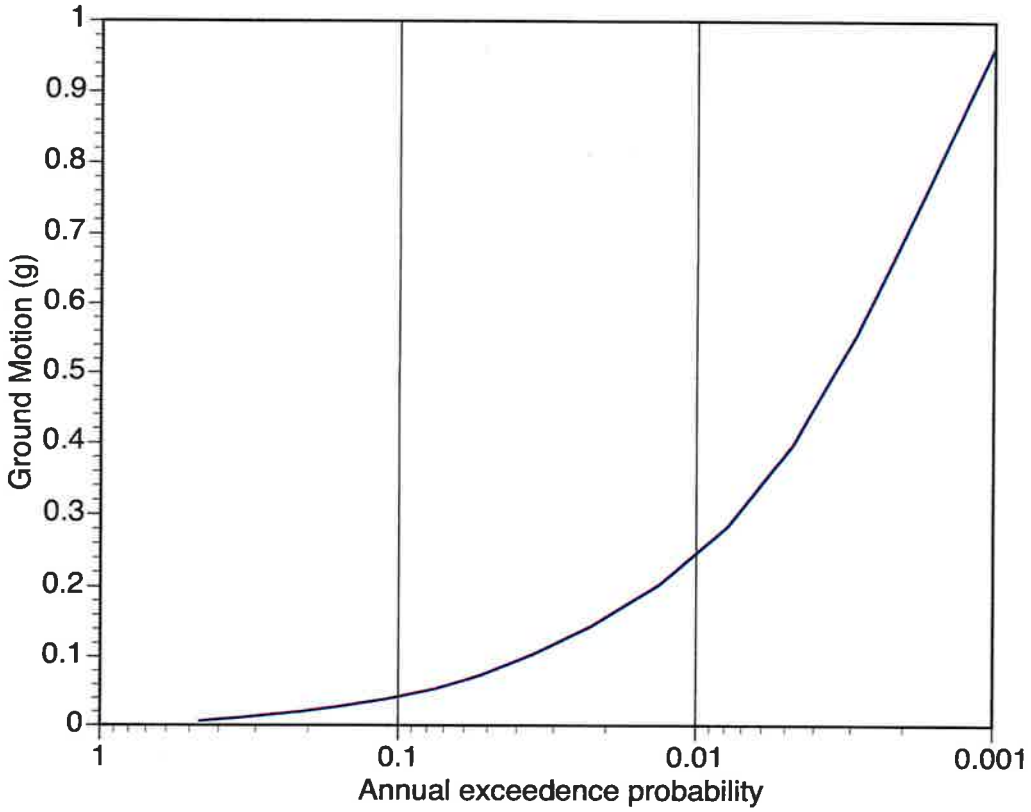

WLA

Chart of Ground Shaking Hazard (10% in 50 Years/475-year Return Period)

LA CONCHITA LANDSLIDE – PHASE 2

Figure 9.1

02 JAN 08, 1885, CSH

Major fault zones capable of producing large earthquakes in or near La Conchita include the Red Mountain fault, the Oak Ridge fault, the Simi-Santa Rosa fault system, the Santa Ynez fault, the Santa Susana fault, and the San Andreas fault among others (see Table A.1; Appendix A). Additional buried, or "blind" thrust faults present within Ventura County and offshore are potential seismic sources.

9.2.1 Liquefaction Hazard within La Conchita

The community of La Conchita lies completely within the CGS liquefaction hazard zone (CGS, 2002). CGS zones areas with late Holocene deposits as potentially liquefiable if ground shaking levels (PGA) with a ten percent probability of being exceeded in fifty years (475-year return period) are greater than or equal to 0.10g and the water table is potentially less than forty feet below the ground surface. Inclusion of La Conchita within the zone of required investigation primarily was based on the presence of soil of late Holocene age, the unknown depth of groundwater beneath the community, and the absence of specific geotechnical data that would preclude potential liquefaction (personal communication, Ralph Loyd (CGS), April, 2007). Only six geotechnical borehole logs containing depth to groundwater and corrected soil density data within the Pitas Point Quadrangle were compiled during the CGS zoning process, with none located in the community of La Conchita (CGS, 2002)

Three general geotechnical conditions are necessary for liquefaction to occur: (1) the presence of shallow (less than fifty feet deep) groundwater within the potentially liquefiable material; (2) the presence of granular soil that meets a specific range of grain sizes (typically with a fines content of less than thirty-five percent); and (3) the soil is of low to moderate relative density. If all those conditions are present and strong ground shaking occurs, portions of the soil column could liquefy depending upon the intensity and duration of the ground shaking.

Liquefaction typically occurs in loose, saturated granular soil materials (sand, silty sand, and potentially clayey sand). Although variable, subject to seasonal and tidal fluctuations, groundwater typically is found at depths ranging from ten to sixty feet but is absent beneath much of the community based on available subsurface data. Groundwater, where present beneath La Conchita, is typically encountered at an elevation of ten feet above sea level. With surface elevations ranging from approximately twenty to eighty feet within the community, the depths of potentially liquefiable terrace sands and thickness of overlying clay-rich soil increases landward from West Surfside Street.

Geotechnical boring logs and Cone Penetrometer (CPT) soundings provide lithologic data that are useful for assessing liquefaction susceptibility. For example, geotechnical borings commonly include information on soil texture (USCS) from field observations and laboratory particle size distribution analyses. Compiled borings and recent geotechnical reports (Pacific Materials Laboratories, 2006) suggest that deposits under La Conchita are predominately fine-grained (Figure 9.2). Site conditions consist generally of clayey artificial fill, dense beach sands and hard clayey Pico Formation at depth.

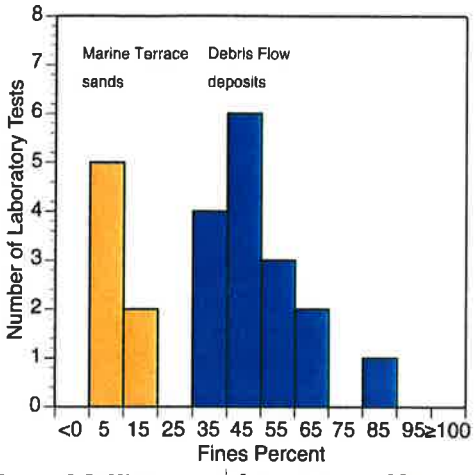

Figure 9.2 Histogram of percentage of fines in buried marine terrace sands versus debris flow deposits derived from laboratory grain-size analyses in geotechnical reports.

Existing shallow borehole data provide the primary means to assess the density of deposits beneath La Conchita. Geotechnical properties measured include dry unit weight, penetration resistance, and relative compaction. Field blow count and CPT data suggest that liquefaction potential in the beach sands within the buried marine terrace is low (Figure 9.3). CPT tip resistance values are generally above 150 tons per square foot (tsf) and locally above 200 tsf (Fugro West, 2007). Field blow counts in the underlying terrace deposits generally are above thirty-five blows per foot. Corrected blow counts (SPT) in the overlying debris fan deposits typically range from nine to thirty-seven, with an average value of approximately twenty-two. However, these deposits have a high fines content (Figure 9.2). Combined with a high fines content and deep groundwater, the potential for liquefaction-related ground deformation is minor.

Differential settlement caused by liquefaction can damage building foundations, occasionally causing structural collapse, but rarely is associated with direct loss of life. Currently, there are two published methods for assessing amounts of settlement in clean sands (Tokimatsu and Seed, 1987; Ishihara and Yoshimine, 1992), both of which require detailed, site-specific subsurface geotechnical data to depths of 50 feet. These methods estimate that typical volumetric strains for clean sands range from one to five percent (Jones and others, 1994). Given that the total thickness of the liquefiable sands is less than 10 to 15 feet, at depths of 40 to 670 feet, any settlement would be on the order of inches.

As noted in Fugro (2007), based on continuous CPT data collected near the entrance of La Conchita at Highway 101 seismic settlement estimates are less than one to two inches. Therefore, the hazard of ground settlement at any given location within La Conchita likely is minor to non-existent. However, as mandated by State law, a geotechnical study is required for proposed residential structures within the liquefaction zone to ensure that local site conditions are not conducive to liquefaction-related failure.

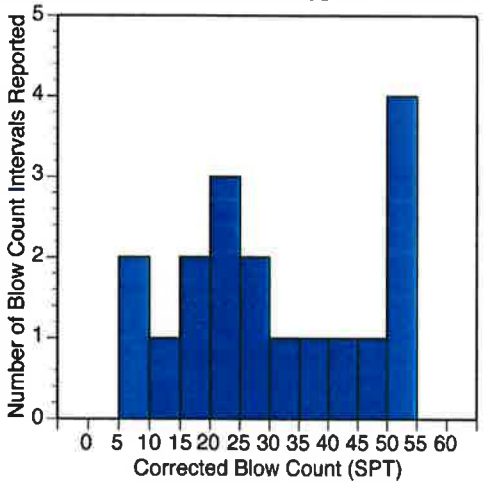

Figure 9.3 Histogram of percentage of fines in buried marine terrace sands versus debris flow deposits derived from borehole logs in geotechnical reports.

9.3 Surface Fault Rupture

Ground surface displacement, or surface rupture, caused by an earthquake is a major consideration in the assessment of seismic hazard. Surface rupture occurs when movement on a fault deep within the earth breaks through to the surface. Most surface faulting is confined to a relatively narrow zone several to tens of feet wide, making avoidance (i.e., building setbacks) the common mitigation method. Fault rupture typically follows preexisting faults, which are zones of weakness. Specific geomorphic features commonly coincide with the locations of repeated fault rupture. Thus, identification of active faults that might produce surface rupture requires: (1) location of existing faults and, (2) evaluation of the recency of activity on the faults. The most useful and direct method of evaluating fault activity is to document the youngest geologic unit faulted and the oldest unit that is not faulted to constrain the timing of the most recent surface offset on the fault.

The Alquist-Priolo Earthquake Fault Zone Act of 1972 was established by the California Legislature to mitigate the potential hazards of surface rupture associated with seismic activity. The Act requires the California Geological Survey (CGS) to evaluate and delineate active faults throughout the state. A fault or fault zone is considered active under the provisions of the Act if there is evidence of surface displacement within the last 11,000 years (Holocene time). Under the Alquist-Priolo Act, if faults are "sufficiently active" and "well-defined," they are zoned and construction along them is regulated. A fault is thought to be sufficiently active if one or more of its segments or strands show evidence of surface displacement during Holocene time. A fault is considered well defined if its trace can be clearly identified by a trained geologist at the ground surface or in the shallow subsurface, using standard professional techniques, criteria, and judgment (Hart and Bryant 1997).

The Red Mountain fault is not well located in the La Conchita area, particularly across the cliff face inland, upslope, of the town. In 1991, the fault was zoned as part of the official State of California map of earthquake fault zones (CGS, 1991). The official Alquist-Priolo fault zone extends across the cliff face upslope of the community of La Conchita. More recently, the CGS mapped strands of the Red Mountain fault during regional mapping activities, also placing the main trace of the fault across the cliff face upslope of the community of La Conchita (CGS, 2003). The CGS (1991, 2003) main map trace of the fault extends across undeveloped land upslope of, and upcoast of, the community of La Conchita. This strand, zoned by CGS (1991), extends across the plateau beneath La Conchita Ranch, along the face of the cliff landward of La Conchita, and across West Barranca upcoast of La Conchita.

9.3.1 Estimates of Maximum Earthquake Magnitude and Fault Displacement

Based on the revised California probabilistic seismic hazard maps (Cao and others, 2003) and preliminary documentation for the 2007 update of the U. S. national seismic hazard maps (National Seismic Hazard Mapping Project, 2007), the Red Mountain fault has an estimated length of 62 miles (100 km), a down-dip rupture width of 10.5 miles (17 km), and an approximate slip rate of 2.0 ± 1.0 mm/yr. Given the 656 square mile (1,700 km^2) fault plane area (A) for the Red Mountain fault, the maximum earthquake magnitude (Mmax) associated with the fault is estimated to be Mw7.2 to Mw7.3, based on the fault plane area regressions of Wells and Coppersmith (1994) for all slip types and reverse slip faults, respectively.

The revised California probabilistic seismic hazard maps (Cao and others, 2003) utilize a logic tree with two, equally weighted branches to assign Mmax. These branches are (1) the combination of the Wells and Coppersmith (1994) relation for $A < 500$ km^2 and the WGCEP (2003) relation for $A \geq 500$ km^2; and (2)

combination of the Wells and Coppersmith (1994) relation for A < 468 km^2 and the Hanks and Bakun (2002) relation for A ≥ 468 km^2. Based on the Cao and others (2003) logic tree, Mmax for the Red Mountain fault is M_w 7.3.

Table 9.1 provides ranges of possible surface displacement on the Red Mountain fault based on empirical relations established by Wells and Coppersmith (1994) for all fault types and for reverse-slip faults similar to the Red Mountain fault. Our mapping suggests the presence of multiple strands of the fault north of the community of La Conchita (Figure 5.2). Based on the exposure of the northern strand of the fault adjacent to Ocean View Road (Figure 5.6), a significant amount of past offset on the Red Mountain fault has occurred on this inferred secondary strand. Therefore the total amount of fault offset on the strand of the Red Mountain fault mapped, and zoned, by CGS (1991, 2003) may be less than that calculated across the entire fault zone.

Table 9.1 Calculated values of coseismic displacement based on regressions and standard deviations given by Wells and Coppersmith (1994), using estimated input parameters.

	Surface Displacement based on regression for all slip types			Surface Displacement based on regression for reverse-slip faults*		
	Mean value	1 standard deviation	2 standard deviations	Mean value	1 standard deviation	2 standard deviations
Surface rupture length = 100 km (62 miles)						
maximum	4.6 m	4.2 to 5.0	3.8 to 5.4 m	***2.5 m***	*2.1 to 2.9 m*	*1.7 to 3.4 m*
displacement	15.1 ft	13.8 to 16.4 ft	12.5 to 17.7 ft	***8.2 ft***	*6.9 to 9.5 ft*	*5.6 to 11.2 ft*
average	2.1 m	1.8 to 2.5 m	1.4 to 2.9 m	***1.1 m***	*0.7 to 1.5 m*	*0.3 to 1.9 m*
displacement	6.9 ft	5.9 to 8.2 ft	4.6 to 9.5 ft	***3.6 ft***	*2.3 to 4.9 ft*	*1.0 to 6.2 ft*
Earthquake magnitude = M_w 7.3						
maximum	3.4 m	2.9 to 3.8 m	2.5 to 4.2 m	***1.9 m***	*1.5 to 2.3 m*	*1.1 to 2.7 m*
displacement	11.2 ft	9.5 to 12.5 ft	8.2 to 13.8 ft	***6.2 ft***	*4.9 to 7.5 ft*	*3.6 to 8.9 ft*
average	1.7 m	1.4 to 2.1 m	1.0 to 2.5 m	***0.7 m***	*0.3 to 1.1 m*	*0 to 1.5 m*
displacement	5.6 ft	4.6 to 6.9 ft	3.3 to 8.2 ft	***2.3 ft***	*1.0 to 3.6 ft*	*0 to 4.9 ft*

* Regressions for reverse-slip relationships shown in italics are not significant at a 95% probability level. Values shown in bold are preferred for conceptual level design.

9.3.2 Probability of Fault Displacement

Variability in total surface displacement predicted for a certain magnitude earthquake along a fault rupture results in uncertainties that are a sizable fraction of the total displacement estimated for any major fault. However, the greatest contribution to uncertainty in the calculations is in the empirical displacement-magnitude relation. Because data on displacement per event at a site are uncommon for reverse faults like the Red Mountain fault, estimating coseismic displacements typically is based on empirical data (e.g., Wells and Coppersmith, 1994), as calculated above. Uncertainty in the rupture model is significant, as characterizations of earthquake behavior are based on a short historical record compared to earthquake recurrence times.

The "simplified approach" for calculating the probability of fault rupture is based on a fault model consisting of a single, characteristic earthquake that has an estimated magnitude and recurrence (return period). This approach assumes that the 475-year return period displacement can be estimated as the median value of the average displacement for the characteristic earthquake. Thus the approximate value of fault displacement on the Red Mountain fault would be roughly two to four feet. This estimate is roughly the same as using the inferred slip rate on the fault to estimate how long would be required to produce enough stored strain on the fault to produce estimated slip per event displacement. A slip rate of between two to six mm/yr would require from 115 to 550 years between major earthquakes.

Finally, the estimates of offset on the fault within the cliff area may be somewhat high because of: (1) the presence of multiple fault strands; and, (2) the conditional probability of fault displacement at the ground surface should incorporate the possibility that earthquake rupture may not reach the surface. The 1989 Mw6.9 Loma Prieta and 1994 Mw6.7 Northridge earthquakes are examples of large, damaging earthquakes that did not reach the surface and thus would not present a fault rupture hazard. Coefficients from a globally-derived dataset of 276 earthquakes by Wells and Coppersmith (1993) predict that 81% of the Mw6.8 earthquakes, 87% of the Mw7 earthquakes, and 98% of the Mw7.9 earthquakes will rupture to the surface.

9.4 Tsunami Inundation

Tsunami are waves generated by rapid displacement of a large volume of seawater, typically resulting from submarine faulting, volcanic eruptions, or large-scale submarine slides. Tsunami generated due to earthquake-related deformation of the seafloor, especially those caused by great earthquakes with large rupture dimensions and high seismic moment, can travel across oceanic basins and produce widespread damage to distant coastal communities and environments (e.g. Indian Ocean Tsunami of 2004). Trans-oceanic tsunami travel at 350 to 500 miles per hour in the open ocean. As a tsunami approaches the shoreline, the wave height increases, resulting in potentially destructive onshore impacts.

Historical records and recent field observations indicate that the severity of tsunami-generated damage depends on the type and size of the tsunami source, coastal topography, and the direction of the incoming waves. The waves slow and increase in amplitude as water depths shallow. Tsunami current velocities in the near-shore environment can be on the order of thirty to sixty feet per second. Hazards from tsunamis therefore include: (1) run-up where tsunami waves wash ashore at heights above normal wave action, and (2) strong currents that can cause localized coastal erosion.

There are three major types of tsunamigenic sources for future tsunami that could potentially impact La Conchita. These include local offshore faults and regional earthquake sources along the Pacific Ocean margin. Earthquake-related movement of the seafloor can result in an accompanying displacement of the ocean surface. The displaced water column is unstable and immediately begins to flow outward from the displacement. The resulting change in potential energy provides the energy for the tsunami wave (Okal and Synolakis, 2003). The energy imparted to the tsunami from coseismic seafloor displacement is sufficient for the tsunami to pose both a local and trans-oceanic hazard.

Tsunami also are produced from local submarine slope failure when the movement of the slide mass creates a bulge on the seafloor at its toe and a mass deficiency, or depression, on the seafloor at the head of the failure with associated displacement of the overlying water column. Because the physical mechanism and speed of the mass dislocation in the slope failure is slow compared to seismic-related seafloor movement, the energy imparted from a submarine slope failure typically is less than that of large earthquakes, and the resulting tsunamis attenuate or die out more rapidly. For this reason, tsunami generated from submarine slope failures typically are local in nature and do not pose a transoceanic inundation hazard (Okal and Synolakis, 2003).

9.4.1 Tsunamigenic Earthquake Sources

Given the number of mapped active faults in the southern California offshore area, and an overall offshore regional rate of strike-slip displacement estimated at five to ten mm/yr, large offshore tsunamigenic earthquakes may have recurrence times of 200-500 years (Legg and others, 2003). Large offshore earthquakes may directly generate tsunami through tectonic seafloor uplift or indirectly by

triggering large submarine slope failures. Vertical movement on reverse faults can cause significant displacement of the seafloor producing tsunami. In addition, offshore strike-slip faults have sinuous traces with structural bends or step-overs that can cause local uplift or subsidence during an earthquake, triggering tsunami (Legg and Kennedy, 1991). Numerous major on-shore fault systems extend offshore in the vicinity of La Conchita, including the Red Mountain and Oak Ridge faults (Figure 9.4). Offshore sources of particular interest for tsunami generation include the Channel Islands Thrust, a north-dipping blind thrust fault responsible for uplift of the Channel Islands and possibly capable of generating six feet (two meters) run-up heights with up to sixty feet (eighteen meters), if a large enough earthquake is associated with triggered submarine landslides (Borrero and others, 2004).

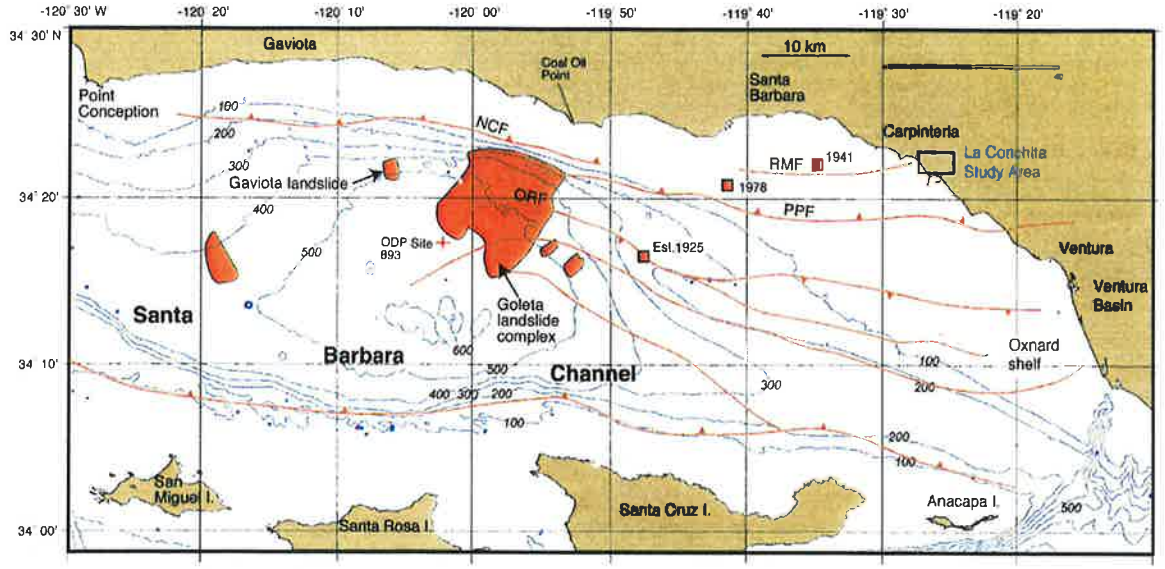

Figure 9.4 Map of the western Santa Barbara Channel showing known submarine landslides, major faults (red lines), and historical earthquakes (red squares). Faults include the Pitas Point (PPF), the Red Mountain (RMF), the North Channel (NCF), and the Oak Ridge (ORF) faults (from Fisher and others, 2005).

9.4.2 Tsunamigenic Landslide Sources

Submarine slope failures have the potential to cause localized and severe tsunami. The 1998 Sissano Lagoon tsunami in Papua New Guinea was triggered by a near-shore, seismically-induced slope failure. The tsunami had a run-up height of up to fifty-two feet (sixteen meters) and caused over 2,000 fatalities (Synolakis and others, 2002). The 1992 Flores Island tsunami in Indonesia also was caused by an earthquake-triggered slope failure and had a run-up height of eighty-five feet (twenty-six meters; Yeh and others, 1993). These events were caused by the sudden displacement of sea floor sediment in large submarine landslides. However, the mechanics leading to tsunami generation from submarine slope failure are complex and as yet incompletely understood (Bardet and others, 2003). As such, these events are not routinely considered in the engineering of major infrastructure projects.

Recent studies have identified possible landslide sources for tsunami in the Santa Barbara channel offshore of La Conchita (Figure 9.5). Of these possible sources, the Goleta landslide complex is the largest and best characterized. This large, approximately eight miles (fourteen kilometers) long by seven

miles (eleven kilometers) wide, series of landslides could be associated with failures on the order of five billion cubic yards of material. A nearby smaller submarine landslide, the Gaviota landslide, has a total volume of roughly a quarter of a billion cubic yards and is thought to be capable of generating a local tsunami run-up heights of about six feet (two meters), based on research by Fisher and others (2005). However, even a tsunami this large from a submarine landslide located immediately offshore likely is insufficient to significantly inundate the community of La Conchita.

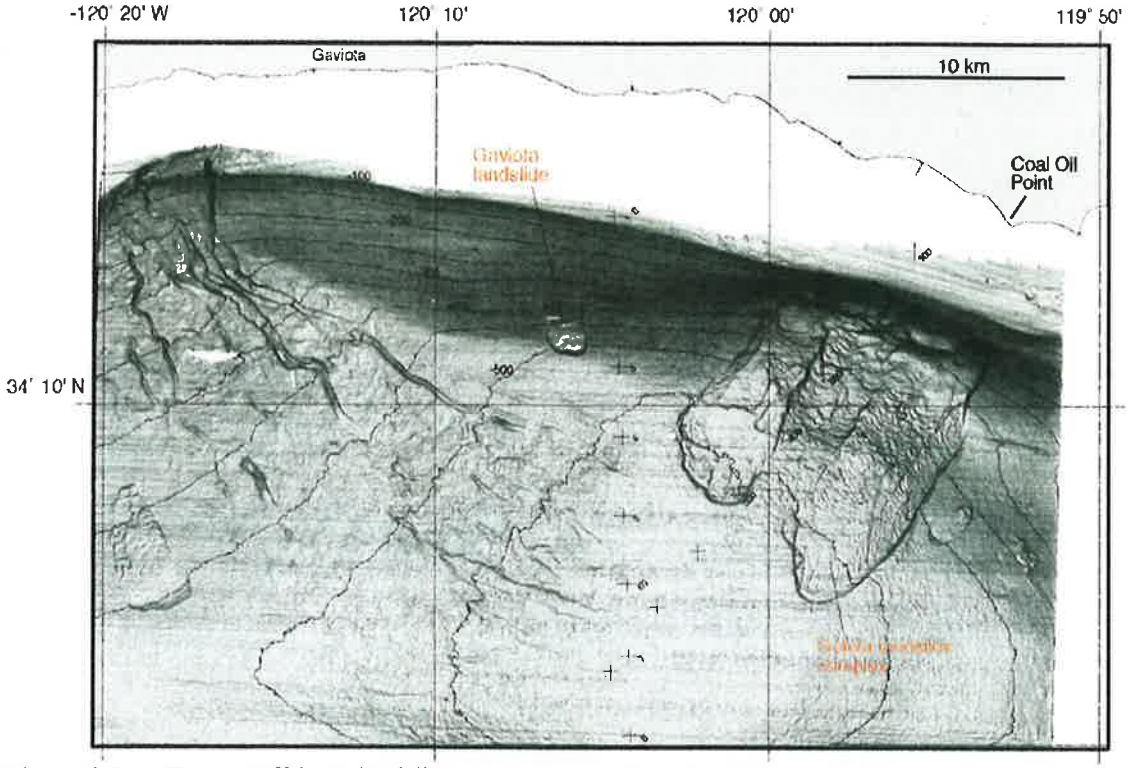

Figure 9.5 Known offshore landslide sources, including the Goleta landslide complex and Gaviota landslide (as mapped by Fisher and others, 2005).

A larger submarine landslide such as failures associated with the Goleta landslide complex could generate tsunami run-ups of up to sixty feet (twenty meters), sufficient to damage La Conchita. (Fisher and others, 2005). However, inundation from waves triggered by submarine landslides is expected to be highly focused with only narrow (five to six miles, or roughly ten kilometers, wide) sections of the immediate shoreline impacted. As shown on Figure 9.6, the estimated distribution of tsunami run-up heights from the offshore Goleta slides does not exceed the minimum elevation threshold for inundation of La Conchita. In addition, similar large landslide been not been identified immediately offshore of La Conchita. However, other possible landslide sources may exist in deeper water or off the Channel Islands. Further study is required to better characterize potential additional sources but current research suggests that known offshore landslide sources for tsunami run-up are unlikely, or at least have a low probability, of causing sufficient run-up to inundate the community of La Conchita.

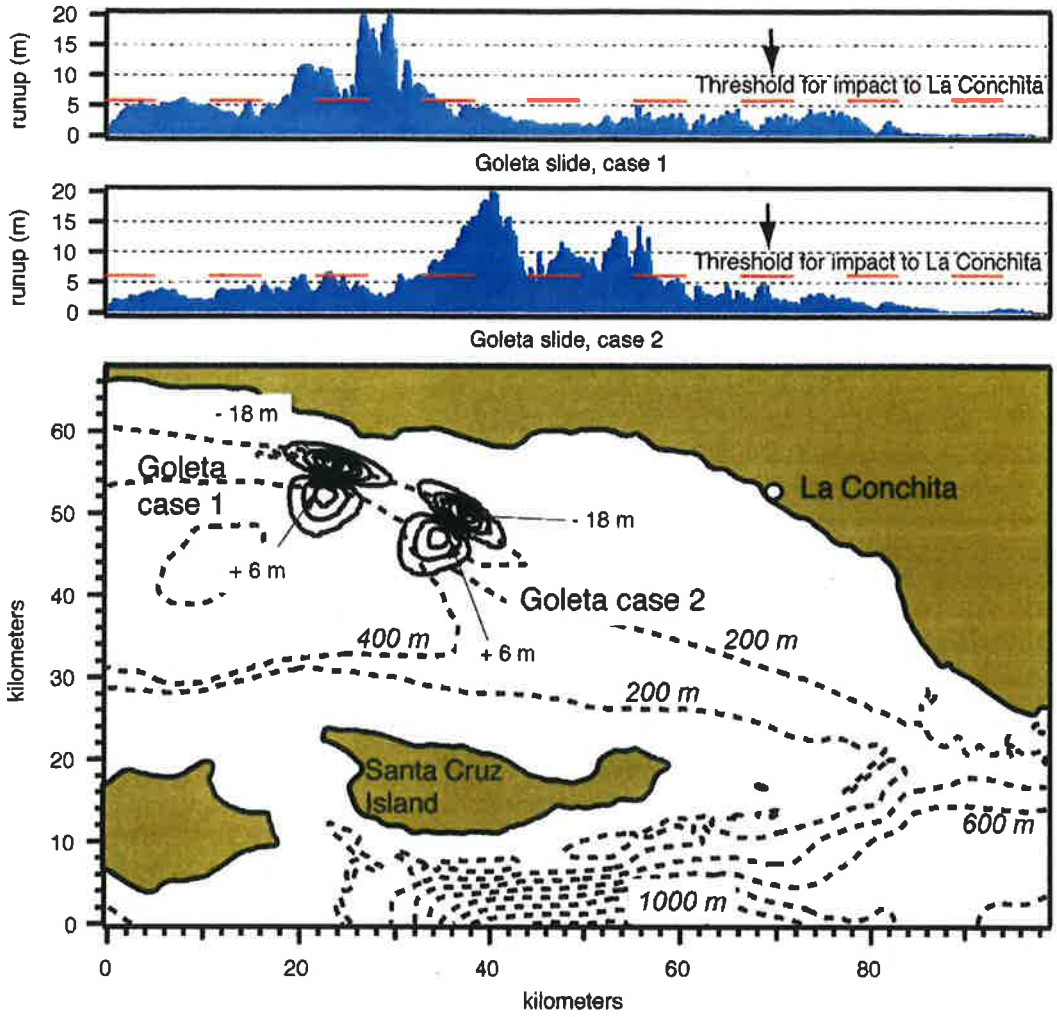

Figure 9.6 Estimated tsunami run-up from the Goleta offshore landslide sources (Fisher and others, 2005).

9.4.3 Historical Tsunami Catalog

The historical record indicates that at least eleven tsunami have been documented with coastal run-ups in the Santa Barbara, Ventura, or Los Angeles Counties since 1806 (Table 9.2). This results in an average of about one tsunami every twenty years. The only historical tsunami to cause significant damage and loss of life along the California coast occurred as a result of the 1964 Alaska earthquake (McCulloch, 1985). Smaller tsunamis recorded along the Ventura coastline over the past 200 years have generally accounted for run-up heights of less than three to four feet (Table 9.2; McCulloch, 1985). However, the potential exists for a future major tsunami from distant sources that might inundate portions of the Ventura Coast, and possibly the community of La Conchita.

9.4.4 Probability of Tsunami Run-up

Although Probabilistic Seismic Hazard Assessments (PSHA) usually are conducted to obtain estimates of the ground shaking hazard from all likely earthquakes, more recently the same approach has been extended to estimate tsunami run-up at the shoreline. Tsunami run-up is the depth of water above a certain datum caused by tsunami inundation. In PSHA, the estimation of ground shaking level for a specified magnitude and distance is based on ground motion attenuation relations. This approach is not feasible for tsunami, because the orientation of source of the tsunami and local ocean bathymetry can cause large variability in local wave height, which is not a simple function of distance. To estimate the tsunami run-up at a particular location on a coast for a given earthquake, a waveform excitation and propagation approach is used rather developing attenuation relations similar to those used to characterize earthquake waves.

In order to identify the appropriate waveforms for use in a Probabilistic Tsunami Hazard Assessment (PTHA), a seismic source model is first developed (as also done for PSHA) that describes the location of potential earthquake sources, range of earthquake magnitudes, earthquake recurrence intervals, and style of faulting. Landslide occurrence is an additional aspect of the PTHA source model.

Table 9.2 Documented Tsunami Run-ups in Southern California (from 1806 through 2008).

Tsunami Source			Tsunami Run-up		
Date Year Month/Day	**Source Location**	**Source**	**Run-up location**	**Run-up (meters)**	**Comments**
1806 3/24	S. California	E?	Santa Barbara	Observed	Boats beached.
1812 12/21	S. California	L	El Refugio	3.4	Anchored ship drifted up canyon.
			Santa Barbara	2	Estimated run-up.
			Ventura	2	Estimated run-up.
1854 5/31	S. California	L	Santa Barbara	Observed	Sea agitated. Heavy swell. Not recorded.
1877 5/10	N. Chile	E	Anaheim	0.9	Swift currents.
			Gaviota	1.8	Observed.
1931 10/3	Solomon Is.	E	San Diego	<0.1	
			Santa Barbara	<0.1	
1932 6/3	Jalisco, Mexico	E	Long Beach	0.1	
			San Diego	<0.1	
			Santa Barbara	<0.1	
1946 4/1	Aleutian Is.	E, L	Los Angeles	0.4	
			Santa Barbara	Observed	
			Ventura.	Observed	Observed by swimmers
1952 11/4	Kamchatka Peninsula, Russia	E	La Jolla	0.1	Recorded on marigram
			Long Beach	0.3	"
			Los Angeles	0.3	"
			Port Hueneme	0.7	"
1957 3/9	Aleutian Is.	E	La Jolla	0.3	Minor damage
			Long Beach	0.3	Recorded on marigram
			Los Angeles	0.3	"
			San Diego	0.2	Wall of water 1 m high reported at Shelter Is.
			Santa Monica	0.5	
1960 5/22	Chile	E	Long Beach	0.7	$500,000 - $1 million damages
			Los Angeles	0.8	1 drowned, 1 injured
			San Diego	0.7	80 m of dock destroyed
			Santa Barbara	1.4	$20,000 damages
			Santa Monica	1.6	Boats broke mooring
1964 3/28	Gulf of Alaska	E	Long Beach	Observed	8 docks destroyed.
			Los Angeles	0.5	$200,000 damages
			Oxnard	Observed	Heavy surf
			San Diego	0.6	3.6 m above MLLW
			Santa Barbara	0.8	
			Ventura	Observed	2.6 m above MLLW, bore up Little River

Note: Run-up heights provided in Table 9.2 represent the observed or estimated heights at specific locations in Southern California, not an estimate of run-up for La Conchita. Run-up is the depth of water above a certain datum caused by tsunami inundation. The key to the cause of the event is as follows: L = Landslide E = Earthquake

Once the source model is developed, a complete tsunami wave field can then be computed for each scenario earthquake and landslide in the model. This method provides a means of evaluating the total risk (seismic and tsunami) to coastal communities. The PTHA can be used to identify whether a significant tsunami hazard exists at a particular coastal location or over a stretch of coastline. If the hazard is found to be significant, then the approach allows further analyses including:

- Probabilistic tsunami run-up and inundation calculations at the site based on the probabilistic tsunami wave height at the shoreline; and,
- Probabilistic tsunami loss calculations based on the probabilistic run-up and inundation.

However, a PTHA currently does not exist for the portion of coast that includes La Conchita. In addition, the basic information required for detailed analysis and input for such a study is not readily available. Given the scope of our study, and mandate to provide conceptual mitigation alternatives, we have performed 'back of the envelope' calculations using existing published data to evaluate; (1) whether the likely return period of tsunami hazard is significant within the time periods evaluated for the overall hazard study, (2) determine general parameters for inclusion in an overall view of hazards, and (3) whether more detailed study is required to analyze the possible impacts of future tsunami to La Conchita.

Tsunami heights for 100-year and 500-year return periods were estimated at 10.5 feet and 21.7 feet for Ventura in a 1974 U.S. Army Corps of Engineers report (Eisner, Borrero, and Synolakis, 2001). Topographic surveys indicate that most of the community of La Conchita is between an elevation of twenty feet (six meters) and sixty feet (eighteen meters), or at elevations at or above these estimated tsunami wave run-up elevations. More recently, work suggest that the probability of large tsunami with associated amplitudes and run-ups sufficient to damage La Conchita have even lower probabilities, with an extremely low annual probability of exceedence. Watts (2004) calculated cumulative probabilities for tsunami having amplitudes equal to twenty to sixty feet (local tsunami run-up may be greater) as less than one to five percent of all tsunami generated in the Pacific (Figure 9.7). This suggests that the average return period of tsunami associated with wave heights greater than twenty feet is even greater than that previously estimated.

In summary, based on the historical record, past tsunami have not been large enough to inundate the community of La Conchita. Recent research has identified nearby offshore landslide and fault sources with the potential to generate large tsunami. However, insufficient information currently exists to fully evaluate the probability of future tsunami inundation and run-up heights in the vicinity of La Conchita. Our review of the available research strongly suggests that tsunami run-up is not a significant hazard within the 100- and 500-year periods of interest, compared to more frequent and potentially damaging landslide hazards.

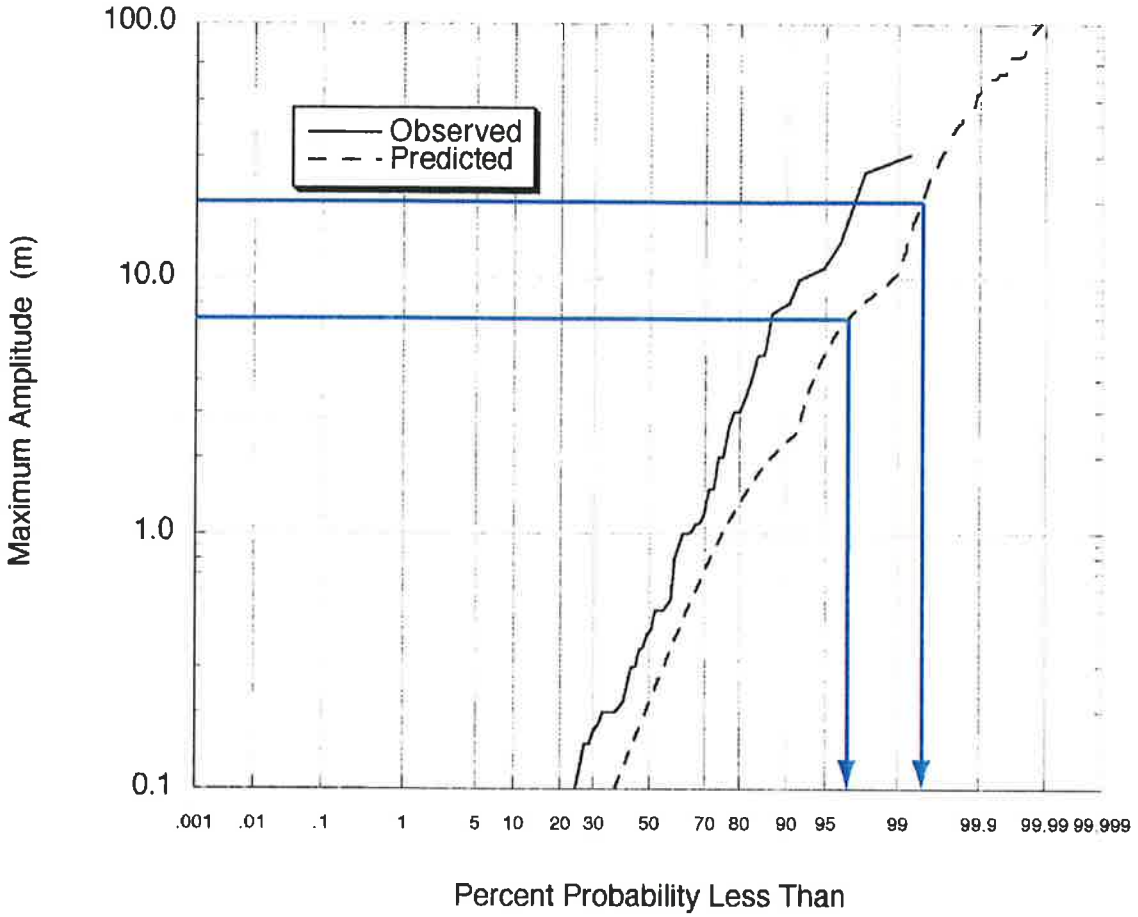

Figure 9.7 Comparison of the predicted tsunami amplitude probability distribution of Southern California versus the measured peak run-up of Pacific Basin tsunami during the 1990s (from Watts, 2004). Blue arrows show the approximate range of tsunami amplitude required to inundate La Conchita. Further study is required to determine whether additional near-shore bathymetry may influence local tsunami run-up in the La Conchita Study Area.

9.5 Summary of Seismic Hazards

Seismic hazards within the La Conchita Study Area are comparable to those present for other developed portions of Ventura County. Hazards identified by previous studies, and zoned by the State of California and County of Ventura, include earthquake-induced liquefaction, fault rupture, tsunami inundation, and strong ground shaking. Of these hazards, liquefaction and tsunami hazards are the least probable to occur with the lowest potential for structural damage and loss of life within the time periods (50, 500, and 1000 years) examined for this study.

Fault rupture on the Red Mountain fault, although also a low probability hazard, does have the potential for causing up to eight feet of displacement, much of it consisting of vertical separation across the fault. Surface rupture across the fault, however, likely would not extend under existing structures. Based on mapping of inferred strands of the Red Mountain fault by the State of California (CGS 1991; 2003), the surface traces of the fault extend across undeveloped land landward of, and upcoast of, the community of La Conchita. Surface rupture associated with a large earthquake on the Red Mountain fault likely would

occur along the mapped main trace of the fault across the plateau beneath La Conchita Ranch, along the face of the cliff landward of La Conchita, and across West Barranca upcoast of La Conchita.

Exposure to the likelihood of strong ground shaking is the greatest seismic hazard to the community of La Conchita. The probability of ground shaking during the next fifty years is high, and even higher over a 500-year period, given the number of nearby active fault sources. Consequences of strong ground shaking may include structural collapse with the potential for loss of life. In addition, strong ground shaking may trigger movement of large landslides within the cliff landward of La Conchita, with the lateral displacement of the landslide toes possibly encroaching upon residences. La Conchita has experienced strong ground shaking from nearby historical earthquakes including moderate to large offshore earthquakes in 1812, 1925, 1941, and 1978 (Table 3.2).

10.0 CONCLUSIONS

Results of this study include new surface and subsurface data providing information on the geologic, hydrologic, and structural conditions present with the Study Area. New mapping performed for this study, based on high-resolution topography data derived from high-resolution LiDAR surveys, provides new information on the lateral extent of landslides and debris flow sources. Five large-diameter borings provide information on the depths and orientation of landslide failure planes, as well as the types of material involved in landsliding. Two hollow-stem augers borings to depths of over 150 feet in the landslides provided samples for geotechnical testing and downhole geophysics (shear wave velocity) profiles. Laboratory testing of radiocarbon samples provide limited constraints on landslide and debris flow deposits. Shear-wave profiles in the downcoast slide ('soil slide') and upcoast slide ('bedrock' slide) document variation in apparent material properties, including possibly landslide deposits density, between the two slides.

Although we present new data and provide new interpretation of the site geology and structure, our conclusions are constrained by both the limited data available and the overall purpose of this study. The scope of our study is to support conceptual designs for possible mitigation alternatives to reduce overall hazard to the community of La Conchita and commerce along the coastal corridor. To the degree possible, we have examined major and minor geologic and seismic hazards within the Study Area, in order to provide a comparison of the relative probability and impact of these hazards. Table 10.1 presents an overall comparison of the major hazards. Although the hazard from earthquake-induced ground failure and associated tsunami inundation from offshore sources can not be ignored, our analyses clearly show that the most frequent and highest consequence hazards to the community of La Conchita are from future slope failures.

Table 10.1 Geologic and Seismic Hazards ranked by probability, from most common to least frequent.

Hazard	Minimum Threshold	Annual Probability	Average Return Period (years)	Associated Damage	Life Safety
Debris Flow from West Barranca	Deposition on fan that reaches town or railroad	0.0526	19	Moderate (localized flooding of H101/railroad/town)	Low
Small landslide along bluff face (back of Vista Del Rincon)	25 ft horizontal displacement	0.0244	41	Moderate (localized severe structural damage)	Low
Debris Flow inundation into town from hillslope	<=1 ft thick flow that extends to Vista Del Rincon	0.0167	60	Moderate (localized flooding)	Low
Strong Ground Shaking (>0.3 g)	>= 0.34 g*	0.0063	158	High (structural damage including partial collapse)	High
Liquefaction-induced ground deformation	>=0.4 g	0.0047	211	Low (~2-4 inches settlement)	Low
Major debris flow inundation into town from hillslope	>=2 ft inundation seaward of Vista Del Rincon	0.0038	265	High (localized severe structural damage)	High
Tsunami Inundation - Surfside Street	inundation of 20 foot elevation	0.0020	500	Moderate (localized flooding)	Moderate
Surface Fault Rupture	M6.5 or greater earthquake on Red Mountain fault	0.0008	1,250	Low** (not mapped through town)	Low
Earthquake-triggered Large Landslide (triggering PGA?)	Earthquake on RMF or strong ground shaking	-	>1,250 (for Red Mountain fault earthquake)	High (localized severe structural damage)	High
Tsunami Inundation - Entire town***	60 feet runup elevation	0.0007	1,500	High (severe structural damage)	High

* Correlative to Mercalli Intensity VIII,very strong to severe ground shaking associated with initiation of structural damage to buildings, including partial collapse (based on Wald et al., 1999)

** Local associated ground shaking would be high. However, this hazard is addressed above in ground shaking (USGS (1996) probabilisitic estimates of ground shaking with 1250-yr return period are great than 1.0 g)

*** 100-year and 500-year tsunami probabilities were estimated in a 1974 U.S. Army Corps of Engineers Report (Eisner, Borrero, and Synolakis, 2001) for Ventura at 10.5 feet and 21.7 feet, respectively. More recently Watts (2004) calculated cumulative probabilities for tsunami with less than 1% having amplitudes equal to 40-60 feet (local tsunami runup may be greater). This suggest that the average return period is very long.

11.0 REFERENCES

Alan Kropp & Associates, Inc., 2007, Phase 1 Report, La Conchita Slope Stabilization Project, La Conchita, Ventura County: Contract No. 3108855 (CRN 17600307169846) submitted to the California Department of General Services (DGS).

Bachman, S., 1998, Geologic and hydrogeologic investigation, La Conchita Ranch; unpublished report dated March 1998.

Bagnold, R.A., 1956. Flow of cohesionless grains in fluids. Philos. Trans., R. Soc. London 249, pp. 235–297.

Bailey, W., 1925, A Study of the Santa Barbara Earthquake of June 29, 1925: Bulletin of the Seismological Society of America, Vol. 15, No. 4, pp. 255-278.

Bardet, J.P., Synolakis, C.E., Davies, H.L., Imamura, F., and E.A. Okal, 2003, Landslide tsunamis: Recent findings and research directions: Pure and Applied Geophysics, v. 160, p. 1793-1809.

Barrows, A. G., Irvine, P., and Tan, S.S., 1995, Geologic Surface Effects Triggered by the Northridge Earthquake: The Northridge, California, Earthquake of 17 January 1994, Special Publication 116, M.C. Woods and W.R. Seiple, Eds., California Division of Mines and Geology, Sacramento, CA, pp. 65-88.

Borcherdt, R. D., 1994, Estimates of site-dependent response spectra for design (methodology and justification): Earthquake Spectra, 10, 617-654.

Borrero, J. C., M. R. Legg, and C. E. Synolakis, 2004, Tsunami sources in the southern California bight, Geophys. Res. Letters, 31, L13211, doi:10.1029/2004GL020078.

Cao, T., Bryant, B.A., Towshandel, B., Branum, D., and Wills, C.J., 2003, The revised 2002 California probabilistic seismic hazard maps, California Geological Survey, (http://www.consrv.ca.gov/cgs/rghm/psha/fault_parameters/pdf/2002_CA_Hazard_Maps.pdf).

California Geological Survey (formerly California Department of Conservation, Division of Mines and Geology), 1991, Revised Official Map of Earthquake Fault Zones, Pitas Point Quadrangle, scale 1:24,000.

California Geological Survey (CGS), 2002, Seismic hazard evaluation of the Pitas Point 7.5-minute quadrangle, Ventura County, California: CGS Seismic Hazard Zone Report 073.

California Geological Survey (CGS), 2003, Preliminary geologic map of the Pitas Point 7.5-minute quadrangle, Ventura County, California: version 1.0 posted on CGS web site http://www.consrv.ca.gov/CGS/rghm/rgm/southern_region_quads.htm.

CALTRANS, 2002, Project Report - VEN 101, From KP R64.0 (PM R39.8) to KP R69.4 (PM R43.1).

Chen, C.L., 1988. Generalized viscoplastic modeling of debris flow. In: J. Hydraul. Div. 114(HY3), ASCE, pp. 237–258.

Clark, M. M., Harms, K. K., Lienkaemper, J. J., Harwood, D. S., Lajoie, K. R., Matti, J. C., Perkins, J. A., Rymer, M. J., Sarna-Wojcicki, R. V., Sharp, R. V., Sims, J. D., Tinsley, J. C., and Ziony, J. I., 1984, Preliminary slip-rate table for late Quaternary faults of California, U. S. Geological Survey Open-File Report 84-06, 12p.

Converse Consultants West, 1994, Final Report - Mitigation and Monitoring, La Conchita Ranch Road Landslide, Dated December 16, 1994, Project No. 94-31-292-02.

Corbett, E.J., Johnson, C.E., 1982, The Santa Barbara, California, earthquake of 13 August 1978: Bulletin of the Seismol. Soc. Am. 72, p. 2201– 2226.

Costa, J.E. and Jarrett, R.D., 1981. Debris flows in small mountain stream channels of Colorado and their hydrologic implications: Bull. Assoc. Eng. Geol. XVIII 3, pp. 309–322

Darton, N. H., 1915, Guidebook of the Western United States, Part C., The Santa Fe Route: USGS Bulletin 618.

Dengler, L., 2005, Dataset for the Historic Tsunami Run Up Map for California (excel spreadsheet): posted at: www.seismic.ca.gov/Appendix_A_Tsunami_Report.html, downloaded 2/27/08.

Dewitte, O., Chung, C.J., and A. Demoulin, 2005, Landslide reactivation hazard mapping in the Flemish Ardennes (W Belgium): Geophysical Research Abstracts, Vol. 7, 01762.

Dibblee, T. W., 1982, Regional Geology of the Transverse Range Province of Southern California, in Fife, S. L. and Minch., J.A., eds., Geology and Mineral Wealth of the California Transverse Ranges, South Coast Geological Society, Inc., Annual Symposium and Guidebook Number 10: Santa Ana, California, p. 7-26.

Dibblee, T.W., Jr., 1988, Geologic map of the Pitas Point and Ventura quadrangles: Dibblee Geological Foundation Map DF-21, map scale 1:24,000.

Denlinger, R. P., and R. M. Iverson, 2001, Flow of variably fluidized granular masses across three-dimensional terrain: 2. Numerical predictions and experimental tests: J. Geophys. Res., 106, 553–566.

Denlinger, R. P., and R. M. Iverson, 2004, Granular avalanches across irregular three dimensional terrain: 1. Theory and computation, Journal of Geophysical Research, 109, F01014, 14 p.

Denlinger, R.P., and D.R.H. O'Connell, 2007, Computing nonhydrostatic shallow water flow over steep terrain, submitted to the ASCE Journal of Hydraulic Research.

Durham, D. L., 2000, Place names of the California Central Coast: Quill Driver Books, Santa Barbara County, 272 pages.

Iverson, R. M., and R. P. Denlinger, 2001, Flow of variably fluidized granular masses across three-dimensional terrain: 1. Coulomb mixture theory, J. Geophys. Res., 106, 537– 552.

Edwards, R.D., Rabey, D.F., and Kouer, R.W., 1970, Soil survey, Ventura area, California: U.S. Department of Agriculture, Soil Conservation Service.

Eisner, R.K., Borrero, J.C., and Synolakis, C.E., 2001, Inundation maps for the State of California, in International Tsunami Symposium 2001, Seattle, WA, p. 67-81.

Ellsworth, W.L., 1990, Earthquake history, 1769–1989. U.S. Geological Survey Professional Papaper 1515, p. 153–187.

Engstrom, W., N., 1996, The California Storm of January 1862: Quaternary Research, Volume 46, Issue 2, Pages 141-148.

Fisher, M.A., Normark, W.R., Greene, H.G., Lee, H.J., and Sliter, R.W., 2005, Geology and tsunamigenic potential of submarine landslides in Santa Barbara Channel, Southern California: Marine Geology, v. 224, p. 1-22.

Frankel, A., Petersen, M. D., Mueller, C. S., Haller, K. M., Wheeer, R. L., Leyendecker, E. V., Wesson, R. L., Harmsen, S. C., Cramer, C. H., Perkins, D. M., and Rukstales, K. S., 2002, Documentation for the 2002 update of the national seismic hazard maps: U.S. Geological Survey Open-File Report OFR 02-420.

Fugro West, Inc., 2007, Foundation Report, Pedestrian Undercrossing beneath Highway 101, La Conchita, Ventura County, California, a letter report to Boyle Engineering Corporation, Ventura, California, FWI Project No. 3044.058.04, dated June 2007.

Fugro West, Inc., 2006, Preliminary Geotechnical Study, Pedestrian Undercrossing beneath Highway 101, La Conchita, Ventura County, California, a letter report to Boyle Engineering Corporation, Ventura, California, FWI Project No. 3044.058, dated December 27.

Fumal, T.E., 1978, Correlations between seismic wave velocities and physical properties of near-surface geologic materials in the southern San Francisco Bay region, California: U.S. Geological Survey Open-File Report 78-1067, 114 p.

Geotechnial Consultants. Inc., 1989, memo to David Orr, La Conchita Ranch, dated December 6, 1989.

Grismer, M.E., Bachman, S., and T. Powers, 2000, A comparison of groundwater recharge estimation methods in a semi-arid, coastal avocado and citrus orchard (Ventura County, California): Hydrological Processes, Volume 14, Issue 14, Pages 2527 – 2543.

Grismer M. E., Snyder R. L, and Faber B. A, 1999a, Determination of avocado and citrus orchard evapotranspiration along the southern California coast: California Agriculture, v. 54, no. 3.

Grismer M. E., 1999b, Longterm evapotranspiration from a coastal avocado/citrus orchard: American Society of Civil Engineers Journal of Irrigation and Drainage Engineering, v126, no.1, p1-7.

Grigsby, F.B., 1988, Structural development of the Ventura Avenue anticlinal trend at the San Miguelito and Rincon oil fields, Ventura County, California in Sylvester, A.G., and Brown, G.C., editors, Santa Barbara and Ventura basins, tectonics, structure, sedimentation, oilfields along an east-west transect: Coast Geological Society Field Guide no. 64, p. 111-124.

Hamilton, R.M., Yerkes, R.F., Brown, R.D., Jr., Burford, R.O., and DeNoyer, J.M., 1969, Geology, petroleum development, and seismicity of the Santa Barbara Channel region, California: United States Geological Survey Professional Paper 679-D, p. 45-77.Hanks, T. C. and Bakun, W. H., 2002, A bilinear source-scaling model for M–log A observations of continental earthquakes: Bull. Seism. Soc. Am., v. 92, p. 1841–1846.

Hanson, R.T., Martin, P., and Koczot, K.M., 2003, Simulation of Ground-Water/Surface-Water Flow in the Santa Clara—Calleguas Ground-Water Basin, Ventura County, California: U.S. Geological Survey Water–Resources Investigations Report 02-4136.

Harden, J.W., Sarna-Wojcicki, A.M., and Dembroff G.R., 1986, Soils Developed on Coastal and Fluvial Terraces near Ventura, California: U.S. Geological Survey Bulletin 1590-B, Soil Chronosequences in the Western United States, pp. B1-B18.

Harp, E. L., Keefer, D.K., and R.C. Wilson, 1978, A comparison of artificial and natural slope failures, the Santa Barbara Earthquake of August 13, 1978: California Geology, May 1980, Vol. 33, No. 5.

Harp E. L., Jibson R. W., 1996, Landslides triggered by the 1994 Northridge, California, earthquake. Seismol Soc Am Bull 86(1B): p. S319–S332.

Hart, E. W. and Bryant, W.A., 1997, Fault-rupture zones in California; Alquist-Priolo Special Studies Zones Act of 1972 with index to special studies zones maps (revised, 1997): California Division of Mines and Geology Special Publication 42.

Hemphill, J.J., 2001, Assessing landslide hazard over a 130-year period for La Conchita, California, in Association of Pacific Coast Geographers Annual Meeting, Santa Barbara, Calif., September 12–15 2001.

Hitchcock, C.S., Loyd, R.C., and Haydon, W.D., 1999, Mapping liquefaction hazards in Simi Valley, Ventura County, California: Environmental & Engineering Geoscience, Vol. V, No. 4, p. 441-458.

Hitchcock, C.S., Lindvall, S.C., Helms, J.D., Randolph, C.E., Weaver K.D., and Lettis, W.R., 2000, Liquefaction hazard mapping, Ventura County, California: Final Technical Report, USGS Award 99-HQ-GR-0117, 21 p, 4 plates.

Huftile, G. J., 1988, Subsurface Connection Between the Red Mountain and San Cayetano Faults, Ventura Basin, California: Eos, v. 69, no. 44, p. 1419.

Huftile, G. J. and Yeats, R. S., 1995, Convergence rates across a displacement transfer zone in the western Transverse Ranges near Ventura, California: Jour. Geophys. Res., v. 100, p. 2043-2067.

Huftile, G. J., Lindvall, S. C. Anderson, L. W. & Gurrola, L. 1997. Paleoseismic investigation and tectonic implications of the Red Mountain Fault, Southern California: Eos Transactions, American Geophysical Union, 78(46) (Supplement), F635.

Hungr, O., Morgan, G.C. & Kellerhalls, R., 1984, Quantitative analysis of debris torrent hazards for design of remedial measures. Can. Geotech. J., 21: 663-677.

Ishihara, K. and Yoshimine, M., 1992, Evaluation of Settlements in Sand Deposits Following Liquefaction During Earthquakes: Soils and Foundations, Vol. 32, No. 1, pp. 173- 188.

Iverson, R. M., and R. P. Denlinger (2001), Flow of variably fluidized granular masses across three-dimensional terrain: 1. Coulomb mixture theory: J. Geophys. Res., 106, 537– 552.

Jackson, P. A., 1980, Structural evolution of the Carpinteria basin, western Transverse Ranges, California: unpub. MS thesis, Oregon State University, Corvallis, Oregon, 107 p.

Jackson, P. A. and Yeats., R.S., 1982, Structural evolution of Carpinteria Basin, Western Transverse Ranges, California: American Association of Petroleum Geologist Bulletin, v. 66, no. 7, p. 805-829.

Jibson, R.W., 1989, Debris flows in southern Puerto Rico, in Schultz, A.P., and Jibson, R.W., eds., Landslide Processes in Eastern North America and Puerto Rico: Geological Society of America Special Paper 236, p. 29–55.

Jibson, R.W., 2005, Landslide Hazards at La Conchita, California: U.S. Geological Survey Open- File Report 2005-1067, 12 p. Available Online: http://pubs.usgs.gov/of/2005/1067/508of05-1067.html

Jibson, R.W., 2006, The 2005 La Conchita, California, Landslide: Landslides Vol. 3, p. 73-78.

Joyner, W.B., 2000, Strong motion from surface waves in deep sedimentary basins, Bull. Seism. Soc. Am., vol. 90, S95-S112.

Kamerling, M.J., Sorlien, C.C., 1999. Quaternary slip and geometry of the Red Mountain and Pitas Point-North Channel faults. California Abs; EOS 46 (80), F1003.

Kamerling, M. J., and Sorlien, C. C, 1999, Quaternary slip and geometry of the Red Mountain and Pitas Point-North Channel faults, California, Supplement to EOS, (Trans. AGU), v. 80, P. F1003.

Kirkbride. W.H.. 1927, The earthquake at Santa Barbara. California. June 2,. 1925, as it affected the railroad of the Southern Pacific Company: Seismological Society of America Bulletin. v. 17. no. 1. p. 1-7.

Lajoie, K. R., and others, 1979, Quaternary marine shoreline and crustal deformation San Diego to Santa Barbara, California, in Geological excursions in the southern California area: San Diego State University, p. 3-15.

Lajoie, K. R., Sarna-Wojcicki, A.M. and Yerkes, R.F., 1982, Quaternary Chronology and Rates of Crustal Deformation in the Ventura Area, California, in Cooper, J. D., ed., Neotectonics of southern California, Field Trip Guidebook: Boulder, Co., Geological Society of America, Cordilleran Section, p. 43-51.

Lajoie, K. R., Ponti, D.J., Powell, C.L., Mathieson, S.A. and Sarna-Wojcicki, A.M., 1991, Emergent Marine Strandlines and Associated Sediments, Coastal California; A Record of Quaternary Sea-Level Fluctuations, Vertical Tectonic Movements, Climatic Changes, and Coastal Processes, in Morrison, R. B., ed., The Geology of North American: Boulder, Co., Geological Society of America, p. 190-214.

Lajoie, K. R. and Sarna-Wojicicki, A.M., 1982, Late Quaternary Coastal Tectonics in the Central and Western Transverse Ranges, Southern California: GSA Abstracts with Programs, v. 14, no. 4, p. 179.

Lander, J.F., ed., 1973, Seismological Notes: January - February 1973. Bulletin of the Seismological Society of America, Vol. 63, No. 5, pp. 1841-1846.

Larsen, S., Agnew, D.C., and Hager, B.H., 1993, Strain accumulation across Santa Barbara Channel, 1970-1988: Journal of Geophysical Research, v. 98(B2), p. 2119-2133.

Larson, K.M., and Webb, F.H., 1992, Deformation in the Santa Barbara Channel from GPS measurements: Geophysical Research Letters, v. 19(14), p. 1491.

Legg, Mark R., Jose Borrero, and Costas E. Synolakis, 2003, Evaluation of Tsunami Risk to Southern California Coastal Cities, The 2003 NEHRP Professional Fellowship Report, Earthquake Engineering Research Institute (EERI), PF2002-11, 32 p.

Legg, M. R., and Kennedy, M. P., 1991. Oblique divergence and convergence in the California Continental Borderland. in Abbott, P.L., and W.J. Elliott (Editors) Environmental Perils of the San Diego Region, San Diego Association of Geologists Guidebook, p. 1-16.

Leighton and Associates, Inc, 1992, La Conchita Ranch, Dated December 11, 1992, Project No. 2920785-02.

Leighton and Associates, Inc, 1993, Summary of Geotechnical Investigations, La Conchita Ranch, Venture County, California, Project No. 2920785-05, dated August 20, 1993.

Lindvall, S. C., Huftile, G. C., Gurrola, L. D., and Bell, M. A., 2002, Paleoseismic investigation of the Red Mountain fault: analysis of the displaced Punta Gorda marine terrace: South Coast Geological Society Field Trip Guidebook, October 12-13, 2002

Lynch, Henry B., 1939, The history of floods in Southern California: American Geophysical Union, Transactions 1939, Pt1, p 6-8.

McCulloch, D. S., 1985. Evaluating tsunami potential, in Ziony, J. I., ed., Evaluating earthquake hazards in the Los Angeles Region—An earth science perspective, U.S. Geological Survey Professional Paper 1360, p. 375-413.

Namson, Jay and Davis, T.L., 1990, Late Cenozoic Fold and Thrust Belt of Southern Coast Ranges and Santa Maria Basin, California, AAPG Bulletin, v.74, n.4, p. 467-492.

National Oceanic and Atmospheric Administration (NOAA), 2-Minute Gridded Global Relief Data (ETOPO2): World Data Center for Marine Geology & Geophysics, Boulder, http://www.ngdc.noaa.gov/mgg/fliers/01mgg04.html

National Oceanic and Atmospheric Administration (NOAA), Tsunami Event Database Search: National Geophysical Data Center (NGDC), http://www.ngdc.noaa.gov/seg/hazard/tsevsrch_idb.shtml

NOAA/NGDC tsunami database accessed at: www.ngdc.noaa.gov/seg/hazard/tsrnsrch_idb.shtml, January 2008.

National Seismic Hazard Mapping Project, 2007, Preliminary documentation of the United States national seismic hazard maps, U. S. Geological Society Open-File Report, 93 p.

Nigbor, R., Imai, T., 1994, The Suspension P-S Velocity Logging Method: in Geophysical Characterization of Sites, ISSMFE Special Publication TC 10.

Okal, E.A. and Synolakis, C.E., 2003, A theoretical comparison of tsunamis from dislocations and landslides: Pure and Applied Geophysics, v. 160, p. 2177-2188.

Orme, A.R., 1998, Late Quaternary tectonism along the Pacific coast of the Californias: a contrast in style: Geological Society, London, Special Publications; 1998; v. 146; p. 179-197.

O'Tousa, James, 1995, La Conchita landslide, Ventura County, California: Association of Engineering Geologists AEG News, v. 38, no. 4, p. 22–24.

O'Tousa, James, 2005, personal communication cited in Jibson, 2005.

Parise, M., and Jibson, R.W., 2000, A seismic landslide susceptibility rating of geologic units based on analysis of characteristics of landslides triggered by the January 17, 1994 Northridge, California, earthquake: Engineering Geology, v. 58, p. 251–270.

Putnam W. C., 1942, Geomorphology of the Ventura Region, California: Bulletin of the Geological Society of America, Vol. 53 pp. 691-754.

Putnam W. C., and Sharp, R.P, 1940, Landslides and Earthflows near Ventura, Southern California: Geographical Review, Vol. 30, No. 4, pp. 591-600.

Reimer, PJ, Baillie, MGL, Bard, E, Bayliss, A, Beck, JW, Blackwell, PG, Buck, CE, Burr, GS, Cutler, KB, Damon, PE, Edwards, RL, Fairbanks, RG, Friedrich, M, Guilderson, TP, Herring, C, Hughen, KA, Kromer, B, McCormac, FG, Manning, SW, Ramsey, CB, Reimer, PJ, Reimer, RW, Remmele, S, Southon, JR, Stuiver, M, Talamo, S, Taylor, FW, van der Plicht, J, and Weyhenmeyer, CE, 2004, IntCal04 Terrestrial radiocarbon age calibration, 0-26 cal kyr BP: Radiocarbon 46, 3, 1029-1058.

Robinson, J.B., Hazell, W.F., and Young, W.S., 1998, Effects of August 1995 and July 1997 storms in the City of Charlotte and Mecklenburg County, North Carolina: U.S. Geological Survey Fact Sheet FS-036-98, 6 p.

Scullin, C.M., 1994, Subsurface exploration using bucket auger borings and down-hole geologic inspection: Bulletin of the Association of Engineering Geologists, v. 31, n. 1, p. 99-105.

Sidler, W. A., 1968, Agua Mansa and the flood of January 22, 1862 Santa Ana river, San Bernadino, California: San Bernadino County Flood Control District.

Shaw, J. and J. Suppe, 1994, Active faulting and growth folding in the eastern Santa Barbara Channel, California, Geol. Soci. of Am. 106, pp. 607-626.

Seeber, L. and C.C., Sorlien, 2000, Listric thrusts in the Western Transverse Ranges, California, Geological Society of America Bulletin, vol. 112; no. 7, p.1067-1079.

Sorlien, C.C., Gratier, J.P., Luyendyk, B.P., Hornafius, J.S., Hopps, T.E., 2000, Map restoration of folded and faulted late Cenozoic strata across the Oak Ridge fault, onshore and offshore Ventura basin, California. Geol. Soc. Amer. Bull. 112, 1080– 1090.

Sidler, W. A., 1968, Agua Mansa and the Flood of January 22, 1862, Santa Ana River: San Bernadino County Flood Control District.

Sorlien, C. C., M. J. Kamerling, L. Seeber, and K. G. Broderick, 2006, Restraining segments and reactivation of the Santa Monica–Dume–Malibu Coast fault system, offshore Los Angeles, California, J. Geophys. Res., 111, B11402, doi:10.1029/2005JB003632.Siebert L, Simkin, T., 2002, Volcanoes of the World: an Illustrated Catalog of Holocene Volcanoes and their Eruptions: Smithsonian Institution, Global Volcanism Program Digital Information Series, GVP-3, (http://www.volcano.si.edu/world/).

Stark, T.D., Choi, H., and McCone, 2005, Drained shear strength parameters for analysis of landslides, Journal of Geotechnical and Environmental Engineering, Vo. 131, No. 5.

Stoney-Miller Consultants, Inc, 1996, Summary Geotechnical Evaluation of the La Conchita Landslide - March 4, 1995, Ventura County, California, for the Bateman Group, Project No: 11203-00, Report No: 5-5042, dated October 18, 1996.

Stoney-Miller Consultants, Inc, 1998, Addendum to the Summary Geotechnical Evaluation of the La Conchita Landslide of March 4, 1995, Ventura County, California, dated March 17, 1998, Project No. 11469-00.

Synolakis, C.E., Bardet, J.P., Borrero, J.C., Davies, H.L., Okal, E.A., Silver, E.A., Sweet, S., and D.R. Tappin, 2002, The slump origin of the 1998 Papua New Guinea Tsunami, Proc. R. Soc. Lond., v. 458, p. 763-789.

Takahashi, T., Nakagawa, H. and Kuang, S., 1987. Estimation of debris flow hydrograph on varied slope bed: in Beschta, R.L., Blinn, T., Grant, G.E., Swanson, F.J. and Ice, G.G., Editors, Erosion and Sedimentation in the Pacific Rim, Publ. No. 165, Int. Assoc. Hydrol. Sci., IAHS Press, Wallingford, pp. 167–177.

Tokimatsu, K., and Seed, H.B., 1987, Evaluation of settlement of sands due to earthquake shaking: Journal of the Geotechnical Engineering Division, ASCE, v. 113, p. 861-878.

Toppazada, et al., 2000, Epicenters of and Areas Damaged by M>=5 California Earthquakes, 1800-1999: California Division of Mines and Geology, Map Sheet 49.

Townley, S.D., 1939, Earthquakes in California, 1769 to 1928: Bulletin of the Seismological Society of America, v. 29, no. 1, pp. 21-252.

Trecker, M.A., Gurrola, L.D., and E.A. Keller, 1998, Oxygen-isotope correlation of marine terraces and uplift of the Mesa hills, Santa Barbara, California: Geological Society, London, Special Publications; v. 146; p. 57-69.

Treiman, J.T., 1989, Fault evaluation report for the Javon Canyon Fault: California Division of Mines and Geology (CGS), FER 213, 9 p.

Troxell, H.C. and others, 1942, Floods of March 1938 in southern California: U.S. Geological Survey Water-Supply Paper 844, 399 p.

U.S. Geological Survey, 2005, National Earthquake Information Center (NEIC) earthquake catalog: http://neic.usgs.gov/neis/epic/epic.html

Ventura County Water Resources and Development Department, 1991, Memorandum dated June 18, 1991 by Joe Hanna.

Ventura County, memorandum from Jim Fisher to Al Echarren, Reconnaissance of Slope Hazard Areas: La Conchita and Ventura Avenue, dated February 14, 1992.

Ventura County Historical Society (VCHS), 2005, A Mountain Ranch: The Quarterly, Vol. 49, nos. 1 and 2, 43 pages.

Waananen, A.O., 1969, Floods of January and February 1969 in central and southern California: U.S. Geological Survey, Open-File Report, 233 p.

Watts, P., 2004, Probabilistic predictions of landslide tsunamis off southern California: Marine Geology, v. 203, p. 281-301.

Weber Jr., F. H. and others, 1973, Geology and Mineral Resources Study of Southern Ventura County, California: California Division of Mines and Geology Preliminary Report 14, 102 p.

Weber, F.H., Jr., and E.W. Kiessling, 1976, General Features of Seismic Hazards of Ventura County, California, in California Division of Mines and Geology, 1976; Special Report - Seismic Hazards Study of Ventura County, California: California Division of Mines and Geology (now California Geological Survey) Open File Report 76-5 LA.

Wells, D.L., and Coppersmith, K.J., 1994, New empirical relationships among magnitude, rupture length, rupture width, rupture area, and surface displacement: Bulletin of Seismological Society of America, v. 84, no. 4, p. 974-1002.

Wieczorek, G.F., 1987. Effect of rainfall intensity and duration on debris flows in central Santa Cruz Mountains, California. In: Debris Flows/Avalanches: Process, Recognition, and Mitigation, Geological Society of America, Boulder, pp. 93–104.

Wills, C.J., Petersen, M.D., Bryant, W.A., Reichle, M.S., Saucedo, G.J., Tan, S.S, Taylor, G.C, and Treiman J.A., 2000, A site conditions map for California based on geology and shear wave velocity: Bulletin of the Seismological Society of America, v. 90, no. 6b, p S187-S208.

Wills, C.J. and Silva, W., 1998, Shear wave velocity characteristics of geologic units in California: Earthquake Spectra, v. 14, p. 533-556.

Wills, C.J., Weldon, R.J., II, and Bryant, W.A., 2008, California fault parameters for the National Seismic Hazard Maps and Working Group on California Earthquake Probabilities, Appendix A in the The Uniform California Earthquake Rupture Forecast, version 2 (UCERF 2): US Geological Survey Open-File Report 2007-1437A and California Geological Survey Special Report 203A, 48 p. [http://pubs.usgs.gove/of/2007/1437/a/].

Working Group on California Earthquake Probabilities (WGCEP), 2003, Earthquake probabilities in the San Francisco Bay region—2002–2031: U. S. Geological Survey Open-File Report 03-214

Yeats, R. S., Lee, W.H.K. and Yerkes, R.F., 1979, Geology and Seismicity of the Red Mountain Fault, Ventura County, California: Tectonophysics, p. 385.

Yeats, R. S., 1983, Large-scale Quaternary detachments in Ventura Basin, Southern California: Journal of Geophysical Research, v. 88, no. B1, p. 569-583.

Yeats, R. S., Lee, W. H. K., and Yerkes, R. F., 1987, Geology and seismicity of the eastern Red Mountain fault, Ventura County: U. S. Geological Survey Professional Paper 1339, p. 161-168.

Yeats, R.S., and Olson, D.J., 1984, Alternate fault model for the Santa Barbara, California, earthquake of 13 August 1978: Bulletin of the Seismological Society of America, v. 74, no. 5, p.1545-1553.

Yeats, R. S., 1988, Late Quaternary slip on the Oak Ridge fault, Transverse Ranges, California: implications for seismic risk: Jour. Geophys. Res., v. 93, p. 12,137-149.

Yeh, H., Imamura, F., Synolakis, C.E., Tsuji, P.L., and S. Shi, 1993, The Flores Island Tsunamis, Eos, v. 74, no. 33, p. 369, 371-373.Wells, D. L. and Coppersmith, K. J., 1994, New empirical relationships among magnitude, rupture length, rupture width, rupture area, and surface displacement: Bull. Seism. Soc. Am., v. 84, no. 4, p. 974-1002.

Zeiser Kling Consultants, Inc, 1998, Vista Del Rincon Avenue Landslide Debris Removal Investigation, La Conchita, County of Ventura, California, Dated October 19, 1998, PN 98092-00.

APPENDIX A: SEISMIC SOURCES AND EARTHQUAKE CATALOG

FAULT NAME AND GEOMETRY	LOCATION	Sense of Slip	LENGTH (km)	+/-	Slip Rate (mm/yr)	+/-	Mean Mmax (Mw)	Down dip Width (km)	+/-	Rupture Top (km)	Rupture Bottom (km)	Dip (deg)	Dip
Northridge	Western Transverse Ranges	Reverse	31	3	1.50	1.00	6.7	22	2	5	20	42	S
Oak Ridge (onshore)	Western Transverse Ranges	Reverse	49	5	4.00	2.00	7.0	14	2	1	14	65	S
Oakridge (blind thrust offshore)	Western Transverse Ranges	Reverse	37	4	3.00	3.00	6.6	10	2	5	10	30	S
Oakridge Mid Channel structure	Western Transverse Ranges	Reverse	37	4	1.00	1.00	6.6	9	2	6	10	28	N
Palos Verdes	Peninsular Ranges	Reverse - right lateral (oblique)	96	10	3.00	1.00	7.3	13	2	0	13	90	-
Pleito Thrust	Transverse Ranges - east	Reverse	44	4	2.00	1.00	7.0	15	2	0	11	45	S
Puente Hills blind thrust	Peninsular Ranges	Reverse	44	4	0.70	0.40	7.1	19	2	5	13	25	N
Raymond	Western Transverse Ranges	Reverse - left lateral (oblique)	23	2	1.50	1.00	6.5	13	2	0	13	75	N
Red Mountain	Western Transverse Ranges	Reverse	100	4	2.00	1.00	7.3	15	2	0	13	60	N
San Andreas-Carrizo	Southern Coast Ranges	Right lateral	146	15	34.00	3.00	7.4	12	2	0	12	90	-
San Andreas-Cholame	Southern Coast Ranges	Right lateral	63	6	34.00	5.00	7.3	12	2	0	12	90	-
San Andreas-Coachella	Western Transverse Ranges	Right lateral	96	10	25.00	5.00	7.2	12	2	0	12	90	-
San Andreas-Mojave	Western Transverse Ranges	Right lateral	103	10	30.00	7.00	7.4	12	2	0	12	90	-
San Andreas-San Bernardino	Western Transverse Ranges	Right lateral	103	10	24.00	6.00	7.5	18	2	0	18	90	-
San Cayetano	Western Transverse Ranges	Reverse	42	4	6.00	3.00	7.0	15	2	0	13	60	N
San Clemente	Continental Boarderland	Right lateral - reverse (oblique)	138	14	2.00	1.00	7.5	13	2	0	13	90	-
San Gabriel	Western Transverse Ranges	Right lateral	72	7	1.00	0.50	7.2	13	2	0	13	90	-
San Luis Range	Southern Coast Ranges	Reverse	64	6	0.20	0.10	7.2	14	2	0	10	45	N

FAULT NAME AND GEOMETRY	LOCATION	Sense of Slip	LENGTH (km)	+/-	Slip Rate (mm/yr)	+/-	Mean Mmax (Mw)	Down dip Width (km)	+/-	Rupture Top (km)	Rupture Bottom (km)	Dip (deg)	Dip
San Joaquin Hills Thrust	Peninsular Ranges	Reverse	28	3	0.50	0.20	6.6	15	2	2	8	23	SW
San Jose	Western Transverse Ranges	Left lateral - reverse (oblique)	20	2	0.50	0.50	6.4	13	2	0	13	75	NW
San Pedro Shelf	Continental Boarderland	Right lateral	107	11	1.00	0.50	7.3	13	2	0	13	90	-
Santa Cruz Island	Western Transverse Ranges	Reverse - left lateral (oblique)	50	5	1.00	0.50	7.0	7	2	0	7	90	-
Santa Monica	Western Transverse Ranges	Reverse - left lateral (oblique)	28	3	1.00	0.50	6.6	13	2	0	13	75	N
Santa Rosa Island	Western Transverse Ranges	Left lateral - reverse (oblique)	56	6	1.00	0.50	7.1	13	2	0	13	90	-
Santa Susana	Western Transverse Ranges	Reverse	27	3	5.00	2.00	6.7	16	2	0	13	55	N
Santa Ynez (east segment)	Western Transverse Ranges	Reverse - left lateral (oblique)	68	7	2.00	1.00	7.1	13	2	0	13	80	-
Santa Ynez (west segment)	Western Transverse Ranges	Reverse - left lateral (oblique)	65	7	2.00	1.00	7.1	13	2	0	13	80	-
Sierra Madre	Western Transverse Ranges	Reverse	57	6	2.00	1.00	7.2	18	2	0	13	45	N
Sierra Madre (San Fernando)	Western Transverse Ranges	Reverse	18	2	2.00	1.00	6.7	18	2	0	13	45	N
Simi-Santa Rosa	Western Transverse Ranges	Reverse	40	4	1.00	0.50	7.0	15	2	1	14	60	N
Upper Elysian Park	Peninsular Ranges	Reverse	20	2	1.30	0.40	6.4	13	2	3	13	50	NE
Ventura-Pitas Point	Western Transverse Ranges	Reverse - left lateral (oblique)	40	4	1.00	0.50	6.9	13	2	1	14	75	N
Verdugo	Western Transverse Ranges	Reverse	29	3	0.50	0.50	6.9	18	2	0	13	45	NE
White Wolf	Transverse Ranges - east	Reverse - left lateral (oblique)	67	7	2.00	2.00	7.3	21	2	0	18	60	S
Whittier	Peninsular Ranges	Right-lateral - reverse (oblique)	38	4	2.50	1.00	6.8	15	2	0	15	75	NE

Table A-1. Fault Parameters

FAULT NAME AND GEOMETRY	LOCATION	Sense of Slip	LENGTH (km)	+/-	Slip Rate (mm/yr)	+/-	Mean Mmax (Mw)	Down dip Width (km)	+/-	Rupture Top (km)	Rupture Bottom (km)	Dip (deg)	Dip
Anacapa-Dume	Western Transverse Ranges	Reverse	75	8	3.00	2.00	7.5	28	2	0	20	45	N
Big Pine	Western Transverse Ranges	Left lateral - reverse (oblique)	41	4	0.80	0.80	6.9	13	2	0	13	90	-
Catalina Escarpment	Continental Boarderland	Right lateral	60	6	1.00	0.50	7.0	13	2	0	13	90	-
Casmalia	Southern Coast Ranges	Reverse	29	3	0.30	0.20	6.5	10	2	0	10	75	SW
Channel Islands Thrust	Western Transverse Ranges	Reverse	63	6	1.50	1.00	7.5	34	2	5	15	17	N
Clamshell-Sawpit	Western Transverse Ranges	Reverse	16	2	0.50	0.50	6.5	18	2	0	13	45	NW
Cucamonga	Western Transverse Ranges	Reverse	28	3	5.00	2.00	6.9	18	2	0	13	45	N
Garlock-west	Transverse Ranges - east	Left lateral	98	10	6.00	3.00	7.3	12	2	0	12	90	-
Hollywood	Western Transverse Ranges	Reverse - left lateral (oblique)	17	2	1.00	0.50	6.4	14	2	0	13	70	N
Holser	Western Transverse Ranges	Reverse	20	2	0.40	0.40	6.5	14	2	0	13	65	S
Hosgri	Southern Coast Ranges	Right lateral	169	17	2.50	1.00	7.5	12	2	0	12	90	-
Lions Head	Southern Coast Ranges	Reverse	41	4	0.02	0.02	6.6	10	2	0	10	75	NE
Los Alamos-West Baseline	Southern Coast Ranges	Reverse	28	3	0.70	0.70	6.9	20.0	2	0	10	30	S
Malibu Coast	Western Transverse Ranges	Left lateral - reverse (oblique)	37	4	0.30	0.20	6.7	13	2	0	13	75	N
Mission Ridge-Arroyo Parida-Santa Ana	Western Transverse Ranges	Reverse	69	7	0.40	0.20	7.2	15	2	0	13	60	N
Newport-Inglewood	Peninsular Ranges	Right lateral (localized uplift)	66	7	1.00	0.50	7.1	13	2	0	13	90	-
North Channel Slope	Western Transverse Ranges	Reverse	68	7	2.00	2.00	7.4	23	2	10	20	26	N

APPENDIX B: GEOLOGIC MAP AND CROSS SECTIONS

Geologic mapping was conducted through compilation of existing mapping, supplemented by interpretation of several generations of aerial photographs and highly detailed LiDAR-based topography generated for this project, and calibrated by field reconnaissance. Surficial information was correlated with subsurface data from borings previously drilled for geotechnical investigations to characterize the lithologic and engineering properties. The borehole data provided lithologic and engineering properties for key map units. Lithologic properties provided within compiled boring logs typically included soil color, type and texture; most often from field observation and less often from laboratory mechanical and hydrometer particle size distribution analysis. Engineering properties typically included dry unit weight, shear strength data, and relative moisture content.

Base Map

The fully digital, preliminary geologic map layer is built upon the merged digital aerial photographic and LiDAR-based terrain map developed for the La Conchita study area (Table B-1). The base map includes one-foot contours derived from the April 2007 LiDAR survey. These contours were interpreted to refine smaller geologic and landslide features previously mapped at a coarser, regional scale. Digital terrain data from the 2007 LiDAR survey were analyzed, along with compiled aerial photography, in order to register and update geologic map units and contacts, as needed.

Sources of Compiled Mapping

Published regional 1:24,000-scale maps by Dibblee (1988) and CGS (2003) were integrated into the project GIS (geographical information system database). A digital copy of the 2003 preliminary geologic map of the Pitas Point quadrangle was obtained from Carlos Gutierrez of CGS (See Table E-1). The Arc export files were converted into ArcGIS shape files; merged into discrete GIS map layers containing mapped geologic units, geologic contacts, and fault traces; and reprojected for direct comparison with the detailed LiDAR-derived topographic base map.

Geologic Mapping

WLA geologists compared the accuracy of mapped lines against high-resolution, georeferenced topography and digital aerial photography. Geologic boundaries on the geologic map were directly overlain, and compared to, topographic features on the updated 2007 LiDAR topographic

base map. The map boundaries also were compared with cultural and vegetation features identified on the 2006 digital aerial photographic base obtained from Air Photo USA.

WLA geologists conducted surface reconnaissance of the La Conchita Study Area on April 26th; May 14th; between May 22nd and 25th; June 6th; June 27th, and December 14th, 2007. Field reconnaissance included: (1) verification of previous mapping of geologic deposits, bedrock geology, and landslides, (2) examination and documentation of road cuts and canyon walls for exposures of key geologic and fault contacts, and (3) identification of boring locations and drill rig access for the evaluation of geologic conditions. Based on field reconnaissance, terrain data were analyzed along with compiled aerial photography to confirm the presence of identified landforms. This mapping was integrated with the compiled map layers to produce the interpretative map of surficial deposits and slope failures on the LiDAR-derived base map (as described in Table B-2). As part of the mapping, we also reviewed and interpreted historic topographic maps, including evaluation of repeated slope failure and ongoing erosion.

Table B-1. Key Data Sources Integrated into Geologic Map.

Dataset	Description	Source	Summary Comments
Topographic Base Map	Processed 30-cm resolution 2007 LiDAR	This study, Airborne1	Used to construct base layer of geologic map.
Digital Aerial Photographic Base Map	Ortho-rectified 2006 aerial photography obtained for this project	This study, IK Curtis	Used as base layer of geologic map and registration of other datasets.
Geotechnical Borings	Hard copy maps from previous geologic and geotechnical studies, including this study.	Various	Locations of geotechnical and water monitoring borings digitized from map plate scans as a point database, with attached tabular descriptive database.
Geologic Maps	Regional mapping by Dibblee (1988) and CGS (2003), and unpublished landslide hazard maps by various consultants.	CGS (2003) map obtained in digital form from CGS.	Digital version of CGS (2003) map obtained and integrated into geologic map.
Fault Locations	A-P fault map by CGS (1991), updated mapping by CGS (2003).	CGS (2003) fault traces obtained in digital form from CGS.	Digital version of CGS (1991) Alquist-Priolo zone map and fault layer from CGS (2003) preliminary geologic map.

Table B-2. Description of Geologic Map Units

Map Symbol	Unit Name and Description (based in part on CGS, 2003)
HISTORICAL DEPOSITS (<300 YEARS OLD).	
Qdf-2005	**Debris flow deposits of the 2005 slope failure** (historic).
Qls-1995	**Landslide deposits of the 1995 slope failure** (historic).
Qb	**Beach sand deposits (historic through Holocene).** This unit includes active beaches. Consists of loose, fine to coarse sand.
Qw	**Stream wash deposits (historic through Holocene).** Historical washes were identified within flat-floored active stream channels and arroyos, including the East and West Barrancas. Locally present within incised gullies and channels. Washes are frequently inundated during and immediately following storms and are subject to scouring or deposition, depending on streamflow and bedload. Washes generally contain more course sediment than the active alluvium. Sediment consists of loose sands, gravels, silts, and clays within poorly- to well-sorted beds. Deposits generally are coarse grained, consisting of poorly-sorted sand, silty sands and clayey sands, often with gravel and in the upland drainages, boulders.
af	**Artificial fill (historic).** Man-made material placed at the earth's surface. Fill may be engineered and/or non-engineered material. Fill shown includes large highway embankments along Highway 101, consisting of engineered fill up to approximately 50 feet thick. Fills whose thicknesses are less than the contour interval (typically 5 to 10 ft) and fills emplaced after the topographic base maps were surveyed are not shown. Small bodies of fill, such as small road embankments associated with the former ranch road across the cliff north of La Conchita are not shown on the preliminary geologic map.
Qlsa	**Active landslide deposits (historic).** Varying composition including poorly sorted, sandy silt with subangular bedrock clasts. Typically loose to moderately dense.
Qlsu (?)	**Landslide deposits (unknown age or queried).** Inferred or potentially active landslide deposits of unknown age and/or composition. Queried where origin of deposits is not known.
Qdf	**Debris fan deposits (historic through Holocene).** Composed of sandy silt with occasional clasts of angular bedrock material.

HOLOCENE (<11,000 years old)

Qf **Latest Holocene alluvial and debris fan deposits**. Alluvial and debris fan sediments judged to be latest Holocene age, based on records of historical inundation or the presence of youthful braid bars and distributary channels. Alluvial fan sediment is deposited by streams emanating from the mountain canyons onto the coastal plain. Most of the latest Holocene fan deposits emanate from a point partway down the alluvial fan slope. Sediments are moderately to poorly sorted and bedded, and may be composed of gravel, sand, silt and clay.

Qlso **Holocene to Pleistocene landslide deposits** (units 2, 3, and 4; with Qlso3 being the youngest identified landslide, Qlso2 intermediate age, and Qlso4 being the oldest). Landslide deposits consist of displaced bedrock of the Monterey and Pico Formations and the Sisquoc Shale. Portions of the landslide deposits include paralic and mass wasting deposits consisting of fine-grained sandy silt with abundant subangular clasts of both Monterey and Pico Formations.

Qhmt **Holocene marine terrace deposits.** Deposits on uplifted marine abrasion platforms, including deposits of the approximately 1,200 to 2,400 year old marine terrace buried beneath the coastal plain at La Conchita. Sediment veneer on the platform, where preserved, is typically 5 to 15 feet thick and consists of loose sand with cobbles. Commonly buried under colluvial deposits of unit Qdf. Not exposed within the Study Area but encountered in borings.

LATE PLEISTOCENE (<300,000 years old)

Qpmw **Pleistocene undivided mass-wasting deposits**. Colluvial, talus, and landslide deposits accumulated on marine wave-cut platforms (Unit Qoa of Dibblee, 1988). Consists of weathered, broken-up (brecciated) fragments of the Monterey Formation.

Qppr-p **Pleistocene marine terrace and paralic deposits** (Unit Qoa of Dibblee, 1988). Deposits on uplifted marine abrasion platforms, including deposits of the 40,000 to 60,000 year old Punta Gorda marine terrace preserved locally beneath the uplifted plateau under La Conchita Ranch. These deposits consist of near-shore marine deposits (beach sands) overlain by non-marine fluvial deposits and colluvium labeled 'paralic' by CGS (2003). These non-marine deposits could more readily be termed 'continental', consisting of a combination of fluvial and mass movement deposits. However, for consistency with the CGS (2003) mapping, we have retained the 'paralic' nomenclature for non-marine deposits overlying the platform. Sediment veneer on the platform, where preserved, is typically greater than 10 feet thick and consists of consolidated clayey sand with gravel lenses. Commonly buried under colluvial deposits of unit Qpmw, or locally stripped by erosional processes.

BEDROCK

Tp **Pliocene undivided Pico Formation**. Composed of claystone, siltstone, sandstone, locally pebbly, generally susceptible to landsliding.

Tpsc **Pliocene Pico Formation containing sandstone and conglomerate**. Composed of claystone and siltstone with interbeds of sandstone and conglomerate. Generally resistant to landsliding.

Tsq **Pliocene-Miocene Sisquoc Shale**. Consists of interbedded silty shale and claystone. Generally susceptible to landsliding.

Tm **Miocene Monterey Formation**. Consists of siliceous and diatomaceous shale with some sandstone and limestone. Generally susceptible to landsliding.

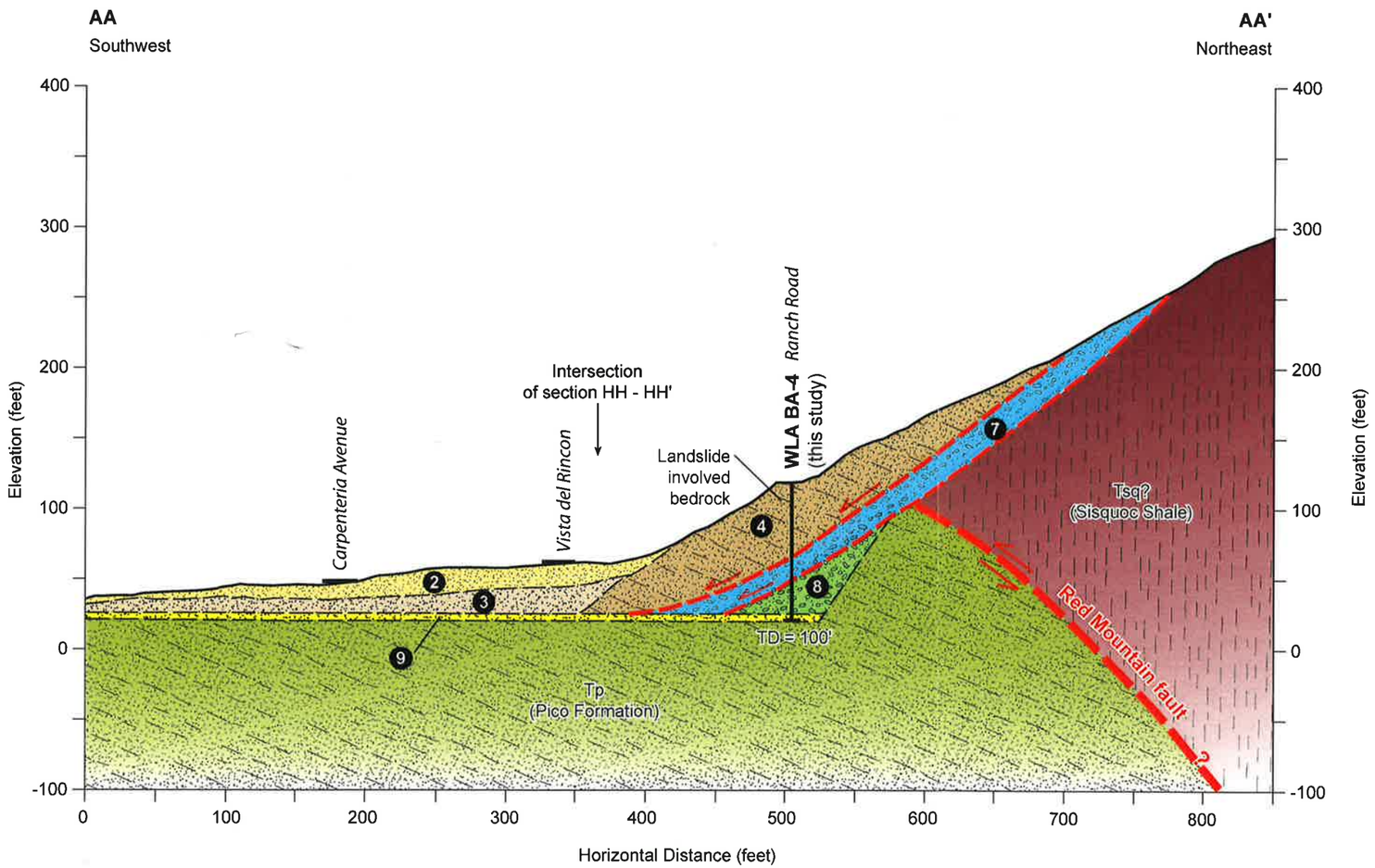

Explanation

Unit Descriptions

- 2 — Qdf, recent debris flow deposits, clayey to sandy silt
- 3 — Qf, holocene debris flow and alluvial fan deposits, clayey to sandy silt
- 4 — Qlsu, older landslide of unknown activity
- 7 — Old landslide deposits ($Qlso_4$)
- 8 — Old colluvial/debris fan deposits, silt with gravel layers
- 9 — Marine terrace deposits, medium- to coarse-grained sand with cobbles
- Tp — Pico Formation, siltstone to sandy siltstone (hachures show approximate dip of bedding)
- Tsq — Sisquoc Shale, light gray silty shale or claystone, locally siliceous and diatomaceous (hachures show approximate dip of bedding)

Symbols

- Lithologic contact, queried where approximately located and poorly constrained
- Landslide plane, queried where inferred
- Fault, arrows show sense of displacement, queried where inferred
- Water encountered
- Water level measured

LA CONCHITA

Geologic Cross Section AA - AA'

WLA William Lettis & Associates, Inc. | Figure B-2

Modified 03.18.08

1885 La Conchita

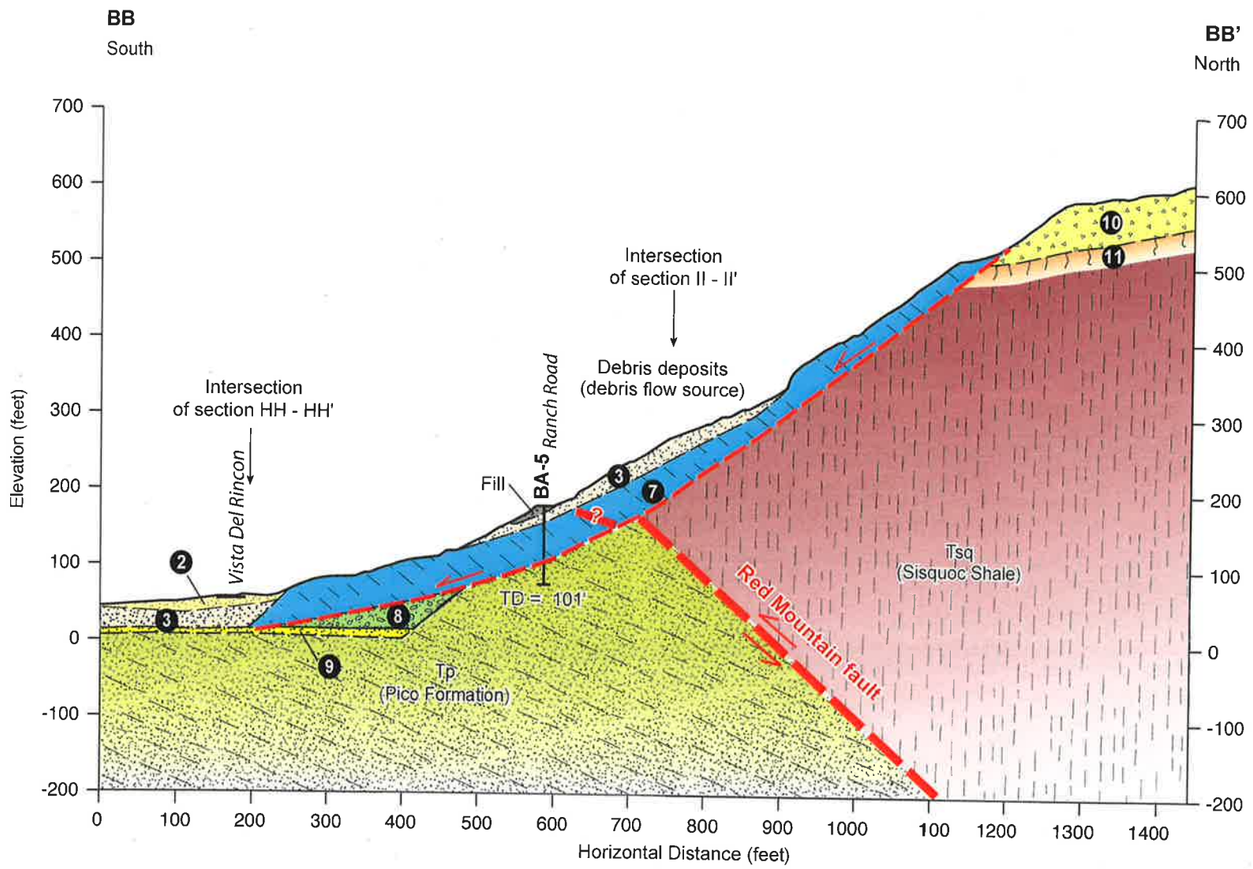

Explanation

Unit Descriptions

- 2 Qdf, recent debris flow deposits, clayey to sandy silt
- 3 Qf, holocene debris flow and alluvial fan deposits, clayey to sandy silt
- 4 Qlsu, older landslide of unknown activity
- 7 Old landslide deposits (Qls_{O4}), bedrock-involved slide
- 8 Old colluvial/debris fan deposits, silt with gravel layers
- 9 Marine terrace deposits, medium- to coarse-grained sand with cobbles

Unit Descriptions (continued)

- 10 Qppr-p, paralic debris deposits with brecciated Monterey clayey to sandy siltstone
- 11 "Paleosol" (buried soil horizon)
- Tp Pico Formation, siltstone to sandy siltstone (hachures show approximate dip of bedding)
- Tsq Sisquoc Shale, light gray silty shale or claystone, locally siliceous and diatomaceous

Symbols

- Lithologic contact, queried where approximately located and poorly constrained
- Fault, arrows show sense of displacement, queried where inferred
- Landslide plane, queried where inferred
- Water encountered
- Water level measured

LA CONCHITA

Geologic Cross Section BB - BB'

WLA William Lettis & Associates, Inc. | Figure B-3

Modified 03.18.08

1885 La Conchita

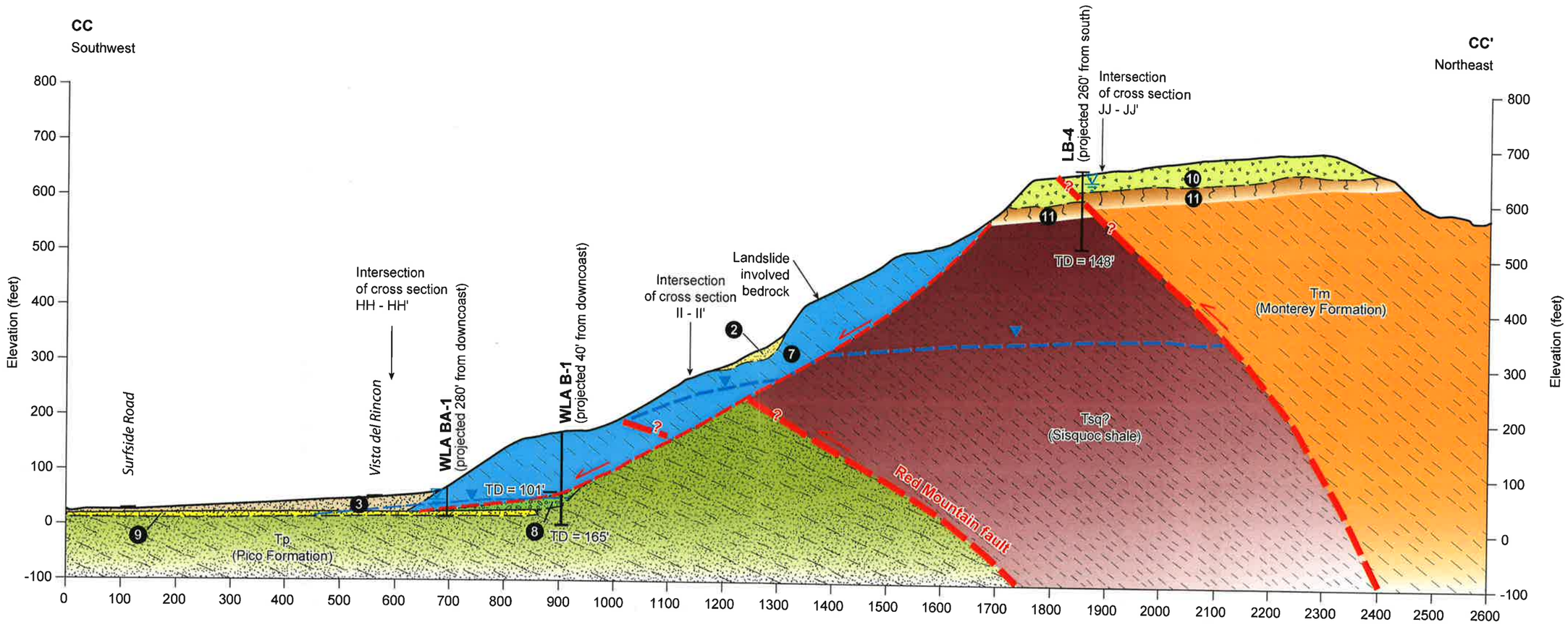

Explanation

Unit Descriptions

- 2 Qdf, recent debris flow deposits, clayey to sandy silt
- 3 Qf, holocene debris flow and alluvial fan deposits, clayey to sandy silt
- 4 Qlsu, older landslide of unknown activity
- 7 Old landslide deposits ($Qlso_4$), bedrock-involved slide
- 8 Old colluvial/debris fan deposits, silt with gravel layers
- 9 Marine terrace deposits, medium- to coarse-grained sand with cobbles

Unit Descriptions (continued)

- 10 Qppr-p, paralic debris deposits with brecciated Monterey clayey to sandy siltstone
- 11 "Paleosol" (buried soil horizon)
- Tp Pico Formation, siltstone to sandy siltstone (hachures show approximate dip of bedding)
- Tsq Sisquoc shale, light gray silty shale or claystone, locally siliceous and diatomaceous
- Tm Monterey Formation, interbedded siltstone and sandstone

Symbols

- Lithologic contact, queried where approximately located and poorly constrained
- Fault, arrows show sense of displacement, queried where inferred
- Landslide plane, queried where inferred
- Water encountered
- Water level measured

LA CONCHITA

Geologic Cross Section CC - CC'

WLA William Lettis & Associates, Inc. | Figure B-4

Modified 03.18.08

1885 La Conchita

DD
Southwest

DD'
Northeast

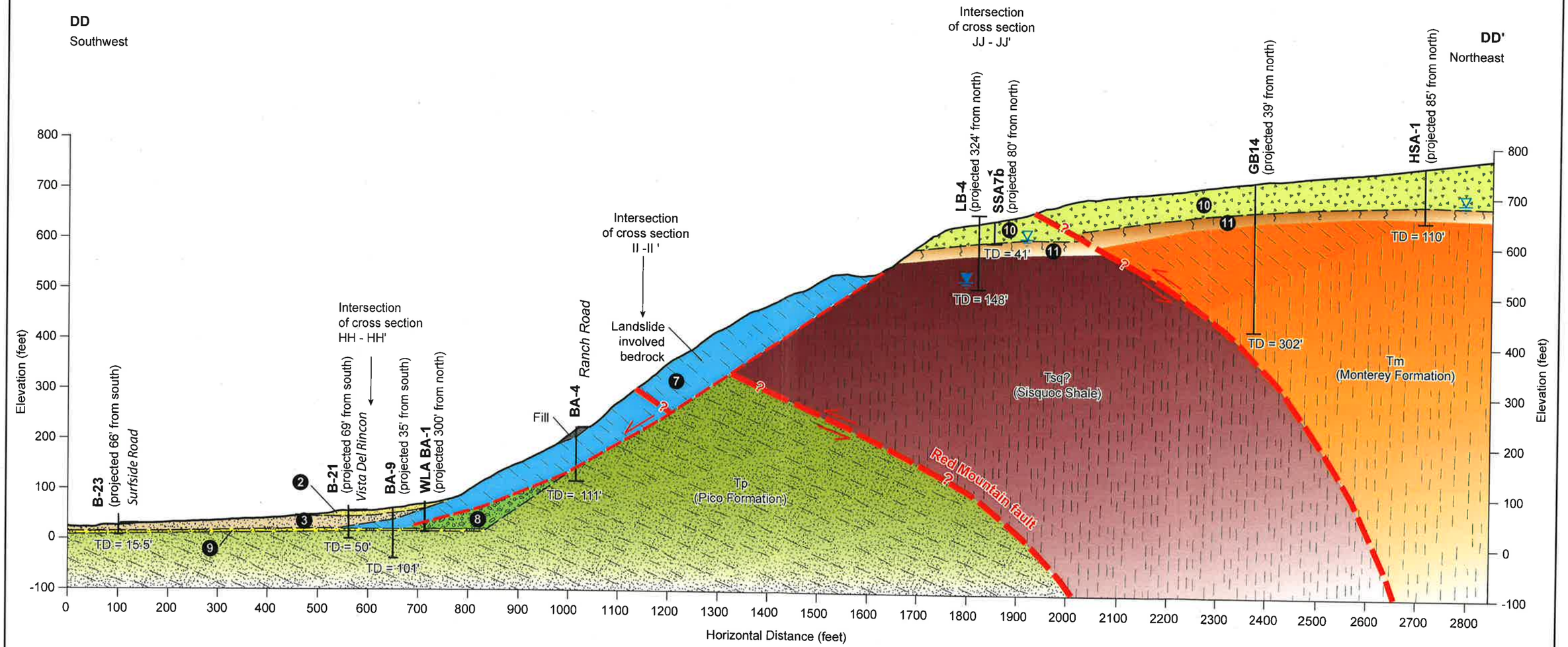

Explanation

Unit Descriptions

- 2 — Qdf, recent debris flow deposits, clayey to sandy silt
- 3 — Qf, holocene debris flow and alluvial fan deposits, clayey to sandy silt
- 4 — Qlsu, older landslide of unknown activity
- 7 — Old landslide deposits ($Qlso_4$), bedrock-involved slide
- 8 — Old colluvial/debris fan deposits, silt with gravel layers
- 9 — Marine terrace (Sea Cliff) deposits, medium- to coarse-grained sand with cobbles

Unit Descriptions (continued)

- 10 — Qppr-p, paralic debris deposits with brecciated Monterey clayey to sandy siltstone
- 11 — "Paleosol" (buried soil horizon)
- Tp — Pico Formation, siltstone to sandy siltstone (hachures show approximate dip of bedding)
- Tsq — Sisquoc Shale, light gray silty shale or claystone, locally siliceous and diatomaceous
- Tm — Monterey Formation, interbedded siltstone and sandstone

Symbols

- Lithologic contact, queried where approximately located and poorly constrained
- Fault, arrows show sense of displacement, queried where inferred
- Landslide plane, queried where inferred
- Water encountered
- Water level measured

LA CONCHITA

Geologic Cross Section DD - DD'

WLA William Lettis & Associates, Inc. | Figure B-5

Modified 01.04.08

1885 La Conchita

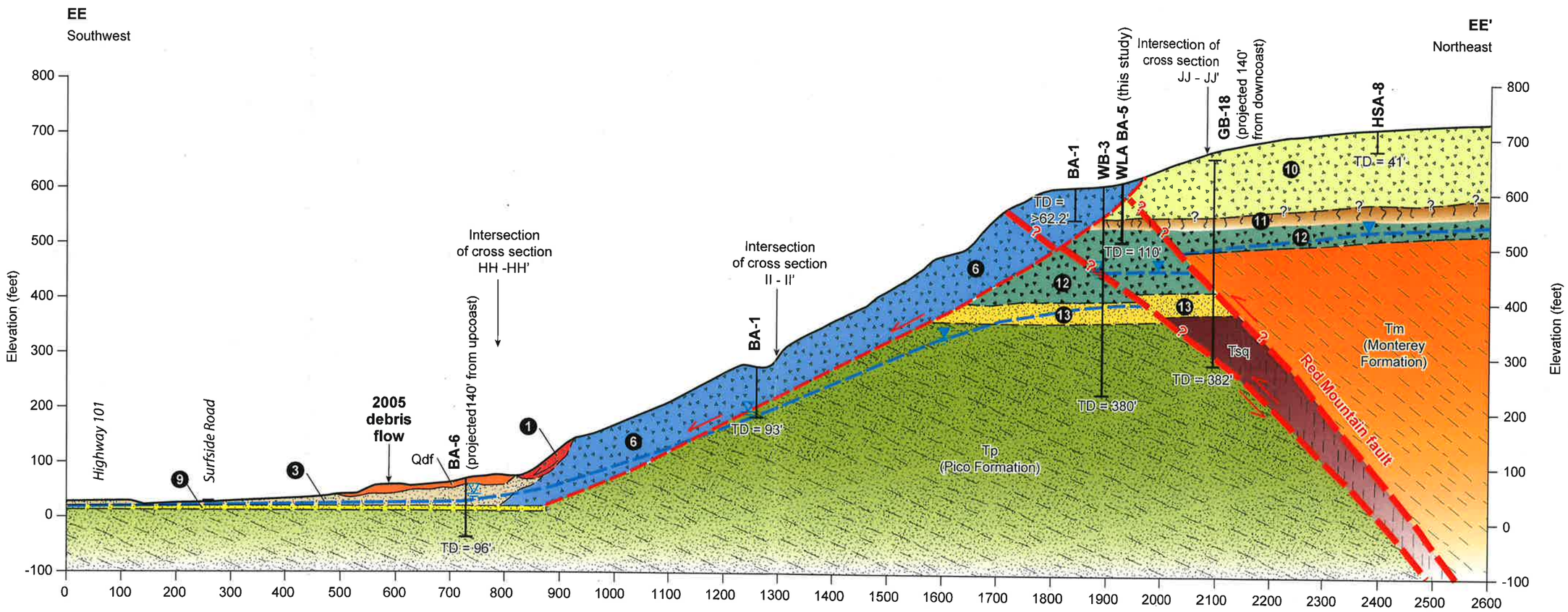

Explanation

Unit Descriptions

- 1 — Qlsa, active landslide
- 2 — Qdf, recent debris flow deposits, clayey to sandy silt
- 3 — Qf, Holocene debris flow and alluvial fan deposits, clayey to sandy silt
- 4 — Qlsu, older landslide of unknown activity
- 6 — Older landslide deposits ($Qlso_2$), silty sand to silt with abundant rock fragments, may include bedrock in downslope portion.
- 9 — Marine terrace deposits, medium- to coarse-grained sand with cobbles

Unit Descriptions (continued)

- 10 — Qppr-p, paralic debris deposits with brecciated Monterey clayey to sandy siltstone
- 11 — "Paleosol" (buried soil horizon)
- 12 — Oldest paralic debris deposits
- 13 — Marine terrace (Punta Gorda) deposits with associated paralic deposits
- Tp — Pico Formation, siltstone to sandy siltstone (hachures show approximate dip of bedding)
- Tsq — Sisquoc Shale, light gray silty shale or claystone, locally siliceous and diatomaceous
- Tm — Monterey Formation, interbedded siltstone and sandstone

Symbols

- Lithologic contact, queried where approximately located and poorly constrained
- Fault, arrows show sense of displacement, queried where inferred
- Landslide plane, queried where inferred
- Water encountered
- Water level measured

LA CONCHITA

Geologic Cross Section EE - EE'

WLA William Lettis & Associates, Inc. | Figure B-6

Modified 07.15.08

1885 La Conchita

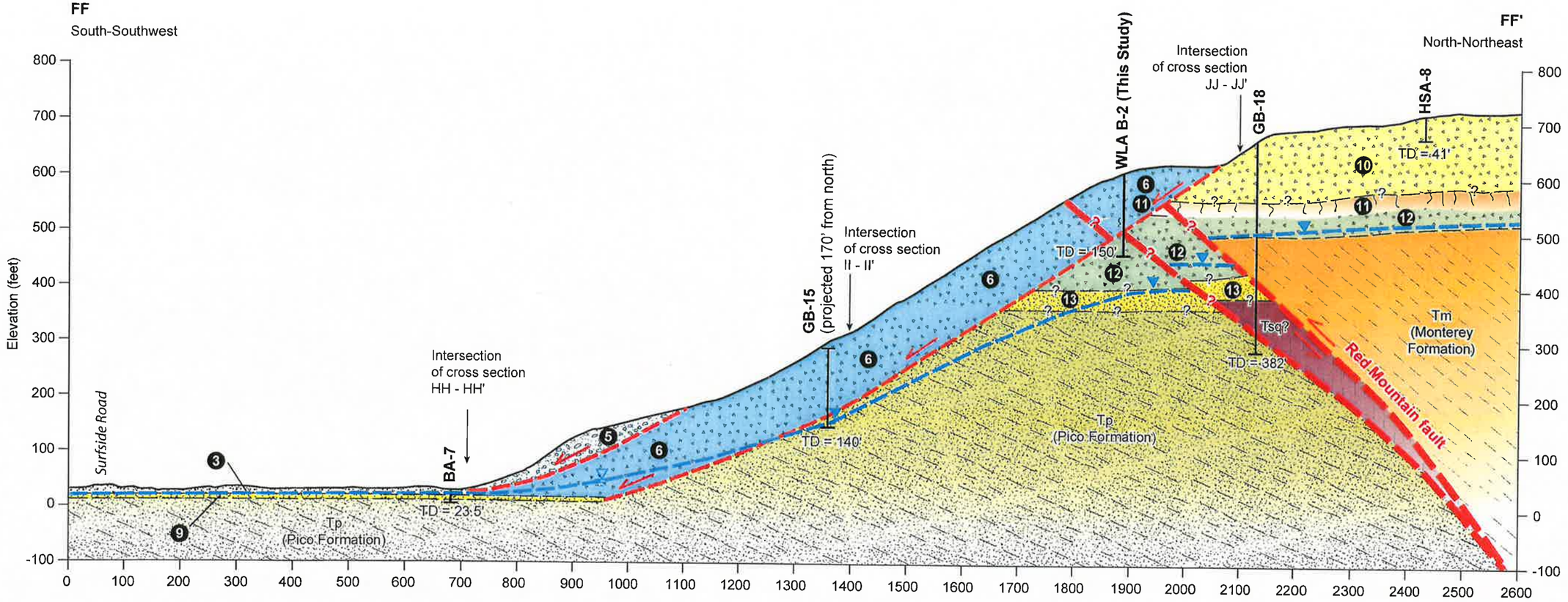

Explanation

Unit Descriptions

- 3 — Qf, Holocene debris flow and alluvial fan deposits, clayey to sandy silt
- 5 — Old landslide deposits ($Qlso_3$), silty sand to silt with abundant rock fragments of siltstone/claystone
- 6 — Older landslide deposits ($Qlso_2$), silty sand to silt with abundant rock fragments
- 9 — Marine terrace deposits, medium- to coarse-grained sand with cobbles
- 10 — Qppr-p, paralic debris deposits with brecciated Monterey clayey to sandy siltstone

Unit Descriptions (continued)

- 11 — "Paleosol" (buried soil horizon)
- 12 — Oldest paralic debris deposits
- 13 — Marine terrace (Punta Gorda) deposits with associated paralic deposits
- Tp — Pico Formation, siltstone to sandy siltstone (hachures show approximate dip of bedding)
- Tsq — Sisquoc Shale, light gray silty shale or claystone, locally siliceous and diatomaceous
- Tm — Monterey Formation, interbedded siltstone and sandstone

Symbols

- Lithologic contact, queried where approximately located and poorly constrained
- Fault, arrows show sense of displacement, queried where inferred
- Landslide plane, queried where inferred
- Water encountered
- Water level elevation or measured

LA CONCHITA

Geologic Cross Section FF - FF'

WLA — William Lettis & Associates, Inc. | Figure B-7

Modified 01.04.08

1885 La Conchita

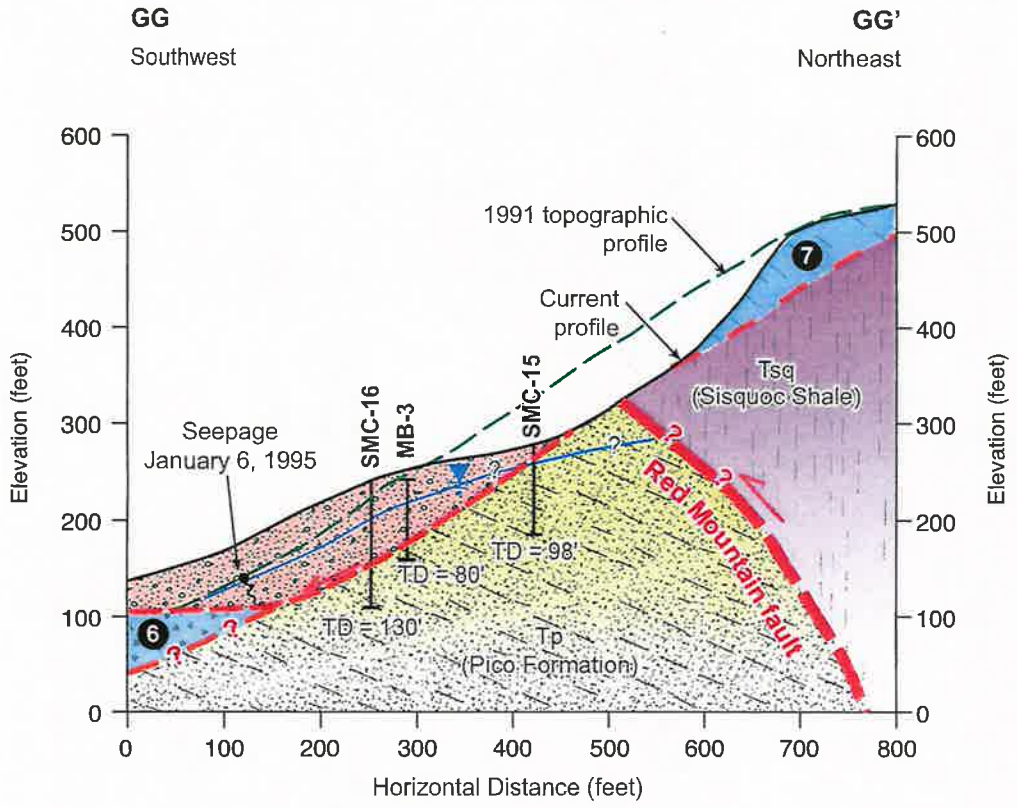

Explanation

Unit Descriptions

- Landslide debris (1995 landslide)
- 6 — Older landslide deposits ($Qlso_2$), may include bedrock within reactivated, translated portions of $Qlso_4$ landslide deposits
- 7 — Old landslide deposits ($Qlso_4$), may include bedrock
- Tp — Pico Formation, siltstone to sandy siltstone (hachures show approximate dip of bedding)
- Tsq — Sisquoc Shale, light gray silty shale or claystone, locally siliceous and diatomaceous

Symbols

- Lithologic contact, queried where approximately located and poorly constrained
- Fault, arrows show sense of displacement, queried where inferred
- Landslide plane, queried where inferred
- Water level measured January 1995

LA CONCHITA

Geologic Cross Section GG - GG'

WLA William Lettis & Associates, Inc. | Figure B-8

Modified 07.24.08

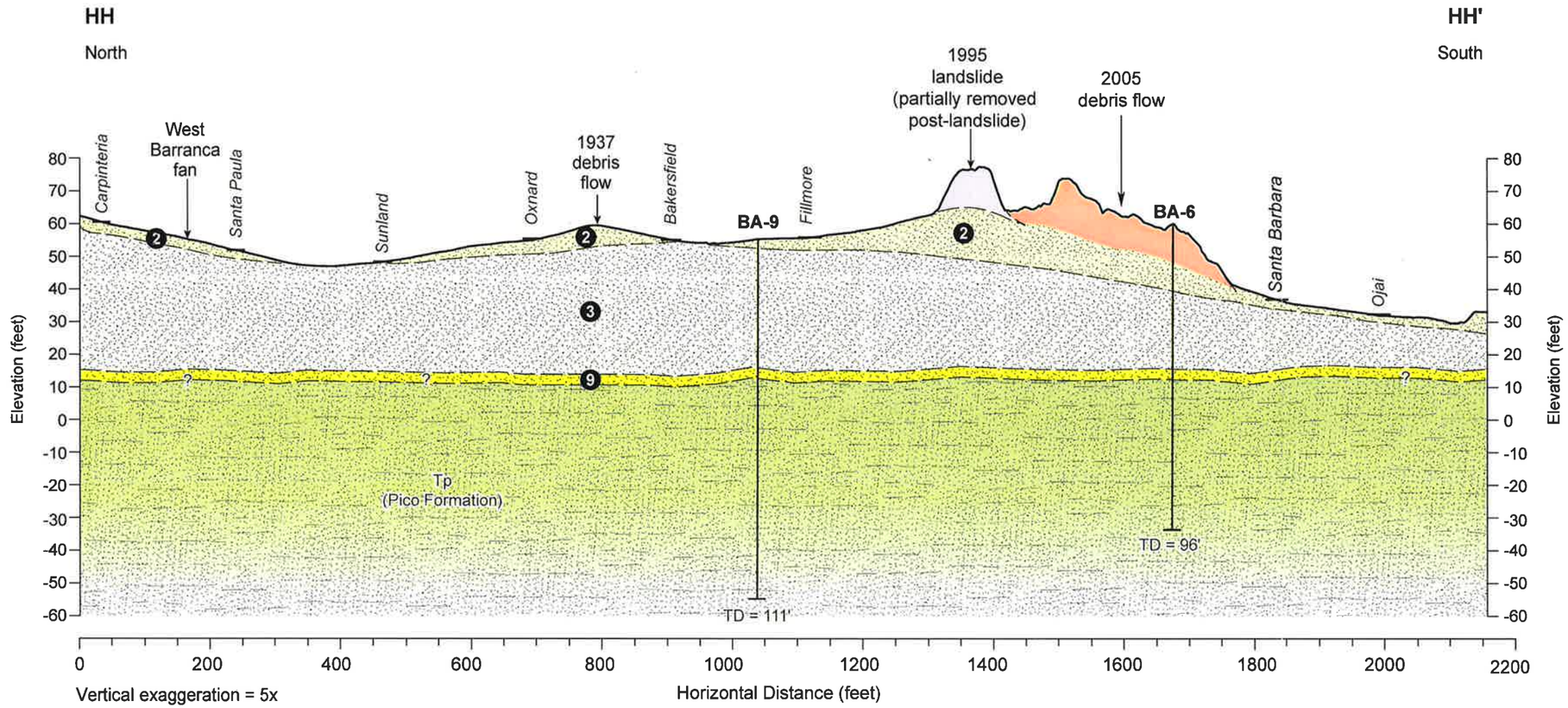

Explanation

Unit Descriptions

- 2 — Qdf, recent debris flow deposits, clayey to sandy silt
- 3 — Qf, holocene debris flow and alluvial fan deposits, clayey to sandy silt
- 9 — Marine terrace deposits, medium- to coarse-grained sand with cobbles
- Tp — Pico Formation, siltstone to sandy siltstone (hachures show approximate dip of bedding)

Symbol

- —?— — Lithologic contact, queried where approximately located and poorly constrained

LA CONCHITA

Geologic Cross Section HH - HH'

WLA William Lettis & Associates, Inc. | Figure B-9

Modified 01.04.08

1885 La Conchita

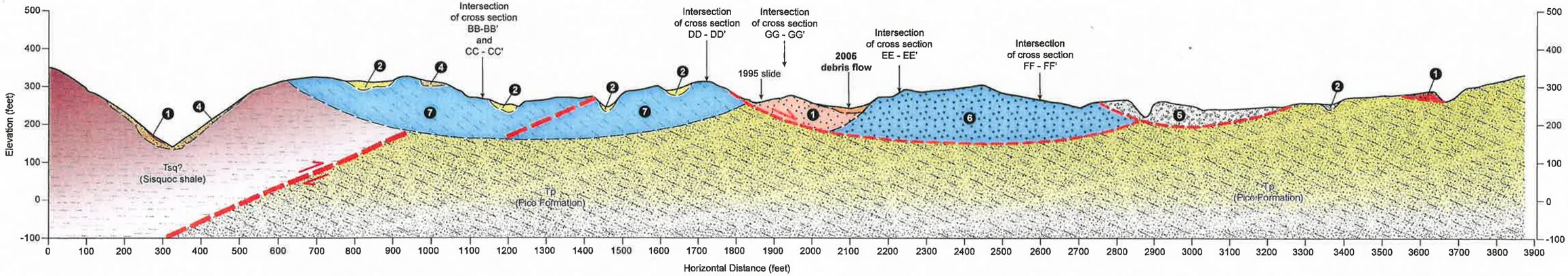

Explanation

Unit Descriptions

1. Qlsa, active landslide
2. Qdf, recent debris flow deposits, clayey to sandy silt
4. Qlsu, older landslide of unknown activity
5. Old landslide deposits ($Qlso_3$), silty sand to silt with abundant rock fragments of siltstone/claystone
6. Older landslide deposits ($Qlso_2$), silty sand to silt with abundant rock fragments
7. Old landslide deposits ($Qlso_4$), bedrock-involved slide

Unit Descriptions (continued)

Tp — Pico Formation, siltstone to sandy siltstone (hachures show approximate dip of bedding)

Tsq — Sisquoc shale, light gray silty shale or claystone, locally siliceous and diatomaceous

Symbols

- Lithologic contact, queried where approximately located and poorly constrained
- Fault, arrows show sense of displacement, queried where inferred
- Landslide plane, queried where inferred
- Water encountered
- Water level measured

LA CONCHITA

Geologic Cross Section II - II'

WLA William Lettis & Associates, Inc. Figure B-10

Modified 07.15.08

1885 La Conchita

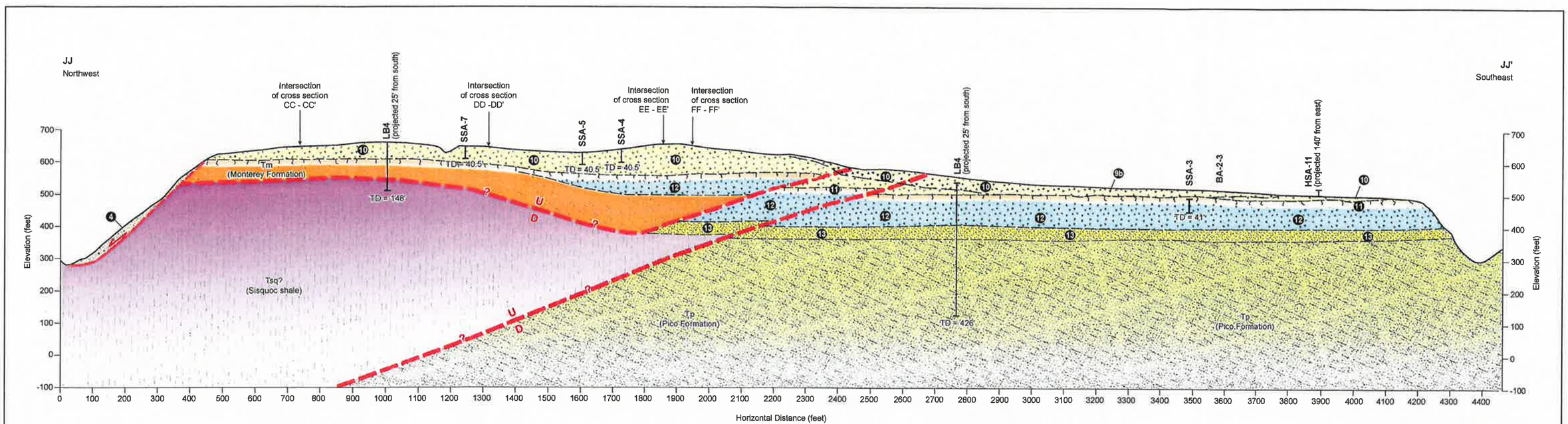

Explanation

Unit Descriptions

- Qlsa, active landslide
- Qlsu, older landslide of unknown activity
- Qpmw, mass wasting deposits (debris flow deposits)
- Qppr-p, paralic debris deposits with brecciated Monterey clayey to sandy siltstone
- "Paleosol" (buried soil horizon)
- Oldest paralic debris deposits
- Marine terrace (Punta Gorda) deposits with associated paralic deposits

Unit Descriptions (continued)

- Tp: Pico Formation, siltstone to sandy siltstone (hachures show approximate dip of bedding)
- Tsq: Sisquoc Shale, light gray silty shale or claystone, locally siliceous and diatomaceous
- Tm: Monterey Formation, interbedded siltstone and sandstone

Symbols

- Lithologic contact, queried where approximately located and poorly constrained
- Fault, arrows show sense of displacement, queried where inferred
- Landslide plane, queried where inferred
- Water encountered
- Water level measured

LA CONCHITA

Geologic Cross Section JJ - JJ'

WILLIAN LETTIS & ASSOCIATES, INC. | Figure B-11

Modified 01.04.08

1885 La Conchita

APPENDIX C: GEOTECHNICAL BORINGS

Small and large diameter borings were drilled in order to characterize key geologic relationships and to collect samples for laboratory testing in order to characterize and engineering properties. Borings were drilled to depths sufficient to document subsurface properties and identify potential slide planes. The locations of the borings were approximately determined by hand-held GPS, typically within 9 to 14 feet, supplemented by location on georectified aerial photographs merged with a detailed topographic contour map derived from high-resolution (30-cm spacing) LiDAR. Ground surface elevations at each boring location were approximately determined by interpolation between 1-ft contours on the LiDAR base map. The locations and elevations of the borings should be considered accurate only to the degree implied by the methods used.

The field exploration program consisted of advancing two rotary wash borings, five large-diameter ('bucket' auger) borings, and downhole geophysical measurements. The borings and geophysics were completed between October 10 and October 26, 2007. The rotary wash drilling subcontractor was C&L Drilling of Los Angeles, California. C&L Drilling used a truck-mounted rotary wash drill rig to advance two borings (WLA-B1 and WLA-B2) to depths of 161 and 151 feet, respectively, between October 23 and October 26, 2007. The borings were logged by Dr. Ross Hartleb, WLA Senior Geologist. Drill holes were sampled using a 2-inch-outside diameter Standard Penetration Test (SPT) split spoon sampler, and a 3-inch-outside diameter Shelby tube sampler. Split-spoon samplers were driven using a 300-pound hammer by means of an 18-inch drop. Groundwater levels could not be obtained from the rotary wash drill holes due to the rig's circulation of water during drilling.

Soil and bedrock conditions beneath the La Conchita Study Area also were explored by drilling and down-hole logging large diameter (24-inch diameter) 'bucket auger' borings. The borings were drilled by TriValley Drilling of Ventura, California, under the supervision of drillers James and Ron Hester. Five large diameter borings were completed to depths of 30 to 110 feet between October 9 and 11, 2007. Each hole was logged by Christopher Hitchcock, Certified Engineering Geologist, after established methods for downhole logging of large-diameter borings (Scullin, 1994). Downhole measurements included use of hand-held shear torvane and pocket penetrometer instruments for assessment of the in-situ (in-place) strength of materials.

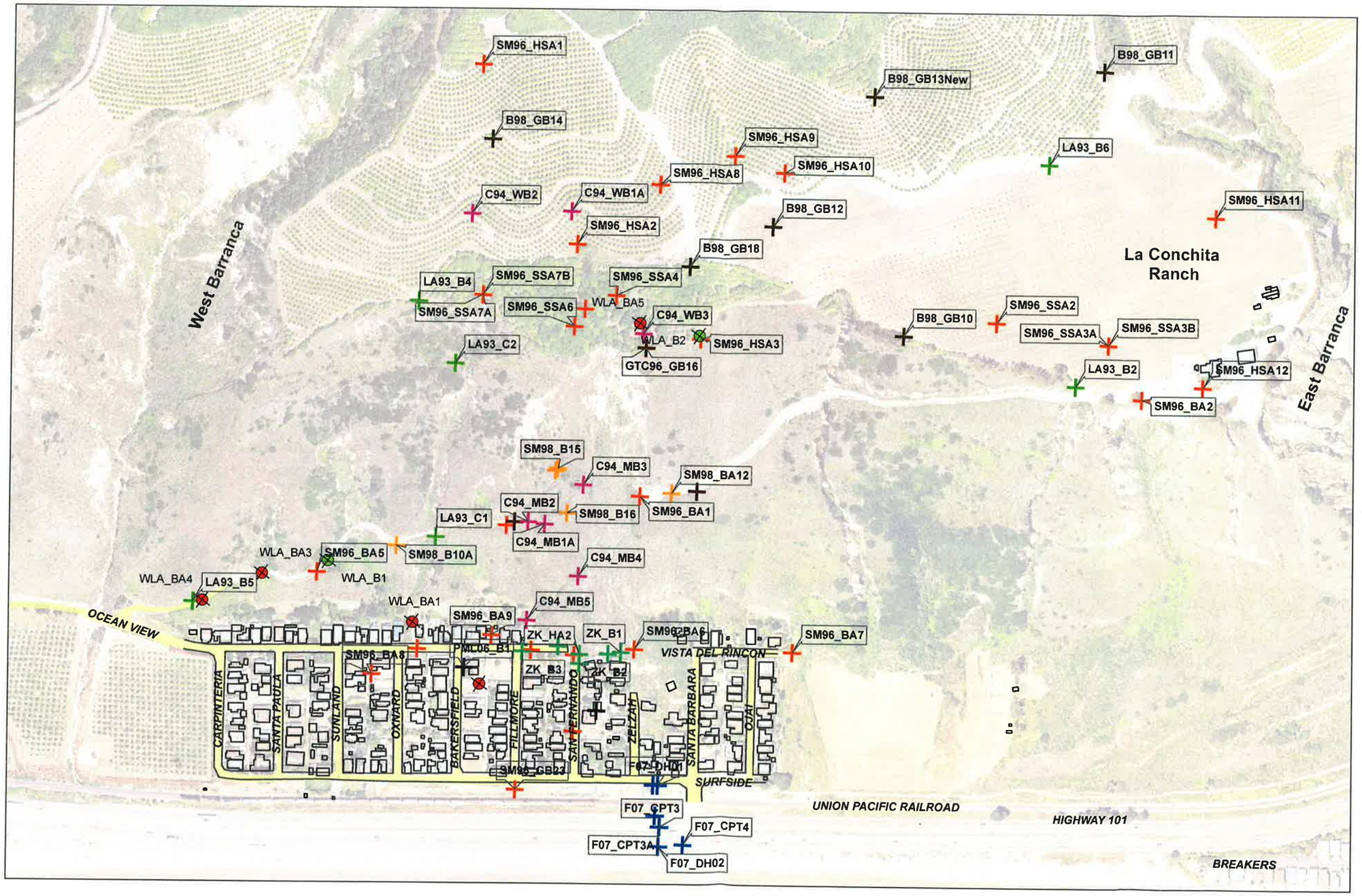

Map Legend

Source of Compiled Borings and Water Wells

- Fugro West, 2007
- Gin Yen & Associates, Inc., 1995
- Converse West Consultants, 1994
- Geotechnical Consultants, Inc (various years from 1994-1998, cited in Bachman, 1998)
- La Conchita Ranch (cited in Bachman, 1998)
- Leighton & Associates, 1992
- Leighton & Associates, 1993
- Pacific Materials Laboratories, 2006 (Hollow stem auger boring for evaluation of liquefaction potential and foundation conditions)
- Stoney-Miller, 1996
- Stoney-Miller, 1998
- Zekser Kling, 1998

Map Symbols

—100— Topographic contour interval, in feet

WLA Boreholes (This Study)

- Bucket Auger
- Mud Rotary

Sources

This compilation of available borings and water-well locations is derived from the following sources:

Bachman, S., 1998, Geologic and hydrogeologic investigations, La Conchita Ranch, unpublished report dated March 1998

Converse Consultants West, 1994, Final report - Mitigation and monitoring, La Conchita Ranch Road Landslide Project, No. 94-31-292-02, unpublished consultant report dated December 16, 1994

Geotechnical Consultants, Inc., 1992, Bedrock and water quality, La Conchita Area, Memorandum, Project No. V88-003, unpublished consultant report dated August 24, 1992

Geotechnical Consultants, Inc., 2007, pers. comm. Ted Powers for La Conchita Ranch, unpublished borings

Leighton and Associates, Inc., 1992, La Conchita Ranch, Dated December 11, 1992, Project No. 2920785-02

Leighton and Associates, Inc., 1993, Summary of Geotechnical Investigations, La Conchita Ranch, Ventura County, California, Project No. 2920785-05, dated August 20, 1993

Pacific Materials Laboratory Inc., 2006, Report No. 7042, Bakersfield Avenue, La Conchita, PML File No. 05-7044.3, unpublished consultant report dated August 2, 2006

Stoney-Miller Consultants, Inc, 1996, Summary Geotechnical Evaluation of the La Conchita Landslide - March 6, 1995, Ventura County, California, for the Bateman Group, Project No. H305-00, Report No. S-5042, dated October 18, 1996

Stoney-Miller Consultants, Inc, 1998, Addendum to the Summary Geotechnical Evaluation of the La Conchita Landslide of March 6, 1995, Ventura County California dated March 17, 1996, Project No. 11469.00

Zekser Kling Consultants, Inc, 1998, Vista Del Rincon Avenue Landslide Debris Removal Investigation, La Conchita, County of Ventura, California, ZKC project number 98002.00, unpublished consultant report dated October 19, 1998

Feet
0 50 100 200 300 400

LA CONCHITA
Phase 2 Report

Figure C-1: Borehole Compilation Map

WLA William Lettis & Associates, Inc.

Table C-1: Summary of location information for compiled geotechnical borings and water wells within the La Conchita study area (see map for boring locations).

Boring Name	Source	X-Coordinate	Y-Coordinate	Local ID (Bachman, 1998)	Boring Information			Monitoring Well?	Surface	Bottom of Hole		Encountered? Y/N			
					Type	Diameter	Date Comp.		Elevation (ft)	Depth (ft)	Elevation (ft)	Slide Plane	Fault	Marine Terrace	Water
LA93_B1	Leighton Associates, 1993	6126960.23	1961111.369		Bucket Auger	30"	11/3/92	N	840	141	699	Y	N	N	Y
LA93_B2	Leighton Associates, 1993	6126941.311	1957103.332	B-2	Bucket Auger	30"	11/4/92	N	500	101	399	N	N	N	Y
LA93_B3	Leighton Associates, 1993	6129168.065	1958288.364		Bucket Auger	30"	11/5/92	N	705	76	629	Y	N	N	N
LA93_B4	Leighton Associates, 1993	6125762.302	1959171.887	B-4	Bucket Auger	30"	11/11/92	N	658	148	510	Y	Y	N	Y
LA93_B5	Leighton Associates, 1993	6124257.193	1959317.587	B-5	Bucket Auger	30"	11/12/92	N	106	88.5	17.5	N	N	N	Y - seep
LA93_B6	Leighton Associates, 1993	6127516.195	1957658.3	B-6	Bucket Auger	30"	11/13/92	N	605	115	490	N	N	N	Y
LA93_B7	Leighton Associates, 1993	6131098.208	1959575.862		Bucket Auger	30"	11/14/92	N	100	28.5	71.5	N	N	N	N
LA93_C1	Leighton Associates, 1993	6125124.782	1958614.102	C1	Longyear-44	2.75"	2/4/93	?	200	185.7	14.3	Y?	N	N	N
LA93_C2	Leighton Associates, 1993	6125663.64	1958932.059	C2	IVI(Air Core)	4.25"	3/7/93	?	521	110.5	410.5	Y?	N	N	Y-minor seep
PML06_B1	Pacific Material Laboratories	6124814.389	1958251.525	B-1	Hollow Stem Auger	2.5"	7/16/06	N	50	50	0	N	N	Y	N
PML79_B1	Pacific Material Laboratories	6124976.702	1957778.215		Hollow Stem Auger	2.5"		N							
SM96_HSA1	Stoney-Miller, 1996	6126579.306	1959496.964	HSA-1	HSA	8"	11/16/95	N	760	110	650	Y?	N	N	Y - wet
SM96_HSA2	Stoney-Miller, 1996	6126267.167	1958839.067	HSA-2	HSA	8"	11/17/95	N	674	75	599				Y - wet
SM96_HSA3	Stoney-Miller, 1996	6126263.892	1958278.121	HSA-3	HSA	8"	11/17/95	N	605	85.5	519.5			N	N
SM96_BA1	Stoney-Miller, 1996	6125683.34	1958114.964	BA-1	Bucket Auger	24"	12/11/95	N	276	93	183			Y	Y - seep
SM96_BA2	Stoney-Miller, 1996	6127049.371	1956884.723	BA-2	Bucket Auger	24"	12/12/95	N	468	91.5	376.5			Y	Y - seep
SM96_BA3	Stoney-Miller, 1996	not in study area	not in study area		Bucket Auger	24"	12/15/95	N	520	90.5	429.5				Y - seep
SM96_BA4	Stoney-Miller, 1996	6125312.52	1958434.968	BA-4	Bucket Auger	24"	4/8/96	N	223	111	112		Y	N	Y - seep
SM96_BA5	Stoney-Miller, 1996	6124770.799	1958877.889	BA-5	Bucket Auger	24"	4/9/96	N	166	101	65	Y?	Y?	N	Y - seep
SM96_BA6	Stoney-Miller, 1996	6125233.895	1957801.337	BA-6	Bucket Auger	24"	5/20/96	N	59	96	-37			Y	Y - seep
SM96_BA7	Stoney-Miller, 1996	6125568.176	1957341.173	BA-7	Bucket Auger	24"	5/21/96	N	29	23.5	5.5	N	N	Y	Y
SM96_BA8	Stoney-Miller, 1996	6124595.516	1958504.148	BA-8	Bucket Auger	24"	5/21/96	N	44	90.8	-46.8			Y	Y
SM96_BA9	Stoney-Miller, 1996	6124966.438	1958242.141	BA-9	Bucket Auger	24"	5/22/96	N	57	101	-44			Y	N
SM96_HSA8	Stoney-Miller, 1996	6126618.075	1958729.575	HSA-8	Hollow Stem Auger	8"	4/22/96	N	711	41	670		N	N	Y - wet
SM96_HSA9	Stoney-Miller, 1996	6126863.138	1958576.802	HSA-9	Hollow Stem Auger	8"	4/22/96	N	670	41	629		N	N	Y - wet
SM96_HSA10	Stoney-Miller, 1996	6126920.476	1958396.73	HSA-10	Hollow Stem Auger	8"	4/22/96	N	668	41	627		N	N	N
SM96_HSA11	Stoney-Miller, 1996	6127729.434	1957063.578	HSA-11	Hollow Stem Auger	8"	4/23/96	N	511	41	470	N	N	N	N
SM96_HSA12	Stoney-Miller, 1996	6127216.198	1956734.177	HSA-12	Hollow Stem Auger	8"	4/23/96	N	465	41	424		N	N	N
SM96_HSA13	Stoney-Miller, 1996	not in study area	not in study area		Hollow Stem Auger	8"	4/23/96	N	530	41	489		N	N	Y - wet
SM96_HSA14	Stoney-Miller, 1996	not in study area	not in study area		Hollow Stem Auger	8"	4/23/96	N	560	41	519		N	N	Y - wet
SM96_SSA1	Stoney-Miller, 1996	not in study area	not in study area		Solid Stem Auger	6"	4/15/96	N	710	27.5	682.5	N	N	N	N
SM96_SSA2	Stoney-Miller, 1996	6126952.517	1957466.818	SSA-2	Solid Stem Auger	6"	4/15/96	N	510	30	480	N	N	N	Y - wet
SM96_SSA3A	Stoney-Miller, 1996	6127132.459	1957095.419		Solid Stem Auger	6"	4/16/96	N	503	6.5	496.5	N	N	N	N
SM96_SSA3B	Stoney-Miller, 1996	6127132.459	1957095.419	SSA-3	Solid Stem Auger	6"	4/18/96	Y-lysimeter	503	41	462	N	N	N	Y - wet
SM96_SSA4	Stoney-Miller, 1996	6126206.41	1958615.124	SSA-4	Solid Stem Auger	6"	4/19/96	Y-Nuke probe	645	40.5	604.5				
SM96_SSA5	Stoney-Miller, 1996	6126099.383	1958677.271	SSA-5	Solid Stem Auger	6"	4/19/96	Y-lysimeters	620	39.5	580.5	N	N	N	Y - wet
SM96_SSA6	Stoney-Miller, 1996	6126026.475	1958669.899	SSA-6	Solid Stem Auger	6"	4/22/96	Y-Nuke probe	605	41	564	N	N	N	N
SM96_SSA7A	Stoney-Miller, 1996	6125919.946	1958999.94		Solid Stem Auger	6"	4/23/96	N	652	23.5	628.5	N	N	N	N
SM96_SSA7B	Stoney-Miller, 1996	6125919.946	1958999.94	SSA-7	Solid Stem Auger	6"	4/22/96	N	652	41.5	610.5	N	N	N	Y - wet
B98_GB10	Geotechnical Consultants, Inc. cited in Bachman, 1998	6126713.25	1957704.096	B-10	Mud Rotary	2"	-	Y	540	491	49			Y?	
B98_GB11	Geotechnical Consultants, Inc. cited in Bachman, 1998	6127905.498	1957697.569	B-11	Mud Rotary	2"	7/16/96	Y	569	252	317				
B98_GB12	Geotechnical Consultants, Inc. cited in Bachman, 1998	6126742.413	1958313.416	B-12	Mud Rotary	2"	7/22/96	Y	636	246	390				
B98_GB13New	Geotechnical Consultants, Inc. cited in Bachman, 1998	6127333.397	1958305.528	B-13	Mud Rotary	2"	7/29/96	Y	707	302	405				
B98_GB14	Geotechnical Consultants, Inc., 1996	6126384.957	1959307.969	B-14	Mud Rotary	2"	8/5/96	Y	729	302.5	426.5				
GTC96_GB15	Geotechnical Consultants, Inc., 1996	6125820.109	1957961.887												
GTC96_GB16	Geotechnical Consultants, Inc., 1996	6126120.423	1958416.833	B-16	Mud Rotary?		8/14/96	N	602	62.2	539.8	N	N	N	?
GTC96_GB17	Geotechnical Consultants, Inc., 1996	6125338.833	1958419.66	B-17	Mud Rotary?		8/14/96	N	230	32.2	197.8	N	N	N	?
B98_GB18	Geotechnical Consultants, Inc. cited in Bachman, 1998	6126447.277	1958465.906	B-18	Mud Rotary	2"	8/19/96	Y	677	382	295			Y?	
SM96_GB20	Stoney-Miller, 1996	6124765.952	1958427.615	GB-20	Bucket Auger	24"	8/12/96	N	58	55	3	N	N	Y	Y
SM96_GB21	Stoney-Miller, 1996	6125008.52	1958097.307	GB-21	Bucket Auger	24"	8/15/96	N	55	49	6	N	N	Y	N
SM96_GB22	Stoney-Miller, 1996	6124867.259	1957801.828	GB-22	Bucket Auger	24"	8/15/96	N	34	27	7	N	N	Y	N
SM96_GB23	Stoney-Miller, 1996	6124576.711	1957842.962	GB-23	Bucket Auger	24"	8/14/96	N	24	15.5	8.5	N	N	Y	N
SM96_GB24	Stoney-Miller, 1996	6125086.069	1957962.595	GB-24	Bucket Auger	24"	8/14/96	N	63	54.5	8.5	N	N	Y	Y
SM98_B10A	Stoney-Miller, 1998	6125015.593	1958709.467	B-10	Bucket Auger	24"	12/2/97	N	192	7	185	N	N	N	N
SM98_BA10B	Stoney-Miller, 1998	6125015.593	1958709.467	B-10	Bucket Auger	24"	12/2/97	N	192	131	61	Y?	N	N	Y - seep
SM98_BA11	Stoney-Miller, 1998	6125574.881	1958411.92	B-11	Bucket Auger	24"	12/8/97	N	282	103	179	Y	N	Y	Y - seep
SM98_BA12	Stoney-Miller, 1998	6125759.382	1958031.746	B-12	Bucket Auger	24"	12/10/97	N	280	45	235	N	N	N	N
SM98_B15	Stoney-Miller, 1998	6125585.815	1958410.575	SMC-15	Solid Stem Auger		12/11/97	Y	285	98	187	Y	N	N	Y - minor
SM98_B16	Stoney-Miller, 1998	6125476.997	1958288.356	SMC-16	Solid Stem Auger		12/10/97	Y	254	130	124	Y?	N	Y?	Y
C94_MB1	Converse West, 1994				TH-60 Air Rotary		10/5/94	Y	234	121	113	N	N	N	N
C94_MB1A	Converse West, 1994	6125397.773	1958328.364		TH-60 Air Rotary		11/4/94	Y	235	148	87	N	N	N	N
C94_MB2	Converse West, 1994	6125368.287	1958381.112		TH-60 Air Rotary		10/6/94	Y	227	80	147	N	N	N	N
C94_MB3	Converse West, 1994	6125592.898	1958302.165		TH-60 Air Rotary		10/7/94	Y	250	80	170	N	N	N	N*
C94_MB4	Converse West, 1994	6125320.498	1958120.282		CME-75 HAS		10/25/94	Y	95	90	5	N	N	N	Y
C94_MB5	Converse West, 1994	6125084.496	1958173.088		CME-75 HAS		10/26/94	Y	110	96	14	N	N	Y?	N
C94_WB1 (aband)	Converse West, 1994	not known	not known		TH-60 Air Rotary		10/10/94	Y - deH2O	690	320	370	Y?	N	N	Y
C94_WB1A	Converse West, 1994	6126348.723	1958925.918	WB-1A	TH-60 Air Rotary		10/18/94	Y - deH2O	690	320	370	Y?	N	N	Y
C94_WB2	Converse West, 1994	6126128.205	1959206.54		TH-60 Air Rotary		10/13/94	Y - deH2O	670	160	510	Y?	N	Y	N
C94_WB3	Converse West, 1994	6126155.779	1958454.89	WB-3	TH-60 Air Rotary		10/31/94	Y - deH2O	670	380	290	Y?	Y	Y?	Y
ZK_B1	Zeiser Kling, 1998	6125196.262	1957833.307	ZB-1	HSA	8"	9/4/98	N	59	51	8	N	N	N	Y
ZK_B2	Zeiser Kling, 1998	6125073.279	1957928.912	ZB-2	HSA	8"	9/4/98	N	59	31	28	N	N	N	N
ZK_B3	Zeiser Kling, 1998	6124986.165	1958119.683	ZB-3	HSA	8"	9/4/98	N	55	31	24	N	N	N	N
ZK_HA1	Zeiser Kling, 1998	6125077.395	1958026.753		Hand Auger		9/4/98	N	65	6	59	N	N	N	Y
ZK_HA2	Zeiser Kling, 1998	6125100.328	1957948.564		Hand Auger		9/4/98	N	67	4	63	N	N	N	N
ZK_HA3	Zeiser Kling, 1998	6125163.113	1957866.81		Hand Auger		9/4/98	N	70	6	64	N	N	N	N
F07_CPT1	Fugro West, Inc., 2007	6124887.833	1957455.891	CPT-1	CPT Sounding	2 1/4"	10/24/06	N	22.5	52	-29.5	N	N	Y	N
F07_CPT2	Fugro West, Inc., 2007	6124804.685	1957385.791	CPT-2	CPT Sounding	2 1/4"	10/24/06	N	26.6	58	-31.4	N	N	Y	Y
F07_CPT3	Fugro West, Inc., 2007	6124781.687	1957348.469	CPT-3	CPT Sounding	2 1/4"	10/24/06	N	26.6	7.5	19.1	N	N	N	N
F07_CPT3A	Fugro West, Inc., 2007	6124781.687	1957348.469	CPT-3A	CPT Sounding	2 1/4"	10/24/06	N	26.6	7.5	19.1	N	N	N	N
F07_CPT4	Fugro West, Inc., 2007	6124781.062	1957243.597	CPT-4	CPT Sounding	2 1/4"	10/24/06	N	25.5	23	2.5	N	N	Y	Y
F07_DH01	Fugro West, Inc., 2007	6124897.531	1957442.812	DH-01	Rotary-wash	5"	10/23/06	Y	22.6	50.5	-27.9	N	N	Y	Y
F07_DH02	Fugro West, Inc., 2007	6124723.680	1957310.524	DH-02	Rotary-wash	5"	10/23/06	N	25.7	51	-25.3	N	N	Y	N
F07_TP01	Fugro West, Inc., 2007			TP-01	Test Pit		10/23/06	N	27	9	18	N	N	N	N

LA - Leighton Associates, 1993
GB - Geotechnical Consultants (Bachman, 1998)
SM - Stoney Miller Consultants
C - Converse, 1994
ZK - Zeiser Kling, 1998
PML - Pacific Materials Laboratories, 2006

Table C-2: Summary of groundwater information for compiled geotechnical borings and water wells within the La Conchita study area (see map for boring locations).

Boring Name	Source	Depth to First Water (ft)	Elevation of First Water (ft)	Comments	Depth to Second Water (ft)	Elevation of Second Water (ft)	Comments	Depth to Third Water (ft)	Elevation of Third Water (ft)	Comments	Water Level Depth (ft)	Elevation of Water Level (ft)	Comments	Water Level Depth (ft)	Elevation of Water Level (ft)	Comments
LA93_B1	Leighton Associates, 1993	85	755	moist to wet	92	748	seepage	---	840		93	747	standing water	100	740	overpressured aquifer
LA93_B2	Leighton Associates, 1993	52	448	slow seepage	53	447	increased seepage	61	439	seepage	84	416	groundwater	---	---	---
LA93_B3	Leighton Associates, 1993	---	---	---	---	---	---	---	---	---	---	---	---	---	---	---
LA93_B4	Leighton Associates, 1993	23	635	moist to wet	30	628	moist to wet, free water locally	48.5	609.5	moist to wet	68.5, 91, 97.5-99, 103.5-104.5, 107-109, 111, 128	589.5, 567, 560.5-559, 554.5-553.5, 551-549, 547, 530	free water and seepage, moist to wet, moist to wet and minor free water, some free water, seepage and heavy caving, free water on fractures, free water on bedding planes	137-138	521-520	wet, noted as groundwater on log
LA93_B5	Leighton Associates, 1993	53.5	52.5	moist to wet clayey sandstone seam	86	20	wet	87	19	seepage	87	19	seepage	---	---	---
LA93_B6	Leighton Associates, 1993	37	568	seepage to 42' (533 el)	47	558	seepage	48.5	556.5	strong seepage	69	536	water (log: at 61' ?)	65	520	water (rises 85' to 79')
LA93_B7	Leighton Associates, 1993	---	100	---	---	100	---	---	100	---	---	100	---	---	100	---
LA93_C1	Leighton Associates, 1993	-	-	-	-	-	-	-	-	-	160	40	water loss stops at 160 "probably GW"	-	-	-
LA93_C2	Leighton Associates, 1993	11	510	slight seepage	---	---	---	---	---	---	---	---	---	---	---	---
PML06_B1	Pacific Material Laboratories	---	50	---	---	50	---	---	50	---	---	50	---	---	50	---
PML79_B1	Pacific Material Laboratories															
SM96_HSA1	Stoney-Miller, 1996	80	680	very moist to wet	-	N/A			760		-	N/A			760	
SM96_HSA2	Stoney-Miller, 1996	19	655	wet cuttings	59	615	some wet surfaces		674		-	N/A			674	
SM96_HSA3	Stoney-Miller, 1996	---	---	---	---	---	---	---	---	---	---	---	---	---	---	---
SM96_BA1	Stoney-Miller, 1996	90	186	wet/seepage	-	-	---	---	---	---	---	---	---	---	---	---
SM96_BA2	Stoney-Miller, 1996	41	427	seepage, wet fractured surfaces	45	423	very moist to wet	52-55	#VALUE!		-	N/A		---	---	---
SM96_BA3	Stoney-Miller, 1996	46	474	abundant seepage	50	470	free water on some frag. faces	---	416-413	very moist to wet, wet fracture surfaces	70, 77, 83	396, 391, 385	slight seepage from fractures, seepage, wet rock faces & seepage	---	---	---
SM96_BA4	Stoney-Miller, 1996	---	---	---	---	---	---	---	---	---	---	---	---	---	---	---
SM96_BA5	Stoney-Miller, 1996	64	102	seepage very slight	75	91	seepage	78	88	seepage	---	166	---	---	166	---
SM96_BA6	Stoney-Miller, 1996	40	19	very moist to wet	48	11	wet, heavy to minor seepage	---	---	---	---	---	---	---	---	---
SM96_BA7	Stoney-Miller, 1996	4	25	very moist to wet	17	12	wet/groundwater		29		17	12	groundwater		29	
SM96_BA8	Stoney-Miller, 1996	36	8	heavy seepage	66	-22	groundwater-end of day	45	-1	groundwater--next morning	66	-22	groundwater		44	
SM96_BA9	Stoney-Miller, 1996	---	---	---	---	---	---	---	---	---	---	---	---	---	---	---
SM96_HSA8	Stoney-Miller, 1996	1	710	very moist to wet	2	709	wet	20	691	very moist to wet, free water on clasts	---	---	---	---	---	---
SM96_HSA9	Stoney-Miller, 1996	1	669	very moist to wet	5	665	wet	20	650	very moist to wet	30	640	very moist to wet	35	635	minor free water on shale
SM96_HSA10	Stoney-Miller, 1996	---	---	---	---	---	---	---	---	---	---	---	---	---	---	---
SM96_HSA11	Stoney-Miller, 1996	10	501	very moist to wet	15	498	wet	20	491	wet	40	471	minor free water on fragments	---	---	---
SM96_HSA12	Stoney-Miller, 1996	---	---	---	---	---	---	---	---	---	---	---	---	---	---	---
SM96_HSA13	Stoney-Miller, 1998		530			530			530			530			530	
SM96_HSA14	Stoney-Miller, 1996		560			560			560			560			560	
SM99_SSA1	Stoney-Miller, 1996		710			710			710			710			710	
SM96_SSA2	Stoney-Miller, 1996	20	490	very moist to wet	25	485	very moist to wet	---	503		---	503		---	503	
SM96_SSA3A	Stoney-Miller, 1996		503			503			---			---			---	
SM96_SSA3B	Stoney-Miller, 1996	14	489	wet	---	---	---	---	---	---	---	---	---	---	---	---
SM96_SSA4	Stoney-Miller, 1996	---	---	---	---	---	---	---	---	---	---	---	---	---	---	---
SM96_SSA5	Stoney-Miller, 1996	8	612	very moist to wet	10	610	very moist to wet	39	581	wet	---	---	---	---	---	---
SM96_SSA6	Stoney-Miller, 1996	---	---	---	---	---	---	---	---	---	---	---	---	---	---	---
SM96_SSA7A	Stoney-Miller, 1996		652			652			652			652			652	
SM96_SSA7B	Stoney-Miller, 1996	36	616	wet	40	612	very moist to wet		652			652			652	
B98_GB10	Geotechnical Consultants, Inc cited in Bachman, 1998		540			540			540			540			540	
B98_GB11	Geotechnical Consultants, Inc. cited in Bachman, 1998		569			569			569			569			569	
B98_GB12	Geotechnical Consultants, Inc cited in Bachman, 1998		636			636			636			636			636	
B98_GB13New	Geotechnical Consultants, Inc. cited in Bachman, 1998		707			707			707			707			707	
B98_GB14	Geotechnical Consultants, Inc cited in Bachman, 1998		729			729			729			729			729	
GTC96_GB15	Geotechnical Consultants, Inc , 1996															
GTC96_GB16	Geotechnical Consultants, Inc., 1996	---	---	---	---	---	---	---	---	---	---	---	---	---	---	---
GTC96_GB17	Geotechnical Consultants, Inc., 1996	---	---	---	---	---	---	---	---	---	---	---	---	---	---	---
B98_GB18	Geotechnical Consultants, Inc. cited in Bachman, 1998		677			677			677			677			677	
SM99_GB20	Stoney-Miller, 1996	45	13	wet to the touch	47	11	wet	---	---	---	48	10	groundwater	---	---	---
SM96_GB21	Stoney-Miller, 1996	28.3	26.7	very moist to wet		55			55			55			55	
SM96_GB22	Stoney-Miller, 1996	16.5	17.5	moist to wet		34			34		26	8	groundwater		34	
SM96_GB23	Stoney-Miller, 1996	3.05	20.95	moist to wet	7	17	wet	7.8	16.2	moist to wet	9	15	moist to wet	10	14	moist to wet, no groundwater
SM96_GB24	Stoney-Miller, 1998		63			63			63		53.7	9.3	groundwater		63	
SM98_B10A	Stoney-Miller, 1998		192			192			192			192			192	
SM98_BA10B	Stoney-Miller, 1998	34.5	157.5	wet fracture faces	36	156	seepage		192		101	181	groundwater		192	
SM96_BA11	Stoney-Miller, 1998	101	161	groundwater	---	---	---	---	---	---	---	---	---	---	---	---
SM96_BA12	Stoney-Miller, 1998	---	---	---	---	---	---	---	---	---	40-43	245-242	based on bedrock elevation	---	---	---
SM98_B15	Stoney-Miller, 1998	---	---	---	---	---	---	---	---	---	93	161	based on driller's comments		254	
SM98_B16	Stoney-Miller, 1998		254			254			254			234			234	
C94_MB1	Converse West, 1994		234			234			234			235			235	
C94_MB1A	Converse West, 1994		235			235			235			227			227	
C94_MB2	Converse West, 1994		227			227			227			250			250	
C94_MB3	Converse West, 1994		250			250			250			95			95	
C94_MB4	Converse West, 1994		95			95			95			110			110	
C94_MB5	Converse West, 1994		110			110			110			690			690	
C94_WB1 (aband)	Converse West, 1994		690			690			690							
C94_WB1A	Converse West, 1994	180	510	"hole making some water"	218	472	"hole making sufficient water to stop infection"	---	---	---	---	---	---	---	---	---
C94_WB2	Converse West, 1994	---	670	---	---	670	---	---	670	---	---	670	---	---	670	---
C94_WB3	Converse West, 1994	50	---	groundwater?	---	---	---	---	---	---	157	513	groundwater	---	---	---
ZK_B1	Zelser King, 1998	---	9			59			59		50	9	groundwater?	---	---	---
ZK_B2	Zelser King, 1998	---	#VALUE!			55			55			59			59	
ZK_B3	Zelser King, 1998	---	#VALUE!			65			65			55			55	
ZK_HA1	Zelser King, 1998	5	60			---		---	---			65			65	
ZK_HA2	Zelser King, 1998	---	---	---	---	---	---	---	---	---	---	---	---	---	---	---
ZK_HA3	Zelser King, 1998	---	---	---	---	---	---	---	---	---	---	---	---	---	---	---
F07_CPT1	Fugro West, Inc., 2007		---	---	---	---	---	---	---	---	---	---	---	---	---	---
F07_CPT2	Fugro West, Inc., 2007	15	7.5	groundwater	---	---	---	---	---	---	---	---	---	---	---	---
F07_CPT3	Fugro West, Inc., 2007	18	8.6	groundwater	---	---	---	---	---	---	---	---	---	---	---	---
F07_CPT3A	Fugro West, Inc., 2007	15	11.6	groundwater	---	---	---	---	---	---	---	---	---	---	---	---
F07_CPT4	Fugro West, Inc., 2007	15	11.6	groundwater	---	---	---	---	---	---	---	---	---	---	---	---
F07_DH01	Fugro West, Inc., 2007	15	10.5	groundwater	---	---	---	---	---	---	---	---	---	---	---	---
F07_DH02	Fugro West, Inc., 2007	15	7.6	groundwater	---	---	---	---	---	---	---	---	---	---	---	---
F07_TP01	Fugro West, Inc., 2007	---	---	---	---	---	---	---	---	---	---	---	---	---	---	---
		---	---	---	---	---	---	---	---	---	---	---	---	---	---	---

LA - Leighton Associates, 1993
GB - Geotechnical Consultants (Bachman, 1998)
SM - Stoney Miller Consultants
C - Converse, 1994
ZK - Zelser Kilng, 1998
PML - Pacific Materials Laboratories, 2006

Table C-3: Summary of depth to bedrock information for compiled geotechnical borings and water wells within the La Conchita study area (see map for boring locations).

Boring Name	Source	Depth of First Bedrock (ft)	Elevation of Bedrock (ft)	Bedrock Type
LA93_B1	Leighton Associates, 1993	141	699	Silty clay or claystone - possible bedrock (bottom of boring)
LA93_B2	Leighton Associates, 1993	62	438	Siltstone - Pico Fm.
LA93_B3	Leighton Associates, 1993	63.7	641.3	(possible bedrock) clayey siltstone - Pico?
LA93_B4	Leighton Associates, 1993	39	619	possible bedrock, siliceous bed, @ 43' siltstone & claystone interbedded - Pico Fm
LA93_B5	Leighton Associates, 1993	---	---	
LA93_B6	Leighton Associates, 1993	95	510	all breccia w/ two relict SS beds
LA93_B7	Leighton Associates, 1993		100	clayey siltstone (tight breccia) wet at 100-102'
LA93_C1	Leighton Associates, 1993	116.8	83.2	
LA93_C2	Leighton Associates, 1993	88.5	432.5	sandy siltstone to silty claystone (Pico Fm)
PML06_B1	Pacific Material Laboratories	42.5	7.5	sandy siltstone and shale (Pico Fm)
PML79_B1	Pacific Material Laboratories			silty clay - bedrock, cobble lens 1.5' thick above
SM96_HSA1	Stoney-Miller, 1996	81	679	Pico Formation
SM96_HSA2	Stoney-Miller, 1996	75	599	Claystone/shale
SM96_HSA3	Stoney-Miller, 1996	85.5	519.5	Refusal @ 75'
SM96_BA1	Stoney-Miller, 1996	-	N/A	Refusal @ 85.5' with shale fragments and siltstone/sandstone colluvium at sample tip
SM96_BA2	Stoney-Miller, 1996	---	---	N/A
SM96_BA3	Stoney-Miller, 1996	80	440	
SM96_BA4	Stoney-Miller, 1996	40	183	sandstone - Pico
SM96_BA5	Stoney-Miller, 1996	70	96	siltstone/claystone Tm?/Tp?
SM96_BA6	Stoney-Miller, 1996	50	9	siltstone - Pico. Siltstone occurs at 40' (120' el.), however underlain by clays and sands, and shears
SM96_BA7	Stoney-Miller, 1996	22	7	sandy siltstone - Pico
SM96_BA8	Stoney-Miller, 1996	39	5	sandy siltstone - Pico, overlain by 2' of boulders w/ abundant shells
SM96_BA9	Stoney-Miller, 1996	43	14	sandy claystone - Pico, overlain by 1.5' to 3' of large rocks/boulders w/shells
SM96_HSA8	Stoney-Miller, 1996	35	676	siltstone/claystone - Pico, overlain by 1' of boulders/ lagg deposits
SM96_HSA9	Stoney-Miller, 1996	---	---	predominantly shale - possible bedrock
SM96_HSA10	Stoney-Miller, 1996	30	638	
SM96_HSA11	Stoney-Miller, 1996	---	---	claystone w/orange brown staining (Tm?)
SM96_HSA12	Stoney-Miller, 1996	---	---	
SM96_HSA13	Stoney-Miller, 1996		530	
SM96_HSA14	Stoney-Miller, 1996		560	
SM96_SSA1	Stoney-Miller, 1996		710	
SM96_SSA2	Stoney-Miller, 1996	20	490	
SM96_SSA3A	Stoney-Miller, 1996		503	sandy claystone (Tm?), refusal @ 30' (480 el.) sandy siltstone
SM96_SSA3B	Stoney-Miller, 1996	30	473	
SM96_SSA4	Stoney-Miller, 1996	39.5	605.5	possible bedrock, fragmented siltstone/claystone w/ clay linings
SM96_SSA5	Stoney-Miller, 1996	38	582	siltstone breccia - sounds like Tm
SM96_SSA6	Stoney-Miller, 1996	---	---	claystone/siltstone breccia (Tm?)
SM96_SSA7A	Stoney-Miller, 1996		652	
SM96_SSA7B	Stoney-Miller, 1996		652	
B98_GB10	Geotechnical Consultants, Inc. cited in Bachman, 1998		540	
B98_GB11	Geotechnical Consultants, Inc. cited in Bachman, 1998		569	
B98_GB12	Geotechnical Consultants, Inc. cited in Bachman, 1998		636	
B98_GB13New	Geotechnical Consultants, Inc. cited in Bachman, 1998		707	
B98_GB14	Geotechnical Consultants, Inc. cited in Bachman, 1998		729	
GTC96_GB15	Geotechnical Consultants, Inc., 1996			
GTC96_GB16	Geotechnical Consultants, Inc., 1996	---	---	
GTC96_GB17	Geotechnical Consultants, Inc., 1996	9	221	Montery breccia with silty-sandy matrix
B98_GB18	Geotechnical Consultants, Inc. cited in Bachman, 1998		677	Pico Fm? gray-brn sandy clay to silty fine sand
SM96_GB20	Stoney-Miller, 1996	51	7	
SM96_GB21	Stoney-Miller, 1996	49	6	siltstone/claystone - Pico Fm.
SM96_GB22	Stoney-Miller, 1996	---	---	siltstone - Pico
SM96_GB23	Stoney-Miller, 1996	---	---	
SM96_GB24	Stoney-Miller, 1996	54.5	8.5	
SM98_B10A	Stoney-Miller, 1998		192	sandy siltstone/silty sandstone (Pico)
SM98_BA10B	Stoney-Miller, 1998	114	78	
SM98_BA11	Stoney-Miller, 1998	---	---	Siltstone - Pico Fm.
SM98_BA12	Stoney-Miller, 1998	---	---	
SM98_B15	Stoney-Miller, 1998	43	242	
SM98_B16	Stoney-Miller, 1998	90	164	Siltstone, clayey Silt - Pico
C94_MB1	Converse West, 1994		234	Siltstone clayey silt - Pico?
C94_MB1A	Converse West, 1994		235	
C94_MB2	Converse West, 1994		227	
C94_MB3	Converse West, 1994		250	
C94_MB4	Converse West, 1994		95	
C94_MB5	Converse West, 1994		110	
C94_WB1 (aband)	Converse West, 1994		690	
C94_WB1A	Converse West, 1994	230	460	
C94_WB2	Converse West, 1994		670	"mostly Pico Fm w/intervals of mixed Tm & Tp gravels" @296' (394' el.) Pico Fm Bedrock
C94_WB3	Converse West, 1994	335	335	
ZK_B1	Zeiser King, 1998	---	---	Siltstone - weathered Tp to 370 (300' el.), then competent(?) Tp
ZK_B2	Zeiser King, 1998		59	
ZK_B3	Zeiser King, 1998		55	
ZK_HA1	Zeiser King, 1998		65	
ZK_HA2	Zeiser King, 1998	---	---	
ZK_HA3	Zeiser King, 1998	---	---	
F07_CPT1	Fugro West, Inc., 2007	29	-6.5	Pico Fm/Landslide deposits
F07_CPT2	Fugro West, Inc., 2007	37.5	-10.9	Pico Fm/Landslide deposits
F07_CPT3	Fugro West, Inc., 2007	---	---	
F07_CPT3A	Fugro West, Inc., 2007	---	---	
F07_CPT4	Fugro West, Inc., 2007	---	---	
F07_DH01	Fugro West, Inc., 2007	28	-5.4	Pico Fm/Landslide deposits
F07_DH02	Fugro West, Inc., 2007	41	-15.3	Pico Fm/Landslide deposits
F07_TP01	Fugro West, Inc., 2007	---	---	

LA - Leighton Associates, 1993
GB - Geotechnical Consultants (Bachman, 1998)
SM - Stoney Miller Consultants
C - Converse, 1994
ZK - Zeiser Kling, 1998
PML - Pacific Materials Laboratories, 2006

SOIL LOG LACONCHITA_110207.GPJ WLA9-8-06.GDT 11/09/07

Project Name and Job Number				
La Conchita SSP 1885	WLA William Lettis & Associates, Inc	**SOIL LOG - Boring No. B1**		
Type and Diameter of Boring Mud rotary wash / 5		Boring Location 34.36644 N, 119.44757 W		Total Depth 161 feet
Drilling Contractor and Rig C&L Drilling		Elevation and Datum 165 feet	Ground Water Depth N/A	Depth to Bedrock N/A
Sampling Method SPT/Split Spoon		Sample Driving Hammer/Drop 300 / 18	No. of Samples 11	Date Started 10/24/07
		Borehole Inclination -90	Logged by R. Hartleb	Date Completed 10/26/07

Reviewed by / Date _____

Reviewed by / Date _____

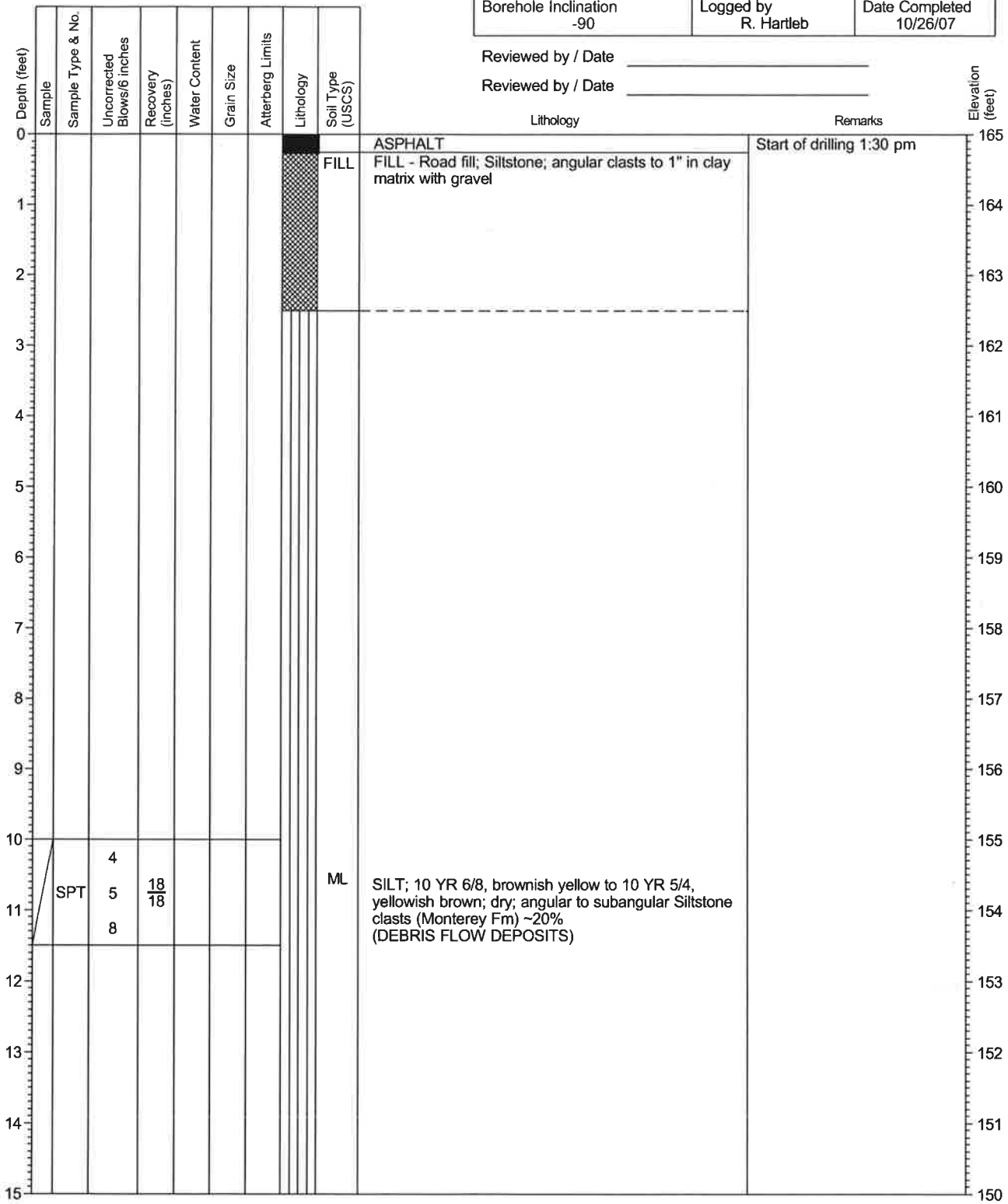

SOIL LOG LACONCHITA_110207.GPJ WLA9-8-06.GDT 11/09/07

Project Name and Job Number
La Conchita SSP
1885

WLA
William Lettis & Associates, Inc.

SOIL LOG - Boring No. B1

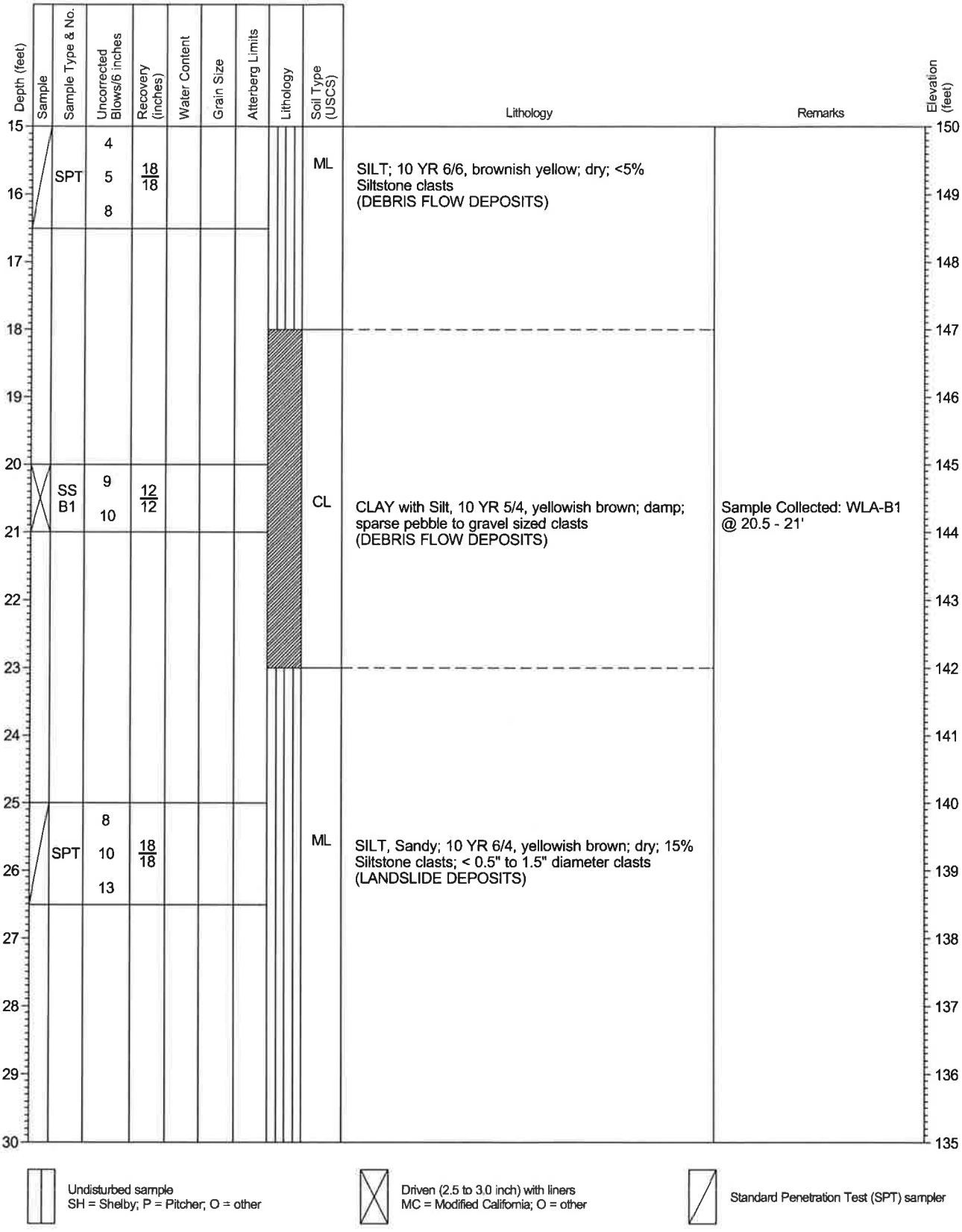

Undisturbed sample
SH = Shelby; P = Pitcher; O = other

Driven (2.5 to 3.0 inch) with liners
MC = Modified California; O = other

Standard Penetration Test (SPT) sampler

SOIL LOG LACONCHITA_110207.GPJ WLA9-8-06.GDT 11/09/07

Project Name and Job Number
La Conchita SSP
1885

William Lettis & Associates, Inc.

SOIL LOG - Boring No. B1

Depth (feet)	Sample	Sample Type & No.	Uncorrected Blows/6 inches	Recovery (inches)	Water Content	Grain Size	Atterberg Limits	Lithology	Soil Type (USCS)	Lithology	Remarks	Elevation (feet)
30									ML	SILT, Sandy; 10 YR 6/4, light yellowish brown; dry; >20% angular Siltstone clasts to 1" (DEBRIS FLOW DEPOSITS - OLD)		135
31		SPT	15 14 17	10.08/18						Same as above with increasing clast content (LANDSLIDE DEPOSITS)		134
32												133
33												132
34												131
35		SS B1	17 25	12/12					ML	SILT; 2.5 Y 5/4, light olive brown; 10% angular Siltstone clasts (LANDSLIDE DEPOSITS)	Sample Collected: WLA-B1 @ 35.5 - 36'	130
36												129
37												128
38												127
39												126
40		SPT	7 8 8	14.04/18								125
41									CL	CLAY, Silty; 2.5 Y 3/2, very dark grayish brown; damp; gypsum veins and visible crystals; Paleosol? Possible Slide Plane?		124
42												123
43												122
44									ML	SILT, Sandy; 2.5 Y 4/4, olive brown; no gravel; no siltstone clasts (LANDSLIDE DEPOSITS?)		121
45												120

Undisturbed sample
SH = Shelby; P = Pitcher; O = other

Driven (2.5 to 3.0 inch) with liners
MC = Modified California; O = other

Standard Penetration Test (SPT) sampler

SOIL LOG LACONCHITA_110207.GPJ WLA9-8-06.GDT 11/09/07

Project Name and Job Number
La Conchita SSP
1885

William Lettis & Associates, Inc.

SOIL LOG - Boring No. B1

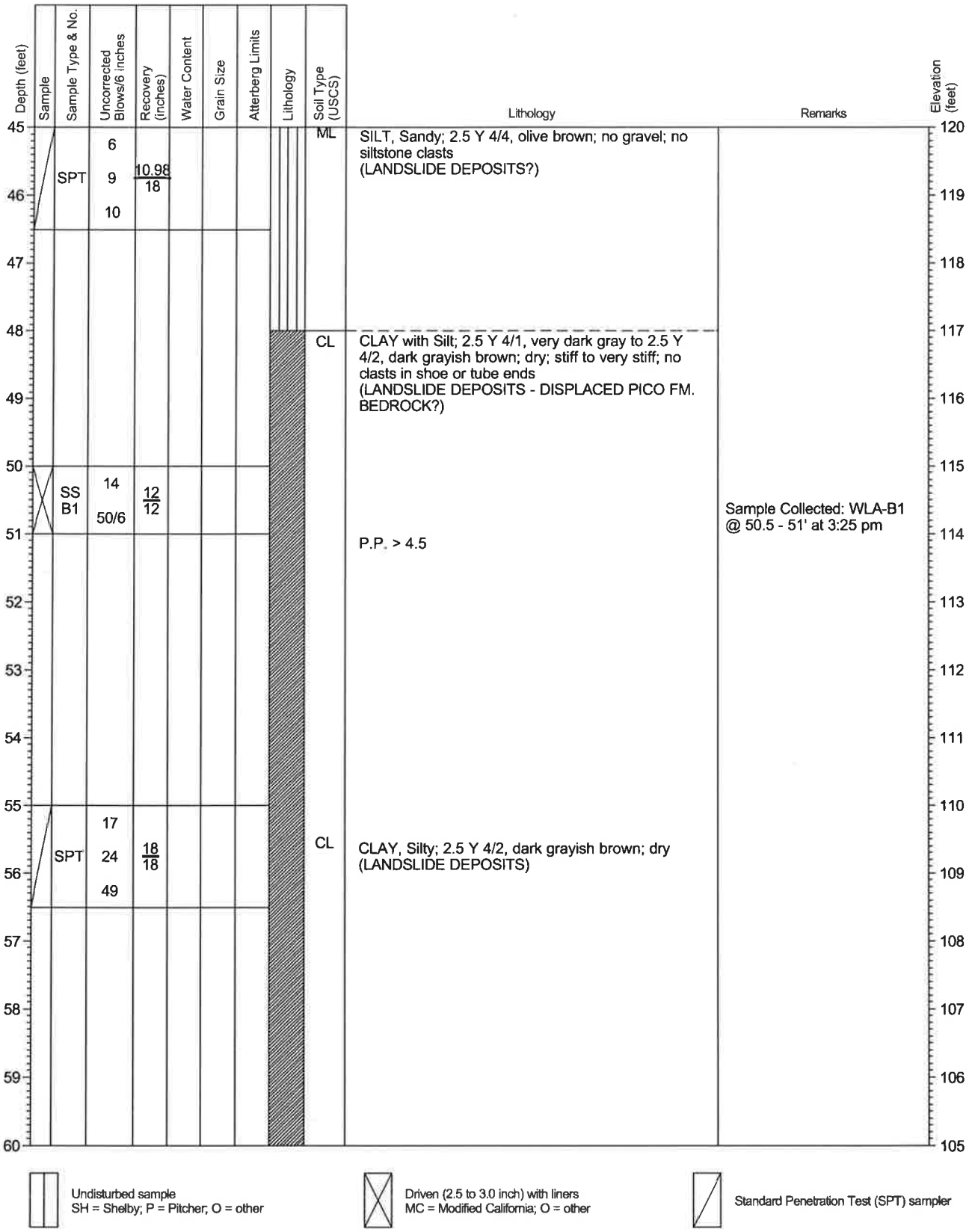

Undisturbed sample
SH = Shelby; P = Pitcher; O = other

Driven (2.5 to 3.0 inch) with liners
MC = Modified California; O = other

Standard Penetration Test (SPT) sampler

SOIL LOG LACONCHITA_110207.GPJ WLA9-8-06.GDT 11/09/07

Project Name and Job Number
La Conchita SSP
1885

William Lettis & Associates, Inc

SOIL LOG - Boring No. B1

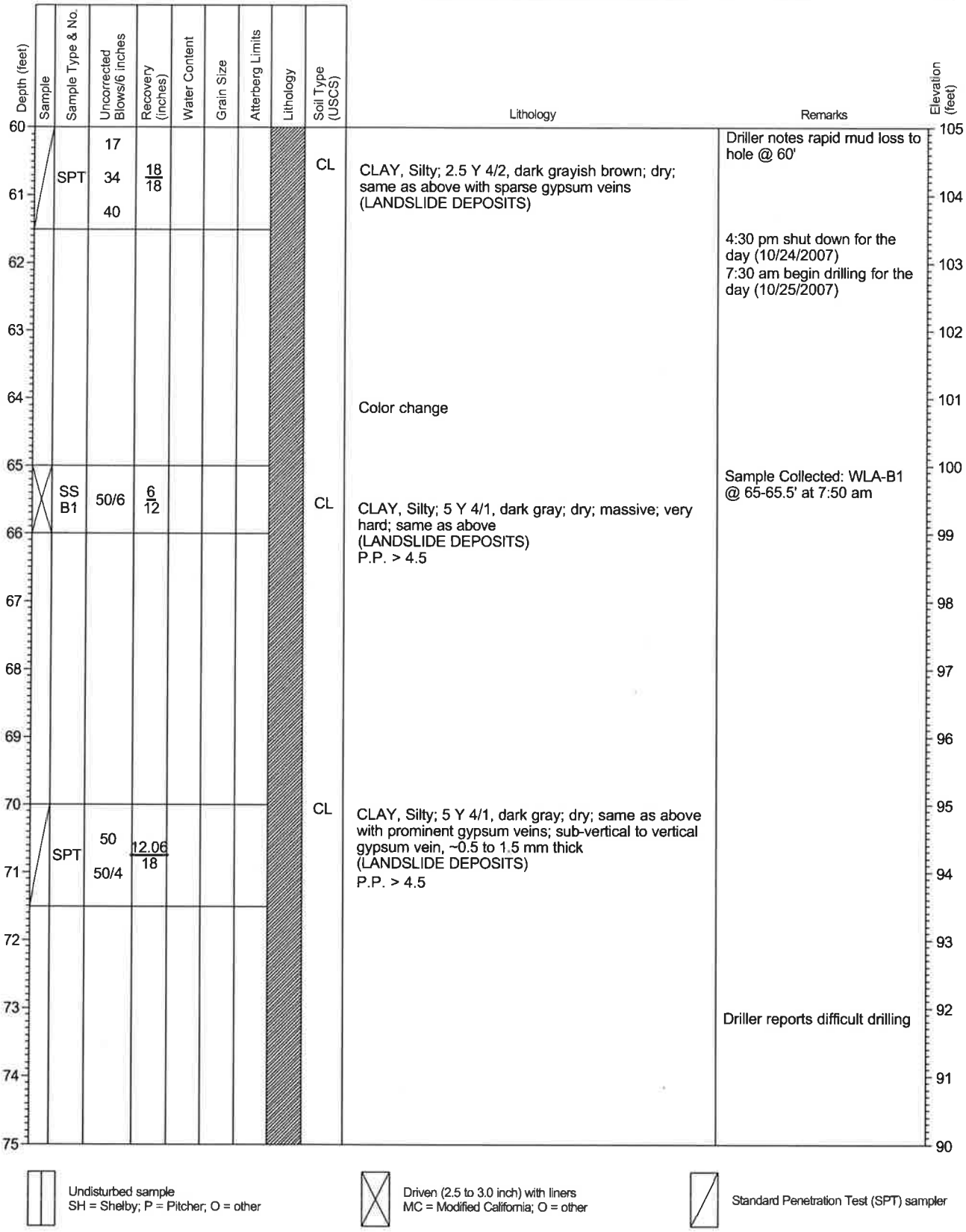

Undisturbed sample
SH = Shelby; P = Pitcher; O = other

Driven (2.5 to 3.0 inch) with liners
MC = Modified California; O = other

Standard Penetration Test (SPT) sampler

SOIL LOG LACONCHITA_110207.GPJ WLA9-8-06.GDT 11/09/07

Project Name and Job Number
La Conchita SSP
1885

William Lettis & Associates, Inc.

SOIL LOG - Boring No. B1

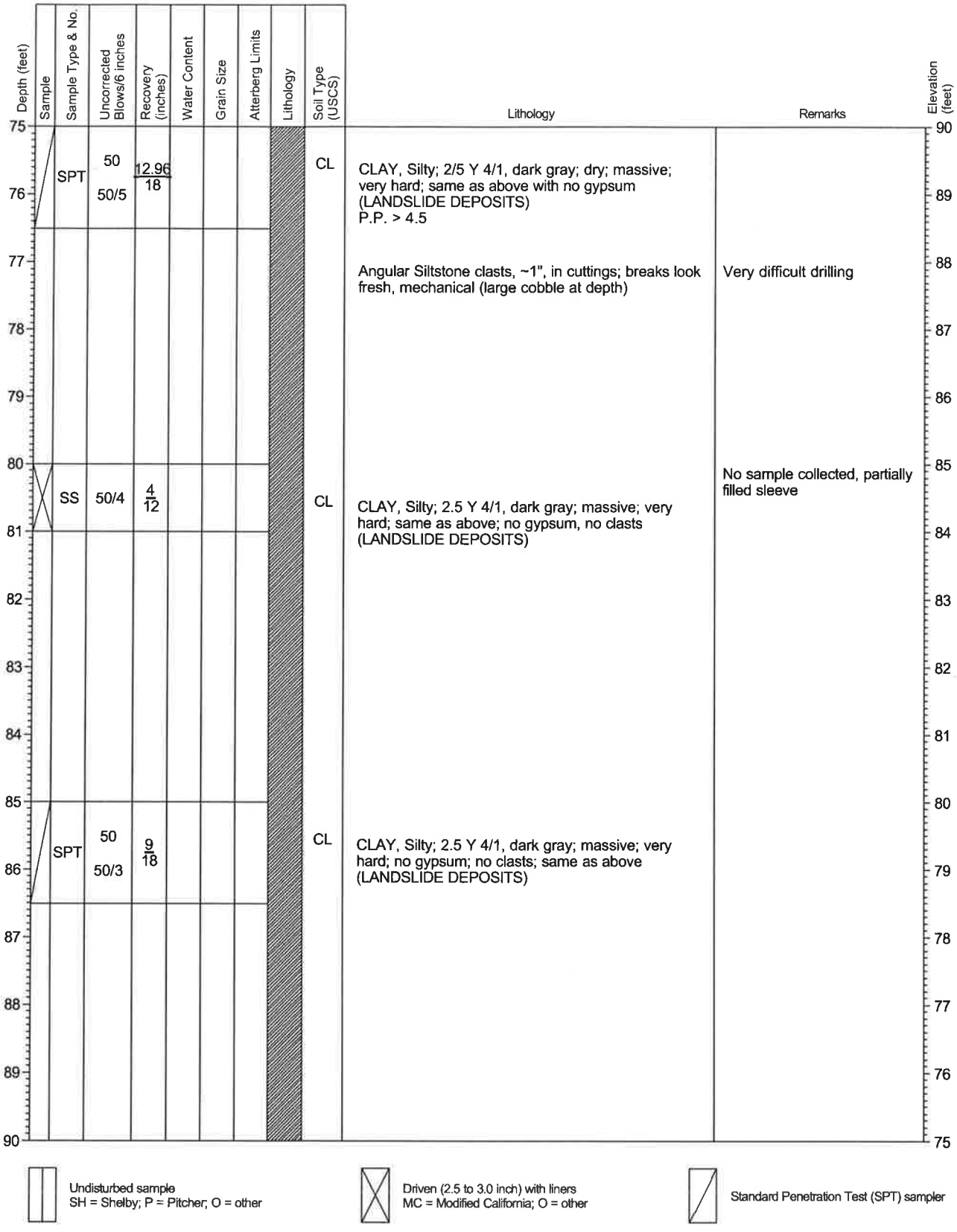

Undisturbed sample
SH = Shelby; P = Pitcher; O = other

Driven (2.5 to 3.0 inch) with liners
MC = Modified California; O = other

Standard Penetration Test (SPT) sampler

SOIL LOG LACONCHITA_110207.GPJ WLA9-8-06.GDT 11/09/07

Project Name and Job Number
La Conchita SSP
1885

William Lettis & Associates, Inc

SOIL LOG - Boring No. B1

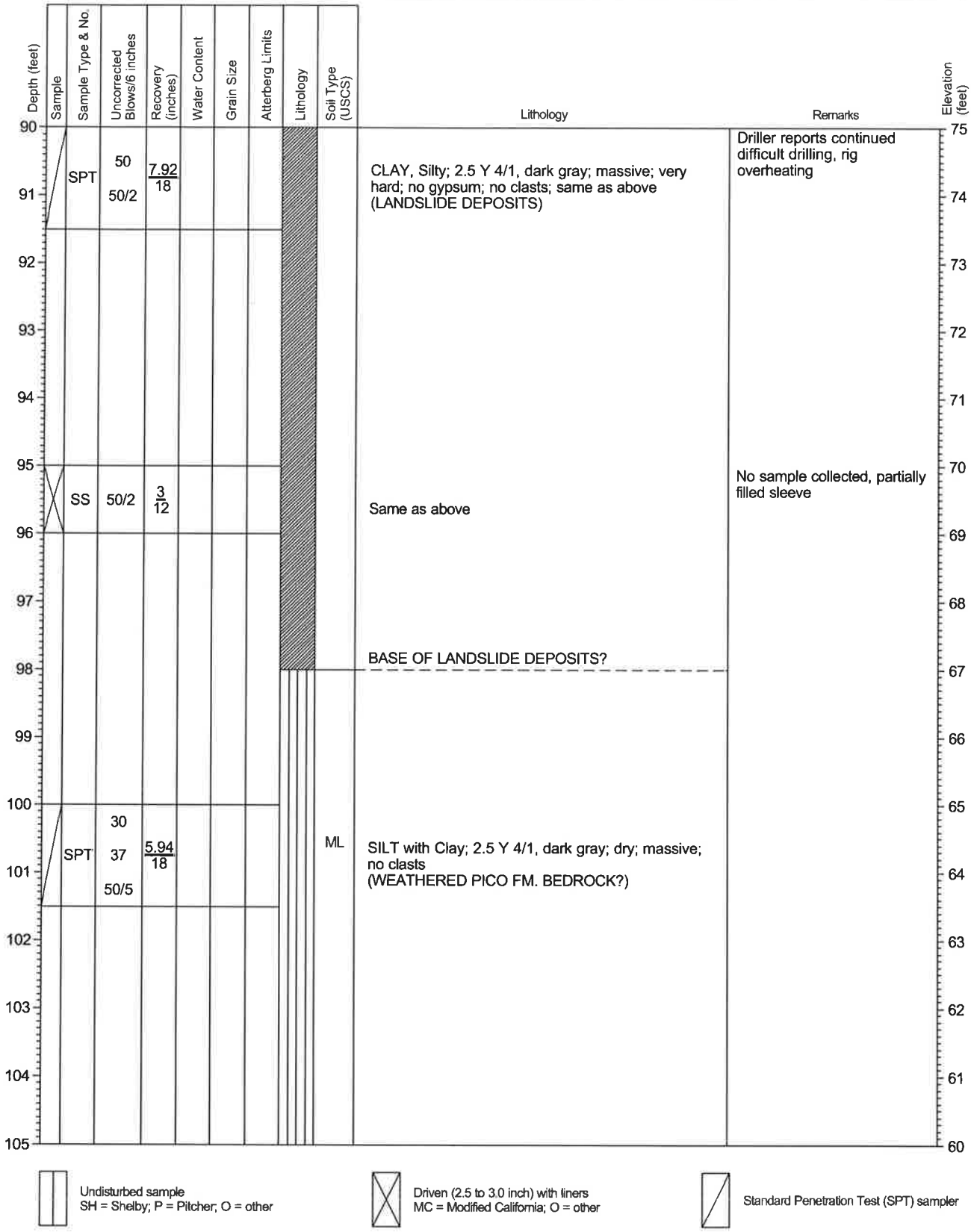

Undisturbed sample
SH = Shelby; P = Pitcher; O = other

Driven (2.5 to 3.0 inch) with liners
MC = Modified California; O = other

Standard Penetration Test (SPT) sampler

SOIL LOG LACONCHITA_110207.GPJ WLA9-8-06.GDT 11/09/07

Project Name and Job Number
La Conchita SSP
1885

William Lettis & Associates, Inc.

SOIL LOG - Boring No. B1

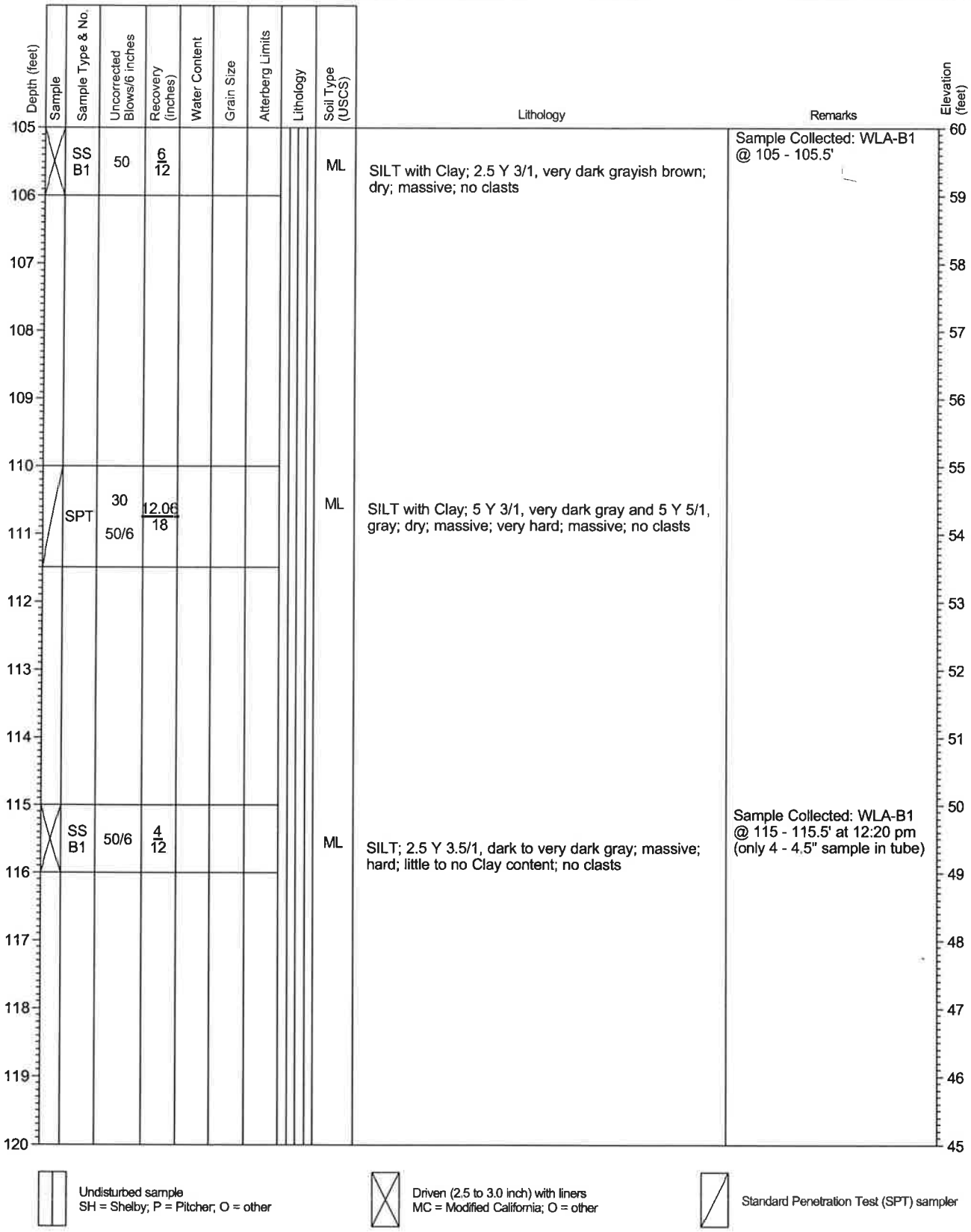

Undisturbed sample
SH = Shelby; P = Pitcher; O = other

Driven (2.5 to 3.0 inch) with liners
MC = Modified California; O = other

Standard Penetration Test (SPT) sampler

SOIL LOG LACONCHITA_110207.GPJ WLA9-8-06.GDT 11/09/07

Project Name and Job Number		SOIL LOG - Boring No. B1
La Conchita SSP 1885	William Lettis & Associates, Inc.	

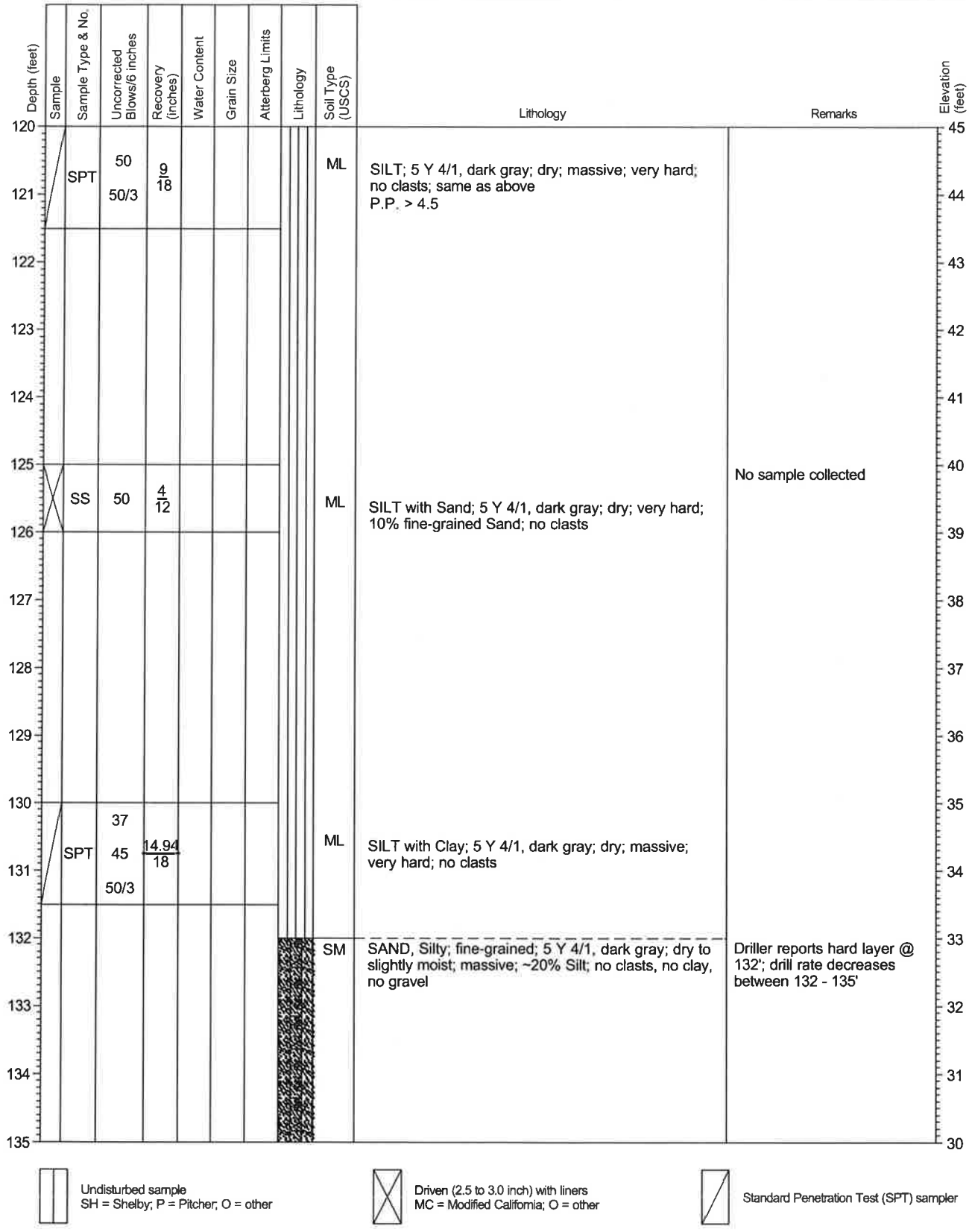

Undisturbed sample
SH = Shelby; P = Pitcher; O = other

Driven (2.5 to 3.0 inch) with liners
MC = Modified California; O = other

Standard Penetration Test (SPT) sampler

SOIL LOG LACONCHITA_110207.GPJ WLA9-8-06.GDT 11/09/07

Project Name and Job Number		SOIL LOG - Boring No. B1
La Conchita SSP 1885	WLA William Lettis & Associates, Inc.	

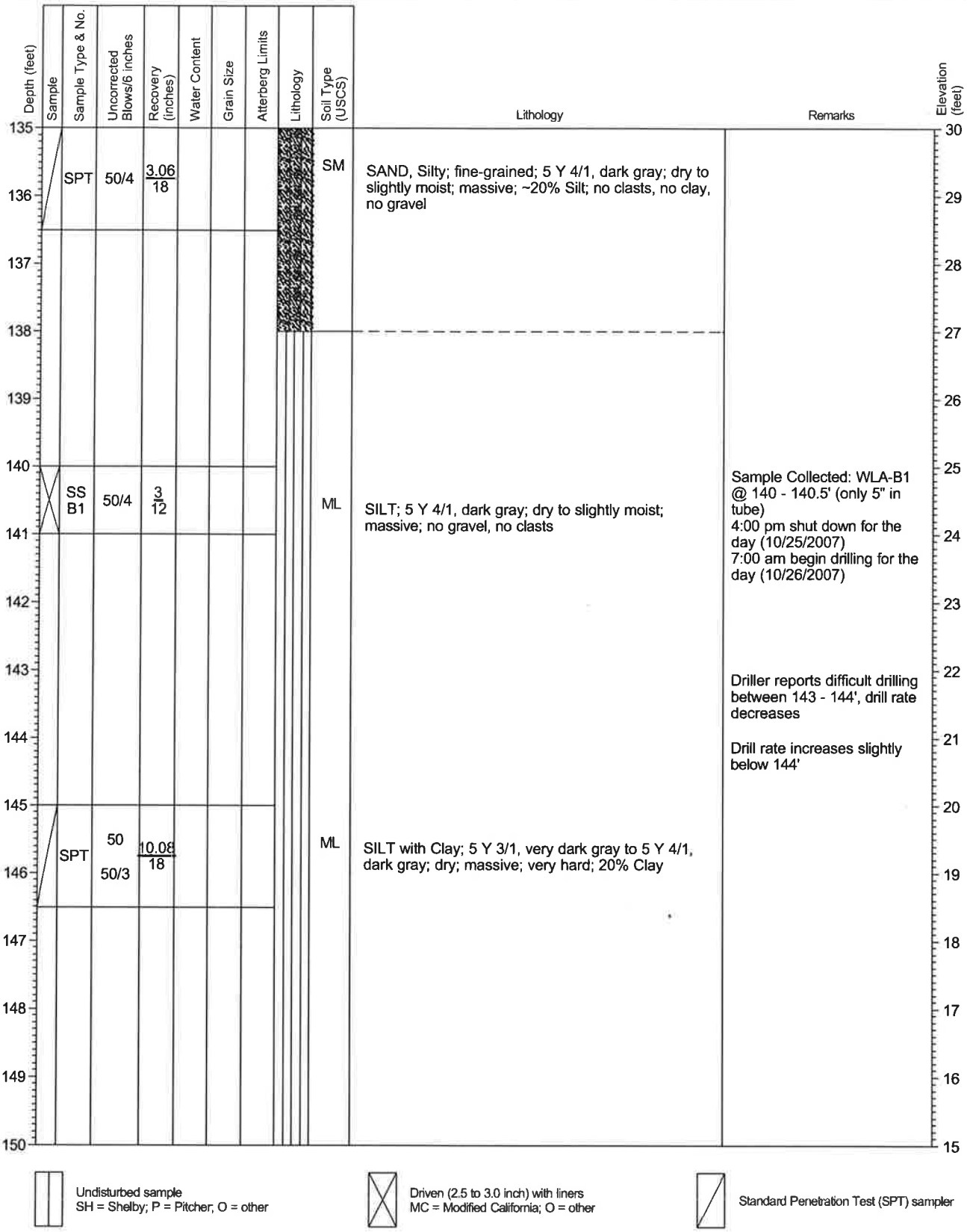

Undisturbed sample
SH = Shelby; P = Pitcher; O = other

Driven (2.5 to 3.0 inch) with liners
MC = Modified California; O = other

Standard Penetration Test (SPT) sampler

SOIL LOG LACONCHITA_110207.GPJ WLA9-8-06.GDT 11/09/07

Project Name and Job Number
La Conchita SSP
1885

William Lettis & Associates, Inc.

SOIL LOG - Boring No. B1

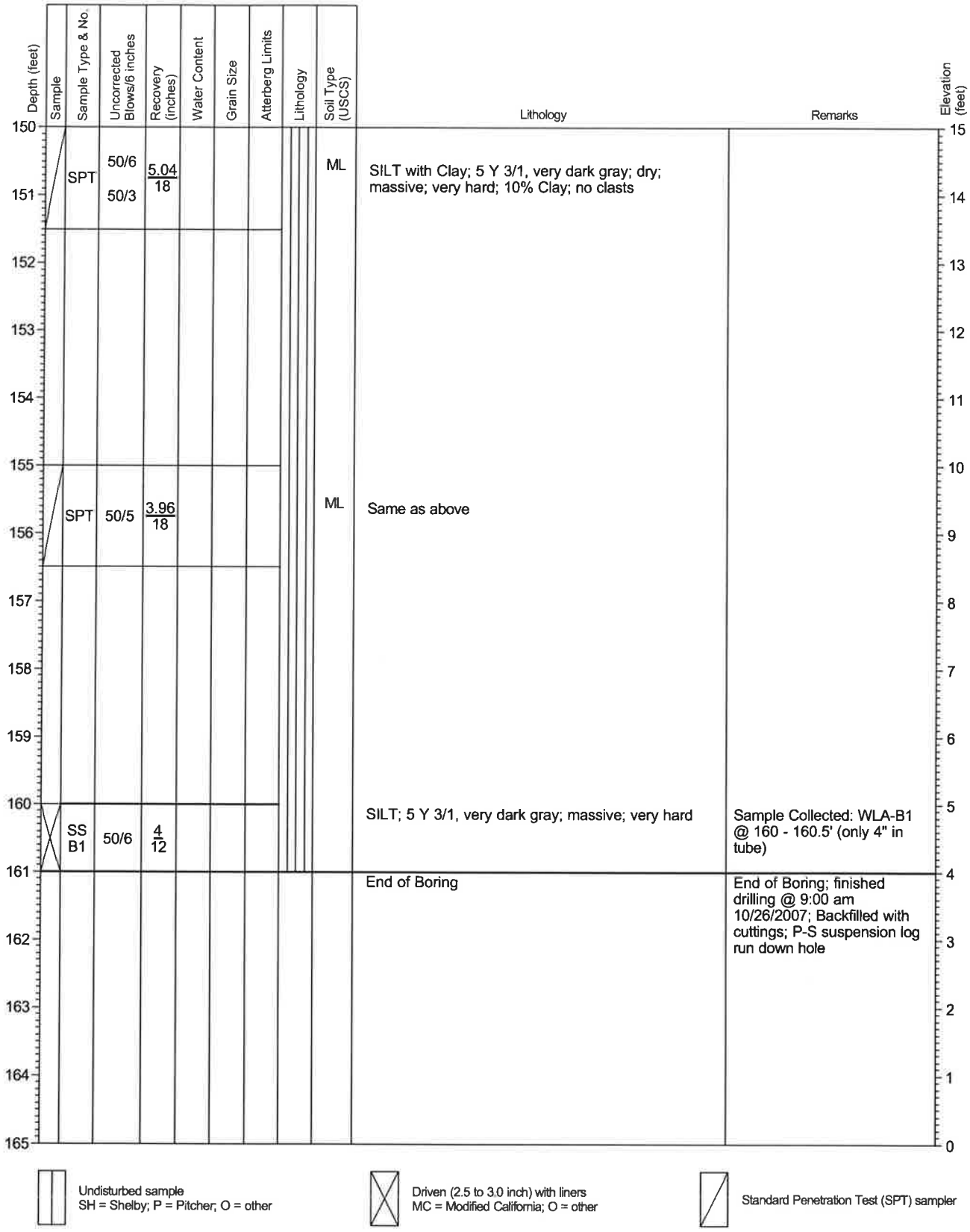

Undisturbed sample
SH = Shelby; P = Pitcher; O = other

Driven (2.5 to 3.0 inch) with liners
MC = Modified California; O = other

Standard Penetration Test (SPT) sampler

Log of Boring WLA BA-2

Project name: State of California, La Conchita Hillside Stabilization	Type & diameter of boring: 1885	Elevation at top of hole: 46 feet	Total depth: 36.5 feet
Type & diameter of boring: 24-inch Diameter Bucket Auger		Groundwater depth: 36-feet	Date started/completed: 10/8/07 - 10/9/07
Sampling method: Downhole Logging, Modified California sampler, 2.5-inch diameter		Sample driving hammer and drop: 1407 lb./36-inch	
Drilling contractor and rig: TriValley Drilling - Earthdrill 42 LHD		Logged by: C. Hitchcock	

Boring location diagram:

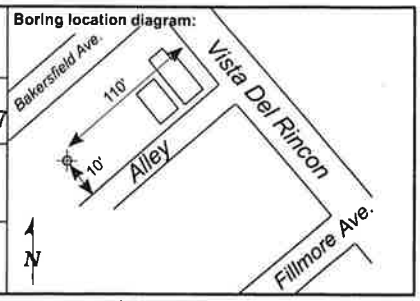

N 34.36447° W119.4476°

Depth (feet)	Description	Remarks
0	Cased to 3-feet, loose gravel with silt. (GW) (FILL)	Start drilling at 1:54 p.m. at 10/8/07, cased to 3-feet
4	GRAVEL, with SILT (GW), yellow brown to orange brown, dry, 50%/50% fine-grained sandstone and siltstone subangular clasts, poorly sorted, moderately dense (DEBRIS FLOW DEPOSITS)	
5	GRAVEL, with SILT (GW), dark brown, moderately dense, poorly sorted, grades upward to clast-rich, siltstone clasts (DEBRIS FLOW DEPOSITS)	Vertical lines denote possible soil horizon At 5-feet PP=4.5 ≠ST
6	SILT, grades to gravely (ML), light brown, dry, 15% subangular gravel with siltstone clasts to 3/4-inch, minor horizontal clay seams (DEBRIS FLOW DEPOSITS)	
8	CLAY, with gravel (CL), brown, dry, stiff, 10% subangular gravel with subangular clasts of siltstone grades to 1/2-inch diameter grades to	Change in soil color in cuttings at 7-feet
10	GRAVEL, with SILT (GW), brown, dry, moderately dense with poorly sorted angular siltstone clasts to 5-inch diameter (DEBRIS FLOW DEPOSITS)	At 10-feet PP=3.5 ST=3.5
12	CLAY (CL), sandy, brown, dry, stiff, minor (<3%) clasts of subangular siltstone (DEBRIS FLOW DEPOSITS)	A-horizon @ 12-feet, 13.5-feet
14	CLAY (CL), dark brown, dry, stiff (DEBRIS FLOW DEPOSITS (A-Horizontal)	Sample BA1-1, detrital charcoal at 15-feet, top of Paleosol
15		

PP = Pocket Penetrometer (in tsf) ST = Shear Torvane (in kg/cm²)

☒ Driven (2.5-inch) with liners, (MC)=Modified California ⊗ Radiocarbon sample

Log of Boring WLA BA-2

Project	Job No.	Logged by
State of California La Conchita Hillside Stabilization	1885	C. Hitchcock

Depth (feet)	Sample	Blows/foot Drive/Recovery No. Rings	Description	Remarks
15			grades to GRAVEL, with SILT (GW), yellowish brown, poorly sorted, subangular siltstone clasts to 4-inch diameter. (DEBRIS FLOW DEPOSITS)	At 15' PP=3 ST=4
16				
17			CLAY (CL), dark brown, dry, massive.	
			grades to	
18			SILT (ML) light brown, dry, <5% subangular siltstone clasts to 1/2-inch diameter.	
19			grades to	
20			SILT, gravelly (ML), brown dry, siltstone clasts to 2-inch diameter.	
			SILT (ML) to CLAY (CL), light brown, dry, stiff, interbedded with fine gravel containing siltstone clasts. (<5%)	Sample BA1-2 charcoal at 20.5-feet in thin layer below contact, top of Paleosol
21				
22			grades to GRAVEL with SILT (GW-GM), yellowish brown, dry, minor calcite, clasts subangular to 3-inches. (DEBRIS ≠ FLOW DEPOSITS)	At 20-feet PP=30 ST=4
23			CLAY (CL), dark brown, dry, stiff, <5% siltstone clasts to 1/2-inch diameter, subangular,	
24			grades to SILT (ML), light brown, dry, massive, stiff, with <5% subangular siltstone clasts <1/4-inch diameter. (DEBRIS FLOW DEPOSITS)	At 23.1-feet, thin paleosol <1/2-inch thick clay layer, subhorizontal
25				At 25-feet PP=2.5 ST=2
26	P +1	9	GRAVEL with SILT (GW-GM), light brown to gray brown, dry, medium dense to loose, poorly sorted, angular clasts of siltstone in chaotic structure to 3-inch diameter.	Sample at 26-feet push +1 Sample: BA2-S1
27				
28			grades to	
29			GRAVELY SILT (ML), light brown to gray brown, dry, >60% siltstone clasts to 5-inch diameter (DEBRIS FLOW DEPOSITS)	
30			SILT (ML), light brown, dry, minor laminar siltstone clasts to 1-inch diameter, subangular, minor carbonate modules (DEBRIS FLOW DEPOSITS) Basal contact is subhorizontal, sharp, appears erosional.	
31				Stop@30-feet @ 3:35 p.m.
32			SAND (SW), light brown, dry, loose, well sorted medium to fine-grained sand with rounded grains, 60-70% quartz, minor (<5%) subrounded o rounded pebbles to 0.5-inch diameter (BEACH SAND/MARINE TERRACE DEPOSITS)	At 30-feet PP=3.5 ST=3
33				Sand at 32-feet, dry
34			10-year 5/3 (brown), non plastic, no dry strength, well-graded SAND (SW), very soft, very sparse shells, <1% opaque minerals	
35				

PP = Pocket Penetrometer (in tsf) ST = Shear Torvane (in kg/cm²)

⊠ Driven (2.5-inch) with liners, (MC)=Modified California ⊗ Radiocarbon sample

Log of Boring WLA BA-2

Project	Job No.	Logged by
State of California La Conchita Hillside Stabilization	1885	C. Hitchcock

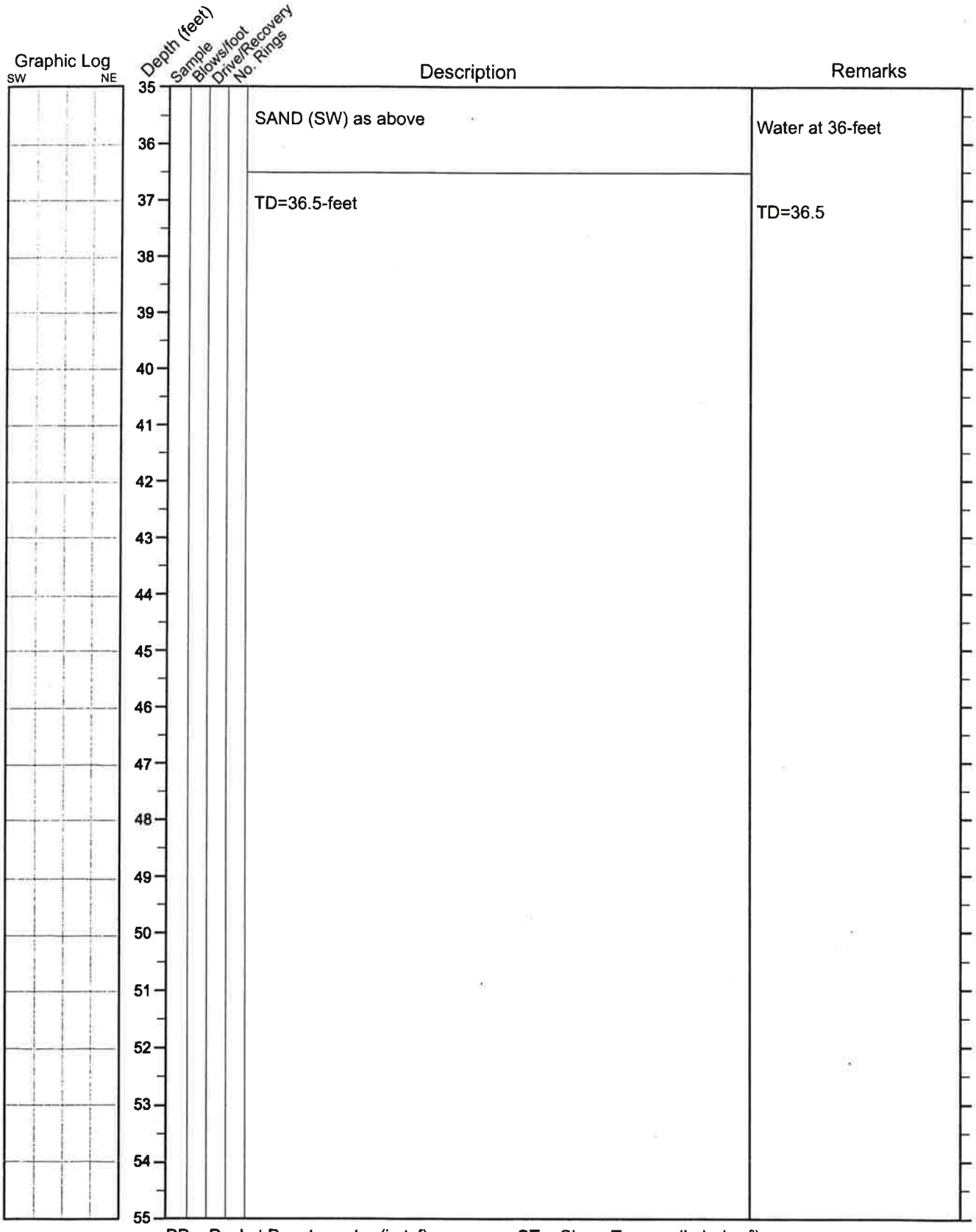

PP = Pocket Penetrometer (in tsf) ST = Shear Torvane (in kg/cm²)

☒ Driven (2.5-inch) with liners, (MC)=Modified California ⊗ Radiocarbon sample

Log of Boring WLA BA-3

Project name: State of California La Conchita Hillside Stabilization	Type & diameter of boring: 1885	Elevation at top of hole: 142 feet	Total depth: 30 feet	Boring location diagram:
Type & diameter of boring: 24-inch Diameter Bucket Auger		Groundwater depth: NA	Date started/completed: 10/9/07	
Sampling method: Downhole Logging, Modified California sampler, 2.5-inch diameter		Sample driving hammer and drop: 1407 lb./36-inch		
Drilling contractor and rig: TriValley Drilling - Earthdrill 42 LHD		Logged by: C. Hitchcock		

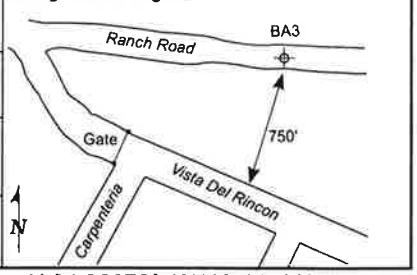

N 34.36678° W119.44820°

Graphic Log (SW–NE)	Depth (feet)	Sample	Blows/foot	Drive/Recovery	No. Rings	Description	Remarks
	0						Start @ 11:54 A.M.
	1					Blocks of CLAY (CL), gravelly, dry, in SILT (ML), with siltstone clasts to 40%	
	2						
	3					(ROAD FILL)	
	4						
	5						At 5-feet PP=2 ST=1.5 at 5-feet push sample BA3-S1
	6	P	18	18	9	SILT (ML), olive to dark gray, damp, decomposed siltstone fragments, subangular to 2-inch diameter up to 20%, abundant gypsum (DEBRIS FLOW DEPOSITS)	
	7						Roots @ 6-feet
	8						
	9						Bulk sample @ 9-feet
	10						At 10-feet PP=3 TS=4 At 10-feet push sample BA3-S2a rings BA3-S2b rings bulk sample @ 12 feet
	11	P	18	18	9	Grades to <5% siltstone clasts.	
	12						
	13						
	14						At 15-feet push sample BA3-S3
	15						

PP = Pocket Penetrometer (in tsf) ST = Shear Torvane (in kg/cm²)

Driven (2.5-inch) with liners, (MC)=Modified California

Log of Boring WLA BA-3

Project	Job No	Logged by
State of California La Conchita Hillside Stabilization	1885	C. Hitchcock

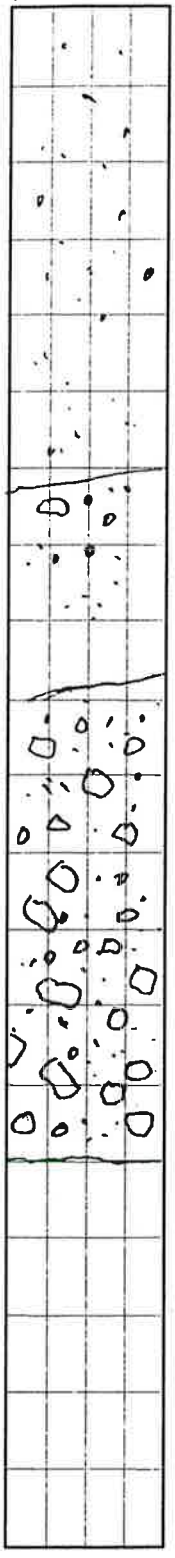

Depth (feet)	Sample	Blows/foot Drive/Recovery No. Rings	Description	Remarks
15			SILT (ML), olive gray, dry, stiff to soft; massive with siltstone, weathered, subangular to 2-inch diameter clasts	At 15-feet PP=1.5 TS=4.5
16				
17			grades to	
18			CLAY, with sand (CL), dark gray, damp, contains 20 percent siltstone clasts to 2-inch with average 3/4-inch, subangular (DEBRIS FLOW DEPOSITS)	
19				
20	P	8 18 9		At 20-feet PP=1 ST=3 sample @ 20-feet BA3-4 fat clay @ 21-feet
21			Sharp contact, dips SW.	
22			CLAY (CL), dark brown, damp, moderately stiff, approximately 30% subangular sandstone (Monterey Fm?) clasts to 5-inch diameter, gypsum stringers and crystals (DEBRIS FLOW DEPOSITS)	
23				
24			Abrupt, SW dipping contact	Change @ 24-feet to clayey, with gravel colluvium? clasts of Monterey formation
25				At 25-feet PP=3 ST=3 increased sandstone clasts @ 28-feet
26				
27			FAT CLAY with GRAVEL (CH), brown to grayish brown, mottled, damp, approximately 30% angular, decomposed clasts of fine-grained sandstone and shale, gypsum stringers and nodules. (COLLUVIUM/LANDSLIDE DEPOSITS)	
28				
29				
30			TD=30 feet	TD=30-feet @ 1:30 p.m.
31				
32				
33				
34				
35				

PP = Pocket Penetrometer (in tsf) ST = Shear Torvane (in kg/cm²)

⊠ Driven (2.5-inch) with liners, (MC)=Modified California

Log of Boring WLA BA-4

Project name: State of California La Conchita Hillside Stabilization	Type & diameter of boring: 1885	Elevation at top of hole: 120 feet	Total depth: 100 feet	Boring location diagram:
Type & diameter of boring: 24-inch Diameter Bucket Auger		Groundwater depth: NA	Date started/completed: 10/9/07-10/10/07	
Sampling method: Downhole Logging		Sample driving hammer and drop: 1407 lb./36-inch		
Drilling contractor and rig: TriValley Drilling - Earthdrill 42 LHD		Logged by: C. Hitchcock		

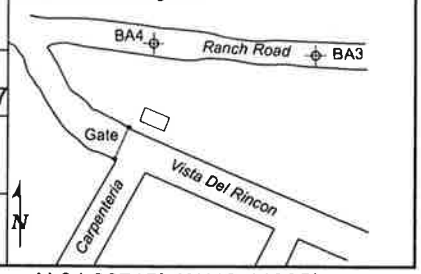

N 34.36715° W119.44895°

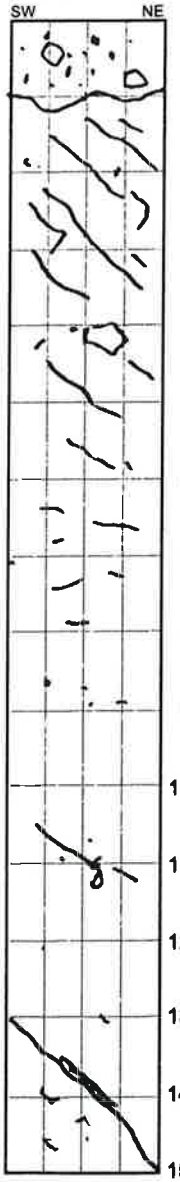

Depth (feet)	Description	Remarks
0	Cased to 2-feet, loose sand and clay with blocks of siltstone (ROAD FILL)	Start drilling at 3:25 p.m.
1	SILTSTONE, gray, bedded to massive, with 3-inch beds dipping NNE (170/55°NE), hard	
2	(PICO FORMATION BEDROCK IN LANDSLIDE)	
3		
4		
5		
6	As above, grayish brown, brecciated, minor fractures	
7		
8	Abundant gypsum veins, subhorizontal to steeply dipping NE	
9		
10	Decreasing gypsum with depth	
11	Gypsum vein dips 30° NE	
12		
13		
14	CLAY to SAND layer to 1-inch thick, dips NE into slope (070/65°N) irregular contact (BEDDING CONTACT)	
15		

PP = Pocket Penetrometer (in tsf) ST = Shear Torvane (in kg/cm²)

Log of Boring WLA BA-4

Project	Job No.	Logged by
State of California La Conchita Hillside Stabilization	1885	C. Hitchcock

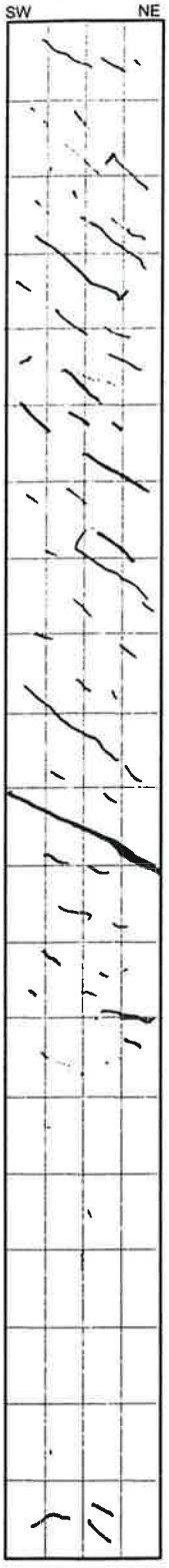

Depth (feet)	Description	Remarks
15	SILTSTONE, grayish brown, dry, very hard, massive with abundant gysum-filled fractures dipping northeast (PICO FORMATION BEDROCK IN LANDSLIDE)	
16		
17		
18		
19		
20		Siltstone fragments at 20-feet, bedrock (PICO FORMATION?)
21	Same as above, dark gray, dry	
22		
23		
24	Increased gypsum with depth in northeast-dipping fractures	
25		
26	Weathered NE-dipping fracture SILTSTONE, grayish brown, dry, hard, massive with minor fractures, minor gypsum (PICO FORMATION BEDROCK IN LANDSLIDE)	
27		
28		
29		
30	Decreasing fractures, gypsum with depth, massive	
31		
32		
33		
34	Minor fractures, no gypsum	
35		

Log of Boring WLA BA-4

Project	Job No.	Logged by
State of California La Conchita Hillside Stabilization	1885	C. Hitchcock

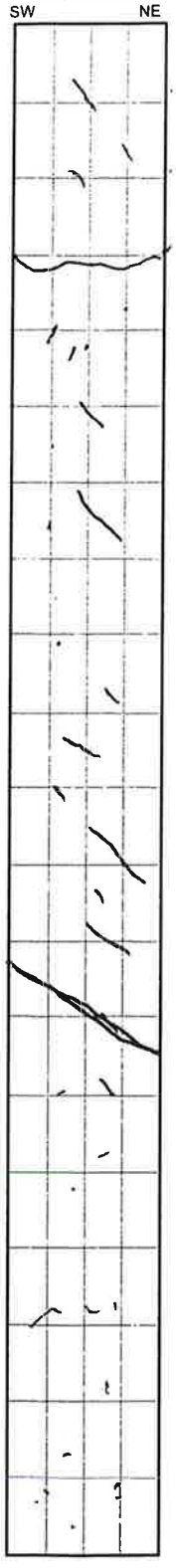

Depth (feet)	Description	Remarks
35	SILTSTONE, grayish brown, dry, very hard, massive, less than 1% gypsum to none, no fractures, increased weathering with depth to reddish brown	
36		
37	(PICO FORMATION BEDROCK IN LANDSLIDE)	
38	Irregular contact, no clay, subhorizontal, (bedding?)	
39	SILTSTONE, gray, dry, hard massive (PICO FORMATION BEDROCK)	
40		
41		
42		42-feet = shale @ 4:00 p.m.
43		
44		
45	As above, grayish brown, dry, hard, massive, minor subvertical fractures, no infilling	
46		
47		
48	Seepage @ 48.5-feet along 1-inch to variable thickness, siltstone seam/bedding contact, dips NNE (080/28° NNE)	
49		
50	SILTSTONE, gray, dry, hard, massive, minor subvertical fractures	
51		
52		
53	Increasing weathering with depth	
54		
55		

Log of Boring WLA BA-4

Project	Job No.	Logged by
State of California La Conchita Hillside Stabilization	1885	C. Hitchcock

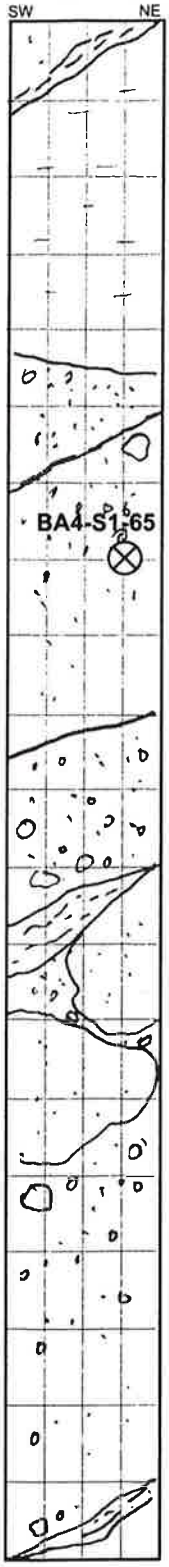

Depth (feet)	Description	Remarks
55	Clay seams in siltstone above SW dipping, approximately 2-inch diffuse sheared contact (OLD LANDSLIDE PLANE?)	Start drilling @ 7:00 a.m. 10/10/07 change to dark gray shale @ 55 to 56-feet PP > 4.5 @ 56-feet
56		
57	CLAY (CL), dark gray, dry very stiff, massive	
58	grades to	
59	GRAVELY LEAN CLAY (CL), dark gray, dry, stiff, subangular siltstone clasts to 1-inch diameter (LANDSLIDE PLANE)	
60	Thin (1-inch) gravelly clay layer, black, dry, with abundant charcoal (BURN layer?), dips 25-30° SW (downslope)	Dark gray siltstone increasing clay upwards landslide/ bedrock transition charcoal sample BA4-S1-65 for blue gray clay with gravel PP=4 @ 62-feet
61		
62	grades to	
63	LEAN CLAY WITH GRAVEL (CL), dark gray, dry, siltstone and sandstone clasts (10%) grades to SILT, (ML), light brown, dry, minor (<5%), sandstone, and siltstone clasts to 1/4-inch diameter	
64		
65	GRAVELY LEAN CLAY, GRAY, dry, hard sandstone, siltstone angular to 5-inch chaotic (DEBRIS FLOW DEPOSITS)	
66	abrupt, sharp SW-dipping (25°) contact base of debris flow, cuts 3-inch clay seam with gravel dipping 30° to SW on sandstone (LANDSLIDE PLANE?)	Change @ 65-feet to brown clay (CL) with gravel, siltstone, sandstone clasts to 3-inch landslide?
67		
68	SANDSTONE, yellow to orange brown, dry, very fine grained, hard BLOCKS in clayey matrix with sandstone clasts to 2-inch diameter	At 67-feet, bright orange brown sandstone
69		
70	grades to	
71	SAND, clayey with gravel (SM), gravel to 40% includes up to 6-inch subangular sandstone, silt, and shaley poorly sorted in chaotic structure (LANDSLIDE/DEBRIS FLOW DEPOSITS)	Water on bucket on 60-feet
72		
73		
74		At 75-feet sand, clayey with gravel, loose brown
75		

Log of Boring WLA BA-4

Project	Job No.	Logged by
State of California La Conchita Hillside Stabilization	1885	C. Hitchcock

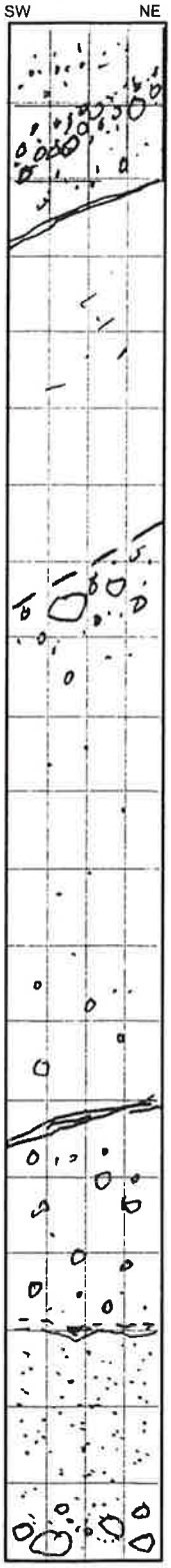

Depth (feet)	Description	Remarks
75	SAND, gravelly (SM) to CLAY, gravelly (CL), gray, dry, stiff, abundant subangular siltstone clasts and occasional sandstone to 1-inch diameter, 2-inch zone at 77-feet of thin sand, fine-grained, sheared, CLAY (CL), gray, dry, massive dips 25°SW	@ 76-feet clast-supported layer of siltstone clasts to 2-inch diameter
77	CLAY (CL), gray, dry, hard (COLLUVIUM/DEBRIS FLOW DEPOSITS)	
80	Contact dips 20° to SW, indistinct, gradational contact? WELL GRADED GRAVEL WITH CLAY (GW-GL), gray, dry, moderately hard, sandstone and siltstone clasts to 3-inch diameter, chaotic structure	Gray shale below approximately 78 to 80-feet
84	grades to	
85	CLAY (CL), gray, dry, massive, hard, no fractures, minor <5% siltstone clasts, subangular to 1/4-inch (DEBRIS FLOW DEPOSITS?)	85-feet at 8:51 a.m.
88	Contact is sharp with irregular laminated sheared clay 1-inch to 5-inch with brecciated gravel	
89	LEAN CLAY WITH GRAVEL (CL), grayish brown, dry, subangular siltstone clasts to 3-inch diameter in clay matrix (LANDSLIDE DEBRIS)	Contact dips 15° SW (base of debris flow deposits?)
92	Contact dips NNE at 15° SAND (SW), light brown, damp, non-plastic soft, medium-grained, rounded to subrounded grains of quartz (50%), mafic (20%), feldspar/siltstone chert (30%) (MARINE TERRACE SAND)	Sample clay at marine bottom on sand, sand at 92-feet Caving @ 93 to 94-feet clay in bucket at 94 to 95-feet
94	GRAVEL, sandy (GW), dark gray, wet, clayey to sandy matrix (coarse-sand) with rounded cobbles to 6-inch diameter (MARINE TERRACE DEPOSITS)	
95		

Log of Boring WLA BA-4

Project	Job No.	Logged by
State of California La Conchita Hillside Stabilization	1885	C. Hitchcock

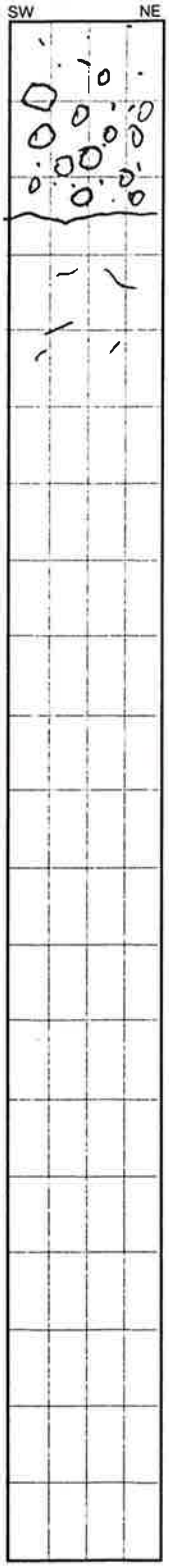

Depth (feet)	Description	Remarks
95		
96	SAND, with cobbles (SW), damp to wet, gray, rounded siltstone and shale cobbles to 6-inches (MARINE TERRACE)	Cobbles
97	(BASE OF MARINE TERRACE)	
98	SHALE, gray, dry, hard, laminar to massive (PICO FORMATION BED-ROCK)	Intact bedrock?
99		
100	TD=100-feet	
101		
102		
103		
104		
105		
106		
107		
108		
109		
110		
111		
112		
113		
114		
115		

Log of Boring WLA BA-5

Project name: State of California, La Conchita Hillside Stabilization	Type & diameter of boring: 1885	Elevation at top of hole: ~ 600-610	Total depth: 110'	Boring location diagram: 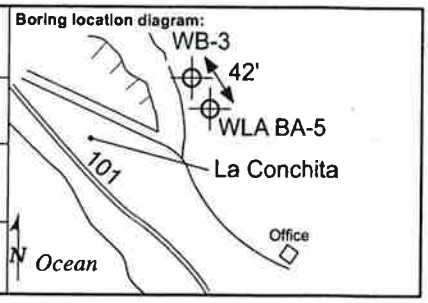
Type & diameter of boring: 24-inch Diameter Bucket Auger		Groundwater depth: NA	Date started/completed: 10/11/07	
Sampling method: Downhole Logging		Sample driving hammer and drop: 1407 lb./36-inch		
Drilling contractor and rig: TriValley Drilling - Earthdrill 42 LHD		Logged by: C. Hitchcock (Ross Hartleb and Pam Irvine present)		

N34.36547 W119.44320

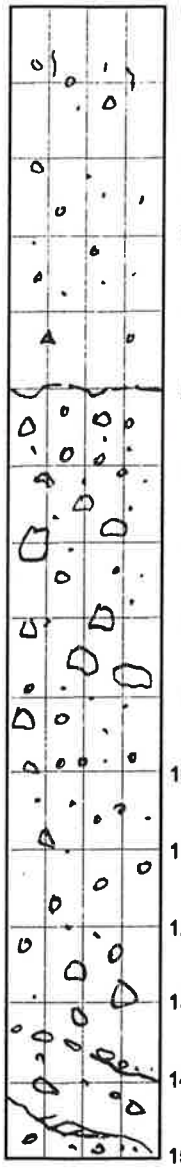

Depth (feet)	Description	Remarks
0	FAT CLAY (CH), black (2.5YR 2.5/1), damp, plastic, with occasional subangular siltstone clasts to 2-inch diameter (<3%) (SOIL; A-HORIZON)	Start drilling at 9:25am
5	Contact is gradational, subhorizontal WELL GRADED GRAVEL with CLAY (GW-GC), light yellowish brown (2.5Y 6/3), wet to damp, subangular Monterey Formation siltstone clasts to 5-inch diameter, 3-inch average diameter in clayey matrix (OLD DEBRIS FLOW DEPOSITS)	Contact @ 5-feet
10		Wet to 10-feet
13	At 14-feet, northeast-dipping bedding in laminar siltstone clast (150/30°NE)	Wet to 13-feet
15		Wet to 15-feet

PP = Pocket Penetrometer (in tsf) ST = Shear Torvane (in kg/cm²)

Log of Boring WLA BA-5

Project	Job No.	Logged by
State of California La Conchita Hillside Stabilization	1885	C. Hitchcock

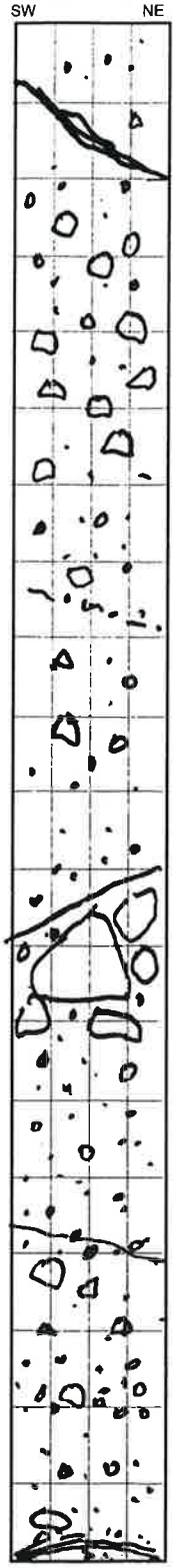

Depth (feet)	Description	Remarks
15	Same as above	Large siltstone clast to 1-foot, increasing silt matrix with depth
16		
17	CLAY, plastic, dark gray, 1 to 3-inch thick, northeast dipping with brecciated siltstone fragments above, minor seepage and manganese coatings on clasts (MINOR FAULT?)	Wet at 17-feet
18		
19	WELL GRADED GRAVEL with CLAY (GW-GL), brown to dark brown (10YR 4/3), damp, sticky, subangular Monterey Formation siltstone clasts to 8-inch diameter to clast supported (OLD DEBRIS FLOW DEPOSITS)	
20		Damp at 19-feet
21		Wet, saturated at 22-feet
22		
23	Bedding dips 25° northeast Fines downward to 2 to 4-inch diameter, average 1/4-inch gravel with clayey to sandy matrix, dark yellowish brown (10YR 4/6), damp and sticky (OLD DEBRIS FLOW DEPOSITS)	
24		
25	Abrupt contact, clayey with brecciated (<1/8-inch) siltstone fragments, dips southwest (130/35°SW) (POSSIBLE SLIDE PLANE?)	Saturated at 25-feet
26		
27	WELL GRADED GRAVEL WITH CLAY (GW-GL), dark yellowish brown (10YR 4/6), damp, sticky clay matrix, Monterey Formation siltstone clasts to 2-feet diameter, fines downward, subangular to angular clasts (OLD DEBRIS FLOW DEPOSITS)	Damp at 27-feet Silty with gravel, hard drilling
28		
29		
30	Depositional, gradational contact dips approximately 20° to northeast	
31		
32		Slightly damp at 32-feet
33	Same as above, WELL GRADED GRAVEL WITH CLAY (GW-GL)	Dry to damp at 35-feet
34	At 35-feet contact, abrupt, south-dipping (20°), FAT CLAY to 1-inch with 2-inch zone of brecciated rock (siltstone) fragments above (LANDSLIDE PLANE)	
35		

PP = Pocket Penetrometer (in tsf) ST = Shear Torvane (in kg/cm²)

Log of Boring WLA BA-5

Project	Job No.	Logged by
State of California La Conchita Hillside Stabilization	1885	C. Hitchcock

Depth (feet)	Description	Remarks
35	WELL GRADED GRAVEL WITH SILT (GW-GM), dark yellowish brown (10YR 4/4), dry, angular siltstone clasts (Monterey Formation) to 3-inch diameter (OLD DEBRIS FLOW DEPOSITS)	35-feet at 10:03 a.m.
36	North-dipping (15° to 20°) clayey zone to 1-inch thick, increasing clayey matrix, dark yellowish brown (10YR 3/4)	
37		
38	As above, WELL GRADED GRAVEL WITH SILT (GW-GM)	
39	Gradational, depositional contact, northeast dipping (130/25 NE)	
	(BASE OF DEBRIS FLOW DEPOSITS/ABRASION PLATFORM?)	
40	As above, gravel with SILT (GW-GM)	
41	SILTSTONE, bedded (2 to 3-inch thick beds), dips northeast (125/45°NE)	Finer at 40-feet, dry to damp
42	(MONTEREY FORMATION BEDROCK)	
43	Contact, south-dipping (35°), 1-inch thick, whitish gray, silty matrix with brecciated blocks of Monterey Formation to 2-feet in rock fragment matrix below (LANDSLIDE PLANE)	Sandier with whitish, clay, fine at 43-feet
44		At 45-feet, subrounded cobbles/clasts to 4-inch, siliceous Monterey Formation
45	WELL GRADED GRAVEL WITH SILT (GW-GM), yellowish brown (10YR 5/4), dry, fines downward to 1-inch subangular siltstone clasts from 1-2 feet diameter at top (OLD DEBRIS FLOW DEPOSITS)	
46		
47		At 47-feet, intact fragments of Monterey Formation, ground up/ sandy
48	Contact, silt layer (bedding?), dips south 15-20°, depositional	At 48-feet damp
49	Well graded gravel (GW-GM), as above, dry, hard, subangular clasts to 2-inch diameter	At 49.5-feet hard, blocks of Monterey Formation siltstone to 1-foot white clay coating
50	SILT, with gravel (ML), whitish gray, dry, to 2-inch thick, dips east (150/27°E), possible ash layer?	
51	Southwest dipping contact, abrupt	
52	SILTSTONE clast, bedded (050/37°E)	
53	(BEDROCK CLAST IN LANDSLIDE DEPOSITS)	
54		
55		

PP = Pocket Penetrometer (in tsf) ST = Shear Torvane (in kg/cm²)

Log of Boring WLA BA-5

Project	Job No.	Logged by
State of California La Conchita Hillside Stabilization	1885	C. Hitchcock

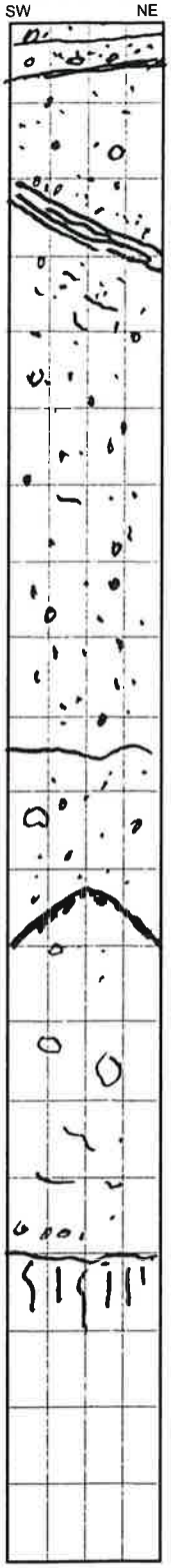

Depth (feet)	Description	Remarks
55	Whitish GRAVEL (GW-GM) with clay, subangular siltstone clasts to 1/4-inch diameter	Monterey Formation clasts ground up to 6-inches, average 1 to 2-inches
56	WELL GRADED GRAVEL (GW), as above	
57	CONTACT, dips east (000/20°E), clay to 3-inch with brecciated rock fragments above	Damp at 57-feet Clayey, fine grained at 58 to 59-feet 10:35 a.m.
58	WELL-GRADED GRAVEL WITH SILT (GW-GM), dark yellowish brown (10YR 4/4), dry, angular siltstone clasts, minor clay seams (DEBRIS FLOW DEPOSITS)	
59		Sand, drier at 61-feet
60		
61	WELL-GRADED GRAVEL WITH SILT (GW-GM), as above	
62		
63		
64	Contact, abrupt, erosional	
65		
66	WELL-GRADED GRAVEL WITH SILT (GW-GM), as above	
67	Layer of whitish gray siltstone clasts dipping south	
68		
69	SILT (ML) to SILTSTONE, massive clasts/boulders, clast supported, abundant gypsum (OLD DEBRIS FLOW DEPOSITS)	
70		
71	FAT CLAY (CL), very dark gray (7.5YR 3/1), grades to clayey silt with minor sand (ML), (PALEOSOL, BURIED SOIL)	At 71.5 FAT CLAY WITH GRAVEL, MOTTLED 11:08 a.m. "paleosol?" photograph minor calcite squeezing on bucket at 73 to 74-feet, gray at 74-feet
72		
73		
74		
75		

PP = Pocket Penetrometer (in tsf) ST = Shear Torvane (in kg/cm²)

Log of Boring WLA BA-5

Project	Job No.	Logged by
State of California La Conchita Hillside Stabilization	1885	C. Hitchcock

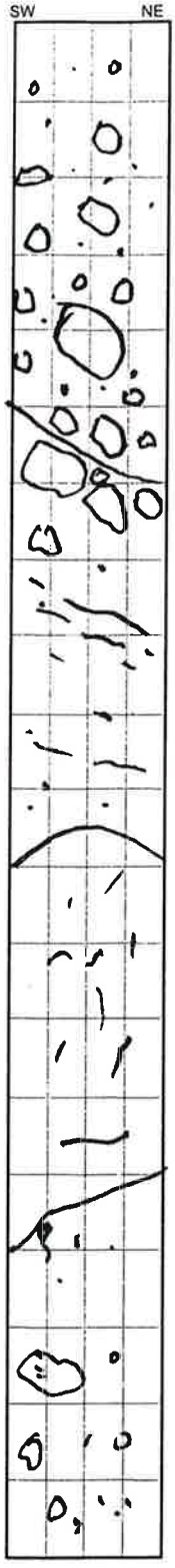

Depth (feet)	Description	Remarks
75	CLAY (CL) to SILT(ML), dark grayish brown (2.5YR 4/2), with subangular to angular Monterey Formation clasts of siltsone, increasing percentage with depth to 3/4-inch average, up to 2-feet diameter (DEBRIS FLOW/LANDSLIDE DEPOSITS)	
76		
77		CLAY at 77-feet, with gravel, grayish white, damp
78		
79		
80		Hard at 81 to 82-feet Monterey Formation, hard, dry, clasts to 1-foot diameter
81	Contact, dips 40°NE, irregular, abrupt, depositional contact	
82		
83	SILT (ML), with gravel, light yellowish brown (2.5-yr 6/3), dry, abundant Monterey Formation clasts to 1-inch, subangular (LANDSLIDE DEBRIS)	
84		
85	Contact dips south, abrupt	
86	SILTSTONE, yellowish-brown (10YR 7/8), dry, hard, massive (BEDROCK IN LANDSLIDE?)	Orangish-brown at 86-feet
87		
88		
89	Fractured, massive	Orange at 89-feet
90		
91	Seepage at 91-feet in fracture within SILTSTONE, dips southwest	
92		
93		93-feet at 12:32 p.m.
94	Increasing gravel clast size with depth Grades to GRAVEL, with clay, dry	
95		

PP = Pocket Penetrometer (in tsf) ST = Shear Torvane (in kg/cm²)

Log of Boring WLA BA-5

Project	Job No.	Logged by
State of California La Conchita Hillside Stabilization	1885	C. Hitchcock

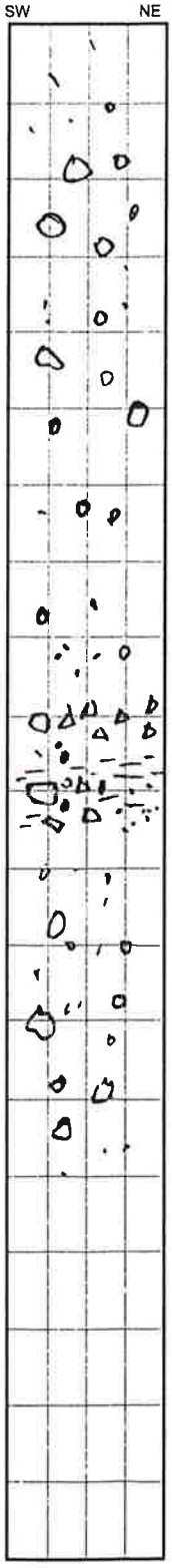

Depth (feet)	Description	Remarks
95	LEAN CLAY to SILT (CL-ML), with gravel, light yellowish brown (2.5-yr 6/4), dry, subangular Monterey Formation clasts to 2-inch diameter (DEBRIS FLOW/LANDSLIDE DEPOSITS)	
104	WELL-GRADED GRAVEL (GW), yellow brown, angular clasts of siltstone, wet	Water at 104-feet wet Monterey Formation angular clasts
105	WELL-GRADED GRAVEL WITH CLAY (GW-GL), dry (DEBRIS FLOW/LANDSLIDE DEPOSITS)	At 105-feet clayey gravel, blocky <1-foot thick zone of seepage/water
109		TD = 110 feet at 1:30 p.m. 10/11/2007
110	TD = 110 feet	
115		

PP = Pocket Penetrometer (in tsf) ST = Shear Torvane (in kg/cm²)

APPENDIX D: DOWNHOLE SHEAR WAVE VELOCITY PROFILES

GEOVision
geophysical services

FINAL REPORT

LA CONCHITA BORINGS WLA B-1 AND WLA B-2 SUSPENSION P & S VELOCITIES

Report 7506-01

November 26, 2007

FINAL REPORT

LA CONCHITA BORINGS WLA B-1 AND WLA B-2 SUSPENSION P & S VELOCITIES

Report 7506-01

November 26, 2007

Prepared for:

William Lettis & Associates
1777 Botelho Drive, Suite 262
Walnut Creek, CA 94596
(925) 256-6070

Prepared by

GEOVision Geophysical Services
1151 Pomona Road, Unit P
Corona, California 92882
(951) 549-1234

SOIL LOG LACONCHITA_110207.GPJ WLA9-8-06.GDT 11/09/07

Project Name and Job Number			
La Conchita SSP 1885	WLA William Lettis & Associates, Inc.	**SOIL LOG - Boring No. B2**	
Type and Diameter of Boring Mud rotary wash / 5	Boring Location 34.36490 N, 119.44290 W		Total Depth 151 feet
Drilling Contractor and Rig C&L Drilling	Elevation and Datum 605 feet	Ground Water Depth N/A	Depth to Bedrock N/A
Sampling Method SPT/Split Spoon	Sample Driving Hammer/Drop 140 / 18	No. of Samples 3	Date Started 10/22/07
	Borehole Inclination -90	Logged by R. Hartleb	Date Completed 10/23/07

Reviewed by / Date _____

Reviewed by / Date _____

Depth (feet)	Sample	Sample Type & No.	Uncorrected Blows/6 inches	Recovery (inches)	Water Content	Grain Size	Atterberg Limits	Lithology	Soil Type (USCS)	Lithology	Remarks	Elevation (feet)
0									CH	CLAY; very dark brown to 2.5 Y 2.5/1, black; moist to damp; plastic; sparse coarse Sand and Gravel clasts; clasts to 1" of Sandstone and Siltstone (Monterey Frm?)	Start of drilling 9:50 am	605
1											Fast, smooth, advancement	604
2										(SOIL; A HORIZON)		603
3												602
4												601
5		SPT	4 10 7	14.94/18					GC-GM	GRAVEL; 2.5 Y 6/3, light yellowish brown; moderately hard to hard fragments; angular to subangular Siltstone and Claystone breccias (Monterey Frm?) in variable matrix (Sand, Silt, Clay) (DEBRIS FLOW DEPOSITS - OLD)		600
6												599
7												598
8												597
9												596
10		SPT	7 6 7	14.04/18					GW-GC	GRAVEL; 10 YR 5/8, yellowish brown; angular to subangular Siltstone breccia (Monterey Frm), Silt and Clay matrix of parent material (DEBRIS FLOW DEPOSITS - OLD)		595
11												594
12												593
13									ML	SILT, Clayey; 10 YR 5/4, yellowish brown; damp; sticky; no clasts, chips, completely weathered Monterey Frm.		592
14												591
15												590

SOIL LOG LACONCHITA_110207.GPJ WLA9-8-06.GDT 11/09/07

Project Name and Job Number
La Conchita SSP
1885

WLA William Lettis & Associates, Inc.

SOIL LOG - Boring No. B2

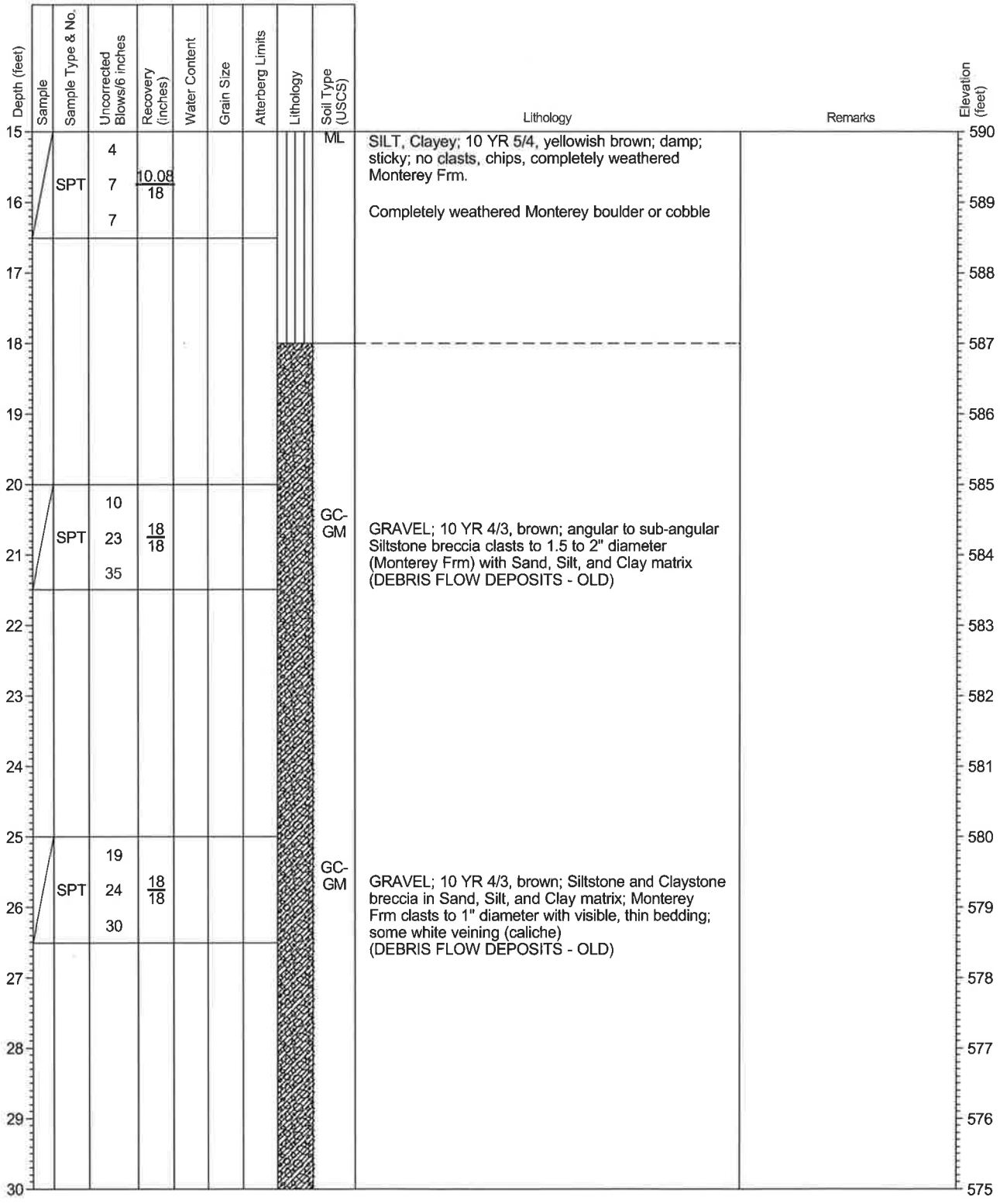

Undisturbed sample
SH = Shelby; P = Pitcher; O = other

Driven (2.5 to 3.0 inch) with liners
MC = Modified California; O = other

Standard Penetration Test (SPT) sampler

SOIL LOG LACONCHITA_110207.GPJ WLA9-8-06.GDT 11/09/07

Project Name and Job Number
La Conchita SSP
1885

WLA
William Lettis & Associates, Inc.

SOIL LOG - Boring No. B2

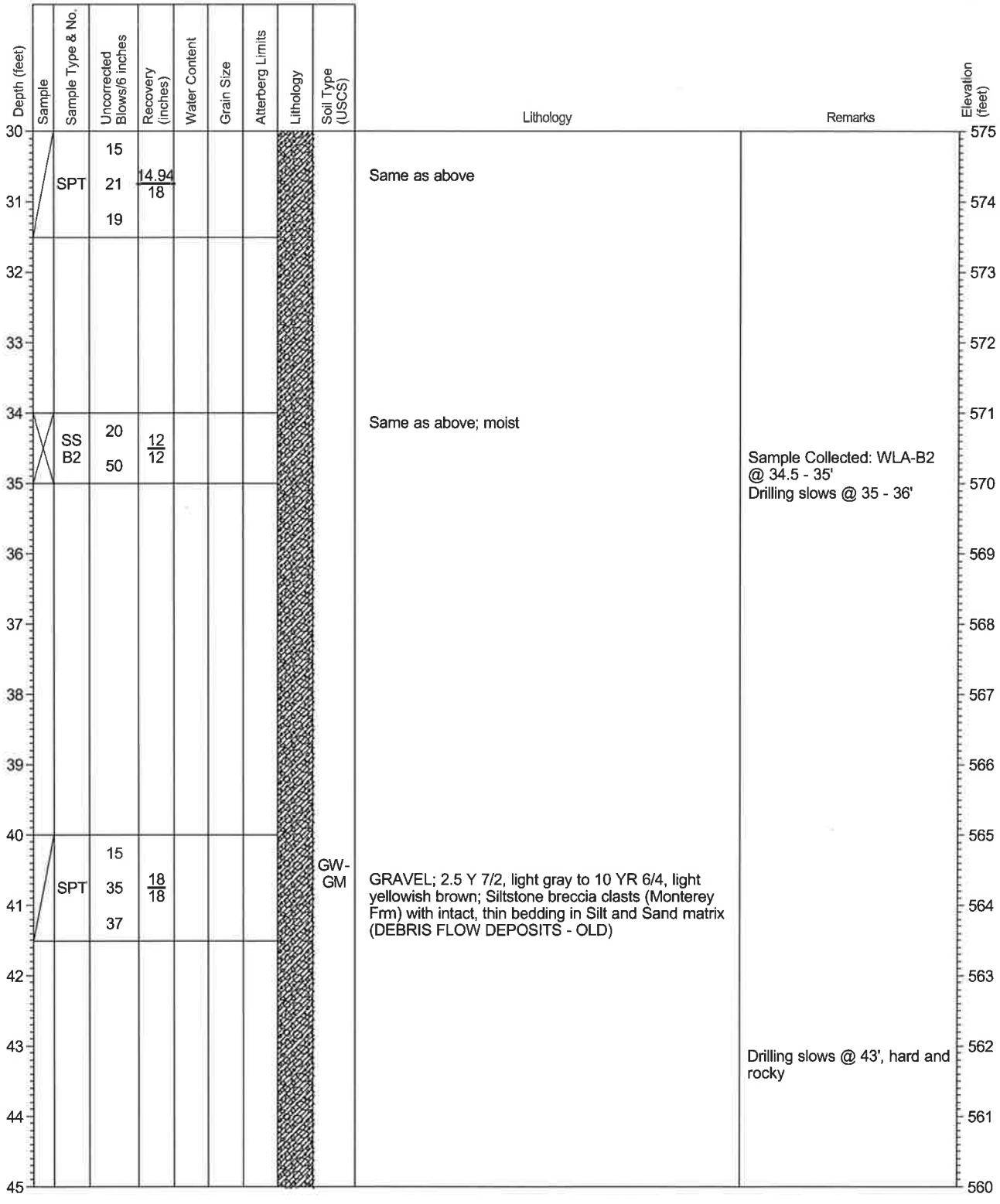

Undisturbed sample
SH = Shelby; P = Pitcher; O = other

Driven (2.5 to 3.0 inch) with liners
MC = Modified California; O = other

Standard Penetration Test (SPT) sampler

SOIL LOG LACONCHITA_110207.GPJ WLA9-8-06.GDT 11/09/07

Project Name and Job Number
La Conchita SSP
1885

William Lettis & Associates, Inc.

SOIL LOG - Boring No. B2

Depth (feet)	Sample	Sample Type & No.	Uncorrected Blows/6 inches	Recovery (inches)	Water Content	Grain Size	Atterberg Limits	Lithology	Soil Type (USCS)	Lithology	Remarks	Elevation (feet)
45											Drilling continues to be hard at 45'	560
46		SPT	27 50	9/18					GC-GM	GRAVEL; 10 YR 6/2, light brownish gray; Siltstone breccia clasts (Monterey Frm) in 10 YR 5/6, yellowish brown, Sand, Silt, Clay matrix; clasts to 1" diameter with fresh mechanical breaks (DEBRIS FLOW DEPOSITS - OLD)		559
47												558
48												557
49												556
50												555
51		SPT	40 50/5	9/18					GW-GM	GRAVEL; 10 YR 6/2, light brownish gray to 10 YR 5/4, yellowish brown; increase in Sand, decrease in Clay in matrix; siliceous angular fragments; thin (mm to < mm thick) laminae (DEBRIS FLOW DEPOSITS - OLD)		554
52												553
53												552
54												551
55												550
56		SPT	27 49 50/3	7.02/18					GC-GM	GRAVEL; 10 YR 6/4, light yellowish brown; Siltstone fragments in Clay, Silt, Sand matrix with an increase in Clay (DEBRIS FLOW DEPOSITS - OLD)		549
57												548
58												547
59												546
60												545

Undisturbed sample
SH = Shelby; P = Pitcher; O = other

Driven (2.5 to 3.0 inch) with liners
MC = Modified California; O = other

Standard Penetration Test (SPT) sampler

Project Name and Job Number
La Conchita SSP
1885

William Lettis & Associates, Inc.

SOIL LOG - Boring No. B2

Depth (feet)	Sample	Sample Type & No.	Uncorrected Blows/6 inches	Recovery (inches)	Water Content	Grain Size	Atterberg Limits	Lithology	Soil Type (USCS)	Lithology	Remarks	Elevation (feet)
60												545
61		SPT	50/5	3.06/18						Same as above		544
62												543
63												542
64											To speed drilling process, will switch to 10' intervals per conversation with C. Hitchcock. Driller will notify of any perceived changes in drilling rate	541
65												540
66											Driller reports slight increase in drill rate, "smoother" advancement	539
67											Drilling advancement slows, less "smooth", increased rig chatter	538
68												537
69												536
70		SS B2	80/5	5/12					GW-GM	GRAVEL; Siltstone and Claystone breccia; angular fragments to 1.5" diameter (DEBRIS FLOW DEPOSITS - OLD)	Sample Collected: WLA-B2 @ 70 - 70.5' Note: Sample advancement halted @ 6"	535
71												534
72												533
73												532
74												531
75												530

Undisturbed sample
SH = Shelby; P = Pitcher; O = other

Driven (2.5 to 3.0 inch) with liners
MC = Modified California; O = other

Standard Penetration Test (SPT) sampler

SOIL LOG LACONCHITA_110207.GPJ WLA9-8-06.GDT 11/09/07

Project Name and Job Number
La Conchita SSP
1885

William Lettis & Associates, Inc.

SOIL LOG - Boring No. B2

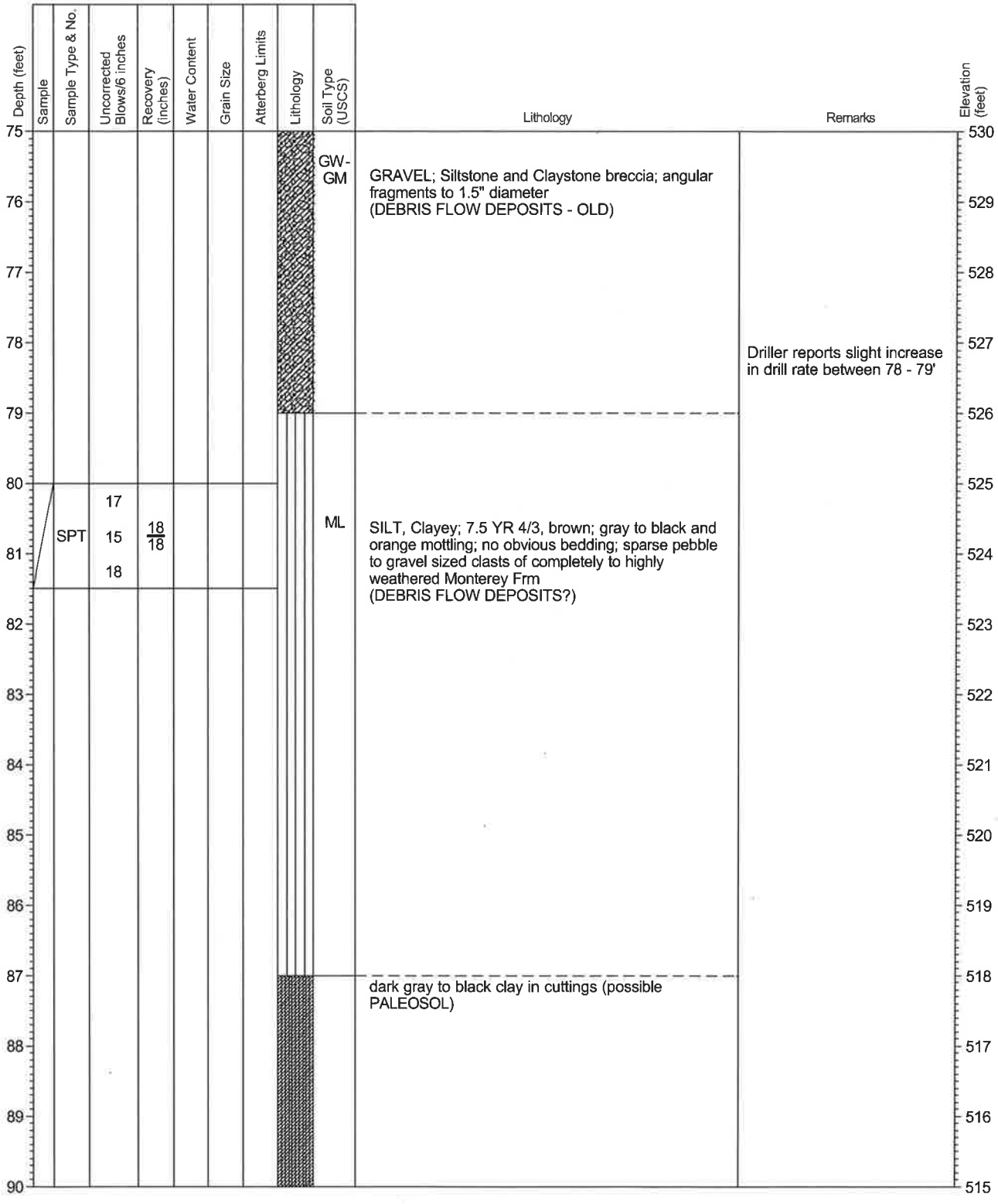

Undisturbed sample
SH = Shelby; P = Pitcher; O = other

Driven (2.5 to 3.0 inch) with liners
MC = Modified California; O = other

Standard Penetration Test (SPT) sampler

SOIL LOG LACONCHITA_110207.GPJ WLA9-8-06.GDT 11/09/07

Project Name and Job Number
La Conchita SSP
1885

William Lettis & Associates, Inc.

SOIL LOG - Boring No. B2

Depth (feet)	Sample	Sample Type & No.	Uncorrected Blows/6 inches	Recovery (inches)	Water Content	Grain Size	Atterberg Limits	Lithology	Soil Type (USCS)	Lithology	Remarks	Elevation (feet)
90											Smooth drilling	515
		SPT	10 13 16	18/18					CL-ML	SILT, Clayey to CLAY, Silty; 10 YR 8/1, white to 10 YR 6/1, gray; no obvious bedding; no clasts (LANDSLIDE DEPOSITS)		
91												514
92												513
93												512
94												511
95												510
96												509
97												508
98												507
99												506
100												505
		SPT	10 17 18	18/18					CL-ML	Same as above		
101												504
102												503
103											4:30 pm shut down for the day (10/22/2007) 7:30 am begin drilling for the day (10/23/2007) Smooth drilling to 105'	502
104												501
105												500

Undisturbed sample
SH = Shelby; P = Pitcher; O = other

Driven (2.5 to 3.0 inch) with liners
MC = Modified California; O = other

Standard Penetration Test (SPT) sampler

SOIL LOG LACONCHITA_110207.GPJ WLA9-8-06.GDT 11/09/07

Project Name and Job Number
La Conchita SSP
1885

William Lettis & Associates, Inc.

SOIL LOG - Boring No. B2

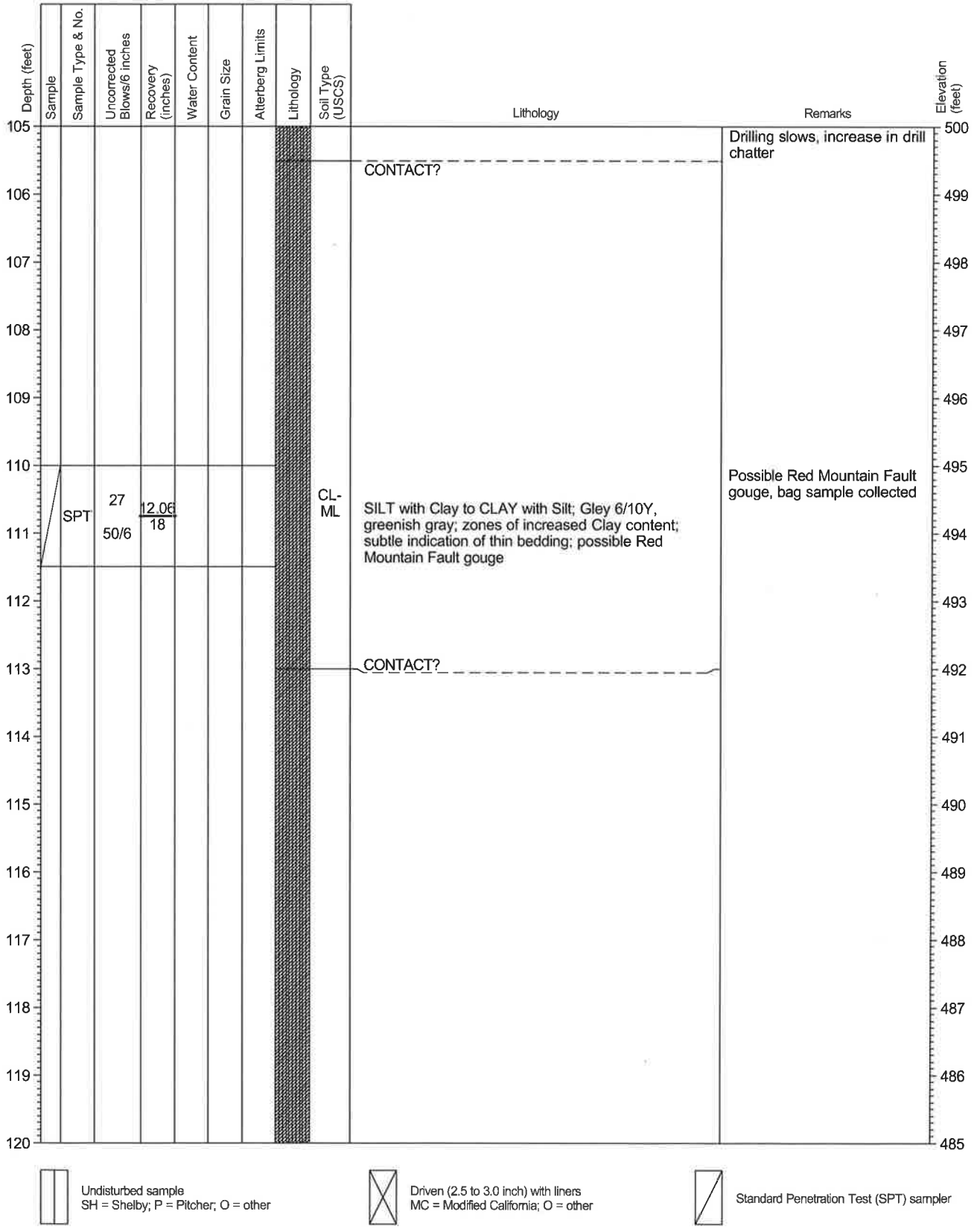

Undisturbed sample
SH = Shelby; P = Pitcher; O = other

Driven (2.5 to 3.0 inch) with liners
MC = Modified California; O = other

Standard Penetration Test (SPT) sampler

SOIL LOG LACONCHITA 110207.GPJ WLA9-8-06.GDT 11/09/07

Project Name and Job Number
La Conchita SSP
1885

WLA
William Lettis & Associates, Inc.

SOIL LOG - Boring No. B2

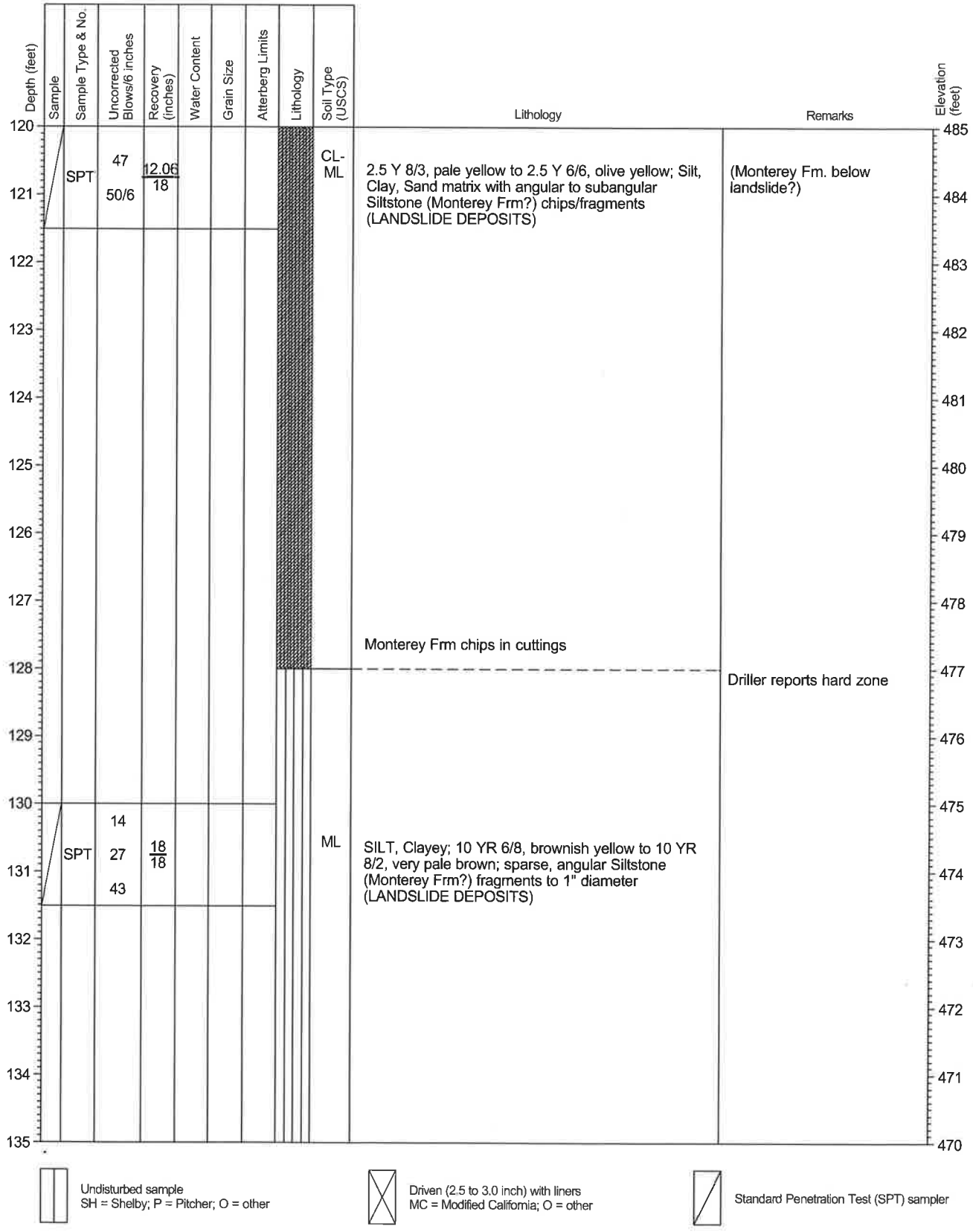

Undisturbed sample
SH = Shelby; P = Pitcher; O = other

Driven (2.5 to 3.0 inch) with liners
MC = Modified California; O = other

Standard Penetration Test (SPT) sampler

SOIL LOG LACONCHITA_110207.GPJ WLA9-8-06.GDT 11/09/07

Project Name and Job Number
La Conchita SSP
1885

WLA
William Lettis & Associates, Inc.

SOIL LOG - Boring No. B2

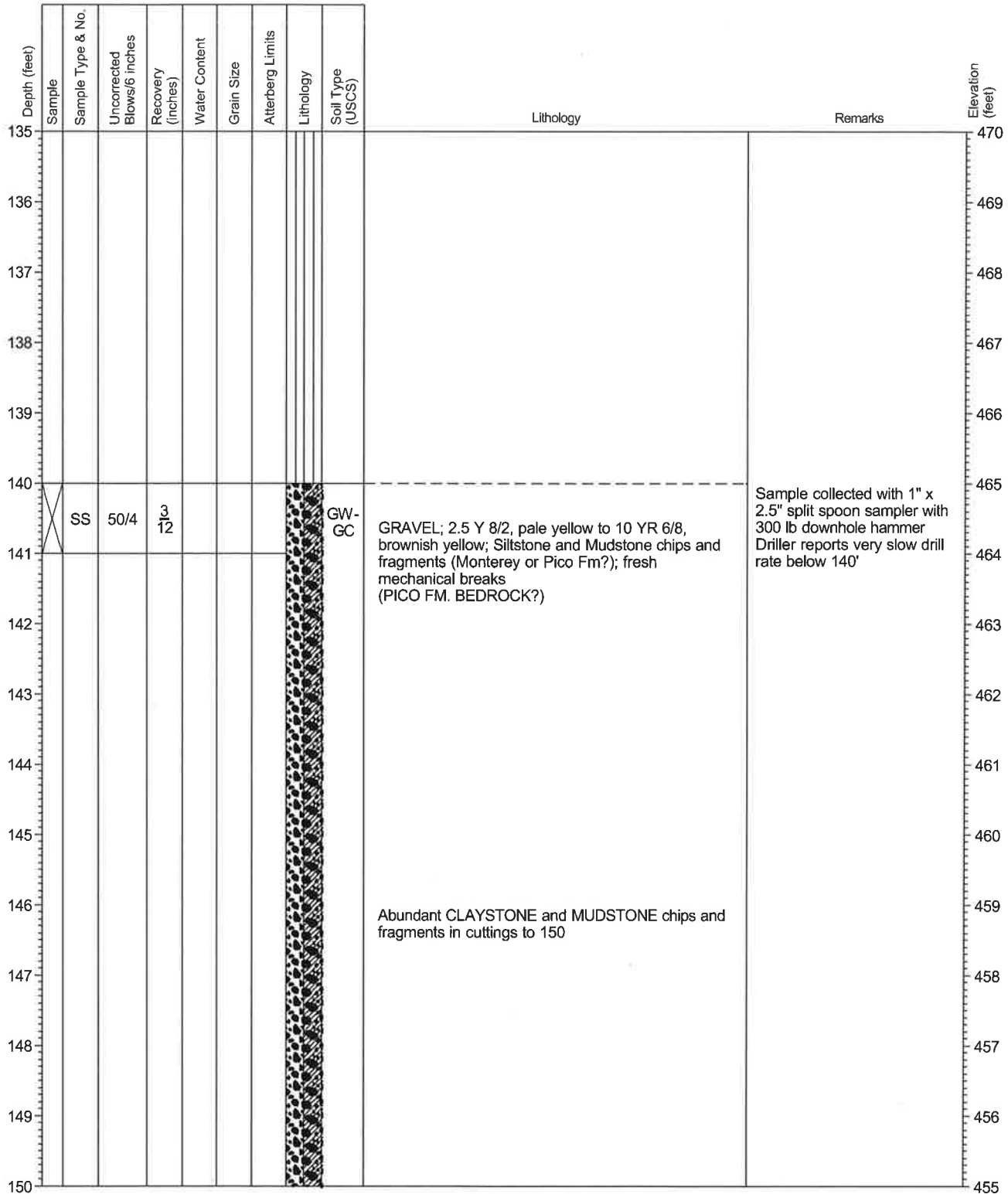

Undisturbed sample
SH = Shelby; P = Pitcher; O = other

Driven (2.5 to 3.0 inch) with liners
MC = Modified California; O = other

Standard Penetration Test (SPT) sampler

SOIL LOG LACONCHITA_110207.GPJ WLA9-8-06.GDT 11/09/07

Project Name and Job Number
La Conchita SSP
1885

William Lettis & Associates, Inc.

SOIL LOG - Boring No. B2

Depth (feet)	Sample	Sample Type & No.	Uncorrected Blows/6 inches	Recovery (inches)	Water Content	Grain Size	Atterberg Limits	Lithology	Soil Type (USCS)	Lithology	Remarks	Elevation (feet)
150		SS B2	50/6	6/12							Sample Collected: WLA-B2 @ 150.5 - 151' at 12: 45 pm	455
151											End of Boring; Backfilled with cuttings on 10/24/2007; P-S suspension log run down hole	454
152												453
153												452
154												451
155												450
156												449
157												448
158												447
159												446
160												445
161												444
162												443
163												442
164												441
165												440

Undisturbed sample
SH = Shelby; P = Pitcher; O = other

Driven (2.5 to 3.0 inch) with liners
MC = Modified California; O = other

Standard Penetration Test (SPT) sampler

Log of Boring WLA BA-1

Project name: State of California, La Conchita Hillside Stabilization	Type & diameter of boring: 1885	Elevation at top of hole: 71 feet	Total depth: 54 feet	Boring location diagram: 90-feet SE of Vista Del Rincon and Oxnard
Type & diameter of boring: 24-inch Diameter Bucket Auger		Groundwater depth: 39 feet	Date started/completed: 10/8/07	
Sampling method: Downhole logging		Sample driving hammer and drop: 1407 lb./36-inch		
Drilling contractor and rig: TriValley Drilling - Earthdrill 42 LHD		Logged by: C. Hitchcock		

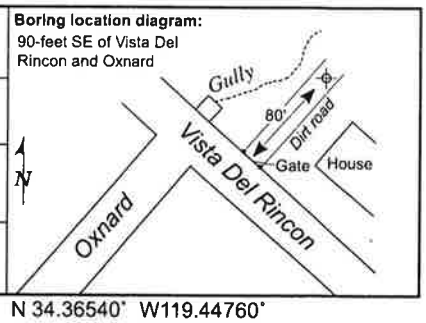

N 34.36540° W119.44760°

Depth (feet)	Description	Remarks
0	SILT to CLAY, with gravel (ML-CL), light to dark brown, dry, medium stiff, 20-30% subangular clasts to cobbles from 1-inch to 1-foot diameter, poorly sorted (DEBRIS FLOW DEPOSITS)	Start drilling @ 8:22 a.m. downhole @10:08 a.m. Hole cased to 3-feet
4	PP=3.0, ST=3.0	
5	SILT, with gravel (ML), light brown, dry, approximately 20% subangular mudstone clasts (Monterey Formation?) to 1-foot diameter; includes lenses of <0.1-inch diameter, clast supported, subangular gravel (DEBRIS FLOW DEPOSITS)	
8	Increasing gravel content with depth, includes <3% very fine-grained sandstone clasts to 2-inch diameter, denser with depth	
9	PP=3, ST=5	Monterey-Formation siltstone clasts to 1-foot diameter
10	LEAN CLAY with GRAVEL (CL), dark brown, dry, 10-20% subangular white mudstone clasts to 1-inch diameter (DEBRIS FLOW DEPOSITS WITH A-HORIZON DEVELOPMENT)	Possible buried soil
12	SILT, with gravel (ML-CL), grayish brown, dry, 10% angular to subangular mudstone and very fine grained sandstone with magnesium coating. (Monterey Formation? clasts) (DEBRIS FLOW DEPOSITS)	At approximately 13 feet; change to light brown sand clay
14	SILT, with sand (ML), yellow brown, dry, subangular clasts to 3-inch diameter of laminar mudstone	15-foot @8:37 a.m.
15		

PP = Pocket Penetrometer (in tsf) ST = Shear Torvane (in kg/cm²)

Log of Boring WLA BA-1

Project	Job No.	Logged by
State of California La Conchita Hillside Stabilization	1885	C. Hitchcock

Depth (feet)	Description	Remarks
15	PP=2.5, ST=4.5 SILT, with sand (ML), yellow brown to range brown, dry angular clasts to 3-inch diameter of banded, laminar mudstone (DEBRIS FLOW DEPOSITS)	
17		Irregular, sharp contact
18	SILT, with gravel (ML), grayish brown, dry, stiff, claystone clasts to 60%, subangular to 3-inch diameter, minor calcite veins (DEBRIS FLOW DEPOSITS)	
19		
20	PP=4.0 ST=3.5	Irregular, subhorizontal sharp contact (erosional?) @ 19.5-feet
21	GRAVELY SILT (ML), yellowish brown, dry, stiff, subangular clasts of yellow brown mudstone to 1-foot diameter forms 40-60% of deposit, coarsens upward (DEBRIS FLOW DEPOSITS)	
22		
23		
24	SILT (ML-CL), gray, semi-plastic, dry, <10% angular mudstone clasts, irregular and discontinuous clay seams dip NNE about 20° (DEBRIS FLOW DEPOSITS)	
25	PP=3.5 ST=2.0	Sample BA1-S1 @ 23.5-feet downhole hand-driven to wall (brass tube)
26		
27	SILT, with gravel (ML), yellow brown, dry, 20% angular clasts of yellowish brown mudstone to 6-inch diameter, minor calcite (DEBRIS FLOW DEPOSITS)	Subhorizontal, sharp, irregular contact @ 26-feet
28		
29	GRAVELLY SILT (ML), grayish white, dry, approximately 30-40% subangular to angular mudstone clasts to 3-inch diameter, poorly sorted with chaotic structure (DEBRIS FLOW DEPOSITS)	
30	PP=4.5 ST=3.0	
31	GRAVELY SILT (ML), yellowish brown to grayish brown, dry, stiff, approximately 40-50% mudstone clasts are subangular to 4-inch diameter and poorly sorted (DEBRIS FLOW DEPOSITS)	
32		
33	SILT to CLAY (ML-CL), yellowish brown, dry, stiff, massive with <5% mudstone clasts to 3-inch diameter, minor clay seams, coarsens downward (DEBRIS FLOW DEPOSITS?)	
34		
35		35-feet @ 8:56 a.m.

PP = Pocket Penetrometer (in tsf) ST = Shear Torvane (in kg/cm²)

Log of Boring WLA BA-1

Project	Job No.	Logged by
State of California La Conchita Hillside Stabilization	1885	C. Hitchcock

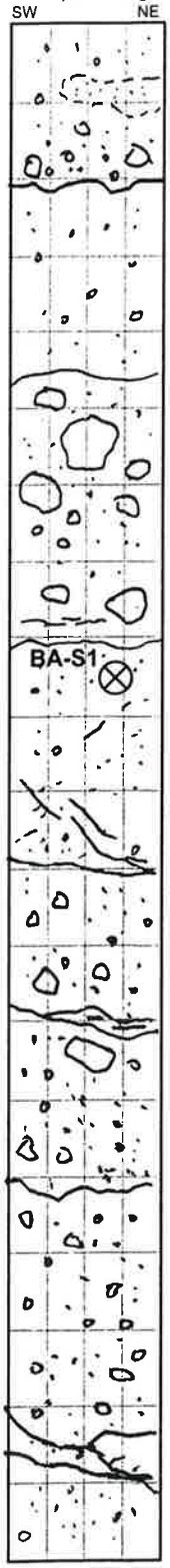

Depth (feet)	Description	Remarks
15	PP=2.5, ST=4.5 SILT, with sand (ML), yellow brown to range brown, dry angular clasts to 3-inch diameter of banded, laminar mudstone (DEBRIS FLOW DEPOSITS)	
17		Irregular, sharp contact
18	SILT, with gravel (ML), grayish brown, dry, stiff, claystone clasts to 60%, subangular to 3-inch diameter, minor calcite veins (DEBRIS FLOW DEPOSITS)	
19		
20	PP=4.0 ST=3.5	Irregular, subhorizontal sharp contact (erosional?) @ 19.5-feet
21	GRAVELY SILT (ML), yellowish brown, dry, stiff, subangular clasts of yellow brown mudstone to 1-foot diameter forms 40-60% of deposit, coarsens upward (DEBRIS FLOW DEPOSITS)	
22		
23	SILT (ML-CL), gray, semi-plastic, dry, <10% angular mudstone clasts, irregular and discontinuous clay seams dip NNE about 20° (DEBRIS FLOW DEPOSITS)	Sample BA1-S1 @ 23.5-feet downhole hand-driven to wall (brass tube)
24		
25	PP=3.5 ST=2.0	
26		
27	SILT, with gravel (ML), yellow brown, dry, 20% angular clasts of yellowish brown mudstone to 6-inch diameter, minor calcite (DEBRIS FLOW DEPOSITS)	Subhorizontal, sharp, irregular contact @ 26-feet
28		
29	GRAVELLY SILT (ML), grayish white, dry, approximately 30-40% subangular to angular mudstone clasts to 3-inch diameter, poorly sorted with chaotic structure (DEBRIS FLOW DEPOSITS)	
30	PP=4.5 ST=3.0	
31	GRAVELY SILT (ML), yellowish brown to grayish brown, dry, stiff, approximately 40-50% mudstone clasts are subangular to 4-inch diameter and poorly sorted (DEBRIS FLOW DEPOSITS)	
32		
33	SILT to CLAY (ML-CL), yellowish brown, dry, stiff, massive with <5% mudstone clasts to 3-inch diameter, minor clay seams, coarsens downward (DEBRIS FLOW DEPOSITS?)	
34		
35		35-feet @ 8:56 a.m.

PP = Pocket Penetrometer (in tsf) ST = Shear Torvane (in kg/cm²)

TABLE OF CONTENTS

Table of Figures

Table of Tables

INTRODUCTION

Boring geophysical measurements were collected in two uncased borings located at the La Conchita Slide, located in Ventura County, California. Geophysical data acquisition was performed on October 23 and 26, 2007 by Rob Steller of **GEO***Vision*. Data analysis was performed by Rob Steller, and reviewed by John Diehl of **GEO***Vision*. Report preparation was performed by Rob Steller and reviewed by John Diehl. The work was performed under subcontract with William Lettis & Associates, Inc., (WLA) with Chris Hitchcock serving as the Project Manager for WLA.

This report describes the field measurements, data analysis, and results of this work.

SCOPE OF WORK

This report presents the results of boring geophysical measurements collected on October 23 and 26, 2007, as detailed in Table 1, below. The purpose of these studies were to supplement stratigraphic information obtained during WLA's soil and rock sampling program and to acquire shear wave velocities and compressional wave velocities as a function of depth, as a component of a slope stability evaluation.

BORING DESIGNATION	DATE LOGGED	COORDINATES - FEET		ELEVATION - FT MSL
		NORTHING	EASTING	
B-1	10/26/2007	NA	NA	NA
B-2	10/23/2007	NA	NA	NA

Table 1. Boring locations and logging dates

The OYO Suspension PS Logging System (Suspension System) was used to obtain in-situ horizontal shear (S_H) and compressional (P) wave velocity measurements in two borings at 1.6 foot intervals. The acquired data was analyzed and a profile of velocity versus depth was produced for both compressional and horizontally polarized shear waves.

INSTRUMENTATION

Suspension Instrumentation

Suspension soil and rock velocity measurements were performed in two borings using the suspension PS logging system, manufactured by OYO Corporation. This system directly determines the average velocity of a 3.3 foot high segment of the soil and rock column surrounding the boring of interest by measuring the elapsed time between arrivals of a wave propagating upward through the soil column. The receivers that detect the wave, and the source that generates the wave, are moved as a unit in the boring producing relatively constant amplitude signals at all depths.

Winch GEOVision 4-conductor
Sheave - Measuring wheel GEOVision S/N 102
OYO/Robertson Suspension PS Logger Borehole Probe, includes:
Telemetry Unit Model 3331 S/N 15014
Receiver/Sensor Model 3385 S/N 12008
Isolation tube, 1m Model 3387B S/N 280068
Source Model 3304 S/N 19043
Driver Model 3386 S/N 27073
Weight Model 3302W S/N 12007

Table 2. Suspension equipment

The suspension system probe consists of a combined reversible polarity solenoid horizontal shear-wave source (S_H) and compressional-wave source (P), joined to two biaxial receivers by a flexible isolation cylinder, as shown in Figure 1. The separation of the two receivers is 3.3 feet, allowing average wave velocity in the region between the receivers to be determined by inversion of the wave travel time between the two receivers. The total length of the probe as used in these surveys is 19 feet, with the center point of the receiver pair 12.1 feet above the bottom end of the probe.

The probe receives control signals from, and sends the amplified receiver signals to, instrumentation on the surface via an armored 7 conductor cable. The cable is wound onto the drum of a winch and is used to support the probe. Cable travel is measured to provide probe depth data, using a 3.28 foot circumference sheave fitted with a digital rotary encoder.

The entire probe is suspended in the boring by the cable, therefore, source motion is not coupled directly to the boring walls; rather, the source motion creates a horizontally propagating impulsive pressure wave in the fluid filling the boring and surrounding the source. This pressure wave is converted to P and S_H-waves in the surrounding soil and rock as it passes through the casing and grout annulus and impinges upon the wall of the boring. These waves propagate through the soil and rock surrounding the boring, in turn causing a pressure wave to be generated in the fluid surrounding the receivers as the soil waves pass their location. Separation of the P and S_H-waves at the receivers is performed using the following steps:

1. Orientation of the horizontal receivers is maintained parallel to the axis of the source, maximizing the amplitude of the recorded S_H -wave signals.
2. At each depth, S_H-wave signals are recorded with the source actuated in opposite directions, producing S_H-wave signals of opposite polarity, providing a characteristic S_H-wave signature distinct from the P-wave signal.
3. The 6.3 foot separation of source and receiver 1 permits the P-wave signal to pass and damp significantly before the slower S_H-wave signal arrives at the receiver. In faster soils or rock, the isolation cylinder is extended to allow greater separation of the P- and S_H-wave signals.

4. In saturated soils, the received P-wave signal is typically of much higher frequency than the received S_H-wave signal, permitting additional separation of the two signals by low pass filtering.
5. Direct arrival of the original pressure pulse in the fluid is not detected at the receivers because the wavelength of the pressure pulse in fluid is significantly greater than the dimension of the fluid annulus surrounding the probe (meter versus centimeter scale), preventing significant energy transmission through the fluid medium.

In operation, a distinct, repeatable pattern of impulses is generated at each depth as follows:

1. The source is fired in one direction producing dominantly horizontal shear with some vertical compression, and the signals from the horizontal receivers situated parallel to the axis of motion of the source are recorded.
2. The source is fired again in the opposite direction and the horizontal receiver signals are recorded.
3. The source is fired again and the vertical receiver signals are recorded. The repeated source pattern facilitates the picking of the P and S_H-wave arrivals; reversal of the source changes the polarity of the S_H-wave pattern but not the P-wave pattern.

The data from each receiver during each source activation are recorded as a different channel on the recording system. The suspension system has six channels (two simultaneous recording channels), each with a 1024 sample record. The recorded data is displayed on a CRT or LCD display as six channels with a common time scale. Data is stored on disk for further processing. Up to 8 sampling sequences can be summed to improve the signal to noise ratio of the signals.

Review of the displayed data on the recorder or computer screen allows the operator to set the gains, filters, delay time, pulse length (energy), sample rate, and summing number to optimize the quality of the data before recording. Verification of the calibration of the suspension digital recorder is performed every twelve months using a NIST traceable frequency source and counter, as outlined in Appendix B.

MEASUREMENT PROCEDURES

Suspension Measurement Procedures

Both borings were logged uncased, filled with drilling mud. In each boring, the probe was positioned with the top of the probe at the top of the mud box, and the electronic depth counter was set to 6.6 feet, the distance between the mid-point of the receiver and the top of the probe, minus the height of the mud box, as verified with a tape measure, and recorded on the field logs. The probe was lowered to the bottom of the boring, stopping at 1.6 foot intervals to collect data, as summarized in Table 3.

At each measurement depth the measurement sequence of two opposite horizontal records and one vertical record was performed, and the gains were adjusted as required. The data from each depth was reviewed on the control computer display and recorded on disk before moving to the next depth.

Upon completion of the measurements, the probe zero depth indication at the depth reference point was verified prior to removal from the boring, and after survey depth error (ASDE) was calculated and recorded on the field log. Field data were backed up to CD-ROM each day upon completion of data acquisition.

BORING NUMBER	TOOL AND RUN NUMBER	DEPTH RANGE (FEET)	TOTAL DEPTH AS DRILLED (FEET)	DEPTH TO BOTTOM OF CASING (FEET)	SAMPLE INTERVAL (FEET)	DATE LOGGED
B-1	SUSPENSION PS	1.6 – 146.0	160	NONE	1.6	10/26/07
B-2	SUSPENSION PS	1.6 – 134.5	150	NONE	1.6	10/23/07

Table 3. Logging dates and depth ranges

DATA ANALYSIS

Suspension Analysis

Using the proprietary OYO program PSLOG.EXE version 1.0, the recorded digital waveforms were analyzed to locate the most prominent first minima, first maxima, or first break on the vertical axis records, indicating the arrival of P-wave energy. The difference in travel time between receiver 1 and receiver 2 (R1-R2) arrivals was used to calculate the P-wave velocity for that 3.3 foot segment of the soil column. When observable, P-wave arrivals on the horizontal axis records were used to verify the velocities determined from the vertical axis data. The time picks were then transferred into an EXCEL template (EXCEL version 2003 SP2) to complete the velocity calculations based upon the arrival time picks made in PSLOG.

The P-wave velocity over the 6.3 foot interval from source to receiver 1 (S-R1) was also picked using PSLOG, and calculated and plotted in EXCEL, for quality assurance of the velocity derived from the travel time between receivers. In this analysis, the depth values as recorded were increased by 4.8 feet to correspond to the mid-point of the 6.3 foot S-R1 interval. Travel times were obtained by picking the first break of the P-wave signal at receiver 1 and subtracting 3.9 milliseconds, the calculated and experimentally verified delay from source trigger pulse (beginning of record) to source impact. This delay corresponds to the duration of acceleration of the solenoid before impact.

As with the P-wave records, using PSLOG, the recorded digital waveforms were analyzed to locate the presence of clear S_H-wave pulses, as indicated by the presence of opposite polarity pulses on each pair of horizontal records. Ideally, the S_H-wave signals from the 'normal' and 'reverse' source pulses are very nearly inverted images of each other. Digital FFT - IFFT lowpass filtering was used to remove the higher frequency P-wave signal from the S_H-wave signal. Different filter cutoffs were used to separate P- and S_H-waves at different depths, ranging from 600 Hz in the slowest zones to 4000 Hz in the regions of highest velocity. At each depth, the filter frequency was selected to be at least twice the fundamental frequency of the S_H-wave signal being filtered.

Generally, the first maxima were picked for the 'normal' signals and the first minima for the 'reverse' signals, although other points on the waveform were used if the first pulse was distorted. The absolute arrival time of the 'normal' and 'reverse' signals may vary by +/- 0.2 milliseconds, due to differences in the actuation time of the solenoid source caused by constant mechanical bias in the source or by boring inclination. This variation does not affect the R1-R2 velocity determinations, as the differential time is measured between arrivals of waves created by the same source actuation. The final velocity value is the average of the values obtained from the 'normal' and 'reverse' source actuations.

As with the P-wave data, S_H-wave velocity calculated from the travel time over the 6.3 foot interval from source to receiver 1 was calculated and plotted for verification of the velocity derived from the travel time between receivers. In this analysis, the depth values were increased by 4.8 foot to correspond to the mid-point of the 6.3 foot S-R1 interval. Travel times were obtained by picking the first break of the S_H-wave signal at the near receiver and subtracting 3.9 milliseconds, the calculated and experimentally verified delay from the beginning of the record at the source trigger pulse to source impact.

These data and analysis were reviewed by John Diehl as a component of **GEO***Vision*'s in-house QA-QC program.

Figure 2 shows an example of R1 - R2 measurements on a sample filtered suspension record. In Figure 2, the time difference over the 3.3 foot interval of 1.88 milliseconds for the horizontal signals is equivalent to an S_H-wave velocity of 1745 feet/second. Whenever possible, time differences were determined from several phase points on the S_H-waveform records to verify the data obtained from the first arrival of the S_H-wave pulse. Figure 3 displays the same record before filtering of the S_H-waveform record with a 1400 Hz FFT - IFFT digital lowpass filter, illustrating the presence of higher frequency P-wave energy at the beginning of the record, and distortion of the lower frequency S_H-wave by residual P-wave signal.

RESULTS

Suspension Results

Suspension R1-R2 P- and S_H-wave velocities are plotted in Figures 4 and 5 and presented in Tables 4 and 5. P- and S_H-wave velocity data from R1-R2 analysis and quality assurance analysis of S-R1 data are plotted together in Figures A-1 and A-2 to aid in visual comparison. It must be noted that R1-R2 data is an average velocity over a 3.3 foot segment of the soil column; S-R1 data is an average over 6.3 feet, creating a significant smoothing relative to the R1-R2 plots. S-R1 data are presented in Tables A-1 and A-2.

Calibration procedures and records for the suspension measurement system are presented in Appendix B.

SUMMARY

Discussion of Suspension Results

Suspension velocity data is ideally collected in an uncased fluid filled boring, drilled with rotary mud (rotary wash) methods. These borings were ideal for collection of suspension velocity data. Suspension velocity data quality is judged based upon 5 criteria:

1. Consistent data between receiver to receiver (R1 – R2) and source to receiver (S – R1) data.
2. Consistent relationship between P-wave and S_H -wave (excluding transition to saturated soils)
3. Consistency between data from adjacent depth intervals.
4. Clarity of P-wave and S_H-wave onset, as well as damping of later oscillations.
5. Consistency of profile between adjacent borings, if available.

These data are of excellent quality, exhibiting all of the above listed criteria.

P- and S_H-wave velocity measurement using the suspension method gives average velocities over a 3.3 foot interval of depth. This high resolution results in the scatter of values shown in the graphs. Individual S_H-wave measurements are very reliable with estimated precision of +/- 5%. Due to the difficulty in picking weak signals, which can be seen in the greater scatter of P-wave arrivals, P-wave measurements have an estimated precision of +/- 10%. Standardized field procedures and quality assurance checks contribute to the reliability of these data.

Quality Assurance

These boring geophysical measurements were performed using industry-standard or better methods for measurements and analyses. All work was performed under WLA and **GEO***Vision* quality assurance procedures, which include:

- Use of NIST-traceable calibrations, where applicable, for field and laboratory instrumentation
- Use of standard field data logs
- Use of independent verification of velocity data by comparison of receiver-to-receiver and source-to-receiver velocities
- Independent review of calculations and results by a registered professional engineer, geologist, or geophysicist.

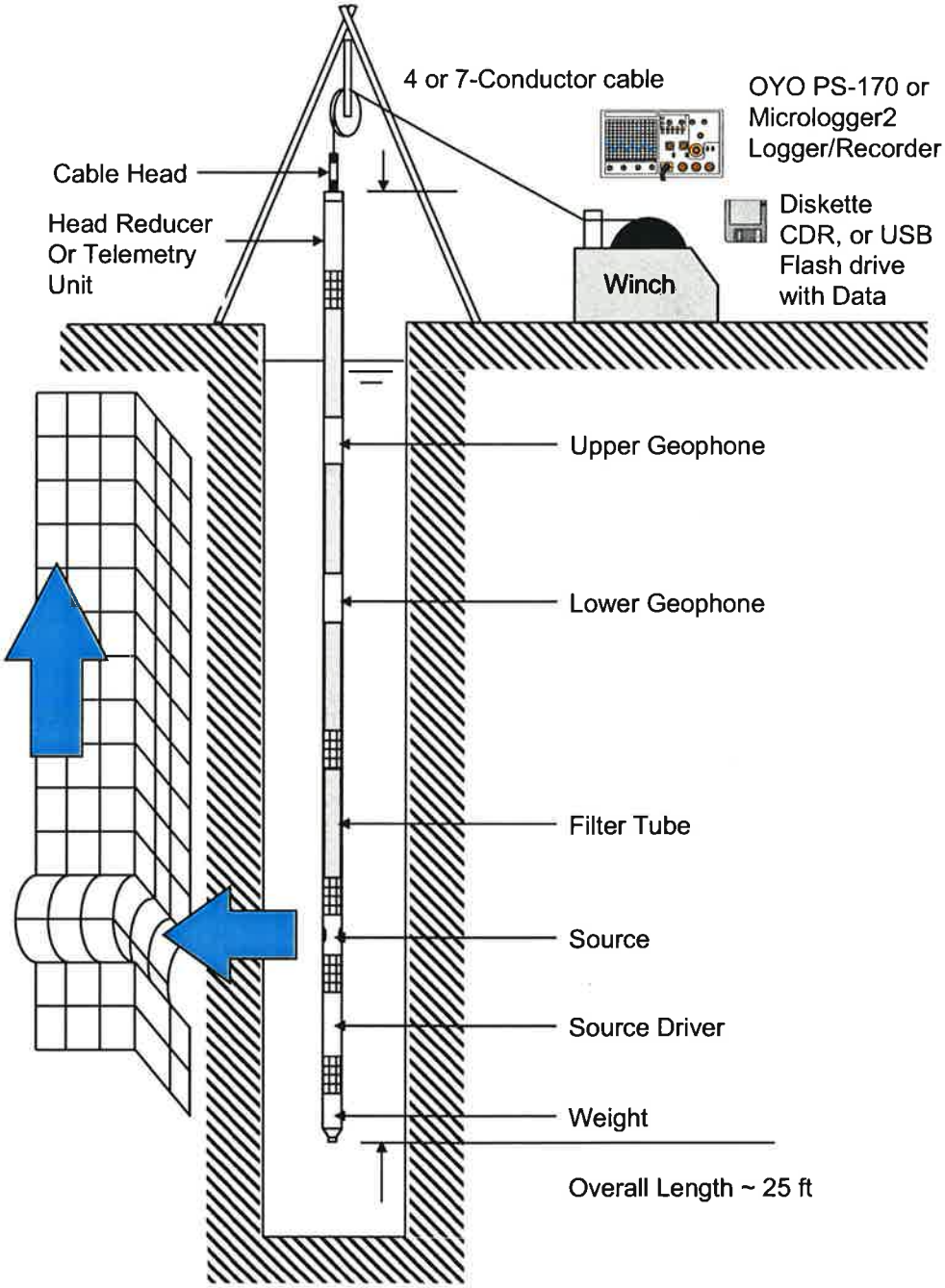

Figure 1: Concept illustration of Suspension logging system

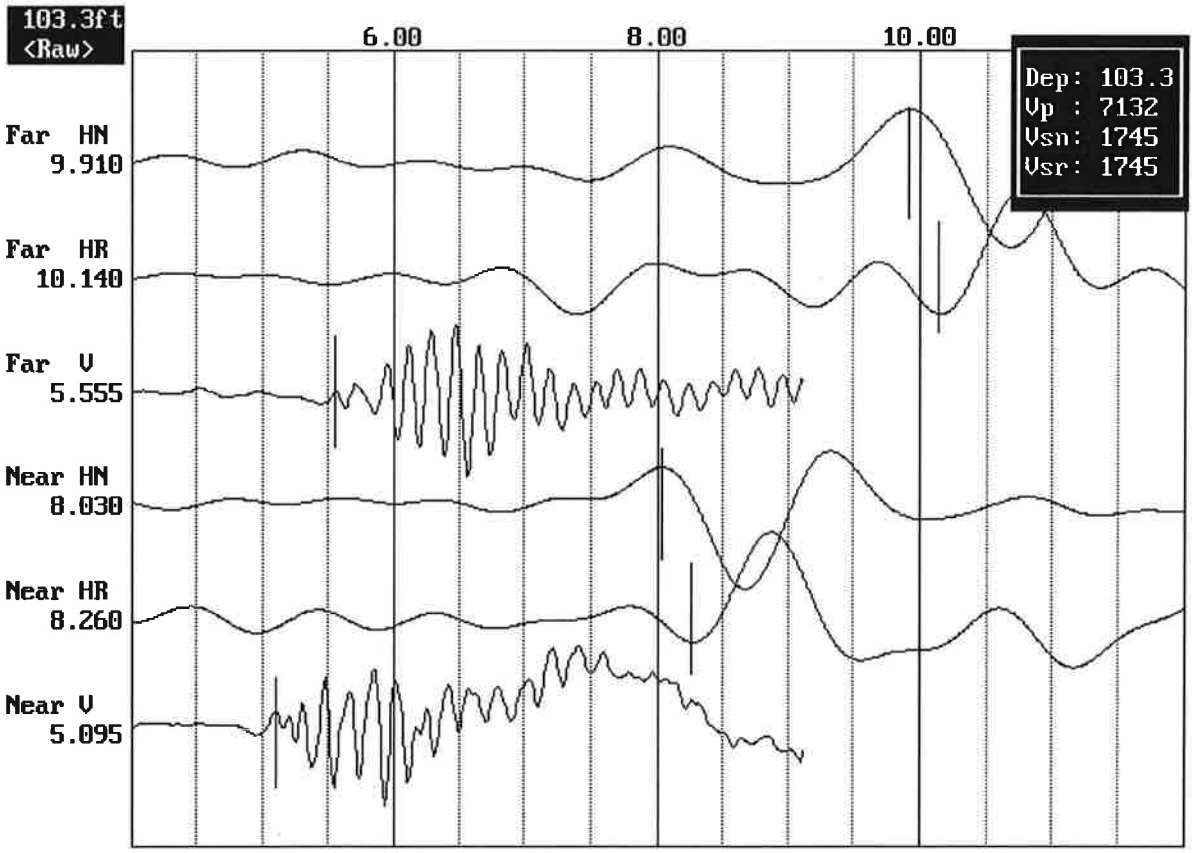

Figure 2: Example of filtered (1400 Hz lowpass) record

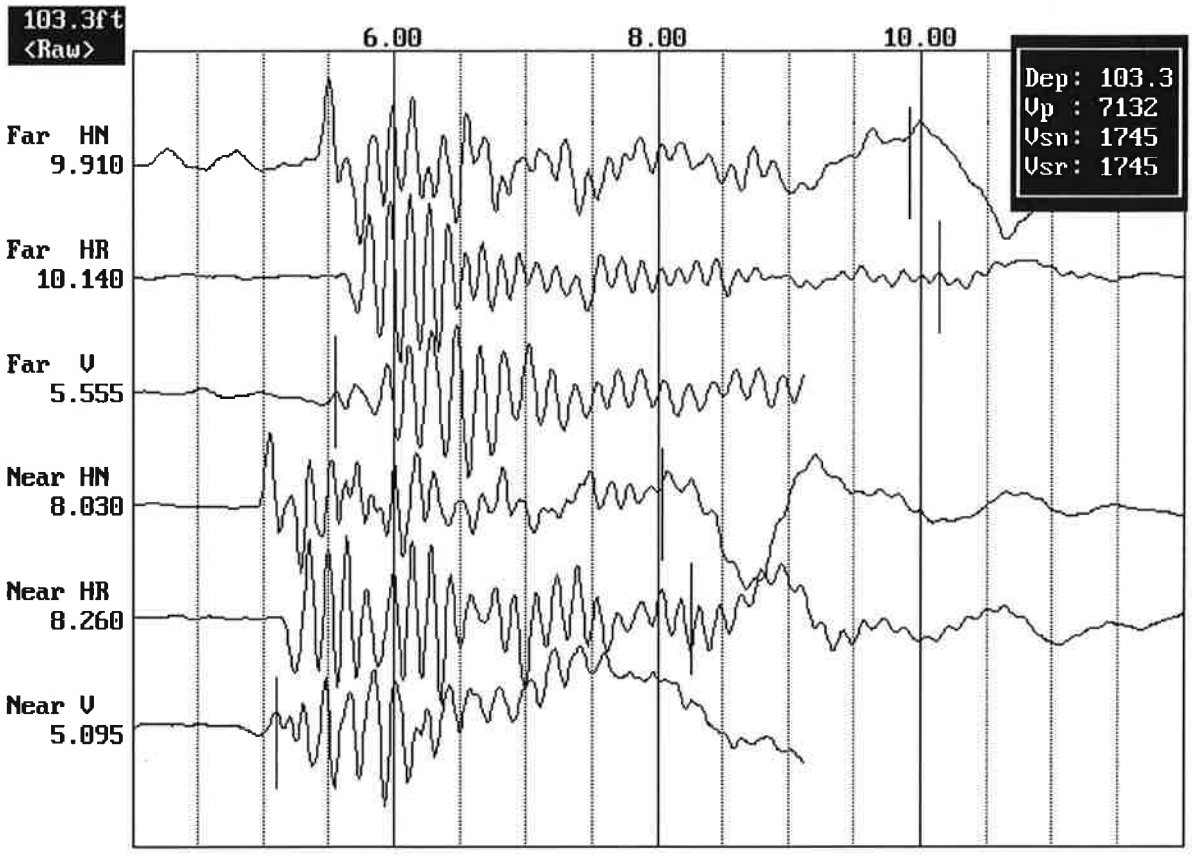

Figure 3. Example of unfiltered record

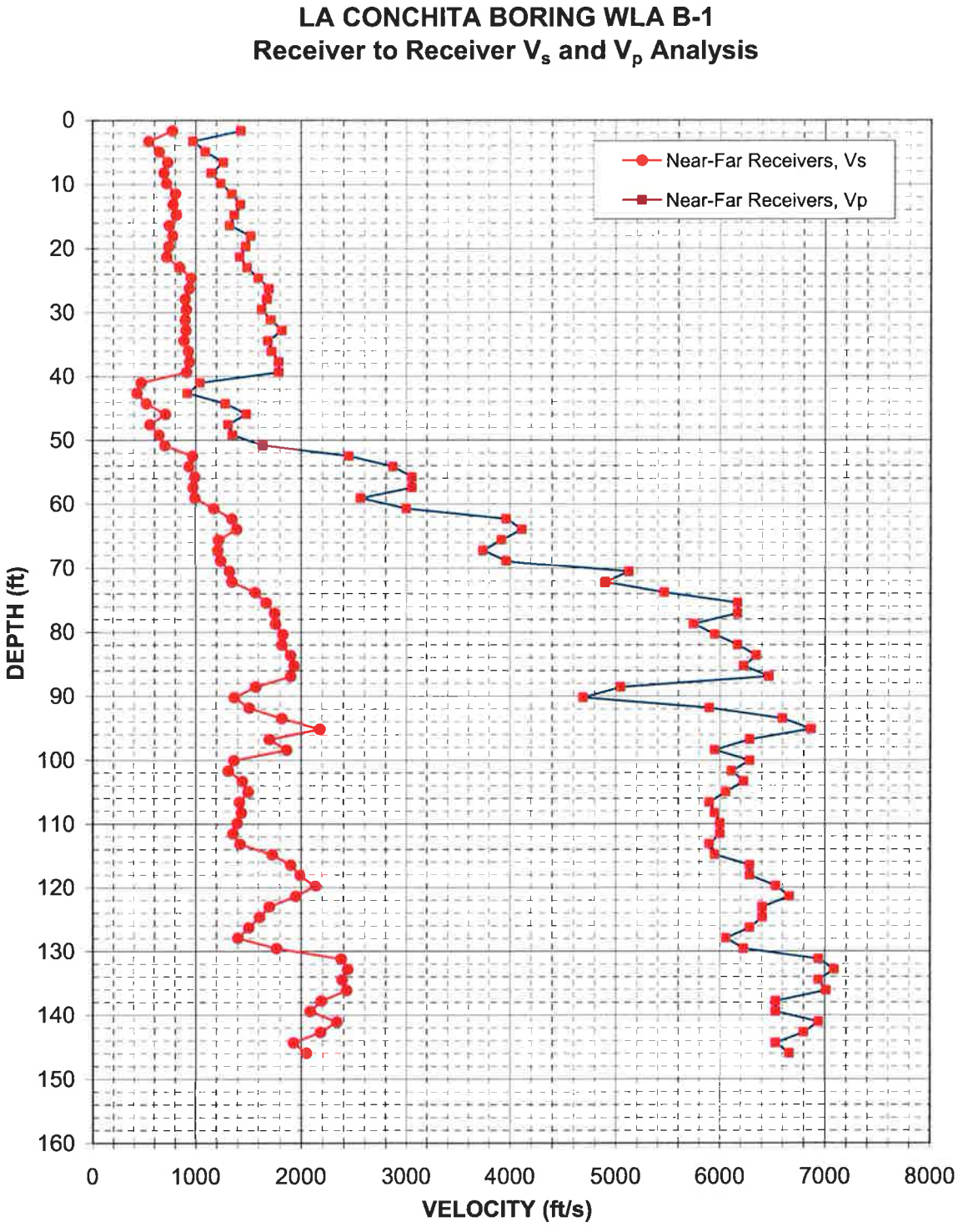

Figure 4: Boring B-1, Suspension R1-R2 P- and S_H-wave velocities

Table 4. Boring B-1, Suspension R1-R2 depths and P- and S_H-wave velocities

Summary of Compressional Wave Velocity, Shear Wave Velocity, and Poisson's Ratio Based on Receiver-to-Receiver Travel Time Data - Borehole WLA B-1

American Units				Metric Units			
Depth at Midpoint Between Receivers	Velocity		Poisson's Ratio	Depth at Midpoint Between Receivers	Velocity		Poisson's Ratio
	V_s	V_p			V_s	V_p	
(ft)	(ft/s)	(ft/s)		(m)	(m/s)	(m/s)	
1.6	780	1440	0.29	0.5	240	440	0.29
3.3	550	980	0.27	1.0	170	300	0.27
4.9	650	1100	0.23	1.5	200	330	0.23
6.6	730	1270	0.25	2.0	220	390	0.25
8.2	700	1150	0.21	2.5	210	350	0.21
9.8	720	1240	0.24	3.0	220	380	0.24
11.5	810	1350	0.22	3.5	250	410	0.22
13.1	790	1430	0.28	4.0	240	440	0.28
14.8	820	1370	0.23	4.5	250	420	0.23
16.4	750	1330	0.27	5.0	230	400	0.27
18.0	780	1530	0.32	5.5	240	470	0.32
19.7	740	1480	0.33	6.0	230	450	0.33
21.3	720	1420	0.33	6.5	220	430	0.33
23.0	850	1490	0.26	7.0	260	460	0.26
24.6	960	1600	0.22	7.5	290	490	0.22
26.3	940	1700	0.28	8.0	290	520	0.28
27.9	900	1680	0.30	8.5	280	510	0.30
29.5	910	1630	0.27	9.0	280	500	0.27
31.2	900	1720	0.31	9.5	280	520	0.31
32.8	910	1820	0.33	10.0	280	560	0.33
34.5	890	1690	0.31	10.5	270	520	0.31
36.1	930	1730	0.29	11.0	280	530	0.29
37.7	940	1790	0.31	11.5	290	550	0.31
39.4	920	1790	0.32	12.0	280	550	0.32
41.0	470	1040	0.37	12.5	140	320	0.37
42.7	430	920	0.36	13.0	130	280	0.36
44.3	520	1290	0.40	13.5	160	390	0.40
45.9	710	1490	0.35	14.0	220	450	0.35
47.6	560	1310	0.39	14.5	170	400	0.39
49.2	650	1360	0.35	15.0	200	410	0.35
50.9	710	1640	0.39	15.5	220	500	0.39
52.5	970	2450	0.41	16.0	300	750	0.41
54.1	940	2870	0.44	16.5	290	880	0.44
55.8	1000	3060	0.44	17.0	300	930	0.44
57.4	980	3060	0.44	17.5	300	930	0.44
59.1	1000	2560	0.41	18.0	300	780	0.41
60.7	1180	3000	0.41	18.5	360	920	0.41
62.3	1350	3970	0.43	19.0	410	1210	0.43

Summary of Compressional Wave Velocity, Shear Wave Velocity, and Poisson's Ratio Based on Receiver-to-Receiver Travel Time Data - Borehole WLA B-1

American Units			
Depth at Midpoint Between Receivers	Velocity		Poisson's Ratio
	V_s	V_p	
(ft)	(ft/s)	(ft/s)	
64.0	1390	4120	0.44
65.6	1230	3920	0.45
67.3	1220	3750	0.44
68.9	1240	3970	0.45
70.5	1330	5130	0.46
72.2	1350	4900	0.46
73.8	1570	5460	0.45
75.5	1680	6170	0.46
77.1	1750	6170	0.46
78.7	1760	5750	0.45
80.4	1830	5950	0.45
82.0	1820	6170	0.45
83.7	1900	6350	0.45
85.3	1940	6230	0.45
86.9	1900	6470	0.45
88.6	1580	5050	0.45
90.2	1370	4690	0.45
91.9	1520	5900	0.46
93.5	1820	6600	0.46
95.1	2190	6870	0.44
96.8	1710	6290	0.46
98.4	1870	5950	0.45
100.1	1370	6290	0.48
101.7	1310	6120	0.48
103.4	1450	6230	0.47
105.0	1500	6060	0.47
106.6	1420	5900	0.47
108.3	1440	5950	0.47
109.9	1400	6010	0.47
111.6	1360	6010	0.47
113.2	1430	5900	0.47
114.8	1730	5950	0.45
116.5	1900	6290	0.45
118.1	2000	6290	0.44
119.8	2140	6540	0.44
121.4	1960	6670	0.45
123.0	1710	6410	0.46
124.7	1610	6410	0.47
126.3	1510	6290	0.47
128.0	1410	6060	0.47
129.6	1770	6230	0.46

Metric Units			
Depth at Midpoint Between Receivers	Velocity		Poisson's Ratio
	V_s	V_p	
(m)	(m/s)	(m/s)	
19.5	430	1250	0.44
20.0	370	1200	0.45
20.5	370	1140	0.44
21.0	380	1210	0.45
21.5	400	1560	0.46
22.0	410	1490	0.46
22.5	480	1670	0.45
23.0	510	1880	0.46
23.5	530	1880	0.46
24.0	540	1750	0.45
24.5	560	1810	0.45
25.0	560	1880	0.45
25.5	580	1940	0.45
26.0	590	1900	0.45
26.5	580	1970	0.45
27.0	480	1540	0.45
27.5	420	1430	0.45
28.0	460	1800	0.46
28.5	560	2010	0.46
29.0	670	2090	0.44
29.5	520	1920	0.46
30.0	570	1810	0.45
30.5	420	1920	0.48
31.0	400	1860	0.48
31.5	440	1900	0.47
32.0	460	1850	0.47
32.5	430	1800	0.47
33.0	440	1810	0.47
33.5	430	1830	0.47
34.0	410	1830	0.47
34.5	440	1800	0.47
35.0	530	1810	0.45
35.5	580	1920	0.45
36.0	610	1920	0.44
36.5	650	1990	0.44
37.0	600	2030	0.45
37.5	520	1950	0.46
38.0	490	1950	0.47
38.5	460	1920	0.47
39.0	430	1850	0.47
39.5	540	1900	0.46

Summary of Compressional Wave Velocity, Shear Wave Velocity, and Poisson's Ratio Based on Receiver-to-Receiver Travel Time Data - Borehole WLA B-1

American Units			
Depth at Midpoint Between Receivers	Velocity		Poisson's Ratio
	V_s	V_p	
(ft)	(ft/s)	(ft/s)	
131.2	2380	6940	0.43
132.9	2440	7090	0.43
134.5	2390	6940	0.43
136.2	2430	7020	0.43
137.8	2190	6540	0.44
139.4	2090	6540	0.44
141.1	2340	6940	0.44
142.7	2190	6800	0.44
144.4	1930	6540	0.45
146.0	2050	6670	0.45

Metric Units			
Depth at Midpoint Between Receivers	Velocity		Poisson's Ratio
	V_s	V_p	
(m)	(m/s)	(m/s)	
40.0	730	2120	0.43
40.5	740	2160	0.43
41.0	730	2120	0.43
41.5	740	2140	0.43
42.0	670	1990	0.44
42.5	640	1990	0.44
43.0	710	2120	0.44
43.5	670	2070	0.44
44.0	590	1990	0.45
44.5	630	2030	0.45

Notes: "-" means no data available at that particular interval of depth.

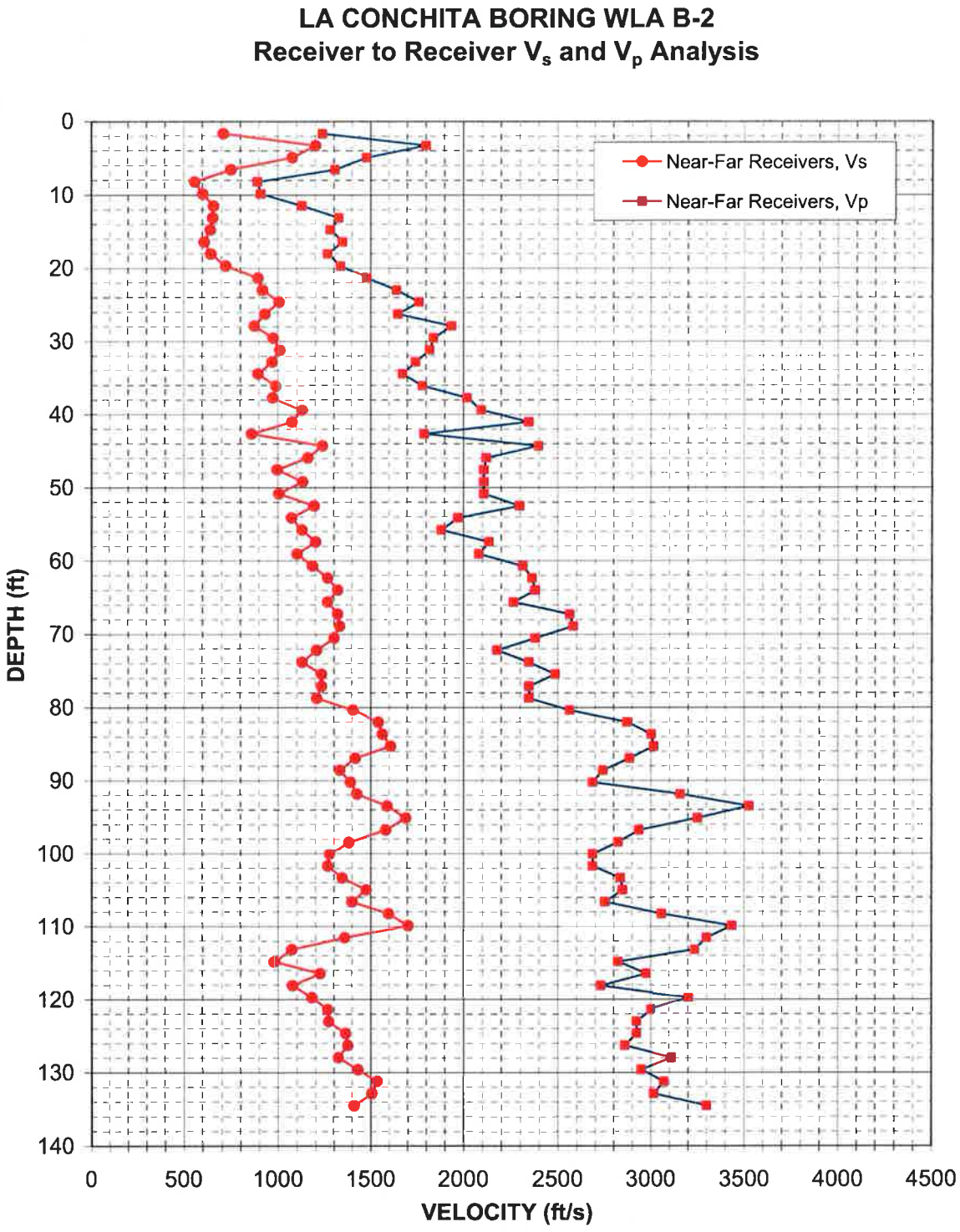

Figure 5: Boring B-2, Suspension R1-R2 P- and S_H-wave velocities

Table 5. Boring B-2, Suspension R1-R2 depths and P- and S_H-wave velocities

Summary of Compressional Wave Velocity, Shear Wave Velocity, and Poisson's Ratio Based on Receiver-to-Receiver Travel Time Data - Borehole WLA B-2

American Units				Metric Units			
Depth at Midpoint Between Receivers	Velocity		Poisson's Ratio	Depth at Midpoint Between Receivers	Velocity		Poisson's Ratio
	V_s	V_p			V_s	V_p	
(ft)	(ft/s)	(ft/s)		(m)	(m/s)	(m/s)	
1.6	710	1240	0.25	0.5	220	380	0.25
3.3	1200	1800	0.10	1.0	370	550	0.10
4.9	1080	1480	-0.06	1.5	330	450	-0.06
6.6	750	1310	0.25	2.0	230	400	0.25
8.2	560	890	0.17	2.5	170	270	0.17
9.8	600	910	0.11	3.0	180	280	0.11
11.5	660	1130	0.24	3.5	200	340	0.24
13.1	660	1330	0.34	4.0	200	400	0.34
14.8	640	1280	0.33	4.5	200	390	0.33
16.4	610	1350	0.37	5.0	190	410	0.37
18.0	650	1270	0.32	5.5	200	390	0.32
19.7	720	1340	0.29	6.0	220	410	0.29
21.3	900	1480	0.21	6.5	270	450	0.21
23.0	920	1640	0.27	7.0	280	500	0.27
24.6	1010	1760	0.26	7.5	310	540	0.26
26.3	930	1650	0.26	8.0	280	500	0.26
27.9	880	1940	0.37	8.5	270	590	0.37
29.5	980	1840	0.30	9.0	300	560	0.30
31.2	1010	1820	0.28	9.5	310	560	0.28
32.8	970	1750	0.28	10.0	300	530	0.28
34.5	900	1680	0.30	10.5	270	510	0.30
36.1	990	1780	0.28	11.0	300	540	0.28
37.7	970	2020	0.35	11.5	300	620	0.35
39.4	1130	2100	0.30	12.0	340	640	0.30
41.0	1080	2350	0.37	12.5	330	720	0.37
42.7	860	1790	0.35	13.0	260	550	0.35
44.3	1240	2400	0.32	13.5	380	730	0.32
45.9	1160	2120	0.29	14.0	350	650	0.29
47.6	1000	2110	0.36	14.5	300	640	0.36
49.2	1130	2110	0.30	15.0	350	640	0.30
50.9	1010	2110	0.35	15.5	310	640	0.35
52.5	1190	2300	0.31	16.0	360	700	0.31
54.1	1080	1970	0.29	16.5	330	600	0.29
55.8	1130	1880	0.22	17.0	340	570	0.22
57.4	1200	2140	0.27	17.5	370	650	0.27
59.1	1100	2080	0.30	18.0	340	640	0.30
60.7	1190	2310	0.32	18.5	360	710	0.32
62.3	1270	2360	0.30	19.0	390	720	0.30

Summary of Compressional Wave Velocity, Shear Wave Velocity, and Poisson's Ratio Based on Receiver-to-Receiver Travel Time Data - Borehole WLA B-2

American Units			
Depth at Midpoint Between Receivers	Velocity		Poisson's Ratio
	V_s	V_p	
(ft)	(ft/s)	(ft/s)	
64.0	1320	2380	0.28
65.6	1270	2270	0.27
67.3	1320	2560	0.32
68.9	1330	2580	0.32
70.5	1300	2380	0.29
72.2	1210	2180	0.28
73.8	1130	2350	0.35
75.5	1230	2490	0.34
77.1	1230	2350	0.31
78.7	1210	2350	0.32
80.4	1410	2560	0.28
82.0	1540	2870	0.30
83.7	1560	3000	0.31
85.3	1610	3020	0.30
86.9	1420	2890	0.34
88.6	1330	2740	0.35
90.2	1390	2690	0.32
91.9	1430	3160	0.37
93.5	1590	3530	0.37
95.1	1690	3250	0.31
96.8	1580	2940	0.30
98.4	1380	2820	0.34
100.1	1280	2690	0.35
101.7	1270	2690	0.36
103.4	1350	2840	0.35
105.0	1480	2850	0.32
106.6	1400	2750	0.33
108.3	1600	3060	0.31
109.9	1710	3440	0.34
111.6	1360	3300	0.40
113.2	1080	3240	0.44
114.8	980	2820	0.43
116.5	1230	2980	0.40
118.1	1080	2730	0.41
119.8	1180	3210	0.42
121.4	1270	3000	0.39
123.0	1270	2920	0.38
124.7	1370	2920	0.36
126.3	1380	2860	0.35
128.0	1330	3120	0.39
129.6	1430	2950	0.35

Metric Units			
Depth at Midpoint Between Receivers	Velocity		Poisson's Ratio
	V_s	V_p	
(m)	(m/s)	(m/s)	
19.5	400	730	0.28
20.0	390	690	0.27
20.5	400	780	0.32
21.0	410	790	0.32
21.5	400	730	0.29
22.0	370	660	0.28
22.5	340	720	0.35
23.0	380	760	0.34
23.5	380	720	0.31
24.0	370	720	0.32
24.5	430	780	0.28
25.0	470	880	0.30
25.5	480	920	0.31
26.0	490	920	0.30
26.5	430	880	0.34
27.0	410	840	0.35
27.5	420	820	0.32
28.0	440	960	0.37
28.5	480	1080	0.37
29.0	520	990	0.31
29.5	480	900	0.30
30.0	420	860	0.34
30.5	390	820	0.35
31.0	390	820	0.36
31.5	410	860	0.35
32.0	450	870	0.32
32.5	430	840	0.33
33.0	490	930	0.31
33.5	520	1050	0.34
34.0	410	1010	0.40
34.5	330	990	0.44
35.0	300	860	0.43
35.5	370	910	0.40
36.0	330	830	0.41
36.5	360	980	0.42
37.0	390	920	0.39
37.5	390	890	0.38
38.0	420	890	0.36
38.5	420	870	0.35
39.0	400	950	0.39
39.5	440	900	0.35

Summary of Compressional Wave Velocity, Shear Wave Velocity, and Poisson's Ratio Based on Receiver-to-Receiver Travel Time Data - Borehole WLA B-2

American Units			
Depth at Midpoint Between Receivers	Velocity		Poisson's Ratio
	V_s	V_p	
(ft)	(ft/s)	(ft/s)	
131.2	1540	3070	0.33
132.9	1510	3020	0.33
134.5	1410	3300	0.39

Metric Units			
Depth at Midpoint Between Receivers	Velocity		Poisson's Ratio
	V_s	V_p	
(m)	(m/s)	(m/s)	
40.0	470	940	0.33
40.5	460	920	0.33
41.0	430	1010	0.39

Notes: "-" means no data available at that particular interval of depth.

REFERENCES

A detailed reference for the suspension velocity measurement techniques used in this study is:

Guidelines for Determining Design Basis Ground Motions, Report TR-102293, Electric Power Research Institute, Palo Alto, California, November 1993, Sections 7 and 8.

APPENDIX A

SUSPENSION VELOCITY MEASUREMENT QUALITY ASSURANCE SUSPENSION SOURCE TO RECEIVER ANALYSIS RESULTS

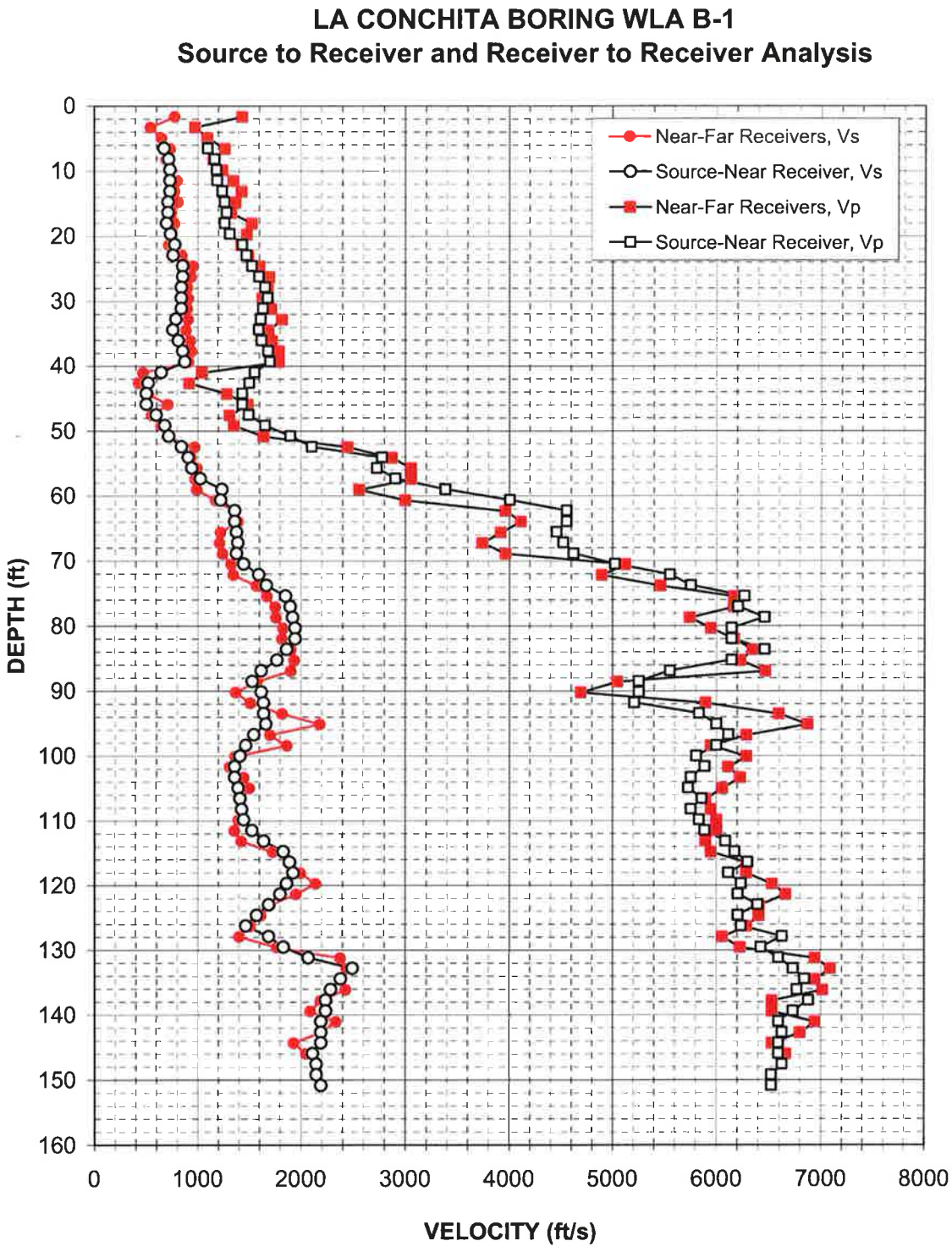

Figure A-1: Boring B-1, Suspension S-R1 P- and S_H-wave velocities

Table A-1. Boring B-1, Suspension S-R1 depths and P- and S_H-wave velocities

Summary of Compressional Wave Velocity, Shear Wave Velocity, and Poisson's Ratio Based on Source-to-Receiver Travel Time Data - Borehole WLA B-1

American Units				Metric Units			
Depth at Midpoint Between Source and Near Receiver	Velocity		Poisson's Ratio	Depth at Midpoint Between Source and Near Receiver	Velocity		Poisson's Ratio
	V_s	V_p			V_s	V_p	
(ft)	(ft/s)	(ft/s)		(m)	(m/s)	(m/s)	
6.5	670	1100	0.20	2.0	200	330	0.20
8.1	720	1160	0.19	2.5	220	350	0.19
9.8	730	1180	0.19	3.0	220	360	0.19
11.4	730	1190	0.20	3.5	220	360	0.20
13.0	730	1240	0.23	4.0	220	380	0.23
14.7	710	1260	0.27	4.5	220	380	0.27
16.3	710	1280	0.28	5.0	220	390	0.28
18.0	700	1260	0.28	5.5	210	380	0.28
19.6	730	1310	0.27	6.0	220	400	0.27
21.2	780	1430	0.29	6.5	240	440	0.29
22.9	760	1470	0.32	7.0	230	450	0.32
24.5	850	1530	0.27	7.5	260	460	0.27
26.2	850	1590	0.30	8.0	260	490	0.30
27.8	840	1650	0.33	8.5	260	500	0.33
29.4	840	1680	0.33	9.0	260	510	0.33
31.1	840	1630	0.32	9.5	260	500	0.32
32.7	790	1610	0.34	10.0	240	490	0.34
34.4	760	1590	0.35	10.5	230	480	0.35
36.0	810	1620	0.33	11.0	250	490	0.33
37.6	850	1680	0.33	11.5	260	510	0.33
39.3	870	1700	0.32	12.0	270	520	0.32
40.9	640	1550	0.40	12.5	200	470	0.40
42.6	520	1500	0.43	13.0	160	460	0.43
44.2	500	1430	0.43	13.5	150	440	0.43
45.8	500	1430	0.43	14.0	150	440	0.43
47.5	600	1490	0.41	14.5	180	460	0.41
49.1	680	1650	0.40	15.0	210	500	0.40
50.8	720	1900	0.42	15.5	220	580	0.42
52.4	840	2100	0.40	16.0	260	640	0.40
54.0	910	2780	0.44	16.5	280	850	0.44
55.7	940	2730	0.43	17.0	290	830	0.43
57.3	1020	2900	0.43	17.5	310	890	0.43
59.0	1230	3390	0.42	18.0	380	1030	0.42
60.6	1220	4010	0.45	18.5	370	1220	0.45
62.2	1360	4550	0.45	19.0	410	1390	0.45
63.9	1360	4550	0.45	19.5	410	1390	0.45
65.5	1380	4460	0.45	20.0	420	1360	0.45

Summary of Compressional Wave Velocity, Shear Wave Velocity, and Poisson's Ratio Based on Source-to-Receiver Travel Time Data - Borehole WLA B-1

American Units				Metric Units			
Depth at Midpoint Between Source and Near Receiver	Velocity		Poisson's Ratio	Depth at Midpoint Between Source and Near Receiver	Velocity		Poisson's Ratio
	V_s	V_p			V_s	V_p	
(ft)	(ft/s)	(ft/s)		(m)	(m/s)	(m/s)	
67.2	1390	4520	0.45	20.5	420	1380	0.45
68.8	1380	4620	0.45	21.0	420	1410	0.45
70.5	1450	5020	0.45	21.5	440	1530	0.45
72.1	1590	5550	0.46	22.0	480	1690	0.46
73.7	1670	5750	0.45	22.5	510	1750	0.45
75.4	1850	6270	0.45	23.0	560	1910	0.45
77.0	1900	6210	0.45	23.5	580	1890	0.45
78.7	1920	6460	0.45	24.0	580	1970	0.45
80.3	1940	6150	0.44	24.5	590	1870	0.44
81.9	1940	6150	0.44	25.0	590	1870	0.44
83.6	1860	6460	0.45	25.5	570	1970	0.45
85.2	1770	6150	0.45	26.0	540	1870	0.45
86.9	1610	5550	0.45	26.5	490	1690	0.45
88.5	1530	5250	0.45	27.0	470	1600	0.45
90.1	1610	5250	0.45	27.5	490	1600	0.45
91.8	1640	5210	0.45	28.0	500	1590	0.45
93.4	1640	5830	0.46	28.5	500	1780	0.46
95.1	1660	6000	0.46	29.0	510	1830	0.46
96.7	1540	6120	0.47	29.5	470	1860	0.47
98.3	1470	6000	0.47	30.0	450	1830	0.47
100.0	1410	5810	0.47	30.5	430	1770	0.47
101.6	1360	5890	0.47	31.0	410	1790	0.47
103.3	1360	5750	0.47	31.5	410	1750	0.47
104.9	1390	5730	0.47	32.0	420	1750	0.47
106.5	1410	5860	0.47	32.5	430	1790	0.47
108.2	1430	5750	0.47	33.0	430	1750	0.47
109.8	1450	5830	0.47	33.5	440	1780	0.47
111.5	1530	5890	0.46	34.0	460	1790	0.46
113.1	1640	6090	0.46	34.5	500	1860	0.46
114.7	1830	6180	0.45	35.0	560	1880	0.45
116.4	1890	6300	0.45	35.5	580	1920	0.45
118.0	1920	6120	0.45	36.0	590	1860	0.45
119.7	1860	6240	0.45	36.5	570	1900	0.45
121.3	1800	6210	0.45	37.0	550	1890	0.45
122.9	1690	6390	0.46	37.5	510	1950	0.46
124.6	1570	6210	0.47	38.0	480	1890	0.47
126.2	1470	6240	0.47	38.5	450	1900	0.47
127.9	1690	6630	0.47	39.0	510	2020	0.47
129.5	1830	6430	0.46	39.5	560	1960	0.46

Summary of Compressional Wave Velocity, Shear Wave Velocity, and Poisson's Ratio Based on Source-to-Receiver Travel Time Data - Borehole WLA B-1

American Units			
Depth at Midpoint Between Source and Near Receiver	Velocity		Poisson's Ratio
	V_s	V_p	
(ft)	(ft/s)	(ft/s)	
131.1	2070	6590	0.45
132.8	2490	6730	0.42
134.4	2380	6840	0.43
136.1	2290	6770	0.44
137.7	2240	6880	0.44
139.3	2240	6730	0.44
141.0	2190	6590	0.44
142.6	2190	6630	0.44
144.3	2190	6590	0.44
145.9	2110	6590	0.44
147.6	2150	6630	0.44
149.2	2150	6530	0.44
150.8	2190	6530	0.44

Metric Units			
Depth at Midpoint Between Source and Near Receiver	Velocity		Poisson's Ratio
	V_s	V_p	
(m)	(m/s)	(m/s)	
40.0	630	2010	0.45
40.5	760	2050	0.42
41.0	730	2090	0.43
41.5	700	2060	0.44
42.0	680	2100	0.44
42.5	680	2050	0.44
43.0	670	2010	0.44
43.5	670	2020	0.44
44.0	670	2010	0.44
44.5	640	2010	0.44
45.0	650	2020	0.44
45.5	650	1990	0.44
46.0	670	1990	0.44

Notes: "-" means no data available at that particular interval of depth.

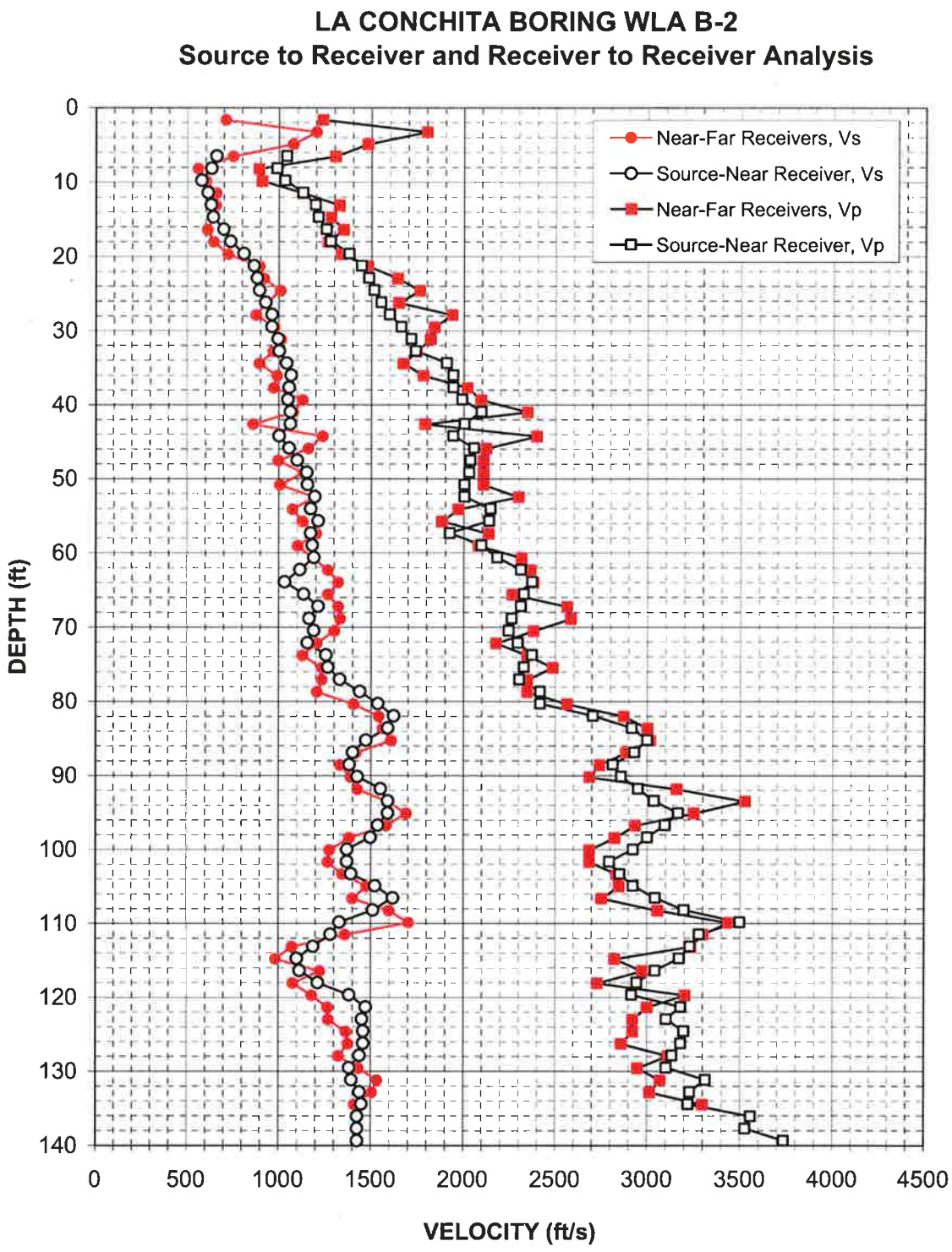

Figure A-2: Boring B-2, Suspension S-R1 P- and S_H-wave velocities

Table A-2. Boring B-2, Suspension S-R1 depths and P- and S_H-wave velocities

Summary of Compressional Wave Velocity, Shear Wave Velocity, and Poisson's Ratio Based on Source-to-Receiver Travel Time Data - Borehole WLA B-2

American Units			
Depth at Midpoint Between Source and Near Receiver	Velocity		Poisson's Ratio
	V_s	V_p	
(ft)	(ft/s)	(ft/s)	
6.5	660	1040	0.17
8.1	630	990	0.16
9.8	580	1030	0.27
11.4	610	1130	0.29
13.0	630	1200	0.31
14.7	640	1210	0.31
16.3	700	1260	0.28
18.0	740	1280	0.25
19.6	810	1380	0.24
21.2	860	1450	0.22
22.9	880	1490	0.23
24.5	890	1510	0.23
26.2	930	1550	0.22
27.8	960	1600	0.22
29.4	960	1660	0.25
31.1	1000	1720	0.25
32.7	1000	1740	0.25
34.4	1040	1910	0.29
36.0	1070	1940	0.28
37.6	1060	1940	0.29
39.3	1050	1990	0.31
40.9	1060	2100	0.33
42.6	1060	2000	0.30
44.2	1000	1940	0.32
45.8	1060	2060	0.32
47.5	1100	2040	0.29
49.1	1150	2030	0.26
50.8	1160	2000	0.25
52.4	1190	2000	0.22
54.0	1170	2150	0.29
55.7	1210	2140	0.26
57.3	1170	1920	0.20
59.0	1180	2100	0.27
60.6	1190	2180	0.29
62.2	1110	2310	0.35
63.9	1030	2370	0.38
65.5	1130	2330	0.34

Metric Units			
Depth at Midpoint Between Source and Near Receiver	Velocity		Poisson's Ratio
	V_s	V_p	
(m)	(m/s)	(m/s)	
2.0	200	320	0.17
2.5	190	300	0.16
3.0	180	310	0.27
3.5	190	340	0.29
4.0	190	360	0.31
4.5	200	370	0.31
5.0	210	380	0.28
5.5	220	390	0.25
6.0	250	420	0.24
6.5	260	440	0.22
7.0	270	450	0.23
7.5	270	460	0.23
8.0	280	470	0.22
8.5	290	490	0.22
9.0	290	510	0.25
9.5	300	520	0.25
10.0	310	530	0.25
10.5	320	580	0.29
11.0	320	590	0.28
11.5	320	590	0.29
12.0	320	610	0.31
12.5	320	640	0.33
13.0	320	610	0.30
13.5	310	590	0.32
14.0	320	630	0.32
14.5	330	620	0.29
15.0	350	620	0.26
15.5	350	610	0.25
16.0	360	610	0.22
16.5	360	650	0.29
17.0	370	650	0.26
17.5	360	590	0.20
18.0	360	640	0.27
18.5	360	670	0.29
19.0	340	700	0.35
19.5	310	720	0.38
20.0	350	710	0.34

Summary of Compressional Wave Velocity, Shear Wave Velocity, and Poisson's Ratio Based on Source-to-Receiver Travel Time Data - Borehole WLA B-2

American Units			
Depth at Midpoint Between Source and Near Receiver	Velocity		Poisson's Ratio
	V_s	V_p	
(ft)	(ft/s)	(ft/s)	
67.2	1210	2310	0.31
68.8	1160	2260	0.32
70.5	1190	2240	0.30
72.1	1160	2290	0.33
73.7	1260	2370	0.30
75.4	1270	2330	0.29
77.0	1330	2300	0.25
78.7	1440	2420	0.23
80.3	1540	2420	0.16
81.9	1620	2710	0.22
83.6	1590	2920	0.29
85.2	1470	3000	0.34
86.9	1400	2930	0.35
88.5	1380	2810	0.34
90.1	1430	2860	0.33
91.8	1550	2950	0.31
93.4	1590	3040	0.31
95.1	1590	3170	0.33
96.7	1540	3100	0.34
98.3	1500	3000	0.33
100.0	1370	2920	0.36
101.6	1370	2790	0.34
103.3	1390	2850	0.34
104.9	1520	2920	0.31
106.5	1620	3040	0.30
108.2	1510	3200	0.36
109.8	1330	3500	0.42
111.5	1280	3280	0.41
113.1	1190	3230	0.42
114.7	1100	3170	0.43
116.4	1110	3040	0.42
118.0	1210	2940	0.40
119.7	1380	2920	0.36
121.3	1470	3180	0.36
122.9	1450	3100	0.36
124.6	1460	3200	0.37
126.2	1460	3180	0.37
127.9	1440	3130	0.37
129.5	1380	3100	0.38

Metric Units			
Depth at Midpoint Between Source and Near Receiver	Velocity		Poisson's Ratio
	V_s	V_p	
(m)	(m/s)	(m/s)	
20.5	370	700	0.31
21.0	350	690	0.32
21.5	360	680	0.30
22.0	350	700	0.33
22.5	380	720	0.30
23.0	390	710	0.29
23.5	410	700	0.25
24.0	440	740	0.23
24.5	470	740	0.16
25.0	490	820	0.22
25.5	480	890	0.29
26.0	450	910	0.34
26.5	430	890	0.35
27.0	420	860	0.34
27.5	430	870	0.33
28.0	470	900	0.31
28.5	480	930	0.31
29.0	480	960	0.33
29.5	470	940	0.34
30.0	460	910	0.33
30.5	420	890	0.36
31.0	420	850	0.34
31.5	420	870	0.34
32.0	460	890	0.31
32.5	490	930	0.30
33.0	460	970	0.36
33.5	410	1070	0.42
34.0	390	1000	0.41
34.5	360	980	0.42
35.0	330	970	0.43
35.5	340	930	0.42
36.0	370	900	0.40
36.5	420	890	0.36
37.0	450	970	0.36
37.5	440	950	0.36
38.0	440	970	0.37
38.5	440	970	0.37
39.0	440	960	0.37
39.5	420	950	0.38

Summary of Compressional Wave Velocity, Shear Wave Velocity, and Poisson's Ratio Based on Source-to-Receiver Travel Time Data - Borehole WLA B-2

American Units			
Depth at Midpoint Between Source and Near Receiver	Velocity		Poisson's Ratio
	V_s	V_p	
(ft)	(ft/s)	(ft/s)	
131.1	1390	3310	0.39
132.8	1440	3230	0.38
134.4	1450	3220	0.37
136.1	1430	3560	0.40
137.7	1430	3530	0.40
139.3	1430	3730	0.41

Metric Units			
Depth at Midpoint Between Source and Near Receiver	Velocity		Poisson's Ratio
	V_s	V_p	
(m)	(m/s)	(m/s)	
40.0	420	1010	0.39
40.5	440	980	0.38
41.0	440	980	0.37
41.5	430	1080	0.40
42.0	430	1070	0.40
42.5	430	1140	0.41

Notes: "-" means no data available at that particular interval of depth.

APPENDIX B

GEOPHYSICAL LOGGING SYSTEMS - NIST TRACEABLE CALIBRATION PROCEDURES AND CALIBRATION RECORDS

CALIBRATION PROCEDURE FOR

GEOVision SEISMIC RECORDER/LOGGER

Reviewed 4/6/06

Objective

The timing/sampling accuracy of seismic recorders or data loggers is required for several GEOVision field procedures including Seismic Refraction, Downhole Seismic Velocity Logging, and P-S Suspension Logging. This procedure describes the method for measuring the timing accuracy of a seismic data logger, such as the OYO Model 170, OYO/Robertson Model 3403, Geometrics Strataview or Geometrics Geode. The objective of this procedure is to verify that the timing accuracy of the recorder is accurate to within 1%.

Frequency of Calibration

The calibration of each GEOVision seismic data logger is twelve (12) months. In the case of rented seismic data loggers, calibration must be performed prior to use.

Test Equipment Required

The following equipment is required. Item #2 must have current NIST traceable calibration.

1. Function generator, Krohn Hite 5400B or equivalent
2. Frequency counter, HP 5315A or equivalent
3. Test cables, from item 1 to item 2, and from item 1 to subject data logger.

Procedure

This procedure is designed to be performed using the accompanying Seismograph Calibration Data Sheet with the same revision number. All data must be entered and the procedure signed by the technician performing the test.

1. Record all identification data on the form provided.
2. Connect function generator to data logger (such as OYO Model 170) using test cable
3. Connect the function generator to the frequency counter using test cable.

4. Set up generator to produce a 100.0 Hz, 0.25 volt (amplitude is approximate, modify as necessary to yield less than full scale waveforms on logger display) peak square wave or sine wave. Verify frequency using the counter and initial space on the data sheet.

5. Initialize data logger and record a data record of at least 0.1 second using a 100 microsecond or less sample period.

6. Measure the recorded square wave frequency by measuring the duration of 9 cycles of data. This measurement can be made using the data logger display device, or by printing out a paper tape. If a paper tape can be printed, the resulting printout must be attached to this procedure. Record the data in the space provided.

7. Repeat steps 5 and 6 three more times using separate files.

Criteria

The duration for 9 cycles in any file must be 90.0 milliseconds plus or minus 0.9 milliseconds, corresponding to an average frequency for the nine cycles of 100.0 Hz plus or minus 1 Hz (obtained by dividing 9 cycles by the duration in milliseconds).

If the results are outside this range, the data logger must be marked with a GEOVision REJECT tag until it can be repaired and retested.

If results are acceptable affix label indicating the initials of the person performing the calibration, the date of calibration, and the due date for the next calibration (12 months).

Procedure Approval

Approved by:

John G. Diehl	President
Name	Title
Signature	April 6, 2006
	Date

Client Approval (if required):

Name	Title
Signature	Date

EDISON ESI℠
A SOUTHERN CALIFORNIA EDISON® Company
Metrology
7300 Fenwick Lane
Westminster, CA 92683
Phone: 866-723-2257

Calibration Report

NVLAP Accredited
Calibration

GEOVision Geophysical Services
1151 Pomona Road, Unit P
Corona, CA 92882

TEST NUMBER
527436

NVLAP®
Lab Code:105014-0

Manufacturer:	Oyo
Model Number:	03331-0000
Description:	Seismograph,
Asset Number:	15014
Serial Number:	15014
PO Number:	7087-070315-01

Condition As Found:	In Tolerance
Condition As Left:	In Tolerance
Calibration Date:	04/13/2007
Calibration Due Date:	04/13/2008
Calibration Interval:	12 Months

Remarks:

The UUT (unit under test) was calibrated using the customer's procedure. The UUT was operated by the customer's personnel and data collection was observed by SCE personnel. The UUT was found to be in tolerance to customer supplied specifications. Frequency is accredited. Please see attached data.

Standards Utilized

I.D.No.	Mfg.	Model No.	Description	Cal. Date	Due Date
S1-03092	Hewlett Packard	5335A OPT 020, 30,40	Counter, Universal,	12/12/2006	06/12/2007
S1-03355	Hewlett Packard	3325B OPT 001, 002	Generator, Function, Synthesizer	11/08/2006	11/08/2007
S1-03686	Fluke	910	Standard, Frequency, Controlled, Gps	01/18/2007	01/18/2008

Procedure: Customer
Temperature: 23° C
Humidity: 38% RH
Test No.: 527436

Calibration Performed By:			Quality Reviewed:	
Branson, Craig A	Metrologist	714-895-0714	Rhonda E. Stinson	4/13/07
Name	Title	Phone	Name	Date

GEOVision
geophysical services

SEISMOGRAPH CALIBRATION DATA SHEET REV 4/6/06

INSTRUMENT DATA

SYSTEM MFR:	OYO	MODEL NO.:	3331
SERIAL NO.:	15014	CALIBRATION DATE:	04/13/2007
BY:	ROBERT STELLER	DUE DATE:	04/13/2008
COUNTER MFR:	HEWLETT PACKARD	MODEL NO.:	5335A
SERIAL NO.:	2626A10854	CALIBRATION DATE:	12/12/2006
BY:	SCE #S1-03092	DUE DATE:	06/12/2007
FCTN GEN MFR:	HEWLETT PACKARD	MODEL NO.:	3325B
SERIAL NO.:	2847A14447	CALIBRATION DATE:	11/08/2006
BY:	SCE #S1-03355	DUE DATE:	11/08/2007

SYSTEM SETTINGS:

GAIN:	10
FILTER:	20 KHZ
RANGE:	100 MILLISEC
DELAY:	0
STACK: 1 (STD)	1
PULSE:	1.6
DISPLAY:	NA
SYSTEM: DATE = CORRECT DATE & TIME	04/13/2007, 09:21AM

PROCEDURE:
SET FREQUENCY TO 100.0HZ SQUAREWAVE WITH AMPLITUDE APPROXIMATELY 0.25 VOLT PEAK. RECORD BOTH ON DISK AND PAPER TAPE, IF AVAILABLE. ANALYZE AND PRINT WAVEFORMS FROM ANALYSIS UTILITY. ATTACH PAPER COPIES OF PRINTOUT AND PAPER TAPES, IF AVAILABLE, TO THIS FORM. AVERAGE FREQUENCY MUST BE BETWEEN 99.0 AND 101.0 HZ.

AS FOUND 100.0 AS LEFT 100.0

WAVEFORM	FILE NO	FREQUENCY	TIME FOR 9 CYCLES Hn	TIME FOR 9 CYCLES Hr	TIME FOR 9 CYCLES V	AVERAGE FREQ.
SQUARE	201	100.0	90.0	90.0	90.0	100.0
SQUARE	202	100.0	90.0	90.0	90.0	100.0
SINE	203	100.0	90.0	90.0	90.0	100.0
SINE	204	100.0	90.0	90.0	90.0	100.0

CALIBRATED BY: ROBERT STELLER (NAME) 04/13/2007 (DATE) Robt Steller (SIGNATURE)

OYO S/N 15014

Suspension 170 1.42

ID_NO. : 201
HOLE NO. : 0
DEPTH : 0.0 [m]
DATE : 13/04/07 09:23:34 AM
H-SAMPLE RATE: 100 [μSEC]
V-SAMPLE RATE: 100 [μSEC]
PULSE WIDTH : 1.6 [mSEC]
DELAY TIME : 0 [mSEC]

	H1	/H1	V1	H2	/H2	V2
GAIN	X 10	X 10	X 10	X 10	X 10	X 10
LCF[Hz]	5	5	5	5	5	5
HCF[Hz]	20K	20K	20K	20K	20K	20K
STACK	1	1	1	1	1	1

TRACE SIZE : 1
H-TIME SCALE: 1.00 [mSEC/LINE]
V-TIME SCALE: 1.00 [mSEC/LINE]

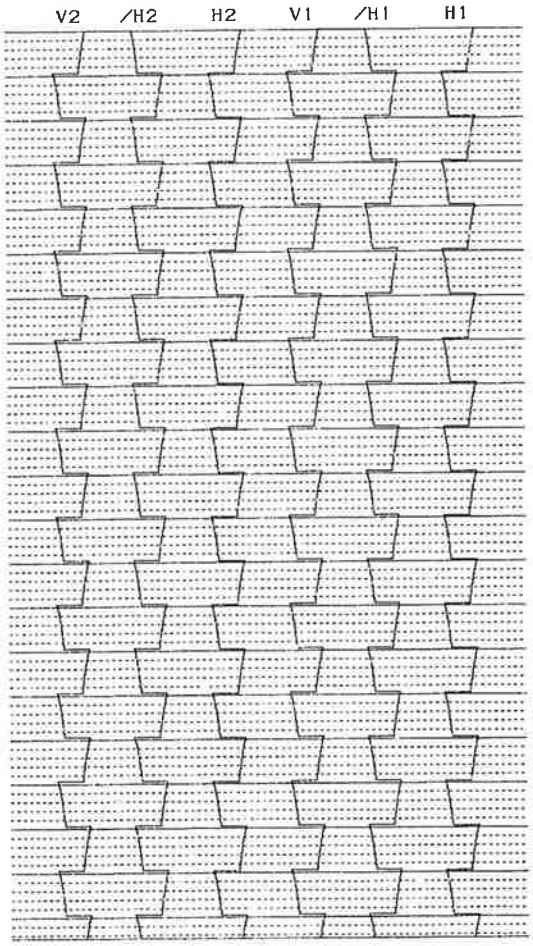

OYO S/N 15014

Suspension 170 1.42

ID_NO. : 202
HOLE NO. : 0
DEPTH : 0.0 [m]
DATE : 13/04/07 09:24:47 AM
H-SAMPLE RATE: 100 [μSEC]
V-SAMPLE RATE: 100 [μSEC]
PULSE WIDTH : 1.6 [mSEC]
DELAY TIME : 0 [mSEC]

	H1	/H1	V1	H2	/H2	V2
GAIN	X 10	X 10	X 10	X 10	X 10	X 10
LCF[Hz]	5	5	5	5	5	5
HCF[Hz]	20K	20K	20K	20K	20K	20K
STACK	1	1	1	1	1	1

TRACE SIZE : 1
H-TIME SCALE: 1.00 [mSEC/LINE]
V-TIME SCALE: 1.00 [mSEC/LINE]

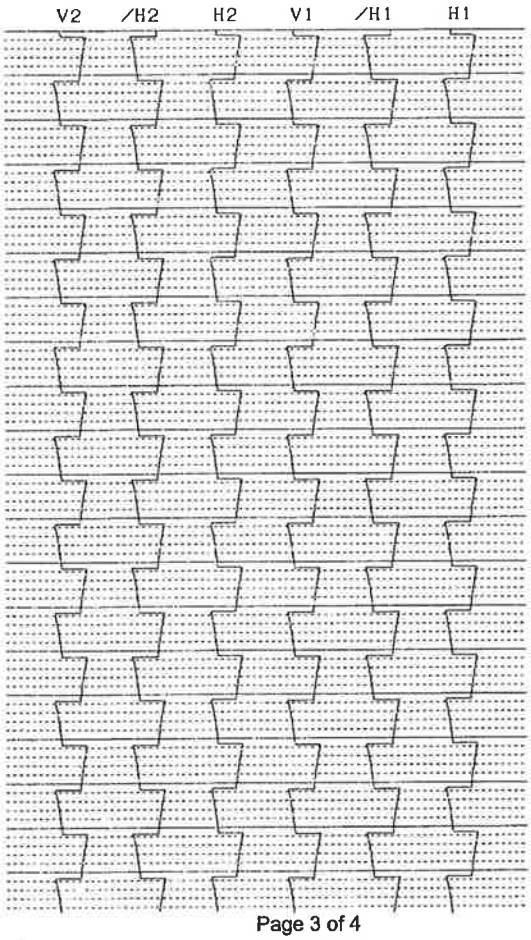

OYO S/N 15014

Suspension 170 1.42

ID_NO. : 203
HOLE NO. : 0
DEPTH : 0.0 [m]
DATE : 13/04/07 09:25:23 AM
H-SAMPLE RATE: 100 [μSEC]
V-SAMPLE RATE: 100 [μSEC]
PULSE WIDTH : 1.6 [mSEC]
DELAY TIME : 0 [mSEC]

	H1	/H1	V1	H2	/H2	V2
GAIN	X 10	X 10	X 10	X 10	X 10	X 10
LCF[Hz]	5	5	5	5	5	5
HCF[Hz]	20K	20K	20K	20K	20K	20K
STACK	1	1	1	1	1	1

TRACE SIZE : 1
H-TIME SCALE: 1.00 [mSEC/LINE]
V-TIME SCALE: 1.00 [mSEC/LINE]

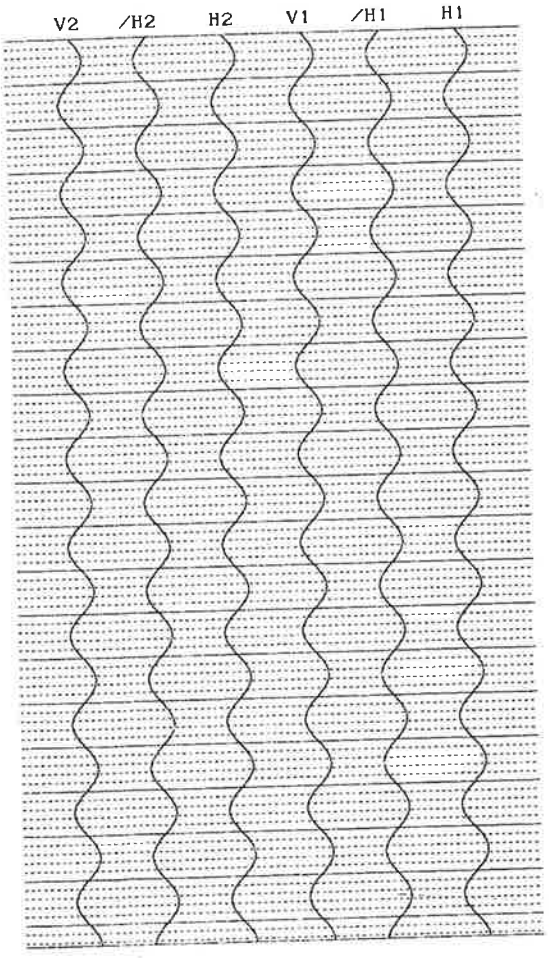

OYO S/N 15014

Suspension 170 1.42

ID_NO. : 204
HOLE NO. : 0
DEPTH : 0.0 [m]
DATE : 13/04/07 09:26:03 AM
H-SAMPLE RATE: 100 [μSEC]
V-SAMPLE RATE: 100 [μSEC]
PULSE WIDTH : 1.6 [mSEC]
DELAY TIME : 0 [mSEC]

	H1	/H1	V1	H2	/H2	V2
GAIN	X 10	X 10	X 10	X 10	X 10	X 10
LCF[Hz]	5	5	5	5	5	5
HCF[Hz]	20K	20K	20K	20K	20K	20K
STACK	1	1	1	1	1	1

TRACE SIZE : 1
H-TIME SCALE: 1.00 [mSEC/LINE]
V-TIME SCALE: 1.00 [mSEC/LINE]

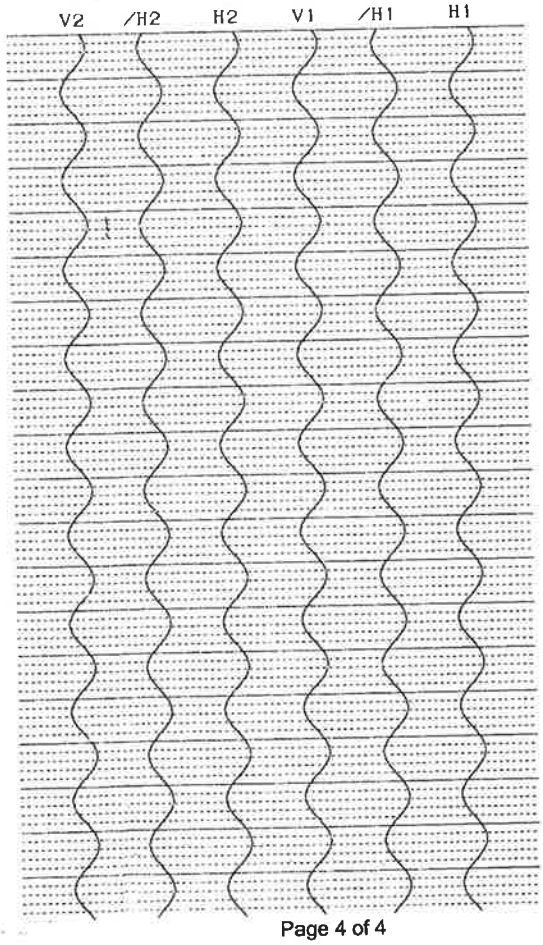

GEOVision Borehole Geophysics depth wheel verification

Performed by Robert Steller on September 23, 2006

	Depth reading in #1	Depth reading out	Depth reading in #2
Depth wheel S/N 101 500 pulse/revolution Circumference = 983mm (3225.07 millifeet)	100.1 feet (30.51 m)	99.95 feet (30.46 m)	100.05 feet (30.50 m)
Depth wheel S/N 102 500 pulse/revolution Circumference = 994mm (3261.15 millifeet)	100.00 feet (30.48) m	100.05 feet (30.50 m)	100.00 feet (30.48) m
Aries winch 200 pulse/revolution Circumference = 305.9mm (1003.51 millifeet)	100.05 feet (30.50) m	100.05 feet (30.50 m)	100.00 feet (30.48) m
Depth wheel S/N 103 500 pulse/revolution Circumference = 1000mm (3.281 feet)			
Comprobe winch 500 pulse/revolution Circumference = 1000mm (3.281 feet)			

All measurements taken with a Stanley 100ft flexible stainless steel tape model number 34-130, and a Keeson 300 foot fiberglass tape, both marked in feet, inches and 1/8ths of inches. Enough cable was spooled off of the winch to allow the cable and tape measures to be laid flat on the parking lot surface side-by-side. A permanent marker was used to mark a 100.0 foot interval on the cable, and the marks were also tagged with electrical tape for visibility. The cable was then spooled back onto the winch. When the first mark was at the top of the measuring wheel, a matching permanent mark was placed, and the recording system (Robertson Micrologger) was set to 0.0 feet depth. The cable was spooled in to the second mark, and the distance was recorded. The recording system was set to 0.0 feet again, and the cable spooled out to the first mark again, and the distance was recorded. The process was repeated one more time to spool the cable back onto the winch, and the distance was recorded.

Estimated accuracy is of these measurements is +/- 0.1 foot or +/- 0.03m.

GEOVision Suspension PS probe Receiver 1–Receiver 2 (R1-R2) spacing verification

Performed by Robert Steller on September 23, 2006

	R2 center to R1 center hanging dry	R2 center to R1 center hanging submerged	R1 bottom to source center hanging submerged with 1m isolation tube S/N 280068
Receiver S/N 30086	40.2in 1.02m	40.0in 1.02m	76.0in 1.93m
Receiver S/N 20042	39.8in 1.01m	39.6in 1.01m	75.7in 1.92m
Receiver S/N 12008	40.2in 1.02m	40.0in 1.02m	76.0in 1.93m

All measurements taken with a Lufkin 3.7m flexible steel tape model number HV1034DM, marked in mm and 100th of feet. Probe suspended in 3-inch diameter clear PVC pipe, using chain clamp placed between bottom and center of Receiver 2 hard section (See Figure). Probe "bounced" to establish unrestricted hanging length before measurement. Probe allowed to relax for 5 minutes prior to each measurement. Water level set to submerge bottom of Receiver 2 hard section.. Estimated accuracy due to hysterisis in rubber section approximately +/- 0.01' or +/- 0.003m.

APPENDIX E: RADIOCARBON DATING LABORATORY RESULTS

Consistent Accuracy
Delivered On Time.

Beta Analytic Inc.
4985 SW 74 Court
Miami, Florida 33155 USA
Tel: 305 667 5167
Fax: 305 663 0964
beta@radiocarbon.com
www.radiocarbon.com

MR. DARDEN HOOD
Director

Mr. Ronald Hatfield
Mr. Christopher Patrick
Deputy Directors

November 21, 2007

Mr. Christopher Hitchcock
William Lettis and Associates
1777 Botelho Drive, Suite 262
Walnut Creek, CA 94596
USA

RE: Radiocarbon Dating Results For Samples BA2-1, BA2-2, BA4-S1-65

Dear Mr. Hitchcock:

Enclosed are the radiocarbon dating results for three samples recently sent to us. They each provided plenty of carbon for accurate measurements and all the analyses proceeded normally. As usual, the method of analysis is listed on the report with the results and calibration data is provided where applicable.

As always, no students or intern researchers who would necessarily be distracted with other obligations and priorities were used in the analyses. We analyzed them with the combined attention of our entire professional staff.

If you have specific questions about the analyses, please contact us. We are always available to answer your questions.

Our invoice is enclosed. Please, forward it to the appropriate officer or send VISA charge authorization. Thank you. As always, if you have any questions or would like to discuss the results, don't hesitate to contact me.

Sincerely,

Darden Hood

BETA

BETA ANALYTIC INC.

DR. M.A. TAMERS and MR. D.G. HOOD

UNIVERSITY BRANCH
4985 S.W. 74 COURT
MIAMI, FLORIDA, USA 33155
PH: 305/667-5167 FAX: 305/663-0964
E-MAIL: beta@radiocarbon.com

REPORT OF RADIOCARBON DATING ANALYSES

Mr. Christopher Hitchcock

Report Date: 11/21/2007

William Lettis and Associates

Material Received: 10/19/2007

Sample Data	Measured Radiocarbon Age	13C/12C Ratio	Conventional Radiocarbon Age(*)
Beta - 236230	1200 +/- 40 BP	-25.8 o/oo	1190 +/- 40 BP
SAMPLE : BA2-1			
ANALYSIS : AMS-Standard delivery			
MATERIAL/PRETREATMENT : (charred material): acid/alkali/acid			
2 SIGMA CALIBRATION : Cal AD 710 to 750 (Cal BP 1240 to 1200) AND Cal AD 760 to 900 (Cal BP 1190 to 1050) Cal AD 920 to 960 (Cal BP 1040 to 990)			
Beta - 236231	1570 +/- 40 BP	-23.8 o/oo	1590 +/- 40 BP
SAMPLE : BA2-2			
ANALYSIS : AMS-Standard delivery			
MATERIAL/PRETREATMENT : (charred material): acid/alkali/acid			
2 SIGMA CALIBRATION : Cal AD 390 to 560 (Cal BP 1560 to 1390)			
Beta - 237365	9910 +/- 60 BP	-22.5 o/oo	9950 +/- 60 BP
SAMPLE : BA4-S1-65			
ANALYSIS : AMS-Standard delivery			
MATERIAL/PRETREATMENT : (organic sediment): acid washes			
2 SIGMA CALIBRATION : Cal BC 9740 to 9730 (Cal BP 11690 to 11680) AND Cal BC 9680 to 9280 (Cal BP 11630 to 11230)			

Dates are reported as RCYBP (raduicarbon years before present, "present" = 1950A.D.). By International convention, the modern reference standard was 95% of the C14 content of the National Bureau of Standards' Oxalic Acid & calculated using the Libby C14 half life (5568 years). Quoted errors represent 1 standard deviation statistics (68% probability) & are based on combined measurements of the sample, background, and modern reference standards.

Measured C13/C12 ratios were calculated relative to the PDB-1 international standard and the RCYBP ages were normalized to -25 per mil. If the ratio and age are accompanied by an (*), then the C13/C12 value was estimated, based on values typical of the material type. The quoted results are NOT calibrated to calendar years. Calibration to calendar years should be calculated using the Conventional C14 age.

CALIBRATION OF RADIOCARBON AGE TO CALENDAR YEARS

(Variables: C13/C12=-25.8:lab. mult=1)

Laboratory number: **Beta-236230**

Conventional radiocarbon age: **1190±40 BP**

2 Sigma calibrated results: (95% probability) **Cal AD 710 to 750 (Cal BP 1240 to 1200) and Cal AD 760 to 900 (Cal BP 1190 to 1050) and Cal AD 920 to 960 (Cal BP 1040 to 990)**

Intercept data

Intercept of radiocarbon age with calibration curve: Cal AD 870 (Cal BP 1080)

1 Sigma calibrated result: (68% probability) Cal AD 780 to 890 (Cal BP 1170 to 1060)

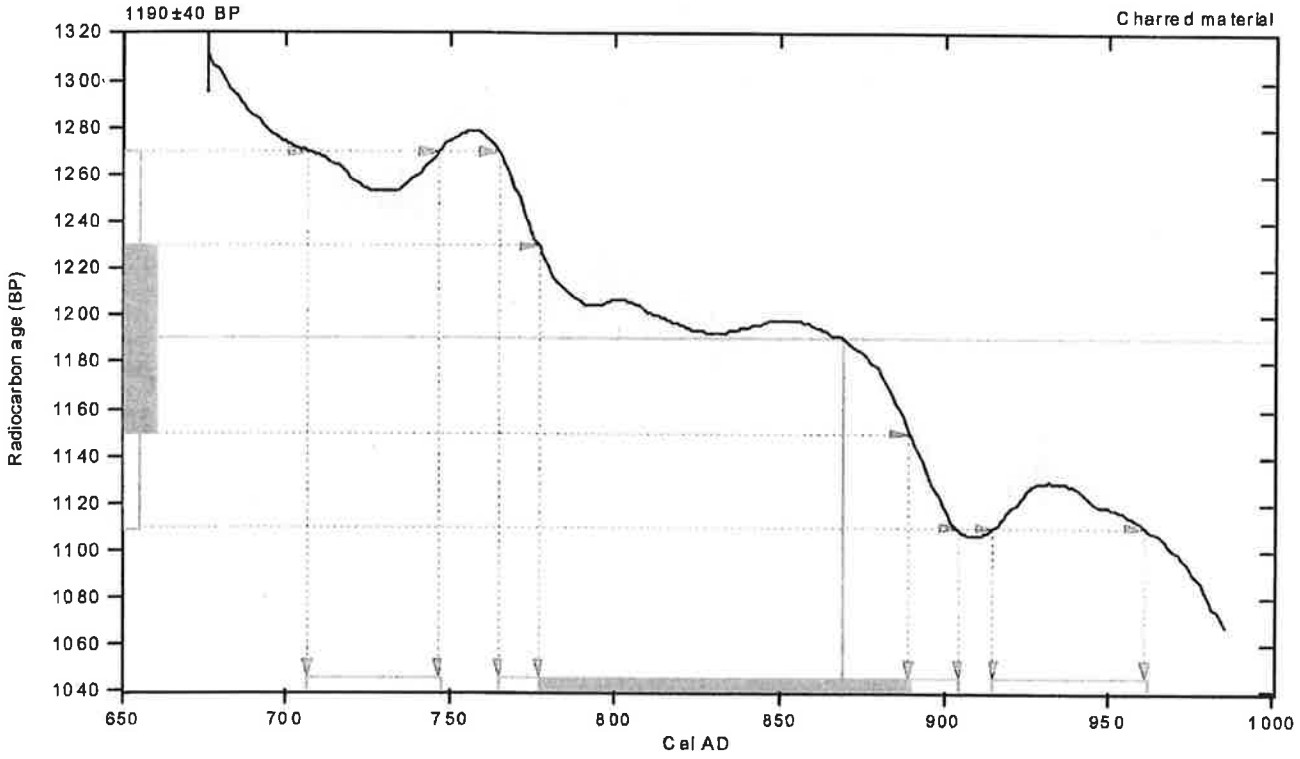

References:

Database used

INTCAL04

Calibration Database

INTCAL04 Radiocarbon Age Calibration

IntCal04: Calibration Issue of Radiocarbon (Volume 46, nr 3, 2004).

Mathematics

A Simplified Approach to Calibrating C14 Dates

Talma, A. S., Vogel, J. C., 1993, Radiocarbon 35(2), p317-322

Beta Analytic Radiocarbon Dating Laboratory

4985 S.W. 74th Court, Miami, Florida 33155 • Tel: (305)667-5167 • Fax: (305)663-0964 • E-Mail: beta@radiocarbon.com

CALIBRATION OF RADIOCARBON AGE TO CALENDAR YEARS

(Variables: C13/C12=-23.8:lab. mult=1)

Laboratory number: **Beta-236231**

Conventional radiocarbon age: **1590±40 BP**

2 Sigma calibrated result: (95% probability) **Cal AD 390 to 560 (Cal BP 1560 to 1390)**

Intercept data

Intercept of radiocarbon age with calibration curve: Cal AD 430 (Cal BP 1520)

1 Sigma calibrated result: (68% probability) Cal AD 420 to 540 (Cal BP 1530 to 1410)

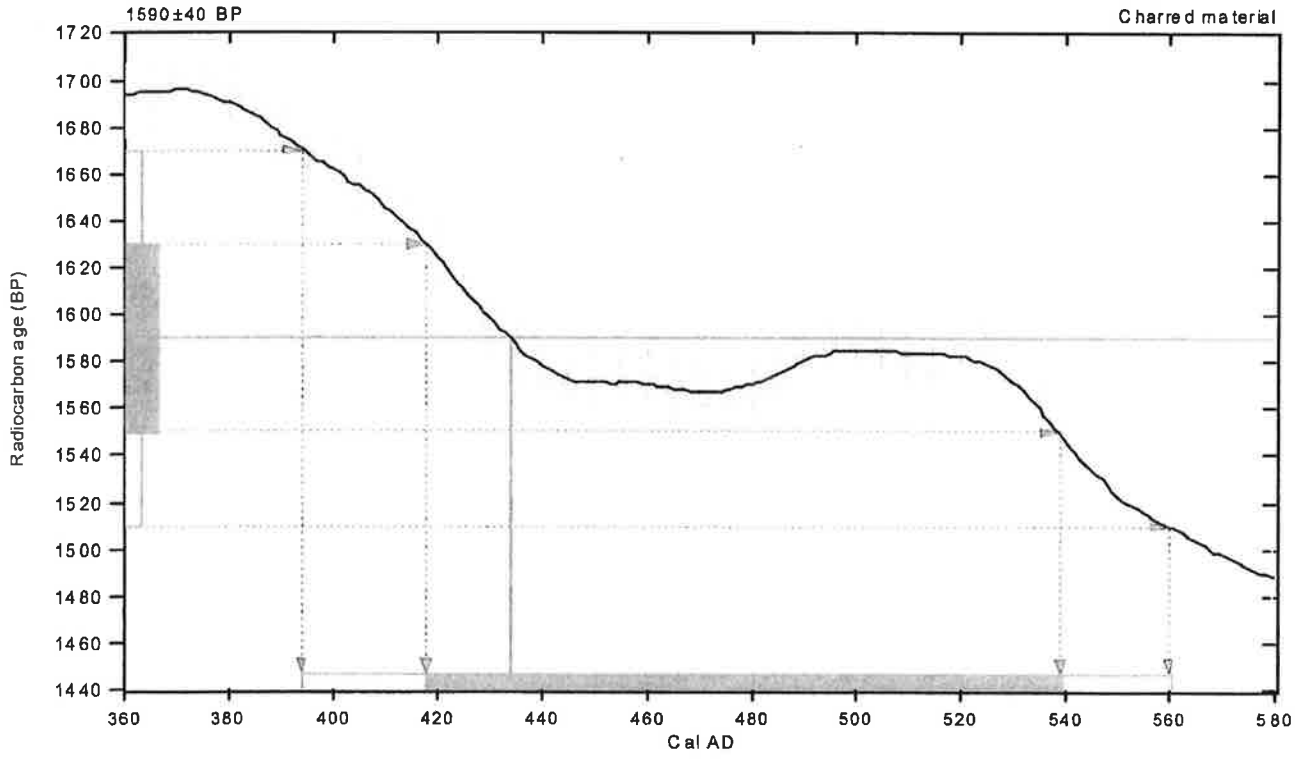

References:

Database used

INTCAL04

Calibration Database

INTCAL04 Radiocarbon Age Calibration

IntCal04: Calibration Issue of Radiocarbon (Volume 46, nr 3, 2004).

Mathematics

A Simplified Approach to Calibrating C14 Dates

Talma, A. S., Vogel, J. C., 1993, Radiocarbon 35(2), p317-322

Beta Analytic Radiocarbon Dating Laboratory

4985 S.W. 74th Court, Miami, Florida 33155 • Tel: (305)667-5167 • Fax: (305)663-0964 • E-Mail: beta@radiocarbon.com

CALIBRATION OF RADIOCARBON AGE TO CALENDAR YEARS

(Variables: C13/C12=-22.5:lab. mult=1)

Laboratory number: **Beta-237365**

Conventional radiocarbon age: **9950±60 BP**

2 Sigma calibrated results: (95% probability) **Cal BC 9740 to 9730 (Cal BP 11690 to 11680) and Cal BC 9680 to 9280 (Cal BP 11630 to 11230)**

Intercept data

Intercept of radiocarbon age with calibration curve: Cal BC 9370 (Cal BP 11320)

1 Sigma calibrated result: (68% probability) Cal BC 9450 to 9310 (Cal BP 11400 to 11260)

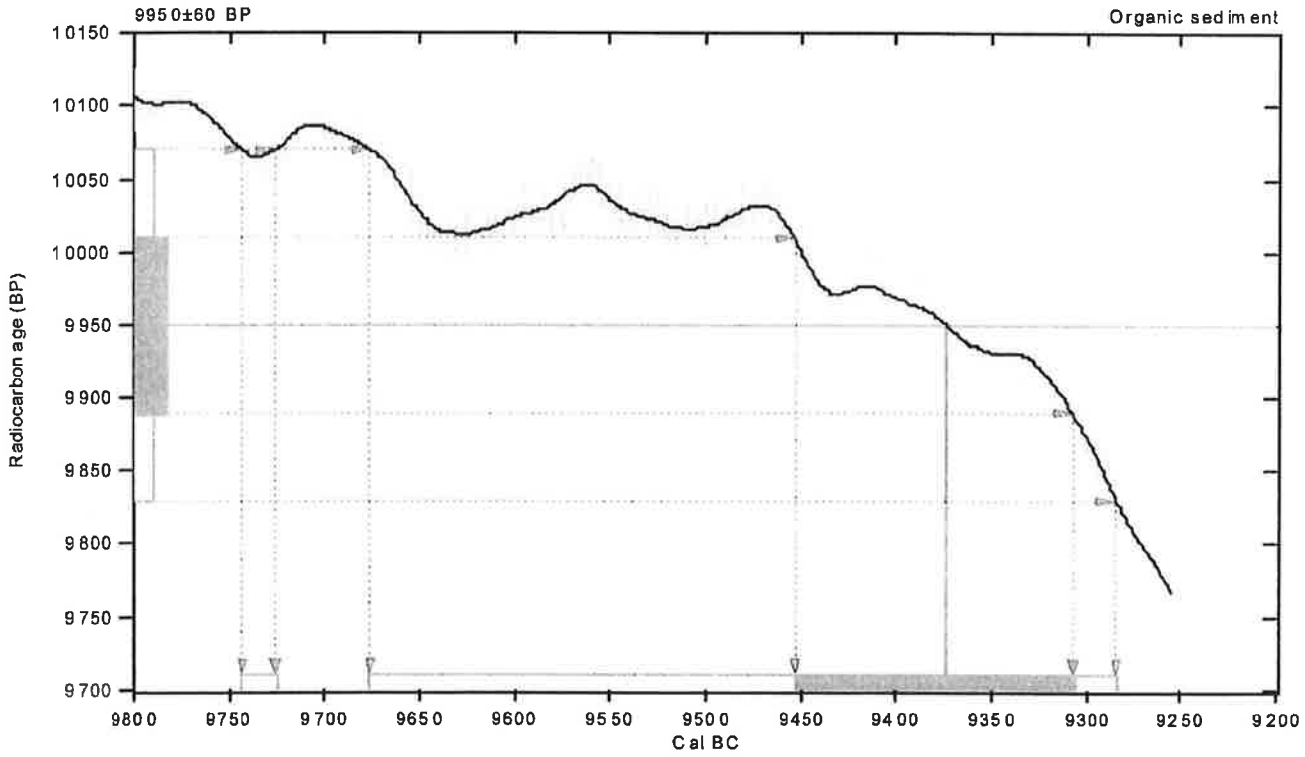

References:

Database used

INTCAL04

Calibration Database

INTCAL04 Radiocarbon Age Calibration

IntCal04: Calibration Issue of Radiocarbon (Volume 46, nr 3, 2004).

Mathematics

A Simplified Approach to Calibrating C14 Dates

Talma, A. S., Vogel, J. C., 1993, Radiocarbon 35(2), p317-322

Beta Analytic Radiocarbon Dating Laboratory

4985 S.W. 74th Court, Miami, Florida 33155 • Tel: (305)667-5167 • Fax: (305)663-0964 • E-Mail: beta@radiocarbon.com

BETA ANALYYTIC INC. - 4985 SW 74 Court, Miami, Florida 33155 USA - Tel: 305-667-5167 - Fax 305-663-0964 - beta@radiocarbon.com

PRETREATMENT GLOSSARY
Standard Pretreatment Protocols at Beta Analytic

Unless otherwise requested by a submitter or discussed in a final date report, the following procedures apply to pretreatment of samples submitted for analysis. This glossary defines the pretreatment methods applied to each result listed on the date report form (e.g. you will see the designation "acid/alkali/acid" listed along with the result for a charcoal sample receiving such pretreatment).

Pretreatment of submitted materials is required to eliminate secondary carbon components. These components, if not eliminated, could result in a radiocarbon date, which is too young or too old. Pretreatment does not ensure that the radiocarbon date will represent the time event of interest. This is determined by the sample integrity. Effects such as the old wood effect, burned intrusive roots, bioturbation, secondary deposition, secondary biogenic activity incorporating recent carbon (bacteria) and the analysis of multiple components of differing age are just some examples of potential problems. The pretreatment philosophy is to reduce the sample to a single component, where possible, to minimize the added subjectivity associated with these types of problems. If you suspect your sample requires special pretreatment considerations be sure to tell the laboratory prior to analysis.

"acid/alkali/acid"

The sample was first gently crushed/dispersed in deionized water. It was then given hot HCl acid washes to eliminate carbonates and alkali washes (NaOH) to remove secondary organic acids. The alkali washes were followed by a final acid rinse to neutralize the solution prior to drying. Chemical concentrations, temperatures, exposure times, and number of repetitions, were applied accordingly with the uniqueness of the sample. Each chemical solution was neutralized prior to application of the next. During these serial rinses, mechanical contaminants such as associated sediments and rootlets were eliminated. This type of pretreatment is considered a "full pretreatment". On occasion the report will list the pretreatment as "acid/alkali/acid - insolubles" to specify which fraction of the sample was analyzed. This is done on occasion with sediments (See "acid/alkali/acid - solubles"

Typically applied to: charcoal, wood, some peats, some sediments, and textiles "acid/alkali/acid - solubles"

On occasion the alkali soluble fraction will be analyzed. This is a special case where soil conditions imply
That the soluble fraction will provide a more accurate date. It is also used on some occasions to verify the present/absence or degree of contamination present from secondary organic acids. The sample was first pretreated with acid to remove any carbonates and to weaken organic bonds. After the alkali washes (as discussed above) are used, the solution containing the alkali soluble fraction is isolated/filtered and combined with acid. The soluble fraction, which precipitates, is rinsed and dried prior to combustion.

"acid/alkali/acid/cellulose extraction"

Following full acid/alkali/acid pretreatments, the sample is bathed in (sodium chlorite) $NaClO_2$ under very controlled conditions (Ph = 3, temperature = 70 degrees C). This eliminates all components except wood cellulose. It is useful for woods that are either very old or highly contaminated.

Applied to: wood

"acid washes"

Surface area was increased as much a possible. Solid chunks were crushed, fibrous materials were shredded, and sediments were dispersed. Acid (HCl) was applied repeatedly to ensure the absence of carbonates. Chemical concentrations, temperatures, exposure times, and number of repetitions, were applied accordingly with the uniqueness of each sample. The sample was not be subjected to alkali washes to ensure the absence of secondary organic acids for intentional reasons. The most common reason is that the primary carbon is soluble in the alkali. Dating results reflect the total organic content of the analyzed material. Their accuracy depends on the researcher's ability to subjectively eliminate potential contaminants based on contextual facts.

Typically applied to: organic sediments, some peats, small wood or charcoal, special cases

BETA

Consistent Accuracy ...
Delivered On Time.

Beta Analytic Inc.
4985 SW 74 Court
Miami, Florida 33155 USA
Tel: 305 667 5167
Fax: 305 663 0/97
Beta@radiocarbon.com
Www.radiocarbon.com

Mr. Darden Hood
Director

Mr. Ronald Hatfield
Mr. Christopher Patrick
Deputy Directors

Final Report

The final report package includes the final date report, a statement outlining our analytical procedures, a glossary of pretreatment terms, calendar calibration information, billing documents (containing balance/credit information and the number of samples submitted within the yearly discount period), and peripheral items to use with future submittals. The final report includes the individual analysis method, the delivery basis, the material type and the individual pretreatments applied. The final report has been sent by mail and e-mail (where available).

Pretreatment

Pretreatment methods are reported along with each result. All necessary chemical and mechanical pretreatments of the submitted material were applied at the laboratory to isolate the carbon which may best represent the time event of interest. When interpreting the results, it is important to consider the pretreatments. Some samples cannot be fully pretreated, making their ^{14}C ages more subjective than samples which can be fully pretreated. Some materials receive no pretreatments. Please look at the pretreatment indicated for each sample and read the pretreatment glossary to understand the implications.

Analysis

Materials measured by the radiometric technique were analyzed by synthesizing sample carbon to benzene (92% C), measuring for ^{14}C content in one of 53 scintillation spectrometers, and then calculating for radiocarbon age. If the Extended Counting Service was used, the ^{14}C content was measured for a greatly extended period of time. AMS results were derived from reduction of sample carbon to graphite (100% C), along with standards and backgrounds. The graphite was then detected for ^{14}C content in one of 9 accelerator-mass-spectrometers (AMS) .

The Radiocarbon Age and Calendar Calibration

The "Conventional ^{14}C Age (*)" is the result after applying $^{13}C/^{12}C$ corrections to the measured age and is the most appropriate radiocarbon age. If an "*" is attached to this date, it means the $^{13}C/^{12}C$ was estimated rather than measured (The ratio is an option for radiometric analysis, but included on all AMS analyses.) Ages are reported with the units "BP" (Before Present). "Present" is defined as AD 1950 for the purposes of radiocarbon dating.

Results for samples containing more ^{14}C than the modern reference standard are reported as "percent modern carbon" (pMC). These results indicate the material was respiring carbon after the advent of thermo-nuclear weapons testing (and is less than ~ 50 years old).

Applicable calendar calibrations are included for materials between about 100 and 19,000 BP. If calibrations are not included with a report, those results were either too young, too old, or inappropriate for calibration. Please read the enclosed page discussing calibration.

BETA

Consistent Accuracy ...
Delivered On Time.

Beta Analytic Inc.
4985 SW 74 Court
Miami, Florida 33155 USA
Tel: 305 667 5167
Fax: 305 663 0/97
Beta@radiocarbon.com
Www.radiocarbon.com

Mr. Darden Hood
Director

Mr. Ronald Hatfield
Mr. Christopher Patrick
Deputy Directors

Calendar Calibration at Beta Analytic

Calibrations of radiocarbon age determinations are applied to convert BP results to calendar years. The short-term difference between the two is caused by fluctuations in the heliomagnetic modulation of the galactic cosmic radiation and, recently, large scale burning of fossil fuels and nuclear devices testing. Geomagnetic variations are the probable cause of longer-term differences.

The parameters used for the corrections have been obtained through precise analyses of hundreds of samples taken from known-age tree rings of oak, sequoia, and fir up to about 10,000 BP. Calibration using tree-rings to about 12,000 BP is still being researched and provides somewhat less precise correlation. Beyond that, up to about 20,000 BP, correlation using a modeled curve determined from U/Th measurements on corals is used. This data is still highly subjective. Calibrations are provided up to about 19,000 years BP using the most recent calibration data available.

The Pretoria Calibration Procedure (Radiocarbon, Vol 35, No.1, 1993, pg 317) program has been chosen for these calendar calibrations. It uses splines through the tree-ring data as calibration curves, which eliminates a large part of the statistical scatter of the actual data points. The spline calibration allows adjustment of the average curve by a quantified closeness-of-fit parameter to the measured data points. A single spline is used for the precise correlation data available back to 9900 BP for terrestrial samples and about 6900 BP for marine samples. Beyond that, splines are taken on the error limits of the correlation curve to account for the lack of precision in the data points.

In describing our calibration curves, the solid bars represent one sigma statistics (68% probability) and the hollow bars represent two sigma statistics (95% probability). Marine carbonate samples that have been corrected for $^{13}C/^{12}C$, have also been corrected for both global and local geographic reservoir effects (as published in Radiocarbon, Volume 35, Number 1, 1993) prior to the calibration. Marine carbonates that have not been corrected for $^{13}C/^{12}C$ are adjusted by an assumed value of 0 %0 in addition to the reservoir corrections. Reservoir corrections for fresh water carbonates are usually unknown and are generally not accounted for in those calibrations. In the absence of measured $^{13}C/^{12}C$ ratios, a typical value of -5 %0 is assumed for freshwater carbonates.

(Caveat: the correlation curve for organic materials assume that the material dated was living for exactly ten years (e.g. a collection of 10 individual tree rings taken from the outer portion of a tree that was cut down to produce the sample in the feature dated). For other materials, the maximum and minimum calibrated age ranges given by the computer program are uncertain. The possibility of an "old wood effect" must also be considered, as well as the potential inclusion of younger or older material in matrix samples. Since these factors are indeterminant error in most cases, these calendar calibration results should be used only for illustrative purposes. In the case of carbonates, reservoir correction is theoretical and the local variations are real, highly variable and dependent on provenience. Since imprecision in the correlation data beyond 10,000 years is high, calibrations in this range are likely to change in the future with refinement in the correlation curve. The age ranges and especially the intercept ages generated by the program must be considered as approximations.)

CALIBRATION OF RADIOCARBON AGE TO CALENDAR YEARS

Variables used in the calculation of age calibration → (Variables: est. C13/C12=-25:lab. mult=1)

Laboratory number: **Beta-123456**

The uncalibrated Conventional Radiocarbon Age (± 1 sigma)

Conventional radiocarbon age[1]: **2400±60 BP**

The calendar age range in both calendar years (AD or BC) and in Radiocarbon Years (BP)

2 Sigma calibrated result: **Cal BC 770 to 380 (Cal BP 2720 to 2330)**
(95% probability)

[1] *C13/C12 ratio estimated*

Intercept data

The intercept between the average radiocarbon age and the calibrated curve time scale. This value is illustrative and should not be used by itself.

Intercept of radiocarbon age with calibration curve: Cal BC 410 (Cal BP 2360)

1 Sigma calibrated result: (68% probability) Cal BC 740 to 710 (Cal BP 2690 to 2660) and Cal BC 535 to 395 (Cal BP 2485 to 2345)

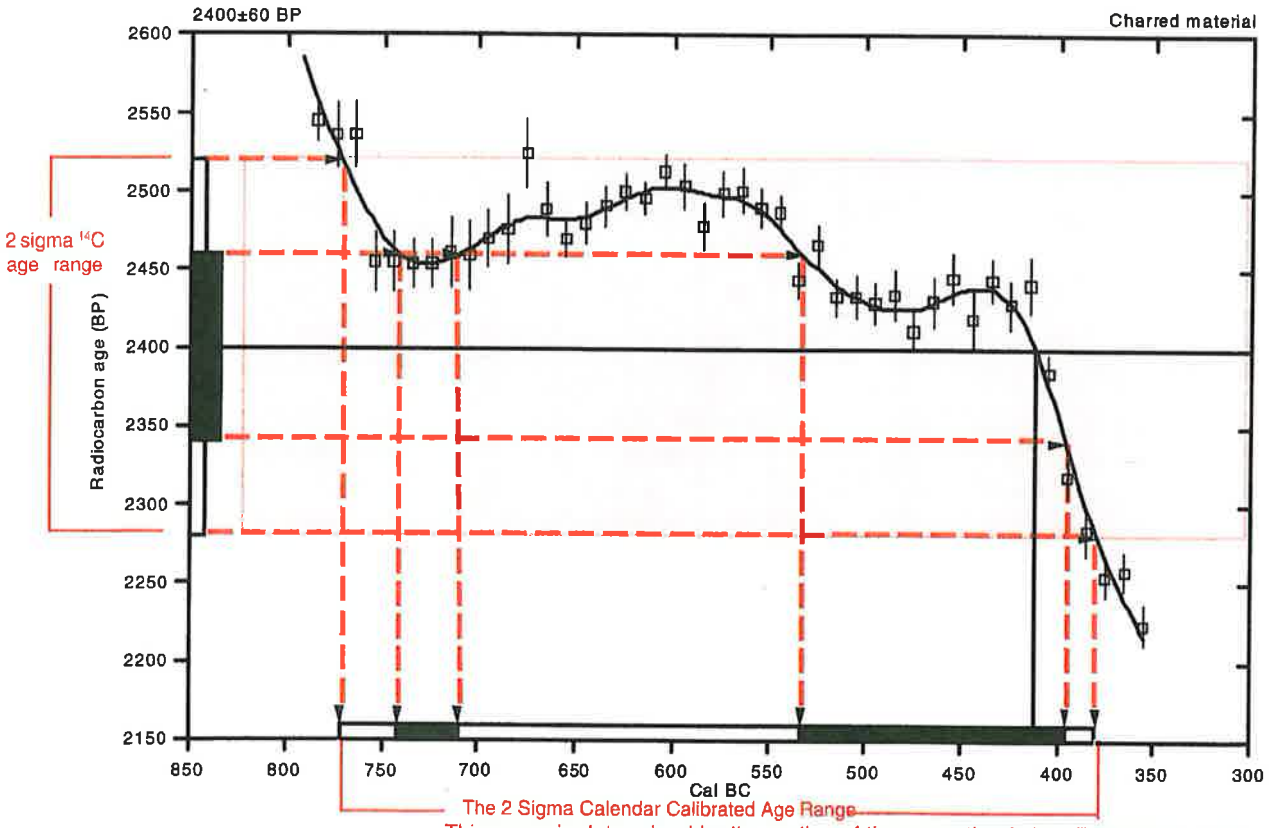

This range is determined by the portion of the curve that is in a "box" drawn from the 2 sigma limits on the radiocarbon age. If a section of the curve goes outside of the "box", multiple ranges will occur as shown by the two 1 sigma ranges which occur from sections going outside of a similar "box" which would be drawn at the 1 sigma limits.

References:

Database used
Intcal 98
Calibration Database
Editorial Comment
Stuiver, M., van der Plicht, H., 1998, Radiocarbon 40(3), pxii-xiii
INTCAL98 Radiocarbon Age Calibration
Stuiver, M., et. al., 1998, Radiocarbon 40(3), p1041-1083
Mathematics
A Simplified Approach to Calibrating C14 Dates
Talma, A. S., Vogel, J. C., 1993, Radiocarbon 35(2), p317-322

References for the calibration data and the mathematics applied to the data. These references, as well as the Conventional Radiocarbon Age and the 13C/12C ratio used should be included in your papers.

Beta Analytic Radiocarbon Dating Laboratory
4985 S.W. 74th Court, Miami, Florida 33155 • Tel: (305)667-5167 • Fax: (305)663-0964 • E-mail: beta@radiocarbon.com

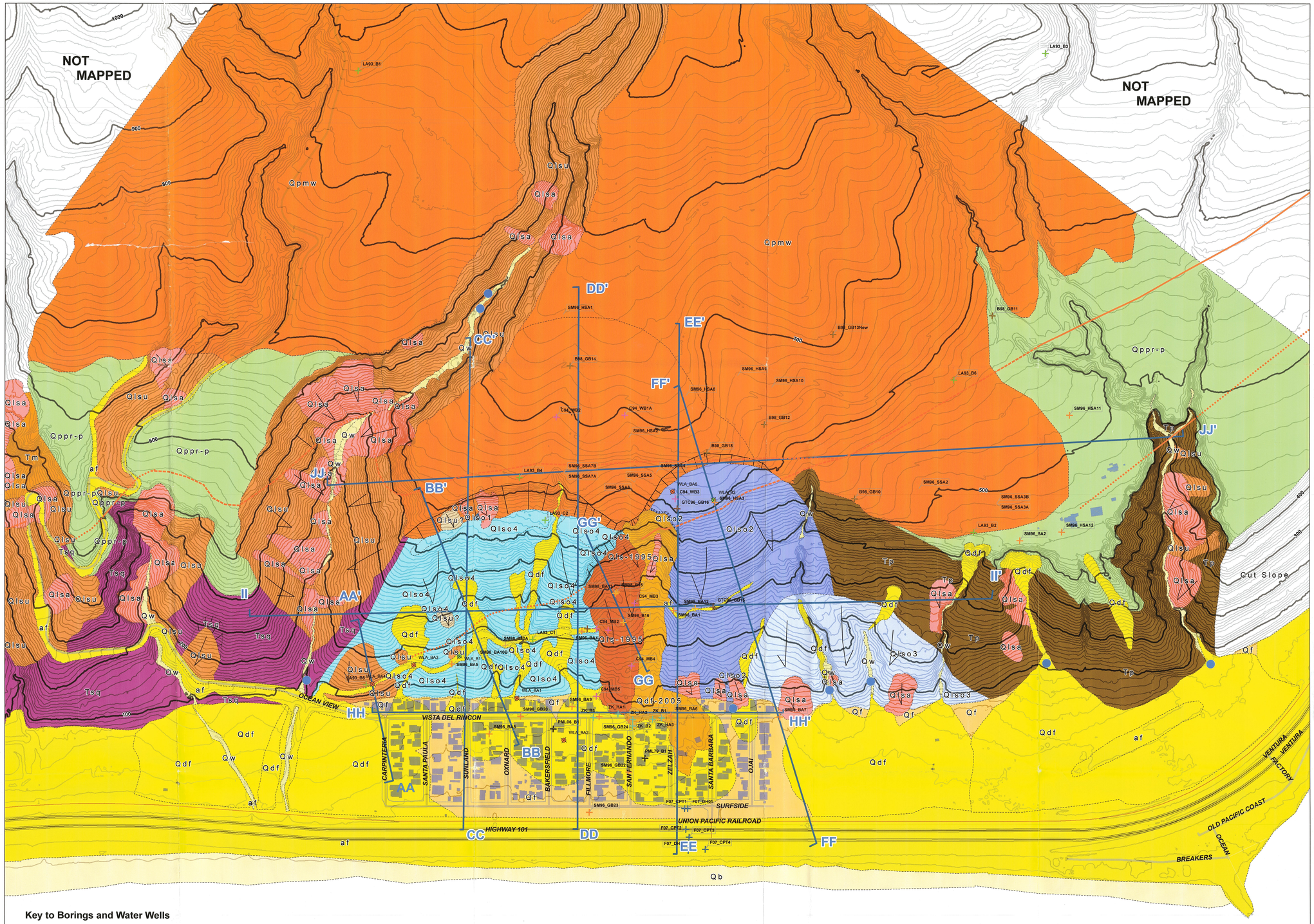

Key to Borings and Water Wells

- Fugro West, 2007
- Bin Yen & Associates, Inc., 1995
- Converse West Consultants, 1994
- Geotechnical Consultants, Inc. (various years from 1994-1998; cited in Bachman, 1998)
- La Conchita Ranch (cited in Bachman, 1998)
- Leighton & Associates, 1992
- Leighton & Associates, 1993
- Pacific Materials Laboratories, 2006 (Hollow-stem auger boring for evaluation of liquefaction potential and foundation conditions)
- Stoney-Miller, 1996
- Stoney-Miller, 1998
- Zeiser Kling, 1998

WLA Boreholes (This Study)

- Bucket Auger
- Mud Rotary

Geologic Map Legend

Explanation of Map Units

Historic (<300 years old)

af	Artificial fill, includes engineered and non-engineered material.
Qb	Active beach deposits, consisting of loose sand.
Qw	Active stream channel and gully wash deposits.
Qdf-2005	Debris flow deposits associated with 2005 slope failure.
Qls-1995	Landslide deposits associated with 1995 landslide.
Qlsa	Active landslide deposits, includes historic landslides identified on aerial photographs and from historical records.
Qdf	Debris flow deposits; including possible source areas, transport gullies, and run-out deposits.

Holocene (>300 years old; <11,000 years old)

Qlsu	Inferred landslide deposits of unknown age and activity, based on geomorphic expression.
Qlsu?	Possible (queried) landslide deposits with unknown activity.
Qf	Late Holocene alluvial fan deposits, may include debris fan deposits.

Holocene/Pleistocene (>300 to 60,000 years old)

Qlso3	Qlso3 - Older landslide deposits.
Qlso2	Qlso2 - Older landslide deposits.
Qlso4	Oldest landslide deposits of unknown age.
Qpmw	Pleistocene debris deposits (mass wasting deposits), contains fragments of Monterey Formation.
Qppr-p	Pleistocene Punta Gorda marine terrace deposits and associated paralic (deposited by the sea but non-marine) deposits, consisting of consolidated clayey sand with gravel lenses.

Bedrock Units (Pliocene and older)

Tp	Pico Formation (Pliocene).
Tsq	Sisquoc Shale (Pliocene-Miocene).
Tm	Monterey Formation (Miocene).

Map Symbols

- 100 — Topographic contour interval, in feet.
- Geologic contact, solid where confirmed dashed where inferred, dotted where covered.
- Fault trace, solid where confirmed, dashed where inferred, dotted where covered.
- Spring location.
- Landslide, hachures indicate scarp area where mappable with exposed geologic deposits or bedrock units shown, queried where existence is questionable, arrows indicate principal direction of movement.

References

This geologic map largely is modified from CGS (2003), based in part on Dibblee (1998).

Topography derived from ultra-high resolution (1m point spacing) LiDAR data obtained by aerial survey in April, 2007 conducted by Airborne1.

California Department of Conservation, Division of Mines and Geology (CGS), 1991, Revised Official Map of Earthquake Fault Zones, Pitas Point Quadrangle, 1:24,000 scale.

California Geological Survey (CGS), 2002, Seismic hazard evaluation of the Pitas Point 7.5-minute quadrangle, Ventura County, California: CGS Seismic Hazard Zone Report 073.

California Geological Survey (CGS), 2003, Geologic map of the Pitas Point 7.5-minute quadrangle, Ventura County, California: A Digital Database: Version 1.0, 1:24,000 scale (digital).

Dibblee, T.W., Jr., 1988, Geologic map of the Ventura and Pitas Point quadrangles: Dibblee Foundation Map no. DF-2, 1:24,000 scale.

Leighton and Associates, Inc, 1992, La Conchita Ranch, dated December 11, 1992: Project No. 2920785-02.

Leighton and Associates, Inc, 1993, Summary of Geotechnical Investigations, La Conchita Ranch, Venture County, California, Project No. 2920785-05, dated August 20, 1993.

Stoney-Miller Consultants, Inc, 1996, Summary Geotechnical Evaluation of the La Conchita Landslide - March 4, 1995, Ventura County, California, for the Bateman Group, Project No: 11203-00, Report No: 5-5042, dated October 18, 1996.

Stoney-Miller Consultants, Inc, 1998, Addendum to the Summary Geotechnical Evaluation of the La Conchita Landslide of March 4, 1995, Ventura County, California, dated March 17, 1998, Project No. 11469-00.

Magnetic Declination / Project North

Feet
0 50100 200 300 400

LA CONCHITA
Final Report

Figure B-1: Geologic Map

WLA William Lettis & Associates, Inc.

11 JULY 2008, 1985, REV 2, CSH